IL
NUOVO CIMENTO
ORGANO DELLA SOCIETÀ ITALIANA DI FISICA
SOTTO GLI AUSPICI DEL CONSIGLIO NAZIONALE DELLE RICERCHE

VOL. XV, N. 1 — *Serie decima* — 1° Gennaio 1960

Proton and Antiproton Diffraction Scattering on Complex Nuclei.

G. BARONI, G. BELLETTINI, C. CASTAGNOLI,
M. FERRO-LUZZI and A. MANFREDINI

Istituto di Fisica dell'Università - Roma
Istituto Nazionale di Fisica Nucleare - Sezione di Roma

(ricevuto il 6 Giugno 1959)

Summary. — A comparison of the results on antiproton and proton diffraction scattering on emulsion nuclei is carried out on the basis of 26.4 m proton track with $\bar{E}=125$ MeV, and 23.15 m of antiproton track with $\bar{E}=150$ MeV. A disagreement is shown to exist between experiment and optical model calculations at 140 MeV.

1. – Introduction.

We report here on the results of a research on the angular distribution of $\bar{p}$ elastic scattering on emulsion nuclei. Preliminary results [1] on one metre track length had suggested the possible existence of destructive interference between nuclear and Coulomb scattering of antiprotons. Therefore we thought it interesting to compare with a better statistics the elastic scattering of protons and antiprotons.

The result of this investigation is that there exists a considerable difference between the proton and antiproton experimental angular distributions, especially at small angles, and that the destructive interference appears to take place for protons rather than for antiprotons.

These experimental results on the angular distribution have been compared with the theoretical predictions of two optical models: an appreciable dis-

(1) ACE (Antiproton Collaboration Experiment): *Phys. Rev.*, **105**, 1037 (1957).

crepancy between the theoretical and experimental angular distributions has been found, for antiprotons; the discrepancy, however, is still larger in the case of protons.

2. – Experimental results.

2·1. *Protons.* – G-5 Ilford plates were exposed at a proton beam of (142 ± 3) MeV energy. Each proton was followed for 1 cm of flat track, starting at 6 mm from the front edge beam end of the stack so as to avoid the distorsions always present at the edge of the emulsion. Thus, taking straggling into account, our results correspond to a mean energy of 125 MeV (from 117 to 133 MeV). All scatterings were recorded regardless of the projected angle α. Only those with $\alpha \geqslant 1°.5$ were used, since we found—as in previous investigations (²)—that the scanning efficiency depends from α only for $\alpha \leqslant 1°.5$.

Measurements on a sample of tracks carried out by different scanners gave an efficiency $\varepsilon = 0.90$; this value was used also for the measurements on the antiprotons. The scanning velocity was ~ 1.5 cm per hour.

Over a total track length of 26.4 m we found 233 elastic scatterings (of which 30 with $\theta > 15°$), and 79 stars. From these data follows λ_e $(\theta \geqslant 1°.5) = (7.3 \pm 0.4)$ cm; $\lambda_{\text{int}} = (33.4 \pm 3.8)$ cm.

The angular distribution of the proton diffraction scattering not corrected for the geometrical cut-off due to the $\alpha \geqslant 1°.5$ limitation, is shown in Fig. 1.

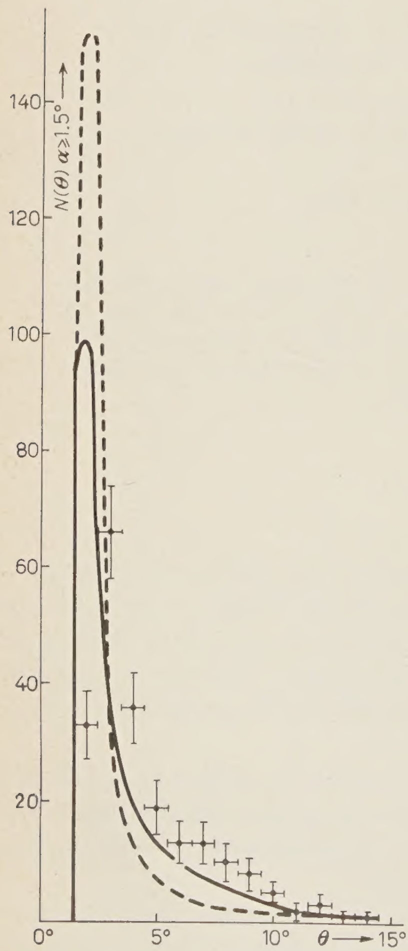

Fig. 1. – Protons. ⊢♦⊣ experimental (Roma); —— according to Bjorklund and Fernbach; – – – according to Glassgold.

(²) A. BARBARO, G. BARONI and C. CASTAGNOLI: *Nuovo Cimento*, 9, 154 (1958).

2·2. *Antiprotons.* – Measurements were carried out by the same scanners and with the same optics as in the previous case, using tracks longer than 3 mm per plate. The plates have been exposed to the antiproton beam of the Bevatron at Berkeley. The energy interval here explored is between 50 and 250 MeV, with a mean energy $\bar{E} = 150$ MeV. For each scattering, besides the angle, also the distance from the end of the range was measured, in order to obtain a scattering measurement as a function of the energy.

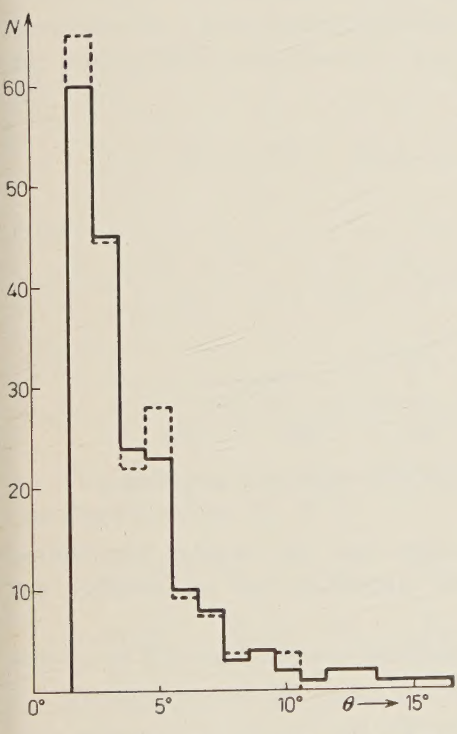

Fig. 2. – $\overline{P}$ diffraction scattering ($\alpha \geqslant 1.5°$). —— Rome ($\alpha \geqslant 1.5)°$; – – – Goldhaber and Sandweiss (normalization factor $f = 0.54$).

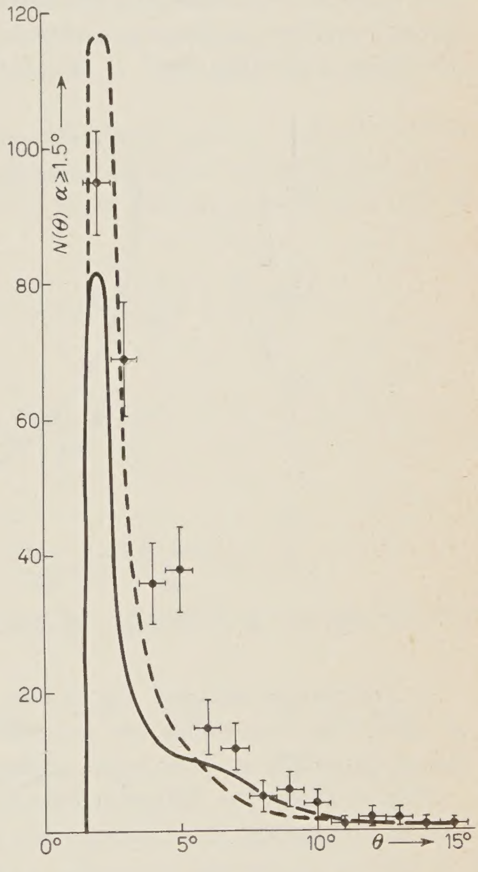

Fig. 3. – Antiprotons. ⊢◆⊣ experimental (Rome, Goldhaber and Sandweiss); —— according to Bjorklund and Fernbach; – – – according to Glassgold.

Over 15.05 m of track we have found 188 scatterings with $\alpha \geqslant 1°.5$. Taking into account the efficiency, we thus obtained $\lambda_e\,(\theta \geqslant 1°.5) = (4.7 \pm 0.7)$ cm. The $\overline{\text{p}}$ diffraction scattering angular distribution, prior to the correction for the geometrical cut-off, is shown in Fig. 2. It may be noticed that the requirement, of at least 3 mm of track per plate, gives rise to a geometrical cut-off

for $\theta > 15°$. A single event of this type was found; the evaluated total number of scatterings with $\theta > 15°$ should not become, in any case, larger than five.

Fig. 2 shows also the comparison of our angular distribution with that obtained by GOLDHABER and SANDWEISS (³) over 8.1 m track length, normalized to the same track length. The agreement is very satisfactory and guarantees the accuracy of the measurement as far as the number of events and the form of the distribution are concerned. Therefore it appears justified to put together our data and these of GOLDHABER *et al.* so as to reduce the statistical error (Fig. 3).

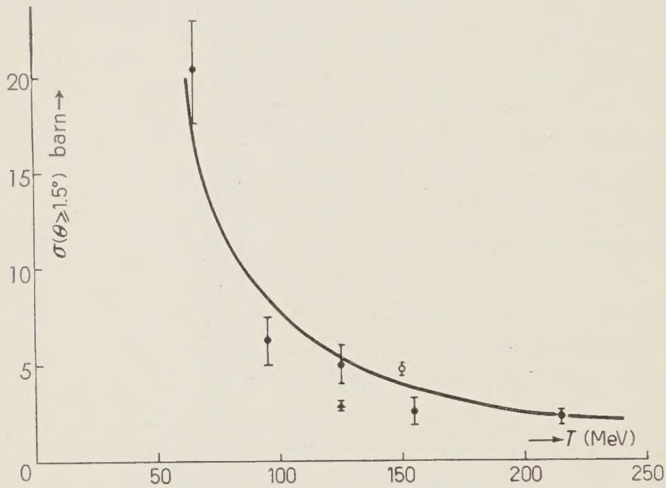

Fig. 4. – ● antiprotons; ○ mean value of antiprotons; ▲ protons.

A comparison between Fig. 1 and 3 shows that the angular distribution of diffraction scatterings for protons and antiprotons are considerably different, especially at very small angles.

Fig. 4. shows the differential elastic scattering cross-section of $\overline{\text{p}}$ as a function of the energy.

3. – Comparison with optical models.

We have compared our experimental results with an optical model computation carried out by GLASSGOLD (⁴) assuming that the p and $\overline{\text{p}}$ interaction with the complex nucleus is given by a Woods-Saxon type potential

$$V(r) = (V + iW)\left\{1 + \exp\left[\frac{r - R}{a}\right]\right\}^{-1},$$

(³) G. GOLDHABER and J. SANDWEISS: *Phys. Rev.*, **110**, 1476 (1958).
(⁴) A. E. GLASSGOLD: *Phys. Rev.*, **110**, 220 (1958).

where $R = 1.3\,A^{\frac{1}{3}}$ fermi, $a = 0.65$ fermi, $V = -15$ MeV, both for p and $\bar{\text{p}}$ and $W = 12.5$ MeV for p and -50 MeV for $\bar{\text{p}}$.

Neither curves, calculated for the actual composition of the emulsion and corrected for geometrical and efficiency biases, fit the experimental data, especially in the case of the protons (see Fig. 1, 3).

Then we tried a comparison of our data with an optical model in which the values of the parameters are deduced from the phase-shifts obtained by CHEW and BALL ([5]) for interpreting the observed antiproton-proton scattering. We recall that Coulomb effects are included in these optical model parameters.

In Fig. 1 and 3 we have plotted the results of such an optical method computation, kindly made under our request by BJORKLUND and FERNBACH ([6]) for protons and antiprotons of 140 MeV. These authors used a potential of the form

$$V = -(V_{CR} + iV_{CI})\varrho(r) + (V_{SR} + iV_{SI})\left(\frac{\hbar}{\mu_C}\right)^2 \frac{1}{r}\frac{\mathrm{d}\varrho}{\mathrm{d}r}\boldsymbol{\sigma}\boldsymbol{L}\,,$$

where

$$\varrho(r) = \left\{1 + \exp\left[\frac{(r - R_0)}{a}\right]\right\}^{-1},$$

with

$$a = 0.65 \text{ fermi}\,, \qquad R_0 = 1.25\,A^{\frac{1}{3}} \text{ fermi}\,.$$

The computations were carried out for Br, Ag and N, using the following parameter values (in MeV):

$$\begin{array}{lllll} \text{for } \bar{\text{p}} & V_{CR} = -15\,, & V_{CI} = 65\,, & V_{SR} = 3.3\,, & V_{SI} = 4.8\,, \\ \text{for p} & V_{CR} = 10\,, & V_{CI} = 20\,, & V_{SR} = 2\,, & V_{SI} = -1.2\,. \end{array}$$

Averaging over the composition of the emulsion and taking into account the geometrical cut-off and the scanning efficiency, the curves of Fig. 1, 3 were obtained.

Experimental and theoretical results differ appreciably. If the experimental data are divided into 3 energy intervals, the angular distributions thus obtained are all alike. This is an indication that the difference between the

---

([5]) J. CHEW and G. BALL: *Phys. Rev.*, **109**, 1385 (1958).

([6]) G. BJORKLUND and S. FERNBACH: private communication. We are grateful to these authors, who have sent us their calculations for $\bar{\text{p}}$, and who have very kindly, on our request, performed the calculations for p.

proton and antiproton distributions does not arise from the difference in energy interval (Fig. 5).

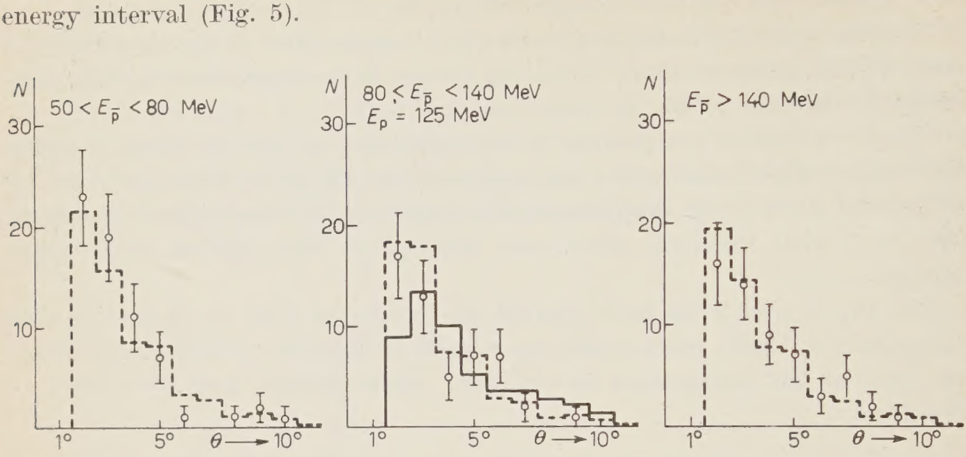

Fig. 5. – – – – Antiprotons; ——— Protons.

In conclusion it appears that the disagreement between the various optical model computations and the experimental data, does not depend appreciably on the details of the adopted model. On the other hand, we believe that this discrepancy can hardly be attributed to experimental reasons, in spite of the rather delicate nature of the measurements involved; in this connection we recall that 1) the experimental curves, for both protons and antiprotons, have been obtained by the same scanners; 2) our antiproton curve is in excellent agreement with that obtained by the Berkeley group, and finally 3) in the case of the protons, the energy band is very narrow and very near to that used in the calculations.

* * *

We would like to thank Dr. F. BJORKLUND and Dr. S. FERNBACH for the kind collaboration; Dr. LOFGREN and the Bevatron staff at Berkeley for providing the exposure of the stack, and Dr. G. GOLDHABER and Dr. G. EKSPONG for information on their experimental results.

RIASSUNTO

Si confrontano i risultati sullo scattering di diffrazione di antiprotoni e protoni contro nuclei dell'emulsione. Essi sono relativi a 26.4 m di traccia di protoni con $\bar{E}=125$ MeV e 23.15 m di traccia di antiprotoni con $\bar{E}=150$ MeV. Si esegue un confronto con le previsioni del modello ottico ad una energia di 240 MeV che mostra un disaccordo tra dati sperimentali e teoria.

IL NUOVO CIMENTO VOL. XV, N. 1 1° Gennaio 1960

The «Catalytic» and «Photo» Decay Modes of the Muon (*).

S. P. ROSEN (**)

Washington University - St. Louis, Mo.

(ricevuto il 25 Giugno 1959)

Summary. — It is shown that, on the basis of the usual baryon-lepton direct coupling theory, the «catalytic» ($\mu + \mathcal{N} \to e + \mathcal{N}$) and the «photo» ($\mu \to e + \gamma$) decays of the muon are expected to occur as second order processes in the effective weak interaction Hamiltonian, $\mathscr{H}_{weak}$. If however, the effective weak interaction itself arises as a consequence of the coupling of baryons and leptons to an intermediate heavy boson («X»), these decays are essentially first order in $\mathscr{H}_{weak}$, and are predicted to go so fast as apparently to contradict experimental data, at least in the case of photo decay. Estimates of the rates of the catalytic and photo decays are given both on the direct coupling and on the «X» theories and a comparison with the available empirical limits on these rates is made.

1. – Introduction.

The remarkable success of the effective weak interaction Hamiltonian, $\mathscr{H}_{weak}$, which couples baryons and leptons directly, in describing the main features of β-decay, μ-capture, μ-decay, and π-μ, π-e decay, together with the apparent equivalence of the electromagnetic properties of the electron and the muon, suggests that the *only* intrinsic difference between these two particles is one of mass ($m_\mu \approx 200\, m_e$). It would therefore appear, *a priori*, reasonable to anticipate the occurrence of processes like the «catalytic» [1]

(*) This research was supported in part by the United States Air Force through the Air Force Office of Scientific Research and Development Command, under Contract no. AF 18(603)-108.

(**) Present address: Midwestern Universities Research Association, Madison, Wis.

(1) The nucleon acts as a kind of catalyst for $\mu \to e$: hence the name.

and « photo » decays of the muon into the electron ($\mathcal{N}$ denotes nucleon):

$$\mu + \mathcal{N} \to e + \mathcal{N}\,, \tag{1}$$

$$\mu \to e + \gamma\,. \tag{2}$$

However, the experimental limits on (1), (2) [2-6] are so low that it seems likely that these processes are either second order in $\mathcal{H}_{\text{weak}}$ or, if in some sense first order, strongly inhibited by an additional selection rule.

The catalytic decay (1) can, obviously, always occur as a second order effect in $\mathcal{H}_{\text{weak}}$,

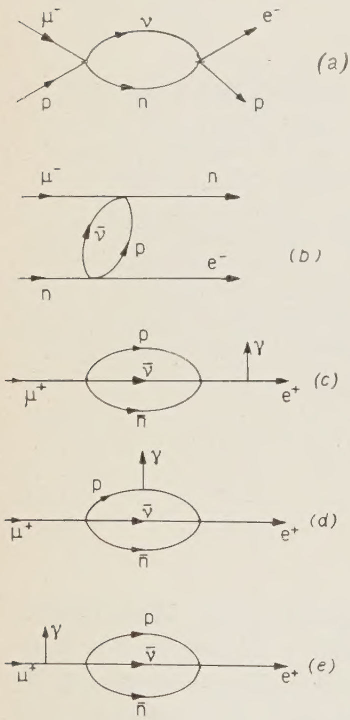

$$\left\{\begin{array}{l}\mu^- + p \to n + \nu \to e^- + p\\ \mu^- + n \to \mu^- + p + \bar{\nu} + e^- \to n + e^-\end{array}\right. \tag{3}$$

while correspondingly, the photo decay (2) can always follow a scheme like (see Fig. 1):

$$\mu^+ \to p + \bar{n} + \bar{\nu} \to e^+ \to e^+ + \gamma\,. \tag{4}$$

Alternatively, if the weak interactions are all generated by the coupling of baryons and leptons to an intermediate heavy boson, « X » [7], then (1), and (2) can also occur via schemes such as [8,9]:

$$\mu^+ \to X^+ + \bar{\nu} \to e^+ \to e^+ + \gamma\,, \tag{5}$$

$$\mu^- + p \to e^- + \gamma + p \to e^- + p'\,. \tag{6}$$

Fig. 1. – Channel (1): (*a*) and (*b*) are diagrams for catalytic decay, and (*c*), (*d*), (*e*) the diagrams for photo decay.

---

(2) A. Lagarrigue and C. Peyrou: *Compt. Rend.*, **234**, 1873 (1952).
(3) J. Steinberger and H. Wolfe: *Phys. Rev.*, **100**, 1490 (1955).
(4) S. Lokanathan and J. Steinberger: *Phys. Rev.*, **98**, 240 (A) (1955).
(5) A. Roberts, H. F. Davis, A. Roberts and T. F. Zipf: *Phys. Rev. Lett.*, **2**, 211 (1959).
(6) D. Berley, J. Lee and M. Barton: *Phys. Rev. Lett.*, **2**, 357 (1959).
(7) See for example M. Gell-Mann: *Gatlinburg Conference* (1958).
(8) G. Feinberg: *Phys. Rev.*, **110**, 1482 (1958).
(9) M. Ebel and F. J. Ernst: preprint.

The rates of the catalytic and photo decays via schemes (3), (4), which are the only ones available in the direct coupling theory, are proportional to g^4, $g^4\alpha$ respectively (g is the universal weak interaction coupling constant and α the fine structure constant); on the other hand, in the X theory the schemes (5), (6) yield rates for these decays proportional to $g^2\alpha$, $g^2\alpha^2$. This suggests that, if the X exists, the schemes (5), (6) will be predominant.

2. – Direct coupling theory.

It is obvious from Fig. 1 that the matrix elements for (3), (4) contain quadratic divergences, and since there is no way of renormalizing them, some form of cut-off must be used. Fortunately such a cut-off may be introduced in a natural way, as follows. If the coupling between leptons and bare nucleons is V, A, then [10,11] the effective interaction Hamiltonian for dressed nucleons is

$$
\begin{aligned}
(7)\qquad \sqrt{2}\,\mathscr{H}_{\text{weak}} = {} & A(q^2)(\bar{\psi}_{\mathcal{N}}\,\tau^+ i\gamma^\lambda\gamma^5\psi_{\mathcal{N}'})\{(\bar{\psi}_\mu i\gamma^\lambda(1+\gamma^5)\psi_\nu) + (\bar{\psi}_e i\gamma^\lambda(1+\gamma^5)\psi_\nu)\} + \\
& + m_\mu B(q^2)(\bar{\psi}_{\mathcal{N}}\,\tau^+\gamma^5\psi_{\mathcal{N}'})\left\{(\bar{\psi}_\mu\gamma^5(1+\gamma^5)\psi_\nu) + \frac{m_e}{m_\mu}(\bar{\psi}_e\gamma^5(1+\gamma^5)\psi_\nu)\right\} + \\
& + \{C(q^2)(\bar{\psi}_{\mathcal{N}}\,\tau^+\gamma^\lambda\psi_{\mathcal{N}}) - iD(q^2)(\bar{\psi}_{\mathcal{N}}\,\tau^+\sigma^{\lambda\varrho}(N'-N)^\varrho\psi_{\mathcal{N}'})\}\cdot \\
& \cdot\{(\bar{\psi}_\mu\gamma^\lambda(1+\gamma^5)\psi_\nu) + (\bar{\psi}_e\gamma^\lambda(1+\gamma^5)\psi_\nu)\} + \text{h.c.}\,,
\end{aligned}
$$

where

$$
(8)\qquad \left\{
\begin{aligned}
A(q^2) &\approx g(\exp[-q^2/4\pi m_p^2])\,, \\
m_\mu B(q^2) &\approx 0.13\,\frac{G^2}{\pi^2}\,m_\mu m_p g\,\frac{1}{m_\pi^2+q^2}\,(\exp[-q^2/4\pi m_p^2]) \\
C(q^2) &\approx g(\exp[-q^2/6](4/7m_\pi)^2) \approx \frac{2m_p}{\mu_p-\mu_n}\,D(q^2)\,, \\
g &\approx 2.5\cdot 10^{-12}\,,
\end{aligned}
\right.
$$

and the $\psi_{\mathcal{N}}$ are, effectively, quantized field amplitudes for dressed nucleons. In (7), (8), $q^2=(N-N')^2$ is the nucleon 4-momentum transfer [12], g and G are the dimensionless weak interaction and pion-nucleon coupling constants, respectively; m_p, m_μ, m_e, m_π are the masses of the proton, muon, electron and pion, and μ_p, μ_n are the proton, neutron anomalous magnetic moments.

---

(10) M. Goldberger and S. B. Treiman: *Phys. Rev.*, **111**, 354 (1958).

(11) A. Fujii and H. Primakoff: *Nuovo Cimento*, **12**, 327 (1959).

(12) 3-momenta, energy are always in units of $m_e c$, $m_e c^2$ respectively and all masses are in units of m_e, the electron mass.

Since the major contributions to the matrix elements for (3), (4) come from large momentum transfers at the weak interaction vertices in Fig. 1, it is clear that the exponential behaviour of A, B, C, D in (8) will remove the divergences. Moreover, since $A(q^2)$ is appreciable for $q^2 \leqslant 4\pi m_p^2$, and since

$$(9) \qquad \frac{4\pi m_p^2}{6(7m_\pi/4)^2} \approx 30\,, \qquad \frac{4\pi m_p^2}{0.13(G^2/\pi^2)m_p m_\mu} \approx 50\,,$$

the dominant term in $\mathscr{H}_{\text{weak}}$ is the axial vector, and so, for the catalytic and photo decay modes

$$(10) \quad \sqrt{2}\,\mathscr{H}_{\text{weak}} \approx A(q^2)(\overline{\psi}_{\mathcal{N}} i\gamma^\lambda\gamma^5\psi_{\mathcal{N}})\{(\overline{\psi}_\mu i\gamma^\lambda(1+\gamma^5)\psi_\nu) + (\overline{\psi}_e i\gamma^\lambda(1+\gamma^5)\psi_\nu)\} + \text{h.c.}$$

2·1 *Catalytic decay.* – Consider first the catalytic decay (Fig. 1*a*, *b*): the nucleon 4-momentum transfers at the vertices are $p_\nu \pm p_e$, $p_\nu \pm p_\mu$ (p_ν, p_e, p_μ are the 4-momenta of ν, e, μ respectively), and for large momentum transfers these are all roughly equal to p_ν. Therefore, from (9), (10), the matrix element for (3) is approximately (in lowest order perturbation theory)

$$(11) \quad M_{\text{weak}} \approx (-i)^2 g^2 \left(\frac{\pi^2 i}{2}\right)\left\langle \begin{matrix} N \\ e \end{matrix} \right| \int \exp[-p_\nu^2/2\pi m_p^2]\, p_\nu\, \mathrm{d}p_\nu \cdot$$
$$\cdot\{\overline{\psi}_{\mathcal{N}}[\gamma^\lambda\gamma^\mu\gamma^\nu(\tau^+\tau^-) + \gamma^\nu\gamma^\mu\gamma^\lambda(\tau^-\tau^+)]\psi_{\mathcal{N}}\}\cdot$$
$$\cdot\{\overline{\psi}_e\gamma^\lambda\gamma^\mu\gamma^\nu(1+\gamma^5)\psi_\mu\}\left| \begin{matrix} N \\ \mu \end{matrix} \right\rangle \delta^4(p_{\mathcal{N}} + p_\mu - p_{\mathcal{N}'} - p_e)\,,$$

with

$$(12) \qquad \int \exp[-p_\nu^2/2\pi m_p^2]\, p_\nu\, \mathrm{d}p_\nu = \pi m_p^2\,,$$

where $p_{\mathcal{N}}$, $p_{\mathcal{N}'}$ are the initial, final four momenta of the nucleon and τ^+, τ^- are the usual isotopic spin operators. Equation (11) can be generalized to give the matrix element for

$$(13) \qquad \mu + \text{nucleus } (A, Z) \to \text{e} + (A, Z)$$

as

$$(14) \quad M_{\text{weak}}(A, Z) \approx \frac{1}{(2\pi)^3}(-i)^2 g^2\left(\frac{\pi^2 i}{2}\right)(\pi m_p^2)\cdot$$
$$\cdot\left\langle \begin{matrix} f \\ e \end{matrix} \right| \overline{\Psi}_f \sum_l \{(10\gamma_l^\lambda + 6\gamma_l^\lambda\gamma_l^5\tau_l^3)(\overline{\psi}_e(x_l)\gamma^\lambda(1+\gamma^5)\psi_\mu(x_l))\}\Psi_i \left| \begin{matrix} i \\ \mu \end{matrix} \right\rangle \delta(E_i + E_\mu - E_f - E_e)\,.$$

Ψ_l, Ψ_i are the wave-functions of the final, initial states f, i of the nucleus (A, Z) with energies E_f, E_i respectively; x_l is the position vector of the l-th

nucleon and $\sum_l$ denotes the sum over all nucleons. E_μ, E_e are energies of the muon, and electron respectively. Terms corresponding to $\mu + \mathcal{N}_1 + \mathcal{N}_2 \to e + \mathcal{N}_1' + \mathcal{N}_2'$ have been neglected in (14) since they are not divergent and should therefore give only a relatively small contribution to the matrix element.

The rate for (13) is estimated by means of a closure method developed by PRIMAKOFF [13] for μ-capture. Assume that the nucleus (A, Z) is initially in its ground state. The muon is taken to be in its lowest Bohr orbit (radius r_0), with orbital wave function $(Z^3/\pi r_0^3)^{\frac{1}{2}}\varphi_\mu(x)$ and the effect of the nuclear Coulomb field on the outgoing electron is neglected. Then $|M_{\text{weak}}(A, Z)|^2$ must be summed over electron spins, averaged over muon spins, and finally summed over all energetically accessible final states, f, of (A, Z). In general $|E_i - E_f| \ll m_\mu$ and so the sum over f can be performed by closure. If the nucleons are treated non-relativistically, this procedure yields, as the total rate for (13),

$$(15) \qquad R_{\text{weak}}(A, Z) \approx \frac{m_e c^2}{\hbar}\left(\frac{g m_p}{\pi}\right)^4 \left(\frac{Z}{r_0}\right)^3 \frac{\langle p_e \rangle^2}{2^{10}} \cdot \langle i | \sum_{lj} [100 + 36\boldsymbol{\sigma}_l \cdot \boldsymbol{\sigma}_j (\tau_l^{(3)} \tau_j^{(3)})] j_0(\langle p_e \rangle x_{lj}) \varphi_\mu(x_l) \varphi_\mu^x(x_j) | i \rangle \,,$$

where $\langle p_e \rangle$, the energy of the electron averaged over the states f is roughly equal to $\frac{3}{4} m_\mu$. (The electron mass is neglected.)

The total rate for μ-capture,

$$(16) \qquad \mu + (A, Z) \to \nu + (A, Z-1)\,,$$

also calculated by the closure method, is roughly given by

$$(17) \qquad \frac{m_e c^2}{\hbar} \frac{g^2}{2\pi^2} \left(\frac{Z}{r_0}\right)^3 \langle p_\nu \rangle^2 \langle i | \sum_{lj} \tau_l^{(+)} \tau_j^{(-)} (1 + \boldsymbol{\sigma}_l \cdot \boldsymbol{\sigma}_j) j_0(\langle p_e \rangle x_{lj}) \varphi_\mu(x_l) \varphi_\mu^x(x_j) | i \rangle \,,$$

where $\langle p_\nu \rangle$, the average neutrino energy, is also $\approx \frac{3}{4} m_\mu$. The « induced pseudoscalar » and anomalous magnetic moment terms of (7) are neglected, since they do affect the order of magnitude of (17); also $q^2 \approx m_\mu^2$, $A \approx C \approx g$ in (8). The nuclear matrix element of (17) can be evaluated by the method of reference [13], and for heavier nuclei ($Z > 6$, $A > 12$)

$$(18) \qquad Z^3 \langle i | \sum_{lj} \tau_l^{(+)} \tau_j^{(-)} (1 + \boldsymbol{\sigma}_l \cdot \boldsymbol{\sigma}_j) j_0(\langle p_\nu \rangle x_{lj}) \varphi_\mu(x_l) \varphi_\mu^x(x_j) | i \rangle \approx \approx (4Z_{\text{eff}})^4 \left| 1 - \frac{3(A-Z)}{2A} \right| \approx (Z_{\text{eff}})^1 \,.$$

[13] H. PRIMAKOFF: *Rev. Mod. Phys.*, **31**, 802 (1959).

In a similar way, the nuclear matrix element of (15) is

$$(19)\qquad \langle i|\sum_{lj}[100+36\boldsymbol{\sigma}_l\cdot\boldsymbol{\sigma}_j(\tau_l^{(3)}\tau_j^{(3)})]j_0(\langle p_e\rangle x_{lj})\varphi_\mu(x_l)\varphi_\mu^*(x_j)|i\rangle\approx 800\cdot A_{\text{eff}}\,,$$

where A_{eff} is defined in a manner analogous to Z_{eff}. The branching ratio of catalytic decay to μ-capture in heavier nuclei ($A>12$) is thus

$$(20)\qquad B_{\text{weak}}\left(\frac{\mu+(A,Z)\to e+(A,Z)}{\mu+(A,Z)\to\nu+(A,Z-1)}\right)\approx\frac{g^2}{\pi^2}\frac{m_p^4}{2^6}10^2\frac{A_{\text{eff}}Z^3}{(Z_{\text{eff}})^4}\approx 10^{-11}\,.$$

2·2 *Photo decay.* – In the case of photo decay, all three diagrams, Fig. 1 *c*, *d*, *e* must be considered so as to obtain a gauge invariant matrix element. (See reference [14] for the analogous case of $\pi\to\mu+\nu+\gamma$.) With (10) for the weak interaction Hamiltonian, the sum of the three diagrams gives a total matrix element, in lowest order,

$$(21)\quad M_{\text{weak}}(\mu\to e+\gamma)\approx\left(-\frac{ie}{(\hbar c)^{\frac12}}\right)5g^2\left\langle{e\atop\gamma}\right|(\bar\psi_e\gamma^\alpha p_\mu^\beta F^{\alpha\beta}(1+\gamma^5)\psi_\mu)\left|\mu\right\rangle\cdot$$
$$\cdot N\delta^4(p_\mu-p_e-p_\gamma)\,,$$

where

$$N=\iint p_{\mathcal{N}}^3\,\mathrm{d}p_{\mathcal{N}}\exp[-p_\nu^2/2\pi m_p^2]p_\nu^3\,\mathrm{d}p_\nu\frac{(\frac12 p_{\mathcal{N}}^2+m_p^2)}{(p_{\mathcal{N}}^2+m_p^2)^2(p_{\mathcal{N}}^2+m_p^2+p_\nu^2)m_\mu^2}\,.$$

p_μ, p_e, p_γ are the four momenta of μ, e, γ, and $p_{\mathcal{N}}$ is that of one of the intermediate nucleons; $F^{\alpha\beta}=A^\alpha p_\gamma^\beta-A^\beta p_\gamma^\alpha$. The appearance of two divergent integrals in (21) is to be expected since the intermediate ν, n, $\bar{\text{p}}$ loop of Fig. 1, *c*, *d*, *e*, contains three momenta which satisfy only one independent condition. As in the catalytic decay calculation, the momentum dependent coupling of (10) introduces a natural cut-off for the neutrino integral. The nucleon divergence is logarithmic and somewhat analogous to the divergence appearing in the matrix element of $\pi\to\mu+\nu$ [14]: since a cut-off at the nucleon mass gives the correct order of magnitude for the rate of $\pi\to\mu+\nu$ it seems reasonable to use the same cut-off in this estimate [11]. Thus

$$(22)\qquad N\approx\frac12(\pi m_p^2)^2\left(\frac{\ln 2}{m_\mu^2}\right),$$

[14] S. B. Treiman and H. W. Wyld jr.: *Phys. Rev.*, **101**, 1552 (1956).

and from (21), (22) the rate for $\mu \to e+\gamma$ is, in the limit of zero muon 3-momentum, (neglecting the electron mass)

$$R_{\text{weak}}(\mu \to e + \gamma) \approx \frac{m_e c^2}{\hbar}\,\alpha\,\frac{g^4}{10}\left(\frac{m_p^2}{2\pi}\right)^4\left(\frac{\ln 2}{m_\mu^2}\right)^2 (m_\mu)^5 . \tag{23}$$

The rate for $\mu \to e+\nu+\bar{\nu}$ is, from V, A coupling,

$$R(\mu \to e + \nu + \bar{\nu}) = \frac{m_e c^2}{\hbar}\,\frac{g^2}{4\pi^3}\,\frac{(m_\mu)^5}{24} , \tag{24}$$

again in the limit of zero muon 3-momentum. Hence, from (23), (24) the branching ratio

$$B_{\text{weak}}\left(\frac{\mu \to e + \gamma}{\mu \to e + \nu + \bar{\nu}}\right) \approx 3 \cdot 10^{-10} . \tag{25}$$

3. – X-theory.

Feinberg's [8] estimate, based on the X theory, for the branching ratio of $\mu \to e+\gamma$ to μ-decay is 10^{-4}: since this value is much higher than the present experimental upper limit [6] of 10^{-6}, it seems unlikely that the X in fact exists. However, this conclusion is not completely certain because EBEL and ERNST [9] have shown that, with suitable choice of X mass, anomalous magnetic moment and cut-off, the theoretical estimate can be reduced to $10^{-6} \div 10^{-7}$. Therefore, in order to examine the catalytic decay on the X-theory, it will be assumed that the photo decay *is* induced by the X with a branching ratio to μ-decay given by

$$\frac{R_X(\mu \to e + \gamma)}{R(\mu \to e + \nu + \bar{\nu})} = T , \tag{26}$$

$$(10^{-6} \geqslant T \geqslant 10^{-7}) .$$

In view of the X-neutrino loop in Fig. 2, the matrix elements for catalytic

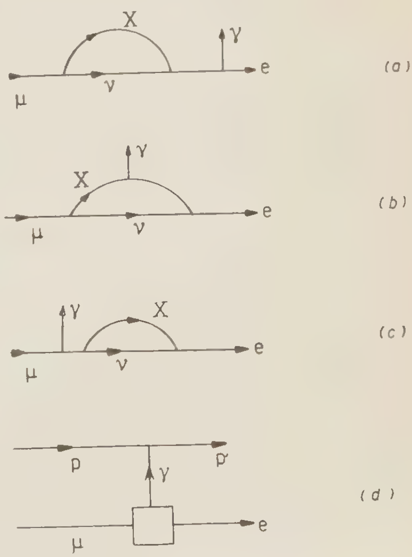

Fig. 2. – Channel (ii): (*a*), (*b*), (*c*) are photo decay. The box in (*d*) represents the production of the γ-ray (in (*a*), (*b*), (*c*)), which is absorbed by the nucleon.

and photo decay will both contain the same divergence. (This should be contrasted with the direct-coupling theory, where the corresponding matrix elements contain one and two divergences respectively: see Section 2·1, 2·2.) These matrix elements may be written (in lowest order)

$$(27)\quad M_X(\mu \to e + \gamma) \approx 2K\,(\overline{\psi}_e \gamma^\alpha p_\mu^\beta F^{\alpha\beta}(1+\gamma^5)\psi_\mu)\,\delta^4(p_\mu - p_e - p_\gamma)\,,$$

$$(28)\quad M_X(\mu + \mathcal{N} \to e + \mathcal{N}) \approx 3K\left(\frac{-ie}{(\hbar c)^{\frac{1}{2}}}\right)(\overline{\psi}_{\mathcal{N}}\tfrac{1}{2}(1+\tau^3)\gamma^\alpha\psi_{\mathcal{N}'})\cdot$$
$$\cdot\,(\overline{\psi}_e\gamma^\alpha(1+\gamma^5)\psi_\mu)\,\delta^4(p_\mu + N' - p_e - N)\,,$$

p_μ, p_e, p_γ are the μ, e, γ, 4-momenta; N', N are the initial final, nucleon 4-momenta. K contains the divergent integrals, coupling constants and various other factors arising in the calculation. The rate for photo decay is then.

$$(29)\qquad R_X(\mu \to e + \gamma) \approx \frac{m_e c^2}{\hbar}\,\frac{K^2\pi}{(2\pi)^{10}}\,(m_\mu)^5\,.$$

The rate of μ-decay is known to be $0.45\cdot 10^6\ \text{s}^{-1}$ and so it follows from (26) and (29) that

$$(30)\qquad K^2 \approx 7T\cdot 10^{-20}\,.$$

Equation (28) can be generalized to give

$$(31)\quad M_X(\mu + (A, Z) \to e + (A, Z)) \approx$$
$$\approx \frac{3}{(2\pi)^3}\,K(4\pi\alpha)^{\frac{1}{2}}\left\langle \begin{matrix} f \\ e \end{matrix}\right| \overline{\Psi}_f\Big[\sum_l \tfrac{1}{2}(1+\tau_l^3)\,\gamma^\alpha(\overline{\psi}_e(x_l)\gamma^\alpha(1+\gamma^5)\psi_\mu(x_l))\Big]\Psi_i\left|\begin{matrix} i \\ \mu \end{matrix}\right\rangle\cdot$$
$$\cdot\,\delta(E_i + E_\mu - E_f - E_e)\,.$$

The notation in (31) is the same as in (14). Using the methods of Sect. 2·1, we find that the rate for catalytic decay is, from (31),

$$(32)\qquad R_X(A, Z) \approx \frac{m_e c^2}{\hbar}\,\frac{9K^2\alpha\langle p_e\rangle^2}{2^6\pi^9}\left(\frac{Z}{r_0}\right)^3\cdot$$
$$\cdot\,\langle i|\sum_{lj}\tfrac{1}{4}(1+\tau_l^{(3)})(1+\tau_j^{(3)})\,j_0(\langle p_e\rangle r_{lj})\,\varphi_\mu(x_l)\,\varphi_\mu^*(x_j)|i\rangle$$

and

$$(33)\quad Z^3\langle i|\sum_l \tfrac{1}{4}(1+\tau_l^{(3)})(1+\tau_j^{(3)})\,j_0(\langle p_e\rangle r_{lj})\,\varphi_\mu(x_l)\,\varphi_\mu^*(x_j)|i\rangle \approx 1\quad \text{(for Hydrogen)},$$

and

$$\approx (Z_{\text{eff}})^4\left(1 + \frac{6Z}{A}\right)\qquad \text{(for } A > 12\text{)},$$
$$\approx 4(Z_{\text{eff}})^4\,.$$

From (32), (33), (17), (18), the branching ratio of catalytic decay to μ-capture, is, for the X-theory

$$(34)\qquad B_X\left(\frac{\mu+(A,Z)\to e+(A,Z)}{\mu+(A,Z)\to \nu+(A,Z-1)}\right)\approx\frac{9K^2\alpha}{g^2\pi^7 2^5}\cdot A \qquad (A>12),$$

$$\approx 3T\cdot 10^{-2} > 3\cdot 10^{-9} \quad \text{and} \quad < 3\cdot 10^{-8}.$$

For hydrogen the branching ratio is one quarter that in (34).

From (27), (28) it is found that

$$(35)\qquad \frac{R_X(\mu+\mathcal{N}\to e+\mathcal{N})}{R_X(\mu\to e+\gamma)}\approx 9\cdot 2^4(\alpha)^4\approx 5\cdot 10^{-7}.$$

Equation (35) does not contradict Feinberg's [8] branching ratio

$$(36)\qquad B_X\left(\frac{\mu\to e+\gamma\to e+e+e}{\mu\to e+\gamma}\right)\approx\frac{1}{150}.$$

The discrepancy between (35), (36) arises from the different densities of final states for $\mu+\mathcal{N}\to e+\mathcal{N}$, and $\mu\to e+e+e$.

To see that (34) and (35) are consistent with each other, consider μ-capture in hydrogen: an extrapolation from Sens' experimental data [15] yields, according to the $(Z_{\text{eff}})^4$-law [16] and taking the Pauli principle inhibition into proper account

$$(37)\qquad R(\mu+p\to\nu+n)\approx 200\ \text{s}^{-1}$$

and so it follows from (34), (37) that

$$(38)\qquad R_X(\mu+p\to e+p)\approx\tfrac{3}{2}T.$$

From (35), (26) and the known rate of μ-decay

$$(39)\qquad R'_X(\mu+p\to e+p)\approx\tfrac{1}{4}T.$$

In view of the crudeness of this calculation, the agreement between (38), and (39) is very good.

We see from this discussion that, if the X exists, there is a simple relation between the rates of catalytic and photo decay (see (26), (34)). Moreover, from the resuts of references [8,9], it is possible to set definite limits on the branching ratio of catalytic decay to μ-capture (34).

---

(15) J. C. Sens: *Phys. Rev.*, **113**, 679 (1959).

(16) H. Primakoff: *Proc. of the Fifth Annual Rochester Conference on High Energy Physics* (New York, 1955), p. 174.

4. – Conclusions.

We have shown in Sections **2**, **3** that the rates of catalytic and photo-decay predicted by the X theory (ii) are at least one hundred times greater than the corresponding rates of the direct coupling theory. In comparing theory with experiment, we may use this difference as a test for the existence of the X. For convenience the results of Sections **2**, **3**, and all available experimental data are presented in Table I.

TABLE I.

Decay mode	Theoretical: direct coupling	Theoretical: X-theory	Experimental	Reference
$B\left(\dfrac{\text{catalytic}}{\mu\text{-capture}}\right)$	10^{-11}	$3T\cdot 10^{-2}$ $\geqslant 3\cdot 10^{-9}$	$\leqslant (4.5\pm 4.5)\cdot 10^{-2}$	(2)
		and $\leqslant 3\cdot 10^{-8}$	$\leqslant 5\cdot 10^{-4}$	(3)
$B\left(\dfrac{\text{photo}}{\mu\text{-decay}}\right)$	$3\cdot 10^{-10}$	T	$\leqslant 2\cdot 10^{-5}$	(5)
		$10^{-6}\geqslant T\geqslant 10^{-7}$	$\leqslant 10^{-5}$	(6)
		(see ref. (9))	$\leqslant 10^{-6}$	(7)

B denotes branching ratio, and T is defined in (26).

The estimates in Table I do not offer much hope of observing the catalytic decay with present muon beams ($10^5 \div 10^7$ muons per second are needed to see one catalytic decay per day!), and it is therefore not surprising that the present experimental upper limits are consistent with the predictions of both theories. On the other hand, at least if Ebel and Ernst's variant of the theory is correct, we may be on the verge of observing the photo decay.

If it is established beyond reasonable doubt that the X does not exist, then some interesting comparison can be made between the catalytic and photo decays of the muon on the one hand and double β-decay on the other: firstly, all three processes are second order in the weak interaction Hamiltonian, $\mathscr{H}_{\text{weak}}$, and secondly, while the matrix element for double β-decay is finite, the predicted rates for the two muon decays are strongly dependent on a cut-off. So far no second order effects of $\mathscr{H}_{\text{weak}}$ have ever been observed and so it is still an open question whether $\mathscr{H}_{\text{weak}}$ is really a bonafide interaction Hamiltonian, usable in principle, to all orders of perturbation theory or whether it is only a phenomenological abbreviation for the calculation of first order transition amplitudes, such as those in β-decay and μ-capture.

Though the cut-off methods used above are fairly standard, they are, nevertheless, quite arbitrary, and so the numerical predictions of this paper should be taken with a certain latitude. The important point to note is that these decay modes of the muon are *observable* processes, depending on a cut-off. Thus we see from this comparison that there are at least two reasons why it is of great basic interest merely to observe the catalytic and photo decays of the muon [17], whatever the rates turn out to be.

* * *

The author is indebted to Professor H. PRIMAKOFF for many helpful suggestions on this subject and also for reading the manuscript: it is a great pleasure to thank him.

[17] $\mu \to 3e$ is expected to occur via the scheme $\mu \to e+\gamma \to e+e+e$. From (36), (26) and (25) the branching ratio of $\mu \to 3e$ to μ-decay is $10^{-8} \div 10^{-10}$ on the X theory and $2 \cdot 10^{-12}$ on the direct coupling theory. Annihilation processes like $\mu^+ + e^- \to \gamma+\gamma$ will be even more suppressed than $\mu \to 3e$.

Note added in proof.

Due to the electron-neutrino scattering term in the « conserved current » theory of Feynman and Gell-Mann (*Phys. Rev.*, **109**, 193 (1958)), the $\mu \to 3e$ decay can occur via the scheme $\mu \to e+\nu+\bar{\nu} \to e+e+e$. If the quadratically divergent element is cut off at the nucleon mass (or, alternatively, if the momentum dependent coupling $A(q^2)$, of equation (8) is used), then the branching ratio of $\mu \to 3e$ to μ-decay is of order $10^{-10} \div 10^{-11}$.

RIASSUNTO (*)

In base alla usuale teoria dell'accoppiamento diretto barione-leptone, si dimostra che il decadimento « catalitico » ($\mu + \mathcal{N} \to e + \mathcal{N}$) ed il « foto » decadimento ($\mu \to e+\gamma$) del muone hanno luogo come processi del secondo ordine nella hamiltoniana effettiva di interazione debole $\mathscr{H}_{\text{weak}}$. Tuttavia, se tale interazione debole effettiva, trae origine dall'accoppiamento di barioni e leptoni con un bosone pesante intermedio (« X »), questi decadimenti sono essenzialmente del primo ordine nel $\mathscr{H}_{\text{weak}}$, e si prevede che essi procedano così rapidamente da contraddire apparentemente, almeno nel caso del decadimento fotonico, i dati sperimentali. Si riportano le stime delle quantità di decadimento catalitico e del fotodecadimento, sia nell'accoppiamento diretto che nelle teorie dell' « X », e si confrontano tali valori con i limiti empirici oggi noti per queste quantità.

(*) *Traduzione a cura della Redazione.*

The Angular Distribution of Secondary Particles in High Energy Nuclear Collisions with Heavy Nuclei of Photographic Emulsion.

J. Bartke, P. Ciok, J. Gierula, R. Hołyński, M. Mięsowicz and T. Saniewska

Cosmic Ray Department, Institute of Nuclear Research - Kraków and Warszawa

(ricevuto il 9 Luglio 1959)

Summary. — 61 jets produced by singly charged and neutral particles of cosmic radiation in photographic emulsion in collisions with heavy nuclei ($N_h > 8$) have been investigated. Primary energies and anisotropy parameters for angular distributions of secondary particles have been calculated. The results were compared with those obtained formerly for events with mall evaporation ($N_h \leqslant 5$). It might be stated that the energy dependence of the anisotropy for both samples of jets is quite similar. The mean anisotropy is however smaller than that predicted by hydrodynamical theories. It was stated that in the same energy interval the anisotropy for particular events differ very much and that the main contribution to high anisotropy is given by the cases in which the angular distribution $\mathrm{d}N/\mathrm{d}(\log \mathrm{tg}\,\theta)$ is not a normal one, but shows two separated maxima. The results were discussed from the point of vew of the two-centre model.

1. – Introduction.

In the previous work of our group (1) the analysis of the angular distributions of secondary particles produced in high energy collisions has been done. Only events with a small number of evaporation tracks ($N_h \leqslant 5$) have been taken. In many ot the events investigated in that work a very typical

(1) P. Ciok, T. Coghen, J. Gierula, R. Hołyński, A. Jurak, M. Mięsowicz, T. Saniewska, O. Stanisz and J. Pernegr: *Nuovo Cimento*, **8**, 166 (1958); P. Ciok, T. Coghen, J. Gierula, R. Hołyński, A. Jurak, M. Mięsowicz, T. Saniewska and J. Pernegr: *Nuovo Cimento*, **10**, 741 (1958).

angular distribution was observed, which was interpreted by our group on the basis of the «two-centre-model». This interpretation was based on the assumption of a nucleon-nucleon collision, although the criterion of a small number of evaporation tracks may be not very efficient in selecting these collisions. On the other hand it is rather easy to qualify an event as a collision of a nucleon with a heavy nucleus in case the number of evaporation tracks N_h is greater than eight. The aim of the present work was to investigate the angular distributions of secondary particles produced in collisions of nucleons with heavy nuclei of photographic emulsions and to compare the results with the predictions of the hydrodynamical «tunnel» theory and with those of the two-centre-model. From all the forms of the tunnel theories, the hydrodynamical theory published recently by MILEHIN (2) presents the results most convenient for comparison with experiments. According to this theory the tunnel contains the nuclear matter taken as a fluid without any structure and the number of nucleons in the tunnel is used only for describing the length or the mass of the tunnel.

2. – Experimental results.

The jets produced in photographic emulsions in collisions with heavy nuclei ($N_h > 8$) found in our laboratory, known from the published papers (3) and also from private communications (*) have been investigated. We compare these jets with events for which $N_h \leqslant 5$, a considerable part of which may be regarded as nucleon-nucleon collisions. Only jets with singly charged or neutral primaries were investigated. The numbers of jets belonging to both groups *i.e.* $N_h \leqslant 5$ and $N_h > 8$ are given in Table I for three intervals of γ-factors.

TABLE I.

γ	Number of jets with $N_h \leqslant 5$	Number of jets with $N_h > 8$
$2.4 \leqslant \gamma < 7.3$	24	29
$7.3 \leqslant \gamma < 23$	28	21
$23 \leqslant \gamma < 140$	19	12

(*) We are very much obliged to Professor N. DOBROTIN for kindly sending us the angular distributions of jets from collaborating laboratories and to Dr. D. H. PERKINS for the material from the H. H. Wills Laboratory, Bristol.

(2) G. A. MILEHIN: *Žurn. Ėksper. Teor. Fiz.*, **35**, 1185 (1958).

(3) D. F. HÄNNI, C. LANG, M. TEUCHER and H. WINZELER: *Nuovo Cimento*, **4**, 1473 (1956).

The γ-factor is defined by the formula

$$\log \gamma = \overline{\log \cot \theta_i}\,, \tag{1}$$

where θ_i are the angles of the secondary particles with the primary direction. γ is therefore the Lorentz factor of a system for which there is symmetry in the forward and backward directions. In the case of nucleon-nucleon collision γ is the energy of each nucleon in the C.M. system expressed in rest mass units. We call the events with $N_h \leqslant 5$ « $\mathcal{N}$-$\mathcal{N}$ »-collisions and those with $N_h > 8$ « $\mathcal{N}$-heavy nucleus »-collisions.

If we express the differential angular distribution in the form $dN/d(\log \operatorname{tg} \theta)$ *vs.* $\log \operatorname{tg} \theta$ we can consider the value of the spread of this distribution defined as

$$\sigma = \sqrt{\frac{\sum (\log \operatorname{tg} \theta_i - \overline{\log \operatorname{tg} \theta_i})^2}{n-1}}\,,$$

as a measure of the anisotropy of the distribution (4). We calculated the σ-values for all events and plotted them as a function of γ. This analysis was formerly done by our group for events with $N_h \leqslant 5$ (1). An analysis of this type was then performed by the Budapest group (5).

The primary energy was determined by using formulae: $E_p = 2\gamma^2$ for jets with $N_h \leqslant 5$ and $E_p = 2n\gamma^2$ for jets with $N_h > 8$, where n is the number of nucleons in the tunnel. The last formula is true if we assume that the symmetry system for which γ was calculated by means of (1) is the CM-system of the primary nucleon and the tunnel. We have found that in the system moving with this γ, forward and backward symmetry in the angular distribution does exist, both in number and shape. This is shown for three energy classes in Fig. 1. As we have well defined nuclei (Ag and Br) in our experiments we take $n = 4$ for the mean length of the tunnel.

In Fig. 2 all the σ-values are plotted against γ. In the same figure the theoretical curves are given for dependence of the anisotropy parameter σ on γ in the form which follows from the hydrodynamical theory given by MILEHIN (2). In this theory the angular distribution in the CM-system may be well approximated by a Gaussian distribution in $\lambda = \ln \gamma \operatorname{tg} \theta$ coordinates in the form $dN/d\lambda \sim \exp[-(\lambda^2/2L)]$, where the parameter L depends on the

(4) N. M. DULLER and W. D. WALKER: *Phys. Rev.*, **93**, 215 (1954); L. v. LINDERN: *Nuovo Cimento*, **5**, 491 (1957).

(5) G. BÓZOKI and E. GOMBOSI: *Nucl. Phys.*, **9**, 400 (1959).

primary energy E and on the length of the tunnel n:

$$L = 0.56 \ln \frac{E}{M} + 1.6 \ln \frac{2}{n+1} + 1.6 \, .$$

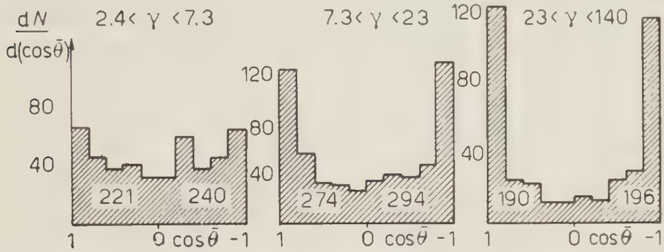

Fig. 1. – Angular distributions transformed with γ-values calculated by the formula (1) for jets with $N_h > 8$.

From Fig. 2 we see that for energies higher than 10^{12} eV for which a comparison with the hydrodynamical theory can be made the observed σ-values (anisotropy parameters) are smaller than the values predicted by this theory for both $N_h \leqslant 5$ and $N_h > 8$.

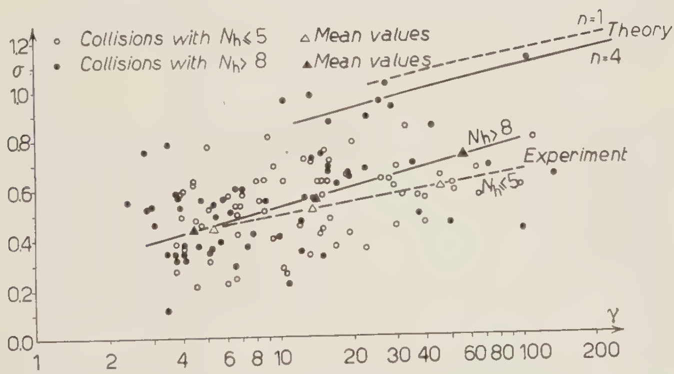

Fig. 2. – Distributions of σ-values in function of γ for all investigated jets.

We tentatively assume that the angular distributions in all jets are of the Gaussian type in $x = \log \operatorname{tg} \theta$ coordinates. This may be expected from the point of view of the hydrodynamical theory. In this case we can ascribe to each σ-value the standard error $\Delta\sigma = \sigma/\sqrt{2(n-1)}$. Applying this formula we can calculate the average anisotropy parameters $\bar{\sigma}$ for each group of jets in the given γ intervals and in the given evaporation group. As a result of this calculation we find that the mean anisotropy $\bar{\sigma}$ is higher for collisions with heavy

nuclei ($N_h > 8$) than for collisions with small evaporation ($N_h \leqslant 5$) in which some important fraction must be nucleon-nucleon collisions (Fig. 2). If any significance could be attributed to the estimation applied, this result is the opposite of the predictions of the hydrodynamical theory.

We have compared the distributions of σ-values for jets with smaller evaporation ($N_h \leqslant 5$) with those for collisions with Ag or Br nuclei ($N_h > 8$) in the highest energy group. From Fig. 3 we see that the spread of σ-values

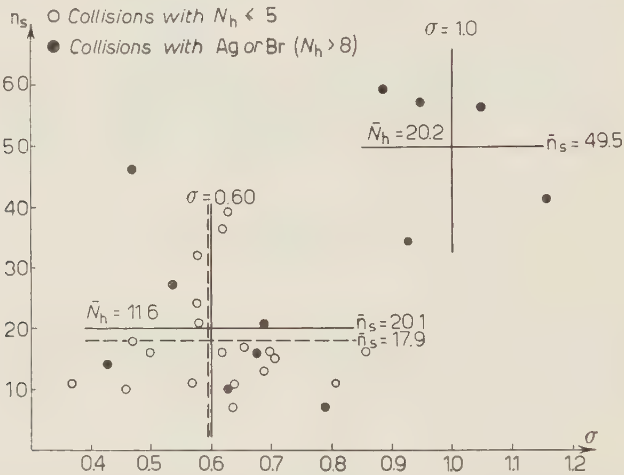

Fig. 3. – Distributions of σ-values as function of n_s for jets with $23 \leqslant \gamma < 140$.

(anisotropy parameters) is significantly smaller for jets with small evaporation than for collisions with Ag or Br nuclei. The latter distribution splits into two groups: the first one with small σ and the second one with large σ. The interesting feature of this grouping is that small n_s and small N_h correspond to small σ while large ones to large σ (see Fig. 3: $\bar{\sigma} = 0.6$ corresponds to $\bar{n}_s = 20.1$, $\bar{N}_h = 11.6$ and $\bar{\sigma} = 1.0$ to $\bar{n}_s = 49.5$, $\bar{N}_h = 20.2$).

All the jets in the large σ group show the characteristic double maximum in the distribution of $x = \log \operatorname{tg} \theta$ (Fig. 4). The deviation

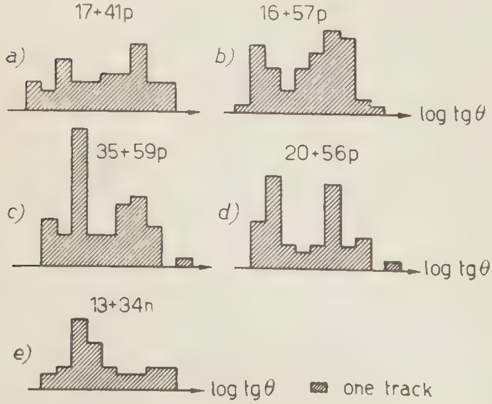

Fig. 4. – Differential angular distributions for five jets with $N_h > 8$ and $23 \leqslant \gamma < 140$ corresponding to the large σ group: *a*) Kraków; *b*) Bristol; *c*) Alma-Ata; *d*) Bern; *e*) Moscow.

of this distribution from the Gaussian one with the same σ value is very pronounced for each individual jet of this group. The Kolmogorov-Smirnov test gives a deviation corresponding to about two standard deviations.

The other interesting thing which may be seen from Fig. 3 is that the mean $\bar{\sigma}$, $\bar{n}_s$, and $\bar{N}_h$ values for jets with small evaporation are very similar to the corresponding values for the small σ group in collisions with Ag or Br nuclei.

3. – Conclusions.

Concluding we can say that both the mean σ and the shape of the angular distribution do not agree with the predictions of the hydrodynamical theory (2).

On the other hand one may try to explain the observed facts on the basis of composite collisions. The angular distributions observed for collisions with heavy nuclei would be a superposition of distributions obtained for $\mathcal{N}$-$\mathcal{N}$- collisions from our two-centre-model (1).

From Fig. 3 we may be tempted to explain the small σ-group for collisions with Ag and Br nuclei as nucleon-nucleon collisions such as those included in the group of jets with $N_h < 5$; since both the mean σ and the mean n_s are very similar. The last group ($N_h \geq 5$) is certainly biased against jets with small n_s and large σ. Such jets are sometimes detected via cascades *e.g.* jet P20 from Bristol (6).

The high σ group may be considered as corresponding to interactions in which the superposition of many such low n_s and high σ collisions occur. This type of collisions shows a distinct double maximum in the angular distribution.

If we consider the double maximum distribution as being the result of peripheric collisions, the approach discussed seems to hold the possibility for obtaining information concerning the unbiased sample of nucleon-nucleon interactions by investigating not the simplest interactions but those in which a nucleon strikes nuclear matter.

* * *

The authors would like to thank Professor M. DANYSZ for many interesting discussions on this subject.

---

(6) B. EDWARDS, J. LOSTY, D. H. PERKINS, K. PINKAU and J. REYNOLDS: *Phil. Mag.*, 3, 237 (1958).

RIASSUNTO (*)

Si sono esaminati 61 getti prodotti in collisioni con nuclei pesanti ($N_h > 8$) della emulsione fotografica da particelle a singola carica o neutre della radiazione cosmica. Si sono calcolate le energie primarie ed i parametri di anisotropia per le distribuzioni angolari delle particelle secondarie. I risultati sono stati paragonati con quelli ottenuti precedentemente per eventi con piccola evaporazione ($N_h \leqslant 5$). Si potrebbe affermare che la dipendenza dell'anisotropia dall'energia in entrambi i tipi di getti è abbastanza simile. L'anisotropia media però è più piccola di quella predetta dalle teorie idrodinamiche. Si è stabilito che nello stesso intervallo energetico l'anisotropia di particolari eventi varia moltissimo e che il maggior contributo all'elevata anisotropia è dato dai casi in cui la distribuzione angolare $dN/d(\log \operatorname{tg} \theta)$ non è normale, ma presenta due massimi separati. I risultati sono stati discussi dal punto di vista del modello a due centri.

(*) *Traduzione a cura della Redazione.*

IL NUOVO CIMENTO Vol. XV, N. 1 1° Gennaio 1960

A Method to Determine the Charge of Nuclei with Nuclear Emulsions.

G. Alvial, L. Grimaldi, J. Riquelme, E. Silva and S. Stantic

Centro de Radiación Cósmica,
Facultad de Ciencias Físicas y Matemáticas - Universidad de Chile

(ricevuto il 3 Agosto 1959)

Summary. — The authors of the present work give their first experimental results on a method to determine the charge of either high and low energy nuclei with nuclear emulsions. They considered only the track thicknesses over a pre-fixed width obtained by measuring the thickness according to the method given by Occhialini and collaborators and determined a criterion to count this type of thickness *which are probably caused by little δ-rays.*

1. – The authors of the present work give their first experimental results on a method to determine the atomic number of either high and low energy nuclei with nuclear emulsions.

We considered only thicknesses over a pre-fixed width obtained by measuring the thickness according to the method given by Occhialini and collaborators [1,2], namely, blobs attached to the edges of the track or relative short columns of silver grains with thickness over the mean track thickness. These particular fluctuations *are probably caused by little δ-rays.* Next we will establish a criterion to define this type of δ-ray.

The experimental curves presented here give the mean integral number of little δ-rays with the residual range for nuclei at the end of their range. For

(1) A. Bonetti, C. Dilworth, M. Ladu and G. Occhialini: *Rend. Acc. Naz. Lincei*, s. viii, **12**, fasc. 6 (Dicembre 1954).

(2) G. Alvial, A. Bonetti, C. Dilworth, M. Ladu, J. Morgan and G. Occhialini: *Suppl. Nuovo Cimento*, **4**, 244 (1955).

high energy nuclei the mean density of little δ-rays is given only. The procedure used to do the thickness measurements as the corresponding technical terms are similar to those described in the OCCHIALINI and collaborator's paper. We do not describe this method here and we recommend the reading of this last article (²).

2. – The measurements were performed by applying the method mentioned above and with a Clausen micrometer of Koristka manufacture fitting the microscope MS2 of the same firm. All the measured tracks were in G-5 Ilford plates of 600 μm original thickness which presented a normal factor of contraction due to the development process.

The adopted cell-measurement was of 0.125 μm length in order to obtain at least three width readings from the thickness measurements of a single grain. With this cell, an experienced observer could measure a 50 μm track length in an average time of 45 minutes.

We took only thicknesses greater than 1.8 times the mean thickness of the last 200 μm of a proton track. This limit was over the mean thickness of each measured track. The ratio between the length of the considered thickness in the direction of the track axis and the mean diameter of single grains belonging to minimum blob density tracks determines the number which *we define as little δ-rays*. In this way, it is easy to calculate *the density of such δ-rays* directly from the thickness readings obtained with the Clausen micrometer.

The thickness limit taken in the previous paragraph was determined experimentally in order to normalize the ratio of little δ-ray densities for protons and α-particles with the ratio of the squares of the respective atomic numbers in points of equal velocity. The same limit was applied to all measured tracks.

In almost all cases it was easy to decide whether or not the thickness corresponds to little δ-rays. Critical cases, as those caused by simultaneous thickening on both sides of the track, were decided by drawing the profile of the track.

3. – Fig. 1 shows the mean integral number of little δ-rays against the residual range for 5 protons, 6 α-particles, 5 lithium nuclei and one beryllium nucleus. The discrimination of these particles, as we see in Fig. 1, can be made in only 60 μm of residual range. Previous identification of the particles was made by applying the standard method for δ-rays of three or more grains. These last measurements were carried out on residual ranges longer than 3 500 μm.

In Fig. 2 we give an example of the measurements for only one lithium and one beryllium both belonging to a plate which presented a strong development gradient.

Fig. 3 shows the mean thickness of 24 α-particles and 10 lithium nuclei against the corresponding angle of dip. These particles were taken from hammer tracks belonging to the same plate. The α-particles had a mean residual range of 18 μm and the lithium nuclei one of 33 μm. In these experimental points we do not observe the same correlation found in a previously mentioned paper (²). In any way, further measurements in plates processed by using different development methods may give an answer to this results.

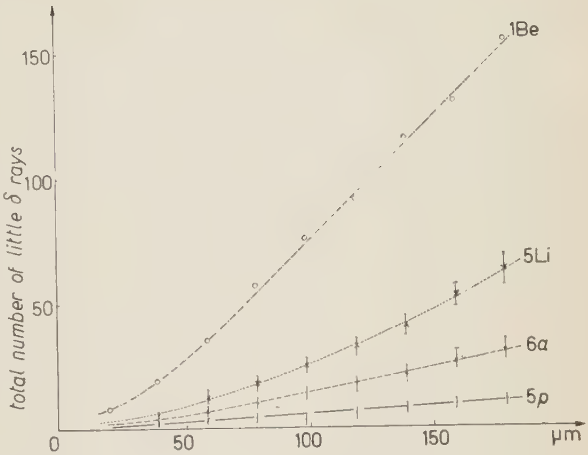

Fig. 1. – The 4 experimental curves give the mean integral number of little δ-rays with the residual range for 1 beryllium nucleus, 5 lithium nuclei, 6 α-particles and 5 protons.

In Fig. 4 are represented the mean integral number of little δ-rays against the residual range for the same 24 α-particles and 10 lithium nuclei. We now observe that the experimental points become arranged on a curve in complete accordance with the curve given in Fig. 1.

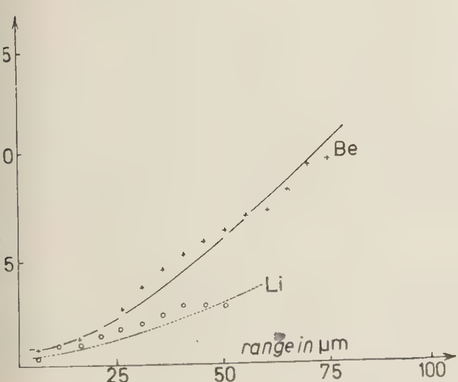

. 2. The experimental points correspond the integral number of little δ-rays against residual range for only one beryllium nucleus and a lithium one.

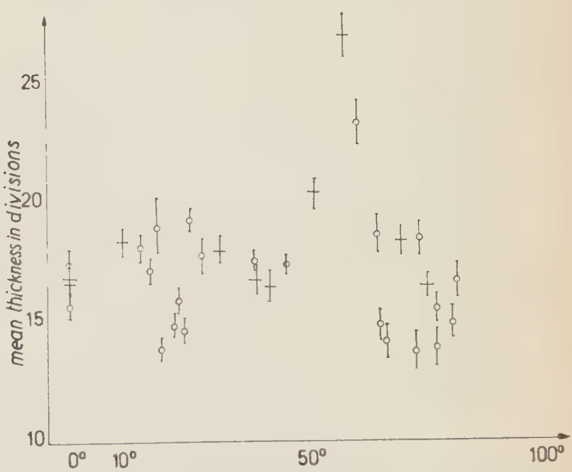

Fig. 3. - Mean thickness in micrometer divisions against the angle of dip for 24 α-particles and 10 lithium nuclei. Circles represent the α-particles and crosses the lithium nuclei.

Moreover we point out that in Fig. 1 the experimental points correspond to tracks of nuclei with dip angles less than 5° and in Fig. 4 to tracks which presented angles of dip as great as those indicated in Fig. 3. Besides, the same accordance with Fig. 1 was found for the lithium and beryllium tracks of Fig. 2 which had angles of dip between 30° and 35°. All these angles were referred to the original emulsion of 600 μm thickness.

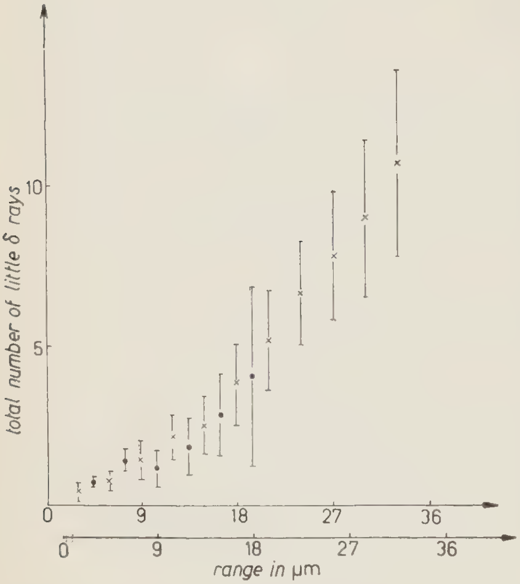

Fig. 4. – Mean integral number of little δ-rays against the residual range for the same α-particles and lithium nuclei represented in Fig. 3. The lower range scale and the points correspond to the α-particles.

These results also seem to indicate a strong independence of the density of the little δ rays from the photographic development.

Finally, Table I is a general summary of the measurements performed on 15 heavy relativistic nuclei of cosmic rays. In the first columns we give the mean density of δ-rays of three or more grains, the range over which this density was determined, the mean thickness of the track in conventional divisions and the mean density of little δ-rays. In the last three columns we find the determined atomic number of these nuclei. In one of the columns is indicated the interval of the atomic number calculated by using the Bradt and Peters curves for relativistic nuclei and calibrated for high energy α-particles of our plates [3]. In these calculations we considered each track as an isolated event. The results of the other two columns were referred to the atomic number of track number 1 which was especially calibrated by making a charge balance in its fragmentation products.

The errors of the measurements are the calculated standard errors. If we take the expression $k/\sqrt{N}$ as the statistical error, we determine for k the value 0.84 ± 0.06 in the case of the standard δ-rays and 0.85 ± 0.06 for little δ-rays. Both values are in complete accordance with the statistical error of the ionization of high energy particles in nuclear emulsions.

[3] H. Bradt and B. Peters: *Phys. Rev.*, **74**, 1828 (1948).

29

TABLE 1.

Track	Number of δ-rays of 3 or more grains per 100 μm	Range in μm on which δ-rays of 3 or more grains were measured	Mean thickness of tracks in divisions of the micrometer	Number of little δ-rays per 5 μm measured in tracks of 100 μm in length	Z determined from Bradt and Peters' curves calibrated for α-particles of our plates	Z is given as fraction number to compare both methods	
						Z determined from the density of δ-rays of three or more grains	Z determined from the density of little δ-rays
1	8.8 ± 0.8	1 945	3.5 ± 0.2	2.5 ± 0.3	$13 \div 16$	15	15
2	3.4 ± 0.2	3 922	2.9 ± 0.1	1.3 ± 0.2	$8 \div 10$	9.3 ± 0.5	10.8 ± 2.2
3	4.0 ± 0.4	3 607	2.9 ± 0.1	0.9 ± 0.1	$9 \div 11$	10.0 ± 0.7	9.0 ± 0.7
4	3.0 ± 0.3	4 000	2.9 ± 0.1	1.0 ± 0.3	$7 \div 10$	8.8 ± 0.6	9.5 ± 1.5
5	6.4 ± 0.5	1 563	2.8 ± 0.1	1.8 ± 0.4	$11 \div 13$	12.8 ± 0.8	12.8 ± 1.6
6	5.2 ± 0.3	2 678	3.8 ± 0.3	1.9 ± 0.3	$10 \div 13$	11.5 ± 0.6	13.1 ± 1.3
7	8.1 ± 0.4	1 722	3.4 ± 0.1	2.5 ± 0.3	$12 \div 16$	14.4 ± 0.7	15.0 ± 1.4
8	9.2 ± 0.4	3 493	4.1 ± 0.1	3.1 ± 0.4	$13 \div 16$	15.4 ± 0.7	16.7 ± 1.5
9	11.5 ± 0.5	775	4.1 ± 0.2	3.8 ± 0.5	$15 \div 18$	17.2 ± 1.1	18.5 ± 1.7
10	12.3 ± 0.3	4 491	4.4 ± 0.1	3.5 ± 0.3	$11 \div 18$	17.7 ± 0.9	17.7 ± 1.4
11	17.5 ± 0.7	1 464	4.4 ± 0.1	3.6 ± 0.5	$18 \div 22$	21.1 ± 1.0	18.0 ± 1.7
12	15.5 ± 0.8	2 242	4.4 ± 0.2	5.2 ± 0.3	$17 \div 20$	19.9 ± 1.0	21.6 ± 1.4
13	10.5 ± 0.4	3 992	4.4 ± 0.1	4.0 ± 0.5	$14 \div 17$	16.5 ± 0.8	19.2 ± 1.6
14	20.8 ± 0.9	2 279	4.6 ± 0.1	4.3 ± 0.3	$20 \div 26$	22.5 ± 1.2	19.7 ± 1.4
15	14.5 ± 1.1	912	4.5 ± 0.1	5.3 ± 0.4	$16 \div 20$	19.3 ± 1.1	21.9 ± 1.5

* * *

We thank very much Prof. Ing. CARLOS MORI GANNA for his valuable help and interest in our works as Dean of the Mathematics and Physics Faculty of the University of Chile.

One of the authors, G. ALVIAL, expresses his acknowledgement to the John Simon Guggenheim Memorial Foundation and Prof. SERGE A. KORFF of the New York University for the valuable opportunities given to continue this work in the United States. At the same time he thanks very much Prof. MARCEL SCHEIN of the University of Chicago for the discussion of this paper and the valuable suggestions and facilities given to continue this work in the Department of Physics of the University of Chicago.

RIASSUNTO

Gli autori del presente lavoro danno un metodo per determinare la carica dei nuclei sia di bassa come di alta energia. Essi considerano soltanto le larghezze delle tracce sopra un certo limite ottenuto applicando il metodo di OCCHIALINI e collaboratori per la determinazione delle larghezze delle tracce. Stabilendo un criterio per ponderare tali grandezze, dovute probabilmente *a piccoli raggi* δ, viene determinata la carica dei nuclei.

Electrons from μ-Capture and the Radius of Fermi Interactions.

B. Jouvet and J.-C. Houard

Laboratoire de Physique Atomique et Moléculaire, Collège de France - Paris

(ricevuto il 7 Agosto 1959)

Summary. — This paper proposes to determine the range of Fermi interactions by measuring vacuum polarisation effects resulting from Fermi couplings. A typical process is studied: the electron emission in muon capture, which would occur if neutrinos emitted in electron and μ-capture were identical. Lower bounds of radii parameters of Fermi interactions are obtained from the actual measured ratio $(\mu \to e)/(\mu \to \nu)$. The implication of this ratio in the single intermediate boson Fermi interaction theories is also discussed, and could be tested by the experiments of nuclei excitation by neutrinos.

1. – Introduction.

Our knowledge of the mixture of Fermi couplings is by now in a fairly good shape. Therefore it becomes of interest to try and determine the range of Fermi interactions. Suggestions have been made as to possible determinations of mass parameters characterizing non-local effects (1). They rely on the influence of such effects on the shape of decay spectra. The main difficulty is that the involved wave lengths are small compared to the «expected» range. (The largest energies coming into play are of the order of 100 MeV which is the maximum energy of the μ-meson electron energy spectrum.) Furthermore mesic and electromagnetic radiative corrections may produce non-negligible alterations of low energy spectrum shapes, which cannot be very accura-

(1) T. D. Lee and C. N. Yang: *Phys. Rev.*, **108**, 1611 (1957); S. Bludman and A. Klein: *Phys. Rev.*, **109**, 550 (1958); A. Sirlin: *Phys. Rev.*, **111**, 337 (1958).

tely computed [2], and therefore only a lower bound of the mass parameter can be obtained.

On the other hand it is worth-while putting an upper bound on this parameter: this can be done indeed by studying electron emission in μ-meson capture [3]: under the assumption that the neutrinos emitted in both muon and electron capture are identical, the electron emission in muon capture can occur through the virtual exchange of a neutrino-nucleon pair. In this process, like in all high energy processes, the range of interactions enters in a essential way. Although the involved matrix element is of second order with respect to the Fermi coupling constant, it is not negligible because of its strong dependence on the interaction radius, even after renormalization.

In Section 2, we define the parameters by means of which we represent the structure of the Fermi interaction occurring in electron and muon capture.

In Section 3, we study the implication of the intermediate boson theory and discuss the possibility of testing this theory by nuclear scattering of neutrinos.

In Section 4, we estimate the values of the range parameters of Fermi interactions as a function of the ratio ($\mu \to \nu/\mu \to e$) in the μ-capture.

2. – Form and structure of Fermi interactions.

On relativistic grounds, one can write the four-particle S-matrix as:

$$\int \mathrm{d}x_1 \mathrm{d}x_2 \mathrm{d}x_3 \mathrm{d}x_4 \sum_{i,j=1}^{16} G_{ij}(x_1, x_2, x_3, x_4) :\bar{\psi}_a(x_1)\theta_i \psi_b(x_2)\, \bar{\psi}_c(x_3)\theta_j \psi_d(x_4): + \text{h.c.}\,, \tag{1}$$

where a, b, c, d, denote the names of the particles or antiparticles; θ_i are the 16-Dirac covariant matrices, and G_{ij} are tensors, functions of the four space-time points where the particles are emitted (absorbed); these functions may contain derivatives.

If we define as « *Fermi interaction* » the corresponding S-matrix occuring in weak interaction, it has the properties that the G_{ij} functions are such that it reduces approximately, for low energy transfers, to the « *form* »

$$\int \mathrm{d}x_1 \ldots \mathrm{d}x_4 \cdot g_F \delta^4(x_1 - x_2)\, \delta^4(x_1 - x_3)\, \delta^4(x_1 - x_4) \cdot \\ \cdot \bar{\psi}_p(x_1)\gamma_\mu(1+\gamma_5)\psi_n(x_2)\bar{\psi}_e(x_3)\gamma_\mu(1+\gamma_5)\psi_\nu(x_4) : + \text{h.c.}\,, \tag{2}$$

([2]) R. E. Behrends, R. J. Finkelstein and A. Sirlin: *Phys. Rev.*, **101**, 866 (1956). S. M. Berman: *Phys. Rev.*, **112**, 267 (1958).

([3]) B. Jouvet and J.-C. Houard: *Compt. Rend.*, **248**, 3275 (1959).

Quote di associazione alla Società Italiana di Fisica e prezzi di abbonamento al *Nuovo Cimento* e al *Supplemento* per il 1960.

Edizioni in carta normale e in carta leggera. Contributi alle spese di stampa.

UOTE SOCIALI PER L'ANNO 1960.

Per l'Italia:		Per l'Estero:	
Soci individuali	L. 9 000	Soci individuali e collettivi	$ 18 (L. 11 250)
» collettivi	» 25 000	Soci sostenitori	$ 96 (» 60 000)
» sostenitori	» 60 000		

Ai Soci vengono inviati gratuitamente *Il Nuovo Cimento*, il *Supplemento* e il *Bollettino* ella Società Italiana di Fisica.

BBONAMENTO AL *Nuovo Cimento* E AL *Supplemento* PER L'ANNO 1960, PER ENTI E PERSONE *non* SOCI DELLA SOCIETÀ ITALIANA DI FISICA.

Per l'Italia:		Per l'Estero:	
abbonam. ordinario	L. 15 000	abbonam. ordinario	$ 28 (L. 17 500)
» sostenitore	» 60 000	» sostenitore	$ 96 (» 60 000)

Agli Abbonati viene inviato gratuitamente il *Bollettino* della Società Italiana di 'isica.

EDIZIONE IN CARTA NORMALE E IN CARTA LEGGERA.

Il *Nuovo Cimento* e il *Supplemento* si pubblicano in due edizioni: una in carta nor-nale e una, in ristretto numero di copie, in carta leggera (India bianca). Il prezzo è il nedesimo per le due edizioni se spedite per posta normale. Salvo richiesta contraria, si pedisce l'edizione in carta normale.

Coloro che desiderino ricevere l'edizione in carta leggera per posta aerea dovranno ssumersi le maggiori spese del trasporto aereo. L'ammontare di dette spese può ri-avarsi considerando che l'edizione per il 1960 in carta leggera peserà in totale (*Nuovo Cimento* e *Supplemento*) circa (4 ÷ 4.5) kg.

CONTRIBUTI ALLE SPESE DI STAMPA.

Si precisa esplicitamente che i contributi alle spese di stampa dei quali si parla nella erza pagina della copertina al quarto capoverso, sono del tutto volontari e che il ritmo ol quale i lavori sono avviati in esame al Comitato di Redazione e poi alla tipografia alla pubblicazione è del tutto indipendente dall'essere o no accolto l'invito a versare detto Contributo.

Circa poi alcune difficoltà di trasferimento di valuta dall'estero in Italia, l'Editore Nicola Zanichelli, al quale va versato il contributo, sarà ben lieto di venire incontro in utti i modi possibili per rimuovere dette difficoltà, in particolare rimandando il versa-mento alla fine d'anno all'atto del rinnovo dell'abbonamento o del versamento della quota di Socio.

Italian Physical Society membership fees and subscription prices to the *Nuovo Cimento* and the *Supplemento* for 1960.

Normal paper and white India paper edition. Publication contributions.

MEMBERSHIP FEES FOR THE YEAR 1960.

For Italy:		For Foreign Countries:	
Individual Members	Lit. 9 000	Individual and Collective Members	\$ 18 (Lit. 11 250)
Collective »	» 25 000		
Sponsoring »	» 60 000	Sponsoring Members	\$ 96 (Lit. 60 000)

To Members *Il Nuovo Cimento*, the *Supplemento* and the *Bollettino* of the Italian Physical Society are sent free of charge.

SUBSCRIPTION FEES TO THE *Nuovo Cimento* AND TO THE *Supplemento* FOR THE YEAR 1960 FOR PERSONS AND INSTITUTIONS *not being* MEMBERS OF THE ITALIAN PHYSICAL SOCIETY.

For Italy:		For Foreign Countries:	
ordinary subscription	Lit. 15 000	ordinary subscription	\$ 28 (Lit. 17 500)
sponsoring »	» 60 000	sponsoring »	\$ 96 (Lit. 70 000)

To subscribers the *Bollettino* of the Italian Physical Society is sent free of charge.

NORMAL PAPER EDITION AND WHITE INDIA PAPER EDITION.

The *Nuovo Cimento* and the *Supplemento* are published in two editions: one on normal paper and the other, in only a limited number of copies, on light paper (white India). The price is the same for both editions when they are shipped by surface mail. Unless instructions to the contrary are given, it is the normal paper edition which will be shipped.

Subscribers who wish to receive the light paper edition by air mail will be charged with the necessary additional postal fees. The amount of these expenses may be gathered from the fact that the white India paper edition (*Nuovo Cimento* and *Supplemento*) will assume for 1960 the total weight of $(4 \div 4{,}5)$ kg.

PUBLICATION CONTRIBUTIONS.

We want to expressly underline that the publication contributions we mention on the 3rd cover page, 4th paragraph, are absolutely not compulsory and that the rythm, at which papers are forwarded to the Publication Board for examination, then to the printer's and to publication is fully independent of the assent to pay these contributions.

As to some difficulties concerning money tranfers from some Foreign Countries to Italy, the Publisher Nicola Zanichelli, to whom the contribution is to be paid, will kindly help in any possible way to remove said difficulties, particularly delaying the payment till the end of the year, to the time of the renewal of the subscription or of the remittance of the association fee.

This approximate form is known from experimental β-decay and capture, in the case when the particles p, n, e, ν, are respectively proton, neutron, electron and neutrino. Very little is known on the actual form of the Fermi interaction occuring in the μ-capture. We postulate, that the form is the same, the μ-meson field occuring instead of that of the electron. The essential point for the considerations developped in the present paper is that the neutrino emitted in μ-capture is the same as that emitted in electron capture (1); this is achieved with that postulated form, we use in explicite calculation, but could have been also done with different types of couplings.

It is convenient for future reference to give the two forms, equivalent to the form (2), obtained by a Fierz transformation:

$$(3)\qquad \int \mathrm{d}x_1 \ldots \int \mathrm{d}x_4 \cdot g_F \delta^4(x_1 - x_2)\delta^4(x_1 - x_3)\delta^4(x_1 - x_4) : \\ : \bar{\psi}_p(x_1)\gamma_\mu(1+\gamma_5)\psi_\nu(x_4)\,\bar{\psi}_e(x_3)\gamma_\mu(1+\gamma_5)\psi_n(x_2) : + \text{h.c.}\,,$$

$$(4)\qquad \int \mathrm{d}x_1 \ldots \int \mathrm{d}x_4 \cdot 2g_F \delta^4(x_1 - x_2)\delta^4(x_1 - x_3)\delta^4(x_1 - x_4) : \\ : \bar{\psi}^c_p(x_1)(1+\gamma_5)\psi_e(x_3)\bar{\psi}_\nu(x_4)(1-\gamma_5)\psi^c_n(x_2) : + \text{h.c.}\,.$$

We are now interested in the space-time *structure* of Fermi interactions. It is entirely defined if we know the x_i dependence of the various G_i functions.

We make in this paper the simplifying assumption that a single scalar function $G(x_i)$, instead of the expression $g\,\delta^4(x_1 - x_2)\,\delta^4(x_1 - x_3)\,\delta^4(x_1 - x_4)$ is enough to take into account the finite volume in which the interaction takes place. This means that the various effects, we discuss later, which produce the non-locality of the interaction, have the same range for the various interaction terms. Let $F(p_1, q_1, p_2, q_2)$ be the Fourier transform, of $G(x_i)$, p_1, q_1, p_2, q_2 being the momenta of the particles p, e, n and ν. For particles on the mass shell, ($p_1^2 = -M_p^2$, $q_1^2 = -m_e^2$, $p_2^2 = -M_n^2$, $q_2^2 = -m_\nu^2 = 0$) and through momentum conservation, F can be expressed as a function $F(u^2, v^2, w^2)$ of the three, total and transverse momenta, $u = p_1 + q_1$, $v = q_2 - q_1 = p_1 - p_2$, $w = p_1 - q_2 = p_2 - q_1$, which are not independent: $u^2 + v^2 + w^2 = p_1^2 + q_1^2 + p_2^2 + q_2^2 = -(M_n^2 + M_p^2 + m_e^2 + m_\nu^2)$. As we are concerned with the *a priori* unknown dependence of the function F on momenta, we cannot assume this function to be a constant in the usually observed processes (*e.g.*, β-decay spectra), and we have to state what we call the « *observable Fermi constant* » g_F. We define the Fermi constants as the values of constants which are factors of various tensor forms in the S-matrix, when the four particles are on the mass shell,

(1) An opposite hypothesis was put forward by E. J. KONOPINSKI and H. M. MAHMOUD: *Phys. Rev.*, **92**, 1045 (1953); K. NISHIJIMA: *Phys. Rev.*, **108**, 907 (1957); Y. TANIKAWA and S. WATANABE: *Phys. Rev.*, **113**, 1344 (1959).

and the neutrino has a null momentum the spinors being written in the order (pn)·(eν). Then $u^2 = -M_n^2 \approx v^2 = -M_p^2 = M^2$, $w^2 = -m_e^2 \approx 0$ and with the above assumption,

$$g_F \simeq F(-M^2, -M^2, 0)\,. \tag{5}$$

What is now the theoretical information we have about the nature and contributions to the space time structure of Fermi interactions? For this discussion we have to admit that the Fermi interaction (S-matrix element) results from some elementary Hamiltonian containing couplings between various fields.

Two kinds of elementary processes produce non-local effects:

— The first ones, come from the vertex corrections produced by the various known boson fields (photon and π-meson); these processes can in principle be evaluated and they depend weakly on the assumed extension of the elementary Fermi coupling and of the structure of particles.

They affect the form of low energy spectra (²) and the values of Fermi constants, but have no important effects on the radius in which the effective interaction takes place.

On the contrary, a coupling of the form $(\varphi_0\partial_\mu\varphi - \varphi\partial_\mu\varphi_0)(\bar{e}\gamma_\mu(1+\gamma_5)\nu)$ as postulated by GELL-MANN (⁵) may extend the interaction volume to a distance of the order of $0.8\cdot 10^{-13}$ cm, as for the proton electric radius.

— The second kind of non-locality pertains to the intrinsic structure of Fermi coupling:

A) The renormalization difficulties in perturbative expansion of Fermi coupling theory make the Yukawa hypothesis of one intermediate boson useful. Three kinds of bosons can be postulated to carry the exchange momenta u, v, w. The corresponding theories are either entirely or only partly renormalizable in perturbative expansion.

Au) Let Λ_u be the mass of the neutral spin 0 boson (⁶), of baryon number 1, which is coupled with the pairs (p, e), (p, μ) and (n, ν) by the coupling constants G^u_{pe} $G^u_{p\mu}$ and $G^u_{n\nu}$. The resulting Fermi non-local couplings are (in obvious notation)

$$(\bar{p}(1+\gamma_5)e^c)\,G^u_{pe}G^u_{n\nu}\frac{1}{u^2+\Lambda_u^2}\,(\bar{\nu}^c(1-\gamma_5)n)\,, \tag{6}$$

$$(\bar{p}(1+\gamma_5)\mu^c)\,G^u_{p\mu}G^u_{n\nu}\frac{1}{u^2+\Lambda_u^2}\,(\bar{\nu}^c(1-\gamma_5)n)\,.$$

(⁵) M. GELL-MANN: *Phys. Rev.*, **111**, 362 (1958); S. S. GERSTEIN and J. B. ZELDOVIČ: *Žurn. Ėksp. Teor. Fiz.*, **29**, 698 (1955).

(⁶) See *e.g.*, S. ONEDA and Y. TANIKAWA: *Phys. Rev.*, **113**, 1354 (1959).

Nucleon stability and the fact that such a boson has not been observed require that Λ_u should be much larger than one nucleon mass, so that, at low energy, where this interaction is observed, $u^2 \approx -M^2_{p} \ll \Lambda^2_u$, and the effective Fermi coupling constant is

$$(7) \qquad |2g_F| \approx |G^u_{pe}G^u_{n\nu}/\Lambda^2_u| \approx |G^u_{p\mu}G^u_{n\nu}/\Lambda^2_u \qquad \text{and} \qquad |G^u_{pe}| \approx |G^u_{p\mu}| .$$

Av) Let Λ_v be the mass of the charged spin one boson, of baryon number 1, which is coupled to the pairs (p, ν), (n, e) and (n, μ) by the constants $G^v_{p\nu}$, G^v_{ne} and $G^v_{n\mu}$. The resulting non-local Fermi couplings are

$$(8) \qquad (\bar{p}\gamma_\mu(1+\gamma_5)\nu)\, G^v_{p\nu}G^v_{n{e \atop \mu}}\left(\delta_{\mu\nu} + \frac{v_\mu v_\nu}{\Lambda^2_v}\right)\left(\left(\frac{\bar{e}}{\bar{\mu}}\right)\gamma_\nu(1+\gamma_5)n\right)\frac{1}{v^2+\Lambda^2_v} \cdot$$

As previously, we know that $\Lambda^2_v \gg M^2_p$, and for low energy, where we defined the Fermi constant, the terms in v_μ are negligible, so that

$$(9) \qquad |g_F| \approx |G^v_{p\nu}G^v_{ne}/\Lambda^2_v| \approx |G^v_{p\nu}G^v_{n\mu}/\Lambda^2_v| \qquad \text{and} \qquad |G^v_{re}| \approx |G^v_{n\mu}| .$$

Aw) Let Λ_w be the mass of the charged spin one boson, of null baryon number, which is coupled to the pairs (np), (eν) and μν), by the constants G^w_{np}, $G^w_{e\nu}$ and $G^w_{\mu\nu}$. Assuming also a high value for the boson mass, one gets like in (*Av*) the non-local Fermi couplings

$$(10) \qquad (\bar{p}\gamma_\mu(1+\gamma_5)n)\left(\delta_{\mu\nu} + \frac{w_\mu w_\nu}{\Lambda^2_w}\right)G^w_{pn}G^w_{({e \atop \mu})\nu}\frac{1}{w^2+\Lambda^2_w}\left(\left(\frac{\bar{e}}{\bar{\mu}}\right)\gamma_\nu(1+\gamma_5)\nu\right),$$

the Fermi constant being

$$(11) \qquad |g_F| \approx |G^w_{pn}G^w_{\mu\nu}/\Lambda^2_w| \approx |G^w_{pn}G^w_{e\nu}/\Lambda^2_w|, \quad \text{and } |G^w_{e\nu}| \approx |G^w_{\mu\nu}| .$$

B) The hypothesis of local Fermi coupling, which has the advantage of decreasing the number of concepts, produces also non-local Fermi interactions and gives raise to intermediate bosons of various masses; however an estimate of constants caracterizing these bosons is related to the unknown and controversial form of the high energy boson propagators (7).

---

(7) B. Jouvet: *Nuovo Cimento*, **5**, 1 (1957).

In any case, whatever the origin of the radii of Fermi interaction may be, one can always represent this structure by some phenomenological parameters related to some assumed form of the function $F(u^2, v^2, w^2)$ defined above. On classical and non-relativistic grounds, one would like to speak about the distances at which the three couples of pairs of particles intervening in a Fermi interaction begin to interact. We define therefore for the nucleon β-decay interaction, three radii

R_u is the classical radius at which the pair (p, e) interacts with the pair (n, ν);

R_v is the classical radius at which the pair (ν, p) interacts with the pair (e, n);

R_w is the classical radius at which the pair (p, n) interacts with the pair (ν, e).

For pratical computation ease we suppose that the form factor which produces an interaction radius R_i is proportional to $1/p_i^2 + \Lambda_i^2$ with $\Lambda_i = 1/R_i$.

With the definition of the Fermi constant given earlier; we consider the effects of the three following types of structure form factors in Fermi interactions,

$$(12) \qquad F_u = g_F \frac{\Lambda_u^2 - M^2}{u^2 + \Lambda_u^2}, \qquad F_v = g_F \frac{\Lambda_v^2 - M^2}{v^2 + \Lambda_v^2}, \qquad F_w = g_F \frac{\Lambda_w^2}{w^2 + \Lambda_w^2}.$$

An essential difference between hypotheses (A) and (B), which produce similar form factors, is for instance that (Au) leads to a well defined interaction $(\bar{p}(1+\gamma_5)e^c)(\bar{e}^c(1-\gamma_5)p)(G^u_{\mathrm{pe}})^2/(u^2+\Lambda_u^2)$, produced by the exchange of the postulated boson Λ_u, whereas by the form factor F_u, we do not mean that Λ_u is the mass of some hypothetical boson, but only a parameter convenient to introduce a radius $R_u = 1/\Lambda_u$, which might be due, for instance, to some many-boson contributions. Therefore we cannot on this basis make the same prediction on the (p-e) interaction.

Concerning the Fermi interaction occuring in muon capture, we introduce similar form factors to represent its structure. Furthermore, we suppose that the radii of this interaction are the same as those involved in β-decay. This assumption is partly supported by the fact that the branching ratio $(\pi \to \mu + \nu / \pi \to e + \nu)$ is consistent with the existence of the same coupling constant for the p.v. couplings of the pion with (μν) and (eν) pairs. Indeed, if these reactions really occur through the processes $(\pi^+ \to (\bar{n}+p) \to \{{}^{\mu+\nu}_{e+\nu}\})$, in which the Fermi interactions enter as final steps, then, the meson coupling constants are proportional to the expressions of the nucleon closed loops, the

values of which depend strongly on the radii $R_v^{e,\mu}$ and (or) $R_u^{e,\mu}$ of the electron and muon Fermi interactions. Therefore these two radii should be equal. This branching ratio does not give any information about the radii R_w^μ and R_w^e; we simply assume that these are equal.

It is known that there is no Fermi interaction of normal strength between the pair (μe) and the nucleon pairs [8]. STEINBERGER and WOLFE have measured the ratio ($\mu \to e$ to $\mu \to \nu$) in the capture of μ-mesons by Cu; they found an upper limit of $5\cdot10^{-4}$.

Let us suppose that there exist $V-A$ types of weak Fermi interactions between the pairs (μe) and the nucleon pairs (nn) and (pp), and let $g_{\text{nn}\mu\text{e}}$ and $g_{\text{pp}\mu\text{e}}$ be the two interaction constants involved. We will show, in Section 4, that these interactions are indeed, to a good approximation of the form $(V-A)$. For the copper nucleus $Z \approx N$; using Wheeler's formula for capture, and the corrective term of Primakoff, which takes into account the Pauli principle, we deduce the ratio

$$\lambda^2 = \frac{g^2_{\text{nn}\mu\text{e}} + g^2_{\text{pp}\mu\text{e}}}{g_F^2} < 5\cdot10^{-4}\,. \tag{13}$$

We will now study the significance o fthis ratio, in the various hypotheses (A) and (B) of Section 2 concerning the structure of Fermi interactions.

3. – The hypotheses Au) and Av).

Au) The hypotheses of existence of the boson A_u leads to the non-local Fermi interactions

$$(\bar{\text{p}}(1+\gamma_5)e^c)(\bar{\mu}^c(1-\gamma_5)p)\, G^u_{\text{pe}} G^u_{\text{pe}}/(u^2+\Lambda_u^2)\,. \tag{14}$$

For energies involved in the capture ($u^2 \approx -M_\text{p}^2$), this interaction is equivalent to a Fermi coupling

$$(\tfrac{1}{2}G^u_{\text{pe}} G^u_{\text{pe}}/\Lambda_u^2 - M_\text{p}^2)(p\gamma_\mu(1+\gamma_5)p)\,(e\gamma_\mu(1+\gamma_5)\mu)\,. \tag{15}$$

One has therefore

$$|g_{\text{ppe}\mu}| \approx \tfrac{1}{2}(G^u_{\text{pe}})^2/\Lambda_u^2\,. \tag{16}$$

---

[8] A. LAGARRIGUE and CH. PEYROU: *Compt. Rend.*, **234**, 1873 (1952); J. STEINBERGER and H. B. WOLFE: *Phys. Rev.*, **100**, 1490 (1955).

This hypothesis does not produce a coupling constant $g_{\mathrm{nne}\mu}$ of comparable order of magnitude.

One deduces from (7), (13) and (16) that $|G^u_{\mathrm{pe}}/G^u_{\mathrm{n\nu}}|^2 = \lambda^2$. However the boson Λ_u can also produce the interaction

$$(17)\qquad (\bar{n}(1+\gamma_5)\nu)(\bar{\nu}(1-\gamma_5)n)(G^u_{\mathrm{n\nu}})^2/(u^2+\Lambda_u^2)\,,$$

which at low energy is equivalent to a Fermi interaction

$$(18)\qquad g_{\mathrm{nn\nu\nu}}(\bar{n}\gamma_\mu(1+\gamma_5)n)(\bar{\nu}\gamma_\mu(1+\gamma_5)\nu)$$

of strength

$$(19)\qquad |g_{\mathrm{nn\nu\nu}}| \simeq \frac{1}{2}(G^u_{\mathrm{n\nu}})^2/\Lambda_u^2 = \frac{1}{\lambda}\left|\left(\frac{1}{2}G^u_{\mathrm{n\nu}}G^u_{\mathrm{pe}}\right)\Big/\Lambda_u^2\right| = \frac{1}{\lambda}|g_F|\,.$$

By such an interaction a beam of neutrinos would produce nuclear excitation with a cross-section $(1/\lambda)^2 > 2\cdot 10^3$ times greater than the already observed neutrino capture cross-section.

A c) The hypothesis of the boson Λ_v leads to the non-local Fermi interaction

$$(20)\qquad (\bar{n}\gamma_\mu(1+\gamma_5)e)(\bar{\mu}\gamma_\nu(1+\gamma_5)n)\left(\delta_{\mu\nu}+\frac{v_\mu v_\nu}{\Lambda_v^2}\right)\frac{1}{v^2+\Lambda_v^2}(G^v_{\mathrm{ne}})^2\,.$$

The effective constant $g_{\mathrm{nne}\mu}$ turns out to be equal to $((G^v_{\mathrm{en}})^2/\Lambda_v^2)$ whereas there is no constant $g_{\mathrm{ppe}\mu}$ of comparable strength; like previously one deduces the ratio $|G^v_{\mathrm{en}}/G^v_{\mathrm{p\nu}}|^2 = \lambda^2$.

This hypothetical Λ_v boson like the previous one, produces an interaction between neutrinos and protons which has the form

$$(21)\qquad g_{\mathrm{pp\nu\nu}}(\bar{p}\gamma_\mu(1+\gamma_5)p)(\bar{\nu}\gamma_\mu(1+\gamma_5)\nu) \qquad \text{with} \qquad |g_{\mathrm{pp\nu\nu}}| \simeq \frac{1}{\lambda}|g_F|\,.$$

giving also scattering cross-sections much larger than that for neutrino capture.

No experiment is known to us which at present permits to rule out the two preceding hypotheses. They produce however a theoretically strange asymmetry of couplings between the neutrino on one side, and the electron and μ-meson on the other side. This strange consequence is avoided either if the neutrinos emitted in electron and muon capture are different [4], or if the one intermediate boson hypotheses of the preceding types are rejected (see Section 2-B).

4. – The hypotheses Aw) and B).

Contrary to the preceding cases, the hypotheses of a boson A_w or of the existence of radii in the Fermi interactions, produce effective μ-e-nucleons Fermi type interactions, only by virtual processes of second order in the elementary Fermi couplings. Corresponding to the three radii $R_i = 1/\Lambda_i$, the various kinds of interactions are represented by the graphs:

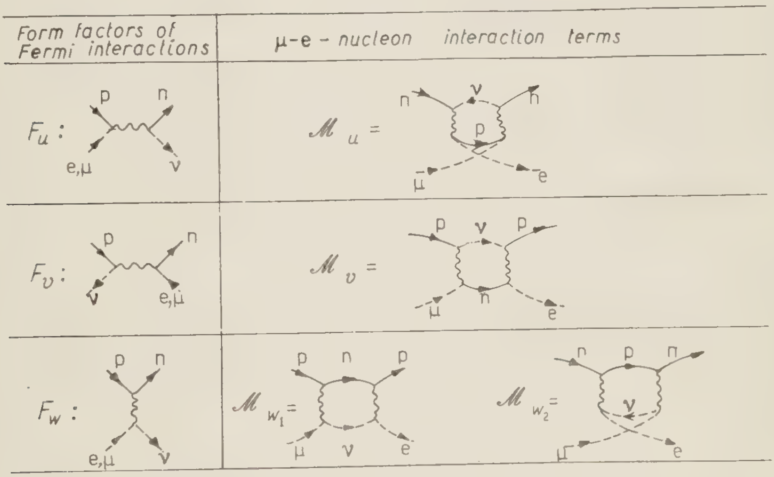

Fig. 1.

It is practical to use respectively the forms (3), (4), (4) and (3) of the interactions to evaluate the matrix elements $\mathscr{M}_u$, $\mathscr{M}_v$, $\mathscr{M}_{w_1}$ and $\mathscr{M}_{w_2}$, the calculation then involving the usual spur expressions for closed loops.

They take the form

$$
(22)\quad
\begin{cases}
\mathscr{M}_u = -\dfrac{1}{2} A(\Lambda_u^2 - M^2)^2 (2\delta^{\mu\varrho}\delta^{\nu\sigma} - \delta^{\varrho\sigma}\delta^{\mu\nu}) I_u^{\varrho\sigma} \cdot (\overline{n}\gamma^\mu(1+\gamma_5)\mu)(\overline{e}\gamma^\nu(1+\gamma_5)n)\,, \\[2ex]
\mathscr{M}_v = A(\Lambda_v^2 - M^2)^2 I_v \cdot (\overline{p}\gamma^\mu(1+\gamma_5)p)(\overline{e}\gamma^\mu(1+\gamma_5)\mu)\,, \\[2ex]
\mathscr{M}_{w_1} = A(\Lambda_w^4) I_{w_1} \cdot (\overline{p}\gamma_\mu(1+\gamma_5)p)(\overline{e}\gamma^\mu(1+\gamma_5)\mu)\,, \\[2ex]
\mathscr{M}_{w_2} = -\dfrac{1}{2} A(\Lambda_w^4)(2\delta^{\mu\varrho}\delta^{\nu\sigma} - \delta^{\varrho\sigma}\delta^{\mu\nu}) I_{w_2}^{\varrho\sigma} \cdot (\overline{n}\gamma^\mu(1+\gamma_5)\mu)(\overline{e}\gamma^\nu(1+\gamma_5)n)\,, \\[2ex]
A = -\dfrac{g_F^2}{4\pi^6} \dfrac{M\sqrt{m\mu}}{\sqrt{E_{p_1}E_{p_2}\varepsilon_{q_1}\varepsilon_{q_2}}}\, \delta^4(p_1 + q_1 - p_2 - q_2)\,.
\end{cases}
$$

where p_1, q_1, p_2, q_2 are respectively the momenta of the incoming nucleon and lepton and outgoing nucleon and lepton.

Explicit expressions for the integrals occuring in $I^{\varrho\sigma}$ and I where calculated under the approximation that the four-momenta q_i of leptons are null. This means that we consider that the lepton masses and energies are negligible with respect to the other masses involved (nucleon masses and cut-off masses). All the integrals can then be derived from the single function

$$J^{\varrho\sigma}(a^2, b^2, \Lambda^2, s) = \int \mathrm{d}^4k \frac{k^\varrho (k+s)^\sigma}{(k^2+a^2)((k+s)^2+b^2)(k^2+\Lambda^2)^2}, \tag{23}$$

where s_μ is the momentum of the incoming nucleon ($s^2 = -M^2$)

$$\left\{\begin{aligned}
I_u^{\varrho\sigma} &= J^{\varrho\sigma}(M^2, 0, \Lambda_u^2, s) = \frac{i\pi^2}{2}(\delta^{\varrho\sigma}J'' + 2s^\varrho s^\sigma K''),\\
I_v &= J^\varrho_{\ \varrho}(M^2, 0, \Lambda_v^2, s) = i\pi^2(2J'' + s^2K''),\\
I_{w_1} &= J^\varrho_{\ \varrho}(0, M^2, \Lambda_w^2, s) = i\pi^2(2J' + s^2K'),\\
I_{w_2}^{\varrho\sigma} &= J^{\varrho\sigma}(0, M^2, \Lambda_w^2, s) = \frac{i\pi^2}{2}(\delta^{\varrho\sigma}J' + 2s^\varrho s^\sigma K'),\\
J' &= \frac{1}{3M^2} - \frac{\Lambda^2 - 3M^2}{6M^4}\log\frac{\Lambda^2}{M^2} + \frac{(\Lambda^2-M^2)(\Lambda^2-4M^2)}{6M^4\sqrt{\Lambda^2|\Lambda^2-4M^2|}}\varphi(\Lambda^2, M^2),\\
K' &= -\frac{1}{M^2}\left\{-\frac{1}{2\Lambda^2} + \frac{2}{3M^2} - \frac{4\Lambda^2 - 9M^2}{12M^4}\log\frac{\Lambda^2}{M^2} + \right.\\
&\qquad\qquad \left. + \frac{10M^4 + 4\Lambda^4 - 17M^2\Lambda^2}{12M^4\sqrt{\Lambda^2|\Lambda^2-4M^2|}}\varphi(\Lambda^2, M^2)\right\},\\
\varphi(\Lambda^2, M^2) &= \begin{cases} \log\left|\dfrac{(2M^2-\Lambda^2-\sqrt{\Lambda^2(\Lambda^2-4M^2)})(\Lambda^2-\sqrt{\Lambda^2(\Lambda^2-4M^2)})}{(2M^2-\Lambda^2+\sqrt{\Lambda^2(\Lambda^2-4M^2)})(\Lambda^2+\sqrt{\Lambda^2(\Lambda^2-4M^2)})}\right|, & \Lambda^2 \geqslant 4M^2,\\[2ex] 2\,\mathrm{arctg}\left(\dfrac{\sqrt{\Lambda^2(4M^2-\Lambda^2)}}{\Lambda^2}\right), & \Lambda^2 \leqslant 4M^2,\end{cases}\\
J'' &= \frac{-\Lambda^2}{3M^2(M^2-\Lambda^2)} - \frac{M^2}{3(M^2-\Lambda^2)^2}\log\frac{\Lambda^2}{M^2} + \frac{\Lambda^2-M^2}{3M^4}\log\left(1-\frac{M^2}{\Lambda^2}\right),\\
K'' &= \frac{4\Lambda^2-3M^2}{6M^4(M^2-\Lambda^2)} + \frac{1}{6(M^2-\Lambda^2)^2}\log\frac{\Lambda^2}{M^2} - \frac{4\Lambda^2-M^2}{6M^6}\log\left(1-\frac{M^2}{\Lambda^2}\right).
\end{aligned}\right. \tag{24}$$

For free particles and null mass leptons we use the relation

$$s_\mu(\bar{e}\gamma^\mu(1+\gamma_5)n) = M(\bar{e}(1-\gamma_5)n) \tag{25}$$

and perform a Fierz transformation to put the interaction into the final form

$$
(26)\quad
\begin{cases}
\mathscr{M}_u = \dfrac{i\pi^2}{2} A(\Lambda_u^2 - M^2)^2 \big\{ (J'' - M^2 K'')(\overline{n}\gamma^\mu(1+\gamma_5)n)(\overline{e}\gamma_\mu(1+\gamma_5)\mu) + \\
\qquad\qquad + (M^2 K'')(\overline{n}\gamma^\mu(1-\gamma_5)n)(\overline{e}\gamma_\mu(1+\gamma_5)\mu) \big\}, \\
\mathscr{M}_v = i\pi^2 A(\Lambda_v^2 - M^2)^2 (2J'' - M^2 K'')(\overline{p}\gamma^\mu(1+\gamma_5)p)(\overline{e}\gamma_\mu(1+\gamma_5)\mu), \\
\mathscr{M}_{w_1} = i\pi^2 A\Lambda_w^4 (2J' - M^2 K')(\overline{p}\gamma^\mu(1+\gamma_5)p)(\overline{e}\gamma_\mu(1+\gamma_5)\mu), \\
\mathscr{M}_{w_2} = \dfrac{i\pi^2}{2} A\Lambda_w^4 \big\{ (J' - M^2 K')(\overline{n}\gamma^\mu(1+\gamma_5)n)(\overline{e}\gamma_\mu(1+\gamma_5)\mu) + \\
\qquad\qquad + (M^2 K')(\overline{n}\gamma^\mu(1-\gamma_5)n)(\overline{e}\gamma_\mu(1+\gamma_5)\mu) \big\}.
\end{cases}
$$

The V and A form of the resulting interactions, is a consequence of the γ_5-gauge invariance of the lepton fields when their masses are neglected.

Compared with a simple Fermi matrix element

$$
(27)\quad \mathscr{M}_F = -ig_F \frac{M\sqrt{m}}{(2\pi)^2\sqrt{E_{p_1}E_{p_2}E_{q_1}}} \cdot
\cdot\, \delta^4(p_1 + q_1 - p_2 - q_2)(\overline{n}\gamma_\mu(1+\gamma_5)p)(\overline{\nu}\gamma_\mu(1+\gamma_5)e),
$$

we get the effective interaction constants governing the μ-e-nucleons interaction:

$$
(28)\quad
\begin{cases}
g^V_{\mathrm{nn\mu e}}(\Lambda_u) = \dfrac{g_F^2}{2\pi^2}(\Lambda_u^2 - M^2)^2 J''(\Lambda_u), \\
g^A_{\mathrm{nn\mu e}}(\Lambda_u) = -\dfrac{g_F^2}{2\pi^2}(\Lambda_u^2 - M^2)^2 (J''(\Lambda_u) - 2M^2K''(\Lambda_u)), \\
g^V_{\mathrm{pp\mu e}}(\Lambda_v) \simeq -g^A_{\mathrm{pp\mu e}}(\Lambda_v) = \dfrac{g_F^2}{\pi^2}(\Lambda_v^2 - M^2)^2 (2J''(\Lambda_v) - M^2K''(\Lambda_v)), \\
g^V_{\mathrm{pp\mu e}}(\Lambda_w) \simeq -g^A_{\mathrm{pp\mu e}}(\Lambda_w) = \dfrac{g_F^2}{\pi^2}\Lambda_w^4 (2J'(\Lambda_w) - M^2K'(\Lambda_w)), \\
g^V_{\mathrm{nn\mu e}}(\Lambda_w) = \dfrac{g_F^2}{2\pi^2}\Lambda_w^4 J'(\Lambda_w), \\
g^A_{\mathrm{nn\mu e}}(\Lambda_w) = -\dfrac{g_F^2}{2\pi^2}\Lambda_w^4 (J'(\Lambda_w) - 2M^2K'(\Lambda_w)).
\end{cases}
$$

For values of Λ much larger than M, we get the approximate expressions:

$$
(29)\quad J' \simeq J'' \simeq \frac{1}{2\Lambda^2} - \frac{M^2}{3\Lambda^4}\log\frac{\Lambda^2}{M^2}; \qquad K' \approx K'' \approx \frac{1}{6\Lambda^4}\log\frac{\Lambda^2}{M^2}.
$$

Then the interactions take the $V-A$ form:

$$(30)\quad \begin{cases} \mathscr{M}_u = \dfrac{i\pi^2 A}{4}\, \Lambda_u^2 (\bar{n}\gamma^\mu (1+\gamma_5)n)\,(\bar{e}\gamma_\mu(1+\gamma_5)\mu)\,, \\ \mathscr{M}_v = i\pi^2 A\, \Lambda_v^2 (\bar{p}\gamma^\mu\, (1+\gamma_5)p)\,(\bar{e}\gamma_\mu(1+\gamma_5)\mu)\,, \\ \mathscr{M}_{w_1} = i\pi^2 A\, \Lambda_w^2 (\bar{p}\gamma_\mu\, (1+\gamma_5)p)\,(\bar{e}\gamma^\mu(1+\gamma_5)\mu)\,, \\ \mathscr{M}_{w_2} = \dfrac{i\pi^2 A}{4}\, \Lambda_w^2 (\bar{n}\gamma_\mu (1+\gamma_5)n)\,(\bar{e}\gamma^\mu(1+\gamma_5)\mu)\,. \end{cases}$$

These expressions are good approximations to compute the values of the constants Λ for which the ratio λ^2 is smaller or equal to the present limit: $\lambda^2 \leqslant 5\cdot 10^{-4}$; we get:

$$(31)\quad \begin{cases} \Lambda_u \leqslant 295\, M_p & \text{or} \quad R_u \geqslant 0.71\cdot 10^{-16}\ \text{cm}\,, \\ \Lambda_v \leqslant 147\, M_p & \text{or} \quad R_v \geqslant 1.42\cdot 10^{-16}\ \text{cm}\,, \\ \Lambda_w \leqslant 145\, M_p & \text{or} \quad R_w \geqslant 1.44\cdot 10^{-16}\ \text{cm}\,. \end{cases}$$

For a cut-off Λ of the order of 10 M, the formulae (30) can still be used, giving for the ratio λ^2 values of the order 10^{-8}.

We must now discuss the corrections to our estimate which might be important. Apart from those already discussed in the calculation, we see four effects. First, there are radiative corrections on each Fermi vertex of the graphs ($\mathscr{M}_i$): by definition, the form factor F_α includes all these effects in theory (B); this would not be the case in theory (Aw). Second, we used for neutrinos and for nucleons the free propagators; by using spectral representation we could, provided we knew the weight function, obtain directly from $J^{\varrho\sigma}(\Lambda^2)$, the modified g. These corrections could be important if there existed $T=\frac{1}{2}$ isobaric states of the nucleon. A third effect comes from the meson radiative corrections to the effective interaction constants $g_{\text{ppe}\mu}$, $g_{\text{nne}\mu}$ (*e.g.* Fig. 2). One expects that such an effect has no reason to be more dangerous than the similar, and so far ununderstood one, which occurs in the simple β-decay vertex.

Fig. 2.

The last correction comes from higher order terms in g_F; these terms are related to the renormalization contribution to the Fermi constant.

On this subject the following question may be raised:

We found that for cut-off much larger than M, the effective μ-e-n-n interactions depend in a very strong manner on the cut-off parameters Λ. This is a very unusual situation, as compared with the experience we have from the renormalizable interactions, where the cut-off parameters, if they exist

at all, enter in small corrective contributions. In some non-renormalizable radiative corrections, we meet only logarithmic dependences on the cut-off (²). Doubts therefore arise as to what extent the renormalization effects would, like in renormalizable theories, damp out this strong dependence on the cut-off, and modify our conclusions on the actual upper limits of Λ_i.

Fig. 3.

By looking at the terms of the S-matrix of higher orders in g_F, one encounters graphs (Fig. 3) of the same structure as those already, treated which would modify the value of the Fermi constant. However, one sees that these corrections are of the order of the ratio $(g^{\text{ren}}/g_F)^2$ which is, with the actual cut-off, equal to $5\cdot 10^{-4}$: therefore they are negligible. We think that this new aspect of strong cut-off dependence, can be better understood if we consider the following model: suppose that there exists only charged mesons, neutrons and protons coupled together, the couplings and field equations being such that the theory is renormalizable. The p-n scattering without charge exchange would occur, in lowest order, according to the process represented by the graph (Fig. 4).

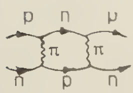

Fig. 4.

This graph is in G^4 and involves the masses of nucleons and mesons. It is commonly accepted, that if G^2 is $\ll 1$, such a graph furnishes a good approximation of the low energy physical process. This graph can equivalently be considered as resulting from a Fermi type interaction between the (pn) pairs, the observable Fermi-type coupling constant being $g = G^2/\mu^2$ and the radius $R = 1/\mu$. The matrix element of this process can then be written in the form $g^2\cdot H(M_p^2, M_n^2, \mu^2, s)$, where the function H represents the value of the closed loop, similar to that calculated in (22) and (24). If, the ratio G^2/μ^2 is kept constant and equal to the actual Fermi constant, when the mass μ is supposed to become much larger than the masses M_p or M_n, and if furthermore one of the masses M_p or M_n is supposed to tend to zero, the function H takes the form $H\sim\mu^2$. Indeed, a part from coefficients of the order of unity which depend on the nature of the couplings, $H(\mu^2)$ involves the same type of functions of μ^2 as the function $\mu^4 J'(\mu^2)$ and $\mu^4 M^2 K'(\mu^2)$ defined in (24) and (29). We mentioned above that our approximation was good provided the ratio $(g^{\text{ren}}/g_F)^2$ is much smaller than unity. We see, with the present model, that this condition reads

$$1 \gg (g_F H(\mu^2))^2 \approx (g_F\mu^2)^2 = G^4\,.$$

which is the usual criterium of validity of a perturbation expansion.

* * *

The present investigation being started, we have been told that a new measurement of the ratio λ^2 was planned at CERN, by BERNARDINI. The object of this new measurement is, following an idea of P. MEYER, to test the existence of the interaction $\mu \to e + \gamma$ which, according to G. FEINBERG (9), would give information on the hypothetical intermediate boson which may explain the μ-meson decay. In this experiment, the γ is virtual, coming simply from the Coulomb field of the nucleus. Very roughly speaking, this intermediate γ-field produces an effective interaction between the pair (μe) and the nucleon pairs, and only a detailed dependence of the ratio λ^2 on the nuclei properties, could eventually permit a distinction between this process and the processes we have discussed in this paper.

(9) G. FEINBERG: *Phys. Rev.*, **110**, 1482 (1958).

RIASSUNTO (*)

Il presente lavoro si propone di determinare il raggio d'azione delle interazioni di Fermi misurando gli effetti di polarizzazione del vuoto che risultano dagli accoppiamenti di Fermi. Si studia un processo tipico: l'emissione dell'elettrone nella cattura del muone che si avrebbe se i neutrini emessi nella cattura di elettroni e di μ fossero identici. Si ottengono i limiti inferiori per i raggi parametri delle interazioni di Fermi partendo dal rapporto effettivamente misurato $(\mu \to e)/(\mu \to \nu)$. Si discute anche il significato di questo rapporto nell'interazione di Fermi di un bosone intermedio singolo che potrebbe anche essere saggiato con esperienze di eccitazione di nuclei per mezzo di neutrini.

(*) *Traduzione a cura della Redazione.*

The Decay and Structure of Hyperfragments - II.

J. Szymański

Institute of Nuclear Research - Warsaw

(ricevuto l'11 Agosto 1959)

Summary. — The energetic and angular distribution of the $^5He_\Lambda$ decay products is calculated. Several hyperfragment shape functions were taken into account. The results indicate a very strong dependence on the hyperfragments structure.

Introduction.

In this paper we shall consider the decay $^5He_\Lambda \to \alpha + p + \pi^-$ and its relation to the structure of hyperfragments. In part I [1] we already discussed the method which will be used here and gave the results for the pion energy distribution under the assumption that the hyperfragments wave function has a form given in the paper of Dallaporta and Ferrari [2] (henceforth referred to as DF). The energy distribution obtained for the DF function clearly favors the high-energy pions and allows practically only decays with pion energies of 24 to 35 MeV. Meanwhile, about 25% of the observed decays lie below 24 MeV. The angular distribution calculated for the DF function is also in clear contradiction to experiment. This disagreement is caused by the fact that $f_0(r)$ decreases too slowly with increasing distance. In the case of the DF function many decays occur at a large distance from the core. As a result the decay products interact weakly and the energy and angular distribution are similar to that obtained for a decay without interaction in the final state. To increase the role of the interaction we must take for $f_0(r)$ a function that decreases more rapidly with distance. To do this we repeated the calculations for the Gaussian function given by Wilhelmson and Zieliński (WZ) [3].

---

(1) J. Szymański: *Nuovo Cimento*, **10**, 834 (1958).
(2) N. Dallaporta and F. Ferrari: *Nuovo Cimento*, **5**, 111 (1957).
(3) H. Wilhelmson and P. Zieliński: *Nucl. Phys.*, **6**, 219 (1958).

The resulting curves fit very well the experimental data. In Section **1** we shall give a sketch of the calculations and the results that are obtained. The discussion of the results and comparison with experiment will be given in Section **2**. We shall discuss in Section **3** the approximations which are made. In Section **4** we shall compare our results with the results of other authors.

1. – Calculations.

The method of calculation is discussed in detail in Part I. We shall calculate here the energy distribution of the pions in the CM system of the hyperfragment and the distribution of the angle between $\hat{l}$ and $\hat{v}$. Here $\hat{l}$ and $\hat{v}$ denote unit vectors with directions $\boldsymbol{l}$ and $\boldsymbol{v}$, where $\boldsymbol{l}$ is the proton momentum relative to the α-particle and $\boldsymbol{v}$ is the pion momentum with respect to the center of mass of the $(\alpha+\text{p})$ system.

For the transition probability (a function ω_π and ϑ) we obtain $(\cos\vartheta = \widehat{\hat{l}\hat{v}})$:

$$\sum_{\text{spin}} |M|^2 \sim g^2(1+\beta^2k^2)\cdot\Bigg\{4f(v, l\cos\delta) -$$
$$-\sum_{Jll'L} \sin^2\delta_{Jl}\, b_l b_{l'} (2J+1)(2l'+1)c^2_{ll'}(L000)\, P_L(\cos\delta) +$$
$$+\sum_{JJ'll'Lj} \sin\delta_{Jl}\sin\delta_{J'l'} \exp[i\delta_{Jl} - i\delta_{J'l'}]\, b_l b_{l'} (-)^{J+J'+l+l'+j+1}\cdot$$
$$\cdot(2l+1)(2l'+1)(2J+1)(2J'+1)(2j+1)c^2_{ll'}(L000)\begin{Bmatrix}\frac{1}{2} & \frac{1}{2} & j\\ l & l' & J\end{Bmatrix}\begin{Bmatrix}\frac{1}{2} & \frac{1}{2} & j\\ l & l & J\end{Bmatrix}\begin{Bmatrix}l & l' & L\\ l' & l & j\end{Bmatrix} P_L(\cos\delta)\Bigg\}.$$

Here we denote by $\begin{Bmatrix}a & b & c\\ d & e & f\end{Bmatrix}$ the 6 j symbols of Wigner, $JJ'll'$ denote the total and orbital angular momentum of the proton and α-particle, respectively: $\delta_{Jl}(\delta_{J'l'})$ is the phase shift for the state $Jl(J'l')$; $f(p)$ is the Fourier transform of $f_0(r)$

$$b_l = \int f(vl\cos\delta) P_l(\cos\delta)\sin\delta\,\mathrm{d}\delta\,. \tag{2}$$

Integrating over the angles and energies we obtain, respectively,

$$W(\omega_\pi) = \int \sum_{\text{Spin}} |M|^2 \delta(E-Q)\varrho_l\varrho_v\,\mathrm{d}l\sin\delta\,\mathrm{d}\vartheta\,,$$

$$W(\cos\delta) = \int \sum_{\text{Spin}} |M|^2 \delta(E-Q)\varrho_l\varrho_v\,\mathrm{d}l\,\mathrm{d}v\,,$$

where E is the kinetic energy of the decay products, Q is the energy of decay of the hyperfragment.

The calculations were carried out for two different extreme functions:

i) The exponential $\exp[-\alpha r]$, $\alpha = 3.67 \cdot 10^{12}$ (DF). For this function the Λ spends most of its time outside the core.

ii) The Gaussian $\exp[-(\alpha/2)(r/a)^2]$, $\alpha = 0.87$, $a = 1.7$ fermi. For this function the Λ spends more or less half the time in the region of the core. The energy distribution obtained for the DF function was given in Part I.

Figs. 1 and 2 show the pion energy and angular distributions obtained with the WZ function, for the decay in s and p states separately. For comparison, we also give the distributions obtained when the interactions are taken into account.

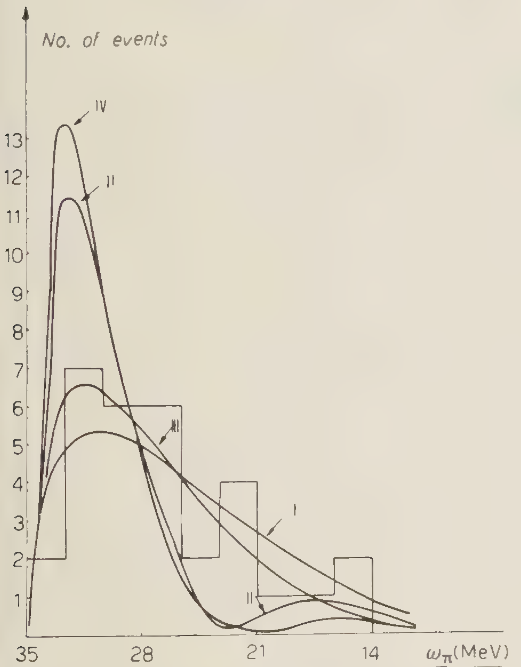

Fig. 1. - Pion energy distribution ($W(\omega_\pi)$) of mesic decays in the s state: (I) without interaction; (II) with interaction; (III) decay in p state without interaction; (IV) with interaction.

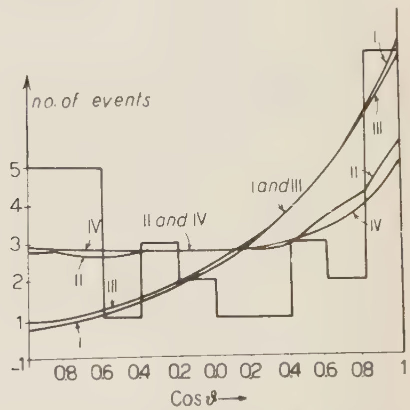

Fig. 2. - Angular distribution ($W(\cos\vartheta)$). Curves I-IV correspond to the same cases as in Fig. 1.

2. - Comparison with experiment.

We compare the theoretical curves with the experimental data given by LEVI SETTI, SLATER, TELEGDI [4]. The authors give 31 cases, 19 of which are well identified and 12 uncertain, which can also be the decay of ${}^5He_\Lambda$ or ${}^4He_\Lambda$. A comparison with experiment requires discussion of the uncertain

---

[4] R. LEVI SETTI, W. SLATER and V. L. TELEGDI: *Suppl. Nuovo Cimento*, **10**, 68 (1958).

cases. HILL and TANG ([5,6]) draw attention to the fact that the inclusion or rejection of these cases can introduce a systematic error. As may be seen from Figs. 1 and 2 the majority of the uncertain cases lie in the region of small angles and rather large pion energies. This is connected with the fact that the identification is more difficult if the recoil track is short. It is these cases which will make a large contribution for high pion energies and small angles. Thus these cases can give rise to a systematic error if they are neglected or included in the analysis. In what follows we shall include the cases of uncertain identity into the statistics and treat them on a par with the well identified cases.

For the comparison with experiment we shall use the Kolmogorov-Smirnov test. We have decided upon an integral test since differential tests (*e.g.* χ^2), in the case of small statistics, are sensitive to the grouping, and would give results that are not single-valued.

From the comparison with experiment we find that for the DF function both the energy and angular distributions lie below 4 standard deviations (in complete disagreement with experiment).

For the WZ function and decay in the s state the energy distribution lies within 3 standard deviations, for the decay in the p state is below 4 standard deviations (which indicates disagreement with experimental data).

On the other hand the angular distribution fits very well with the experimental data. The curves for both the s and p states lie within one standard deviation. The good agreement for the angular distribution and the poor agreement for the energy distribution is understandable if one considers the approximations which we have made. We have assumed a weak disturbance of the act of decay (we have neglected virtual protons Eq. (12) (I), which is probably correct for $\omega_\pi > 26$ MeV). If for $\omega_\pi < 26$ MeV we consider virtual protons in an intermediate state then $W(\omega_\pi)$ can change. But even changes of the order of $(100 \div 200)\%$ give a relatively small change in the angular distribution. That is why we shall base our conclusions mainly on the angular distribution.

The angular distribution clearly depends on the shape of the wave function. The more slowly $f_0(r)$ decreases with an increase in r, the more privileged, for a free decay, are small values of ϑ, and the less is the role of the interaction. The interaction causes an increase in the value of $W(\cos\vartheta)$ for ϑ near π, and a drop in the value of this function for ϑ near 0. Consequently, for slowly decreasing functions $W(\cos\vartheta)$ will have a clearly defined maximum in the forward direction, which is not evident in the experimental distribution. It seems to us that on the basis of our estimations, the necessary condition for

([5]) R. D. HILL: *Nuovo Cimento*, **8**, 459 (1958).
([6]) Y. C. TANG: *Nuovo Cimento*, **10**, 780 (1958).

obtaining good agreement with experiment for the angular distribution is that the Λ spend about 50% of the time or more in the region of the core. This condition eliminates a large number of the $f_0(r)$ functions, and indirectly also the potentials.

On the basis of the angular distribution it is impossible to determine the value of the ratio p/s.

Curves II and IV in Fig. 2 practically coincide. $W(\omega_\pi)$, it is true, depends on p/s, but for the reasons mentioned above, any conclusions based on it are uncertain.

The lack of dependence of the angular distribution on p/s results largely from the fact that the interaction is independent of the state in which the decay takes place. That is why ^{5}He also cannot be used to determine this ratio. The determination of the ratio p/s from hyperfragment decays is discussed in detail in the paper of CHLEBOWSKA and SZYMAŃSKI (7).

3. – Discussion of the approximations.

The approximations which we made reduce roughly to neglecting 5 effects: *a*) deformation of the core, *b*) deformation of the meson cloud surrounding the Λ-particle, *c*) retarded interaction between the initial and final states, *d*) π-α interactions, *e*) virtual protons in an intermediate state.

a) The influence of the deformation of the core of the hyperfragment on the decay was discussed in formulating the problem in Part I. We will not return to this question here. We repeat only the final conclusion, namely, that for the decay $\text{Hf} \to \text{c} + \text{p} + \pi$ this influence can be neglected.

b) The effect of the deformation of the meson cloud surrounding the Λ-particle can be (i) a change in the values of g and β for bound Λ in comparison with a free Λ, (ii) an energy dependence of the coefficients g and β. It seems that these differences should be very small. At present it is supposed that weak interactions take place in the core, and the disturbance of this region even by large changes in the external part of the cloud should be small. On the other hand in a hyperfragment we can expect, at most, small changes. In Fig. 3*b* we give one of the diagrams illustrating the effect of deformation of the cloud on the decay.

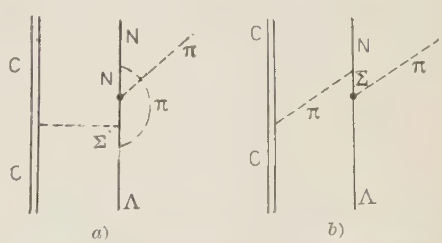

Fig. 3. – Examples of diagrams leading to: *a*) deformations of the cloud; *b*) retarded interactions.

(7) D. CHLEBOWSKA and J. SZYMAŃSKI: to be published in *Bull. Pol. Ac. Sci.*

c) The retarded interaction (Fig. 3*b*) is of the order (v^2/c^2) and therefore the corrections associated with it are rather small. If these corrections were significant, then we should observe among other things, decays with the emission of a π^+. For light hyperfragments ($Z \leqslant 2$) this effect has not been observed thus far. That such meson effects on weak interactions are small is also seen from the fact that in β decay no differences have been observed in the coupling constants determined from the free decay of the neutron and from the decay of various nuclei.

d) Because of the small cross-section for the scattering of pions on α-particles the π-α interaction should not lead to any qualitative changes. A more detailed discussion of this interaction is given by BYERS and COTTINGHAM [8].

e) The most problematic of the approximations we have made is the neglecting in the matrix element

$$M = \langle f | \left(H + T \frac{1}{a} H \right) | i \rangle ,$$

of the main part of the propagator (of virtual protons). Since we know the operator T only on the energy shell we must limit ourselves to that part of the matrix element which contains the δ function, as only this part does not lead us outside the energy shell. We neglect by necessity that part of the matrix element in which there occurs in the propagator the integration by the principal value. This means that we take into account only the protons which are created as real ones and we neglect the virtual particles in the intermediate states.

If the decay takes place outside the core, then this approximation is correct, while if the decay takes place in the core, then corrections may be large. Decays taking place at large distances are those decays on the energy curve for which the pion energy is approximately equal to the energy of a pion from a free decay.

The majority of cases lie in this region. This fact justifies our approximation, at least, for the angular distribution.

4. – Comparison of results with those of other authors.

The mesic decay of ${}^5\mathrm{He}_\Lambda$ was discussed for the first time by HILL [8]. The author drew attention to the existence of resonances in the scattering of protons on the α particles and tried to explain the strong anisotropy observed in the angular distribution in the apparent rest system of the Λ by the formation

---

(8) N. BYERS and W. N. COTTINGHAM: preprint.

of a virtual ^{5}Li in an intermediate state. Our calculations do not show that the formation of ^{5}Li in the ground state plays such an important role; for example, the potential in the $S_{\frac{1}{2}}$ state is repulsive, none the less it causes more important changes in the angular distribution than the interaction in the $P_{\frac{1}{2}}$ state, despite the fact that there is a resonance in this state.

TANG calculated the decay of $^5\mathrm{He}_\Lambda$ by the method of distorted waves. He neglects, like we did, the distortion of the wave function in the region of interaction. In his paper one may find numerical results for Hulthen's functions. Tang's variables are the same as ours (ω_π, θ). He gives the energy distribution for pions and the ratio of mesons emitted forward to those emitted backward as a function of the energy. TANG does not give the angular distribution.

The energy distribution obtained by TANG lies between the distributions obtained by us for the DF and WZ functions. It decreases far more slowly with decreasing energy than the distribution we obtained for the DF function, and somewhat more rapidly than the distribution for the WZ function.

A more detailed discussion on the role of the interaction on the decay products for $^5\mathrm{He}_\Lambda$ was given by BYERS and COTTINGHAM. They assume for the wave function of the final state an exact solution for a square well with parameters for each of the states $S_{\frac{1}{2}}P_{\frac{1}{2}}P_{\frac{3}{2}}$. Owing to this, the role of the interaction is taken into account in considerably more detail than in our paper. The results, depend however, on the model taken for the interaction. Because of the essential differences in the method of calculation it would be interesting to compare our results with those of BYERS and COTTINGHAM, since this could be a way of checking our simplified approach. Unfortunately our calculations are made in a different system. BYERS and COTTINGHAM made their calculations in the apparent rest system of the Λ, which makes comparison with our results quite difficult.

* * *

The author is much indebted to Prof. W. KRÓLIKOWSKI, Prof. J. WERLE and Dr. P. ZIELIŃSKI for helpful discussions.

RIASSUNTO (*)

Si calcolano le distribuzioni angolare ed energetica dei prodotti del decadimento del $^5\mathrm{He}_\Lambda$. Si è tenuto conto di varie funzioni di forma degli iperframmenti. I risultati indicano una fortissima dipendenza dalla struttura degli iperframmenti.

(*) *Traduzione a cura della Redazione.*

IL NUOVO CIMENTO VOL. XV, N. 1 1° Gennaio 1960

Investigation of the Invariance Group in the Three Fundamental Fields Model.

J. E. WESS

CERN - Geneva

(ricevuto il 21 Settembre 1959)

Summary. — For a theory in which elementary particles are represented by products of fundamental fields, consequences of an invariance group are investigated. The invariance group is the three-by-three unitary group. Tensor-calculus is used to investigate the representations, quantum numbers are defined and it is tried to identify certain families of elementary particles with irreducible representations.

Introduction.

The problem as to how many fields are necessary to get all conservation laws which hold in strong interaction, has been studied by W. THIRRING [1]. Through the commutation relations of the conserved quantities and the invariance properties of the Lagrangian-formulism, THIRRING found that at least three massless Weyl fields (or Majorana fields) or six fields with mass are necessary.

In this paper, consideration will be given only to the three-fields case, where the invariance group is the three-by-three unitary group. The group theoretical consequences of this invariance will be investigated.

In Section 1 the tensor representations, the only finite dimensional representations of this group, will be discussed.

Then the co-ordinate system in the representation space is adapted to transformations, which, in our theory, are connected with the isotopic spin and the displacement of the centre of charge. We find that we can label the tensor components in a unique way with numbers which we can associate

(1) W. THIRRING: *Nucl. Phys.*, **10**, 97 (1959).

with the displacement of the centre of charge (u), the isospin (τ), and the third component of isospin (τ_3).

In Section **3** we construct the tensors by means of « fundamental fields ». If we take the fields at the same space-time-point, we learn from the Pauli-principle that only a few representations are possible. These representations will be listed.

Then we try to identify certain families of elementary particles (as n, p, Λ or π-, K-mesons) with these representations. Doing this, we demand an agreement between the quantum numbers of isospin, strangeness and the baryon number.

1. – We consider the quantities $\boldsymbol{T}$ (isotopic spin), N (baryon numer) and U (displacement of the centre of charge), which obey the commutation relations

$$[T_l, T_m] = i\varepsilon_{lmk} T_k\,, \qquad [N, \boldsymbol{T}] = [N, U] = [U, \boldsymbol{T}] = 0\,. \tag{1.1}$$

They form an algebra and it is very easy to be seen that the lowest dimensional faithful representation of this algebra is three-dimensional and that the elements of this algebra can be represented by the following matrices

$$\boldsymbol{t} = \begin{pmatrix} \boldsymbol{\sigma} & \\ & 0 \end{pmatrix}, \qquad n = \begin{pmatrix} 1 & & \\ & 1 & \\ & & 1 \end{pmatrix}, \qquad u = \begin{pmatrix} 1 & & \\ & 1 & \\ & & 0 \end{pmatrix}. \tag{1.2}$$

($\boldsymbol{\sigma}$ are the Pauli matrices).

These matrices are contained in the Lie-algebra of the unitary three-by-three group (but not in the Lie-algebra of the orthogonal three-by-three group).

We will take the full three-by-three unitary group (u_3) although only the algebra (1.2), corresponding to a sub-group of u_3, has been connected with physical quantities up to now. Starting, however, like YAMAGUCHI [2] with three fields (p, n, Λ) and an invariance against unitary transformations between p and n as well as a symmetry against permutations of the three fields, we are again concerned with the full unitary group.

Let us assume now that in physics there is an invariance against our group. Thus, physical quantities have well-defined transformation properties against this group, *i.e.* they belong to certain representations. We assume that they belong to irreducible representations. Therefore, we have to investigate at first the representations of the group and the quantities belonging to the representations (these are the vectors in the representation space). In order

[2] Y. YAMAGUCHI: *A Composite Theory of Elementary Particles. A Model of Strong Interactions.* To be published in *Prog. Theor. Phys. Suppl.*

to construct the representations, it is useful to introduce covariant vectors (x_i) and contravariant vectors (x^i); $x_i x^i$ being an invariant

$$x_i' = u_i{}^k x_k\,, \qquad x^{i'} = u^i{}_k x^k \qquad (i, k = 1, 2, 3), \tag{1.3}$$

where: $\|u_i{}^k\|$ is an element of u_3, and $u^i{}_k = u_i{}^{k*}$.

With the help of these vectors we can build up tensors,

$$A^{l_1 \dots l_s}_{k_1 \dots k_r}\,, \tag{1.4}$$

should be a tensor component with s contravariant and r covariant indices.

From group theory [3] we know that all finite representations are capable of tensor representations and that u_3 induces irreducible representations in the tensor space of a certain rank and symmetry class. Thus, we have to construct tensors of highest symmetry in order to get the irredubicle representations.

When forming the determinant of three vectors

$$\operatorname{Det}(xyz) = \begin{vmatrix} x_1 & x_2 & x_3 \\ y_1 & y_2 & y_3 \\ z_1 & z_2 & z_3 \end{vmatrix}, \tag{1.5}$$

we see that $\operatorname{Det}(x'y'z') = \operatorname{Det}\|u_i{}^k\| \operatorname{Det}(xyz)$. $\operatorname{Det}(xyz)$, therefore is an invariant against the uni-modular unitary group:

$$\varepsilon^{ijk} x_i^{(1)} x_j^{(2)} x_k^{(3)} \sim \text{invariant}\,, \tag{1.6a}$$

$$\varepsilon^{ijk} x_j^{(1)} x_k^{(2)} \sim x^i\,. \tag{1.6b}$$

If we restrict ourselves to the uni-modular group, (1.6b) indicates that a pair of covariant (contravariant) indices, in which a tensor is antisymmetric, can be replaced by one contravariant (covariant) index. Furthermore, three indices form an invariant, if a tensor is antisymmetric in each pair of these three indices (1.6a). Obviously there exists no tensor that is antisymmetric in each pair of more than three indices. Thus if we use covariant and contravariant indices, we have to construct only tensors whose components

$$A^{l_1 \dots l_s}_{k_1 \dots k_r} \tag{1.7}$$

are symmetrical in the r covariant and the s contravariant indices. The space spanned by such a tensor, however, is not irreducible, for it contains an invariant sub-space formed by the linear combinations

$$\sum_i A^{il_2 \dots l_s}_{ik_2 \dots k_r}\,. \tag{1.8}$$

---

(3) H. Weyl: *The Classical Groups, their Invariants and Representations.*

The tensor components therefore should satisfy the following condition

$$\sum_i a^{i l_2 \dots l_s}_{i k_2 \dots k_r} = 0\,, \tag{1.9}$$

(we write small a to indicate that the components obey the condition (1.9)). In such a tensor space the uni-modular unitary group induces an irreducible representation. We call it $a(rs)$. Then $(\operatorname{Det} u_3)^e a(rs)$, ($e$ integer) is a representation of u_3. We call it ${}^e a(rs)$.

Our quantities are the tensor components

$$ {}^e a^{l_1 \dots l_s}_{k_1 \dots k_r}\,. \tag{1.10}$$

From this we learn that all the irreducible representations of u_3 can be labelled with the three numbers e, r, s; (e integer; $r, s \geqslant 0$).

We have, for instance

$$\varepsilon^{ikl} x_k\, y_l \sim {}^1 a^i\,, \qquad \varepsilon^{ikl} x_i y_k z_l \sim {}^1 a\,. \tag{1.11}$$

The tensor space formed by

$$x_j\, {}^e a^{l_1 \dots l_s}_{k_1 \dots k_r}\,, \tag{1.12}$$

contains the invariant sub-spaces spanned by the tensor components

$$ {}^e a^{l_1 \dots l_s}_{k_1 \dots k_r j}\,; \qquad \varepsilon^{i k_1 j} x_j\, {}^e a^{l_1 \dots l_s}_{k_1 \dots k_r}\,; \qquad x_j\, {}^e a^{j l_2 \dots l_s}_{k_1 \dots k_r}\,. \tag{1.13}$$

In these sub-spaces, the representations

$$ {}^e a(r+1, s)\,; \qquad {}^{e+1} a(r-1, s+1)\,; \qquad {}^e a(r, s-1) \tag{1.14}$$

are induced.

If we want to know the degree of the representations, we have to count the linear independent tensor components. This will be done in Appendix I. We find that $\frac{1}{2}(r+1)(s+1)(r+s+2)$ is the degree of the representation ${}^e a(r, s)$.

2. – Under the invariance group physical quantities should transform like vectors in the representation space of this group. Thus, we shall discuss the representation space rather than the representation itself. In this Section we shall characterize the vectors in this space; for this purpose we have to specify the co-ordinate system. This can be achieved by giving a special form to matrices representing certain group elements, so that there is no freedom for equivalence transformations.

The most obvious way is to make diagonal the transformations generated by N, U, T_3. These are the only transformations that are diagonal in the

same co-ordinate system, as we can find no other element in the Lie-algebra of u_3 commuting with N, U, T_3. Then we try to characterize the vectors by labelling them with the eigenvalues of N, U, T_3.

In the three-dimensional vector space the transformations:

$$x_1' = \exp[i\varphi_1]x_1\,, \quad x_2' = \exp[i\varphi_2]x_2\,, \quad x_3' = \exp[i\varphi_3]x_3 \tag{2.1}$$

are generated by N, U, T_3. It follows that the tensor components (r, μ, ν^*, μ^*) (see Appendix I) are eigenvectors with the eigenvalue (= weight of the component)

$$\exp\left[i\{(\nu - \nu^* + e)\varphi_1 + (\mu - \mu^* + e)\varphi_2 + (r - s - \nu + \nu^* - \mu + \mu^* + e)\varphi_3\}\right] \tag{2.2}$$

According to (1.2) the eigenvalues of N, U, T_3 are

$$\left\{\begin{aligned} n &= r - s + 3e\,, \\ u &= \nu - \nu^* + \mu - \mu^* + 2e\,, \\ \tau_3 &= \tfrac{1}{2}(\nu - \nu^* - \mu + \mu^*)\,, \end{aligned}\right. \tag{2.3}$$

We see that the weight depends only on

$$\left\{\begin{aligned} \nu - \nu^* &= \alpha\,, \\ \mu - \mu^* &= \beta\,, \end{aligned}\right. \tag{2.4}$$

so that components with the same value for α and β have the same weight and are not distinguished through labelling with n, u, τ_3.

In Appendix II, it will be shown that there are only

$$\tfrac{1}{2}[(r+1)(s+1)(r+s+2) - rs(r+s)]$$

different pairs $\alpha\beta$, *i.e.* for $r \neq 0$, $s \neq 0$ less than the degree of the representation. Therefore, we have linear independent tensor components with the same weight. If the transformations (2.1) are required to be diagonal, there is still a possibility for equivalence transformations, affecting only components with the same weight. Thus, we cannot characterize the vectors by the numbers n, u, τ_3 only, but we have to distinguish between linear independent vectors with the same n, u, τ_3.

Now we demand that the representations of the sub-group generated by $\boldsymbol{T}$ are contained in ${}^e a(rs)$ in fully reduced form.

The sub-group is a two-by-two unitary uni-modular group (u_2), the irreducible representations of which are well known. They can be characterised by the eigenvalues of $T_1^2 + T_2^2 + T_3^2$, which have the form $\tau(\tau+1)$, or, as usual, with the isospin τ itself. Furthermore, we know that, for a representation of

u_2 characterized by τ, there is exactly one linear independent eigenvector of T_3 to every eigenvalue: $-\tau, -\tau+1, -\tau+2, .. +\tau$. These eigenvectors span the whole representation space.

As U commutes with all $\boldsymbol{T}$ matrices, it follows from the lemma of Schur that U has the same eigenvalue u for all vectors belonging to the same irreducible representation of u_2. From (2.3), we see that the eigenvalue of N depends only on r, s and e and that it has therefore the same value for vectors of the same irreducible representation ${}^e a(rs)$.

From (2.3) (Appendix II, 1) and (Appendix II, 2) it follows that the values which can be taken on by u are

$$(2.5) \qquad 2e-s\,, \quad 2e-s+1\,, \quad \ldots \quad r+2e-1\,, \quad r+2e\,.$$

When forming the sub-space of all the vectors with the same eigenvalue u, we know already that this is an invariant sub-space under the transformations induced by u_2. We are interested in the irreducible invariant sub-spaces contained in this sub-space. For this end we take the vectors belonging to the greatest eigenvalue of $T_3 = \tau_{3\max}$. The number of the linear independent vectors belonging to $\tau_{3\max}$ gives the number of the representations of u_2 with $\tau = \tau_{3\max}$, which are induced in the above mentioned sub-space. Then, we take away the eigenvectors of T_3 belonging to these irreducible representations and start again with the greatest remaining eigenvalue of T_3.

With the help of this procedure we find all the irreducible representations of u_2 induced in the given sub-space and we can adapt the co-ordinate system to these representations. In other words, we label the vectors with τ, τ_3 and u.

The corresponding calculations are also given in Appendix II. The final results are

TABLE I.

For u between	there is exactly one irreducible representation of u_2 for each value of τ
$r-s+2e \leq u \leq r+2e$	$\tau = \frac{u}{2}-e\,, \quad \frac{u}{2}-e+1\,, \quad \ldots, r-\frac{u}{2}+e$
$2e \leq u \leq r-s+2e$	$\tau = \frac{u}{2}-e\,, \quad \frac{u}{2}-e+1\,, \quad \ldots, s+\frac{u}{2}-e$
$-s+2e \leq u \leq 2e$	$\tau = -\frac{u}{2}+e\,, \quad -\frac{u}{2}+e+1\,, \quad \ldots, s+\frac{u}{2}-e$

(we have assumed $r \geq s$).

Thus we find that the quantities can be characterized by the eigen values of U, T_3 and T^2 in a unique way; the possible eigenvalues are listed in Table I. The fact that we need the three numbers indicates that the valueof u does not determine the value of τ in a certain representation.

The irreducible representations can be characterized by n, r and s.

3. – Up to now we have only been concerned with symmetry properties arising from an invariance against the three-by-three unitary group and no other properties of the quantities have been involved. Now we shall consider the case that the vectors in the three-dimensional unitary space (internal space) are fields. We can build up all our tensors with these three « fundamental fields » just as products. As we have taken fields—they are quantities with a known space-time dependence—our quantities have also a certain space-time dependence.

In others words, we shall take fields belonging to the two-dimensional representation of the Lorentz group (Weyl fields) and we shall make products, which then transform according to certain representations of the Lorentz group. We are interested in the spin to which they belong.

If we take the fields in the products at the same space-time point, as will be done throughout this paper, the products are just spin tensors. From spinor-calculus we know the spin representations induced in such a tensor space.

As is well known, an antisymmetric pair of spin-indices forms an invariant under the uni-modular unitary two-by-two group (determinant). In our consideration we need therefore only spin tensors with covariant vector indices, which are symmetrical also. Such a tensor can now be written

$$b_{\varrho_1 \dots \varrho_t} \tag{3.1}$$

and it belongs to a spin representation with spin $t/2$. The tensor space

$$v_\sigma b_{\varrho_1 \dots \varrho_t} \tag{3.2}$$

contains the invariant sub-spaces

$$b_{\varrho_1 \dots \varrho_t \sigma}, \qquad \varepsilon^{\varrho_1 \sigma} v_\sigma b_{\varrho_1 \dots \varrho} \tag{3.3}$$

belonging to the spin $\frac{1}{2}(t+1)$ and $\frac{1}{2}(t-1)$.

W. THIRRING has shown that the Lagrangian formulism is invariant against a unitary group only in case the mass is zero.

Thus we take massless Weyl fields [4]:

$$\psi_{k\sigma}(x)\,, \tag{3.4}$$

$k=1, 2, 3$ is a vector index in the internal space, $\sigma=1, 2$ is a spin index.

Naturally, $\psi^+_{k\sigma}(x)$ transforms contravariant. The fields are supposed to obey the commutation relations

$$\left\{\begin{aligned} &[\psi_{k\sigma}(x),\, \psi(x_{k'\sigma'})]_+ = 0\,,\\ &[\psi^+_{k\sigma}(x),\, \psi^+_{k'\sigma'}(x)]_+ = 0\,. \end{aligned}\right. \tag{3,5}$$

It follows from (3.5)

$$\ldots\,\psi_{k\sigma}\,\ldots\,\psi_{k'\sigma'}\,\ldots = -\,\ldots\,\psi_{k'\sigma'}\,\ldots\,\psi_{k\sigma}\,\ldots\,. \tag{3.6}$$

The products of ψ fields or ψ^+ fields must be antisymmetric in the index pairs $(k\sigma)$, *i.e.* they have to be

symmetric in k and antisymmetric in the corresponding σ

or

antisymmetric in k and symmetric in the corresponding σ.

Thus, forming the irreducible tensor space, we have only the freedom to choose the symmetry class for either the spin or the isospin tensor. This restricts the possible representations to a large extent, for spin tensors are antisymmetric in not more than two indices, isospin tensors in not more than three indices.

In the construction of the irreducible invariant tensor spaces that are spanned by our field products, we follow the way indicated by (1.12), (1.13), (3.2) and (3.3). Taking into account the rules outlined above, it is very easy to find the possible representations. A list of the representations will be given in Table II.

---

(4) W. THIRRING: *Three Field Theory of Strong Interactions*, to be published.

TABLE II.

Field products	Spin	${}^{e}a(r, s)$	Degree of ${}^{e}a(rs)$
$\psi_{k_1\sigma_1}$	$\frac{1}{2}$	${}^{0}a(10)$	3
$\psi_{k_1\sigma_1}\psi_{k_2\sigma_2}$	0	${}^{0}a(20)$	6
	1	${}^{1}a(01)$	3
$\psi_{k_1\sigma_1}\psi_{k_2\sigma_2}\psi_{k_3\sigma_3}$	$\frac{1}{2}$	${}^{1}a(11)$	8
	$\frac{3}{2}$	${}^{1}a(00)$	1
$\psi_{k_1\sigma_1} \cdots \psi_{k_4\sigma_4}$	0	${}^{2}a(02)$	6
	1	${}^{1}a(10)$	3
$\psi_{k_1\sigma_1} \cdots \psi_{k_5\sigma_5}$	$\frac{1}{2}$	${}^{2}a(01)$	3
$\psi_{k_1\sigma_1} \cdots \psi_{k_6\tau_6}$	0	${}^{2}a(00)$	1

The same table holds for products of the form

$$\overset{+}{\psi}_{k_1\sigma_1}(x) \dots \overset{+}{\psi}_{k_l\sigma_l}(x)$$

when we interchange r and s and put $-e$ for e.

In order to get the irreducible representations according to which products of the form

$$\overset{+}{\psi}_{k_1\sigma_1} \cdots \overset{+}{\psi}_{k_l\sigma_l}\psi_{k'_1\sigma'_1} \cdots \psi_{k'_{l'}\sigma'_{l'}} \tag{3.7}$$

transform, we have to reduce the direct product of the corresponding representations as listed in Table II. This can be done by considering all the possibilities, in which the indices available are fully symmetrized.

The tensor space

$$a^{l_1}_{l_2} \times a_{k_1k_2} \tag{3.8}$$

for instance, contains the

Irreducible subspaces	belonging to the representations
$a^{l_1}_{l_2} a_{k_1k_2}$	${}^0a(31)$
$\sum\limits_{l_1} a^{l_1}_{l_2} a_{l_1k_2}$	${}^0a(20)$
$\sum\limits_{l_2l_1} \varepsilon^{l_3l_2k_1} a^{l_1}_{l_3} a_{k_1k_2}$	${}^1a(12)$
$\sum\limits_{l_1l_2k_1} \varepsilon^{l_3l_2k_1} a^{l_1}_{l_3} a_{k_1l_1}$	${}^1a(10)$

The spin, to which the products belong, follows from vector addition, there is no restriction as is in the first case (3.6).

For a certain class of products, *i.e.* products belonging to a baryon number 0 and 1, the representations will be listed in Table III and Table IV.

TABLE III. – *Field products with baryon number* 0.

Field products	Spin	${}^ea(rs)$	Degree of ${}^ea(rs)$
$\psi^+_{k_1\sigma_1} \psi_{k_1'\sigma_1'}$	0, 1	${}^0a(00)$	1
		${}^0a(11)$	8
$\psi^+_{k_1\sigma_1} \psi^+_{k_2\sigma_2} \psi_{k_1'\sigma_1'} \psi_{k_2'\sigma_2'}$	0	${}^0a(00)$	1
		${}^0a(11)$	8
		${}^0a(22)$	27
	1	${}^1a(03)$	10
		${}^0a(11)$	8
		${}^{-1}a(30)$	10
	0, 1, 2	${}^0a(00)$	1
		${}^0a(11)$	8

TABLE III (*continued*).

Field products	Spin	${}^{e}a(rs)$	Degree of ${}^{e}a(rs)$
$\psi^{+}_{k_1\sigma_1}\cdots\psi^{+}_{\sigma_3k_3}\psi_{k'_1\sigma'_1}\cdots\psi_{k'_3\sigma'_3}$	0, 1	${}^{0}a(22)$	27
		${}^{1}a(03)$	10
		${}^{-1}a(30)$	10
		${}^{0}a(11)$	8
		${}^{0}a(00)$	1
	1, 2	${}^{0}a(11)$	8
	0, 1, 2, 3	${}^{0}a(00)$	1
$\psi^{+}_{k_1\sigma_1}\cdots\psi^{+}_{k_4\sigma_4}\psi_{k'_1\sigma'_1}\cdots\psi_{k'_4\sigma'_4}$	0	${}^{0}a(00)$	1
		${}^{0}a(11)$	8
		${}^{0}a(22)$	27
	1	${}^{0}a(11)$	8
		${}^{-1}a(30)$	10
		${}^{1}a(03)$	10
	0, 1, 2	${}^{0}a(00)$	1
		${}^{0}a(11)$	8
$\psi^{+}_{k_1\sigma_1}\cdots\psi^{+}_{k_5\tau_5}\psi_{k'_1\sigma'_1}\cdots\psi_{k'_5\sigma'_5}$	0, 1	${}^{0}a(00)$	1
		${}^{0}a(11)$	8
$\psi^{+}_{k_1\sigma_1}\cdots\psi^{+}_{k_6\sigma_6}\psi_{k'_1\sigma'_1}\cdots\psi_{\sigma'_6k'_6}$	0	${}^{0}a(00)$	1

In Table I we find the possible eigenstates of T^2, T_3 and U for the representations. Thus, we know the possible eigenvalues τ, τ_3 and u of the field products under consideration, as we know the representations to which they belong.

TABLE IV. – *Field product with baryon number* 1.
To products with baryon number-1 belong the contravariant representations.

Field products	Spin	${}^{e}a(rs)$	Degree of ${}^{e}a(rs)$
$\psi_{k'_1\sigma'_1}$	$\frac{1}{2}$	${}^{0}a(10)$	3
$\psi^+_{k_1\sigma_1}\psi_{k'_1\sigma'_1}\psi_{k'_2\sigma'_2}$	$\frac{1}{2}$	${}^{0}a(10)$	3
		${}^{0}a(21)$	15
	$\frac{1}{2}$, $\frac{3}{2}$	${}^{1}a(02)$	6
		${}^{0}a(10)$	3
$\psi^+_{k_1\sigma_1}\psi^+_{k_2\sigma_2}\psi_{k'_1\sigma'_1}\ldots\psi_{k'_3\sigma'_3}$	$\frac{1}{2}$	${}^{1}a(13)$	24
		${}^{0}a(21)$	15
		${}^{1}a(02)$	6
		${}^{0}a(10)$	3
	$\frac{3}{2}$	${}^{1}a(02)$	6
	$\frac{1}{2}$, $\frac{3}{2}$	${}^{0}a(21)$	15
		${}^{1}a(02)$	6
	$\frac{1}{2}$, $\frac{3}{2}$, $\frac{5}{2}$	${}^{0}a(10)$	3
$\psi^+_{k_1\sigma_1}\ldots\psi^+_{k_3\sigma_3}\psi_{k'_1\sigma'_1}\ldots\psi_{k'_4\sigma'_4}$	$\frac{1}{2}$	${}^{1}a(13)$	24
		${}^{1}a(02)$	6
		${}^{0}a(21)$	15
		${}^{0}a(10)$	3
	$\frac{1}{2}$, $\frac{3}{2}$	${}^{0}a(10)$	3
		${}^{0}a(21)$	15
		${}^{1}a(02)$	6
	$\frac{3}{2}$	${}^{1}a(02)$	6
	$\frac{1}{2}$, $\frac{3}{2}$, $\frac{5}{2}$	${}^{0}a(10)$	3

TABLE IV (*continued*)

Field products	Spin	${}^{e}a(rs)$	Degree of ${}^{e}a(sr)$
$\psi^{+}_{k_1\sigma_1} \cdots \psi^{+}_{k_4\sigma_4} \psi_{k'_1\sigma'_1} \cdots \psi_{k'_5\sigma'_5}$	$\frac{1}{2}$	${}^{0}a(21)$	15
		${}^{0}a(10)$	3
	$\frac{1}{2}$, $\frac{3}{2}$	${}^{1}a(02)$	6
		${}^{0}a(10)$	3
$\psi^{+}_{k_1\sigma_1} \cdots \psi^{+}_{k_5\sigma_5} \psi_{k'_1\sigma'_1} \cdots \psi_{k'_6\sigma'_6}$	$\frac{1}{2}$	${}^{0}a(10)$	3

To the representations of Table III and Table IV belong the states with the following quantum numbers.

TABLE V.

Representation	u	τ
${}^{0}a(00)$	0	0
${}^{0}a(11)$	-1	$\frac{1}{2}$
	0	0, 1
	1	$\frac{1}{2}$
${}^{0}a(22)$	-2	1
	-1	$\frac{1}{2}$, $\frac{3}{2}$
	0	0, 1, 2
	1	$\frac{1}{2}$, $\frac{3}{2}$
	2	1
${}^{1}a(03)$	-1	$\frac{3}{2}$
	0	1
	1	$\frac{1}{2}$
	2	0
${}^{-1}a(30)$	-2	0
	-1	$\frac{1}{2}$
	0	1
	1	$\frac{3}{2}$
${}^{0}a(10)$	0	0
	1	$\frac{1}{2}$
${}^{0}a(21)$	-1	$\frac{1}{2}$
	0	0, 1
	1	$\frac{1}{2}$, $\frac{3}{2}$
	2	1

TABLE V (*continued*).

Representation	u	τ
$^1a(02)$	0	1
	1	$\frac{1}{2}$
	2	0
$^1a(13)$	-1	$\frac{3}{2}$
	0	1, 2
	1	$\frac{1}{2}$, $\frac{3}{2}$
	2	0, 1
	3	$\frac{1}{2}$

In a composite model of elementary particles one would try to identify the field products with elementary particles. According to the quantum numbers n, u, τ, τ_3 there are among others the following possibilities:

TABLE VI.

	τ	τ_3	u
ψ_1	$\frac{1}{2}$	$\frac{1}{2}$	1
ψ_2	$\frac{1}{2}$	$\frac{1}{2}$	1
ψ_3	0	0	0

These fundamental fields have the quantum numbers of p, n and Λ as a consequence of (1.2), but they belong to the mass zero. Therefore, we would have to identify these particles with products of at least three fields.

From Table IV we see that the 27 different states formed by the product of three fields belong to different irreducible representations. They have the degrees 3, 15 and spin $\frac{1}{2}$ and degrees 3, 6 and spin $\frac{1}{2}$ or $\frac{3}{2}$.

As we believe that there is no degeneration among states belonging to different irreducible representations, we have to identify the particles with a family of states connected by the same irreducible representation, and we have also some reason to exclude the other states. According to Table V, there are states which we can identify with p, n, Λ, Σ and Ξ particles, but there are several possibilities among which group theory predicts no unique way.

In the case of two-fields product, we can form the following states:

TABLE VII.

Products	τ	τ_3	u	Particles
$\psi_1^+\psi_2$	1	-1	0	π^-
$\psi_1^+\psi_1 - \psi_2^+\psi_2$	1	0	0	π^0
$\psi_2^+\psi_1$	1	1	0	π^+
$\psi_1^+\psi_3$	$\frac{1}{2}$	$-\frac{1}{2}$	-1	$\overline{K^+}$
$\psi_2^+\psi_3$	$\frac{1}{2}$	$\frac{1}{2}$	-1	$\overline{K^0}$
$\psi_3^+\psi_2$	$\frac{1}{2}$	$-\frac{1}{2}$	1	K^0
$\psi_3^+\psi_1$	$\frac{1}{2}$	$\frac{1}{2}$	1	K^+
$\psi_3^+\psi_3 - \psi_i^+\psi_i$	0	0	0	π^{00} (*)

$\sum_i \psi_i^+\psi_i$ again belongs to a different representation and can be excluded.

(*) π^{00} is a state degenerated with the π^- and K^- mesons.

4. – Final comments.

Invariance under a group of transformations yields a great deal of information. We can identify families of physical states with representations of the group, through this we get transformation laws and orthogonality relations for the states. We can deduce conservation laws and define quantum numbers and we obtain branching ratios for processes where several states are involved.

In this paper we started with the knowledge of conservation laws and tried to deduce them from invariance against a transformation group. The conservation laws furnish us with the Lie algebra (1.1), and the corresponding Lie group should be isomorph to the desired group of transformations, or at least to one of their sub-groups.

From (1.1) it is very easy to see that the corresponding Lie group is the direct product of two commuting sub-groups, one generated by the elements T the other by the elements N and U. It follows that the representations are also the direct product of the corresponding representations. The representations of the first group are just the spin representations, the other group is Abelian and has one-dimensional representations only. Thus, from (1.1) alone,

we could get no further information beyond that contained in the isospin theory.

But we can choose a larger group, so that (1.1) corresponds to a sub-group. The choice of this group is rather arbitrary and we have to justify our choice of the three-by-three unitary group.

What we essentially want to do is to connect the group operations of the two commuting groups, so that the whole group does not split into their direct product. To achieve this we can, *e.g.* add to the group operations the permutations of the rows and columns in the representation (1.2). Through this we have introduced Y. Yamaguchi's (2) global symmetry and we can use the arguments given in his paper for the so formed three-by-three unitary group.

On the other hand, W. Thirring (1) has shown that the Lagrangian formalism is invariant either under orthogonal or unitary transformations, corresponding to the cases of non zero mass, or mass zero respectively. Now, the lowest dimensional representation of (1.1) given in (1.2) is contained only in the Lie algebra of the unitary group. This gives again some reason to treat the unitary group; together with massless fields. But all these considerations can only give some arguments. To prove that there is an invariance in physics against a group, isomorph to the three-by-three unitary group, we have to check the consequences.

In this paper the representations have been investigated, quantum numbers have been defined and finally we tried to select certain families of elementary particles and to identify them with irreducible representations. The principle of selection has been the agreement in the quantum numbers. To restrict the number of possible representations, we made use of a composite model of elementary particles, *i.e.* we introduced fundamental fields and we assumed that elementary particles are represented by products of these fields taken at the same space-time point. Using the Pauli principle, we get a strong restriction of the possible representations and moreover it gives us a connection with the spin.

Selecting families, we can think of a family of particles with baryon number zero. From Table III we see that the smallest family has 8 members. According to the quantum numbers, there can be the π- and K-mesons in this family, but there is one more particle degenerated with them. We introduced this particle as a π^{00}-meson in Table VII, where we identified the particles with products of two fields.

For particles with baryon number 1 (-1), we find families of 3, 6, 15 and 24 members (Table IV). The three-dimensional representation connects states which can be identified with p, n and Λ. It is also possible to identify the n, p, Λ, Σ and Ξ particles with the 15 dimensional representation, but there would be 7 more members in this family.

In fact, the representations discussed here appear several times, as can be seen from Table III and Table IV. Thus, even with the help of branching ratios we could not find a unique way to represent elementary particles by field products.

To verify that elementary particle states really transform like vectors in the representation space, we would still have to test branching ratios. This would then justify the assumption that there is an invariance against the whole unitary three-by-three group.

* * *

The author would like to express his thanks to Professor C. J. BAKKER and to CERN for the hospitality extended to him. He his grateful to Professor M. FIERZ and Professor W. THIRRING for suggestions and helpful comments and for useful discussions with Dr. F. CERULUS and Dr. Y. YAMAGUCHI.

APPENDIX I

Degree of the representation ${}^{e}a(rs)$.

If we want to know the degree of a representation, we have to count the linear independent vectors in the representation space. Our representation space is spanned by the tensor components

$$a^{l_1 \dots l_s}_{k_1 \dots k_r},$$

that obey the condition (1.9). (ν, μ, ν^*, μ^*) should be a tensor component with

$$\nu \text{ covariant indices } 1\,,$$

$$\mu \text{ covariant indices } 2\,,$$

and

$$\nu^* \text{ contravariant indices } 1\,,$$

$$\mu^* \text{ contravariant indices } 2\,.$$

For one fixed value of ν $(0 \le \nu \le r)$, μ can be any integer number between 0 and $r-\nu$, that are $r-\nu+1$ different numbers.

When we sum over the values ν can take on, we find that there are $\frac{1}{2}(r+1)(r+2)$ different possibilities to choose the covariant indices. Similarly, we find $\frac{1}{2}(s+1)(s+2)$ possibilities for the contravariant indices. Thus, there are $\frac{1}{4}(r+1)(r+2)(s+1)(s+2)$ tensor components, but condition (1.9) was not yet taken into account.

In order to get the degree of the irreducible representation ${}^{e}a(rs)$, we have to subtract the degree of the invariant subspace formed by the linear combinations:

$$\sum a^{i\,l_2\ldots l_s}_{i\,k_2\ldots k_r}\,. \tag{AI.1}$$

Here, only the indices $k_2 \ldots k_r$, $l_2 \ldots l_s$ can be chosen freely, so that there are $\frac{1}{4}r(r+1)s(s+1)$ linear independent components in the subspace.

Thus, the representation space of ${}^{e}a(rs)$ has the dimension

$$\tfrac{1}{4}[(r+1)(r+2)(s+1)(s+2)-r(r+1)s(s+1)]=\tfrac{1}{2}(r+1)(s+1)(r+s+2)\,. \tag{AI.2}$$

This number is the degree of the representation ${}^{e}a(rs)$.

Appendix II

In Appendix I we have introduced the tensor components (ν, μ, ν^*, μ^*). For ν, μ, ν^*, μ^* being any integer number, greater or equal to zero, and satisfying

$$\nu+\mu\leqslant r\,, \qquad \nu^*+\mu^*\leqslant s\,, \tag{AII.1}$$

there is one tensor component.

As a consequence of (1.8) this tensor space is not irreducible, but contains invariant subspaces. In order to obtain an irreducible subspace, the tensor components have to satisfy condition (1.9); consequently, some of them are linearly dependent; these are always components with the same weight.

Now we want to know the range of α, β as defined in (2.4). From (AII.1) and (2.4) follows

$$-s\leqslant\alpha\leqslant r\,, \qquad -s\leqslant\beta\leqslant r\,, \qquad -s\leqslant\alpha+\beta\leqslant r\,, \tag{AII.2}$$

so that with α fixed, greater or equal to zero, β can take any value between $-s$ and $r-\alpha$; these are $r+s-\alpha+1$ different values. With α smaller than zero, we find $r+s+\alpha+1$ different values.

Next we sum over α between $-s$ and r and obtain

$$\tfrac{1}{2}[(r+1)(s+1)(r+s+2)-rs(r+s)]\,.$$

different pairs.

Let us count now the number $k(\alpha, \beta)$ of linear independent tensor components with the weight determined by α and β. For this end α is kept fixed again and we write down the possible values of ν and ν^*, so that $\nu-\nu^*=\alpha$.

From (AII.1) and (2.4) follows

$$\text{for } \alpha\geqslant 0\colon \begin{cases} \nu\colon & \alpha\,, \quad \alpha+1 \ldots \alpha+x \\ \nu^*\colon & 0\,, \quad 1 \ \ldots \ x \end{cases}, \tag{AII.3}$$

with

$$\alpha + x \leqslant r, \qquad 0 \leqslant x \leqslant s,$$

as a condition for x; and

$$\text{for } \alpha \leqslant 0: \begin{cases} \nu: & 0, \quad 1 \ldots x \\ \nu^*: & -\alpha, \quad -\alpha+1 \ldots -\alpha+x, \end{cases}$$

with

$$0 \leqslant x \leqslant r, \qquad \alpha + x \leqslant s,$$

as a condition for x.

The same applies to β and μ, μ^*. We bear in mind that ν, ν^* are numbers already fixed.

Then we have

$$\text{for } \beta \geqslant 0: \begin{cases} \mu: & \beta, \quad \beta+1 \ldots \beta+y \\ \mu^*: & 0, \quad 1 \ldots y \quad, \end{cases}$$

with

$$\beta + y \leqslant r - \nu, \qquad 0 \leqslant y \leqslant s - \nu^*,$$

as a condition for y; and

$$\text{for } \beta \leqslant 0: \begin{cases} \mu: & 0, \quad 1 \ldots y \\ \mu^*: & -\beta, \quad -\beta+1 \ldots -\beta+y, \end{cases}$$

with

$$0 \leqslant y \leqslant r - \nu, \qquad -\beta + y \leqslant s - \nu^*,$$

as a condition for y.

From the condition for y, we see that we have to distinguish between the following cases:

1) $r - \nu \geqslant \beta \geqslant (r-\nu) - (s-\nu^*) = r - s - \alpha \geqslant 0$

then y runs from zero to $r - \nu - \beta$; these are $r - \nu - \beta + 1$ different values; all of them yield the same β.

2) $r - s - \alpha \geqslant \beta \geqslant 0$

gives $s - \nu^* + 1$ different values for y.

3) $0 \geqslant \beta \geqslant r - s - \alpha$

gives $r - \nu + 1$ different values for y.

4) $0 \geqslant r - s - \alpha \geqslant \beta \geqslant -s + \nu^*$

gives $s - \nu^* + \beta + 1$ different values for y.

Next we have to sum over all the values ν or ν^* that give a certain α. The possible values are listed in (AII.3), but we have also

$$r - \nu \geqslant \beta, \qquad \beta \geqslant -s + \nu^*.$$

For β fixed this is a condition for ν and ν^*. The sum is the number of tensor components with a certain weight, but we want to count only the components in the invariant irreducible subspace determined by (1.9). For this purpose we have to subtract the components with a given weight, which are in the other invariant subspace. From (1.8) it follows that this other subspace is isomorph to the representation space of $(r-1, s-1)$. As a result of the above calculation we obtain the number of vectors in this space also.

Finally, we have to subtract the two numbers, and if we assume $r \geqslant s$ we find

TABLE VIII.

α	β	$k(\alpha\beta)$
$r-s \leqslant \alpha \leqslant r$	$0 \leqslant \beta \leqslant r-\alpha$	$r-\alpha-\beta+1$
	$r-s-\alpha \leqslant \beta \leqslant 0$	$r-\alpha+1$
	$-s \leqslant \beta \leqslant r-s-\alpha$	$s+\beta+1$
$0 \leqslant \alpha \leqslant r-s$	$r-s-\alpha \leqslant \beta \leqslant r-\alpha$	$r-\alpha-\beta+1$
	$0 \leqslant \beta \leqslant r-s-\alpha$	$s+1$
	$-s \leqslant \beta \leqslant 0$	$s+\beta+1$
$-s \leqslant \alpha \leqslant 0$	$r-s-\alpha \leqslant \beta \leqslant r$	$r-\beta+1$
	$0 \leqslant \beta \leqslant r-s-\alpha$	$s+\alpha+1$
	$-s-\alpha \leqslant \beta \leqslant 0$	$s+\alpha+\beta+1$

This Table also contains the character of the representation.

From (2.3) and (2.4) follows

$$u = \alpha + \beta + 2e\,, \qquad \tau_3 = \tfrac{1}{2}(\alpha - \beta)\,. \tag{AII.5}$$

In Sect. 2 we have considered the subspace formed by vectors with the same eigenvalue u. For this reason, we have to find all the possible values of α and β, so that $u = \alpha + \beta$ (we put $e = 0$). $k(\alpha\beta)$ then is the number of the linear independent vectors belonging to the pair $\alpha\beta$ and this is also the number of vectors with the eigenvalues $\tau_3 = \frac{1}{2}(\alpha-\beta)$, $u = \alpha - \beta$.

Let us write down the possible values of α and β which have the sum $\alpha + \beta = u$. Then $k(\alpha\beta)$ can be found in Table VIII.

We have to consider the cases

1) $\quad r - s \leqslant u \leqslant r \qquad (r \geqslant s)$

$$\begin{array}{llllll}
\alpha: & r & \ldots & u & \ldots\ 0 \ldots & u-r \\
\beta: & u-r & \underbrace{\ldots}_{1 \ldots r-\alpha+1} & 0 & \underbrace{\ldots}_{r-u+1}\ u\ \underbrace{\ldots}_{r-\beta+1 \ldots 1} & r \\
k(\alpha\beta): & & & & &
\end{array}$$

2) $0 \leqslant u \leqslant r - s$

$$\begin{array}{lccccccc}
\alpha: & u+s & \dots & u & \dots & 0 & \dots & s \\
\beta: & -s & \dots & 0 & \dots & u & \dots & u+s \\
k(\alpha\beta): & \multicolumn{3}{c}{1 \dots s+\beta+1} & s+1 & \multicolumn{3}{c}{s+\alpha+1 \dots 1}
\end{array}$$

3) $-s \leqslant u \leqslant 0$

$$\begin{array}{lccccccc}
\alpha: & u+s & \dots & 0 & \dots & u & \dots & -s \\
\beta: & -s & \dots & u & \dots & 0 & \dots & u+s \\
k(\alpha\beta): & \multicolumn{3}{c}{1 \dots s+\beta+1} & s+u+1 & \multicolumn{3}{c}{s+\alpha+1 \dots 1}
\end{array}$$

Here the conditions (AII.2) are always satisfied.

In the case of $r - s \leqslant u \leqslant r$ the number of vectors with the eigenvalue $\tau_3 = r - u/2$ is one. It increases steadily by one with decreasing τ_3 and is $r - u + 1$ for $\tau_3 = u/2$. The number is constant until τ_3 becomes $-u/2$, then it decreases and becomes one again for $\tau_3 = -r + u/2$.

In the cases 2) and 3) we get similar results.

RIASSUNTO (*)

Si esaminano, per una teoria in cui le particelle elementari sono rappresentate da prodotti dei campi fondamentali, le conseguenze di un gruppo d'invarianza. Il gruppo di invarianza è il gruppo unitario tre-per-tre. Si usa il calcolo tensoriale per analizzare le rappresentazioni, si definiscono i numeri quantici e si tenta di identificare alcune famiglie di particelle elementari per mezzo di rappresentazioni irriducibili.

(*) *Traduzione a cura della Redazione.*

IL NUOVO CIMENTO Vol. XV, N. 1 1° Gennaio 1960

The Field-Theoretical Definition of Nuclear Potential - II.

J. M. Charap (*) and S. P. Fubini

CERN - Geneva

(ricevuto il 22 Settembre 1959)

Summary. — The results of Part I are extended to include the exchange forces introduced by charged pions. It is shown that the scattering amplitude for a proton and neutron between which acts a potential with an exchange part, is related by symmetrization to that for the scattering of non-identical particles through an isotopic spin dependent potential. This enables the amplitude to be split into two parts, each of which obeys a Khuri-type dispersion relation if the appropriate momentum transfer is kept fixed. The method allows also the generalization of the Mandelstam representation to the case where exchange forces are present. A similar separation of the field-theoretic amplitude is possible into parts which satisfy one-dimensional dispersion relations without the pion singularities for negative energies. A comparison of the dispersion relations and the unitarity condition for the field theoretic amplitudes with those of the potential theory lead to a definition of the potential (which is partly direct, partly exchange) which is capable of simulating the field-theoretic amplitude for energies sufficiently below meson production threshold.

1. – Introduction.

In Part I (1) we considered the scattering of two scalar meson fields. This model deliberately avoids all difficulties connected with exchange forces and with spin. We were able to show that a comparison of the dispersion relations and the unitarity conditions for the field theory on the one hand and the potential theory on the other leads to a definition of a potential adequate to

(*) Now at Enrico Fermi Institute for Nuclear Studies, University of Chicago, Chicago, Ill., U.S.A.

(1) J. M. Charap and S. P. Fubini: *Nuovo Cimento*, **14**, 540 (1959).

reproduce the field-theoretic scattering amplitude for energies sufficiently below meson-production threshold.

In the present paper we shall extend this model to allow for the interaction involving charged mesons. The negative energy cut in the fixed momentum transfer dispersion relation now extends much further towards the origin, because proton and antineutron annihilation into pions is now permitted. It is clear that a direct local potential cannot simulate a scattering amplitude with these analytic properties for any reasonable energy range; the potential must be either non-local or, what comes to the same thing, strongly energy dependent. We are able to show that the non-locality required is of a very special kind, so that a superposition of a local direct potential and a local exchange potential, each of them energy-independent, is sufficient to give an approximation to the scattering amplitude below meson production threshold.

We shall leave over to a later paper the final complications associated with the spins.

The notation throughout this paper will be the same as in Part I, but we recall some of the more important definitions. The centre of mass 3-momentum $\boldsymbol{k}$ has modulus η, and the scattering angle in this reference frame is θ,

$$\tag{1.1} \begin{cases} s = E^2 = M^2 + \eta^2 \,, \\ t = -\frac{1}{2}\eta^2(1-\cos\theta) = -\Delta^2 \,, \\ u = -\frac{1}{2}\eta^2(1+\cos\theta) = -K^2 \,. \end{cases}$$

The potential, V, leads to a scattering matrix s related to the T-matrix by

$$\tag{1.2} \langle \boldsymbol{k}_2 | s | \boldsymbol{k}_1 \rangle = \delta^{(3)}(\boldsymbol{k}_2 - \boldsymbol{k}_1) - 2\pi i\, \delta(W_2 - W_1) \langle \boldsymbol{k}_2 | T | \boldsymbol{k}_1 \rangle \,.$$

In field theory the S-matrix is related to the scattering amplitude G by

$$\tag{1.3} \langle p_2 n_2 | S | p_1 n_1 \rangle = \delta^{(3)}(\boldsymbol{p}_2 - \boldsymbol{p}_1)\delta^{(3)}(\boldsymbol{n}_2 - \boldsymbol{n}_1) - \\ - 2\pi i\, \delta^{(4)}(p_2 + n_2 - p_1 - n_1) \frac{M^2}{E^2} \langle \boldsymbol{k}_2 | G | \boldsymbol{k}_1 \rangle \,.$$

We shall express matrices like T and G in terms of the scalar quantities η^2, t:

$$\tag{1.4} \begin{cases} \langle \boldsymbol{k}_2 | G | \boldsymbol{k}_1 \rangle = G(\eta^2, t) \\ \langle \boldsymbol{k}_2 | T | \boldsymbol{k}_1 \rangle = T(\eta^2, t) \end{cases}$$

or sometimes in terms of s, t.

2. – Exchange effects in potential scattering.

A) Before we discuss the effect of exchange forces, it is instructive to look at the exchange effect introduced by symmetrization when two particles scattering through a potential are identical (*). If the T-matrix for non-identical particles scattering through the potential is $T(s, t)$, that for identical particles is

$$\overline{T}(s, t) = \tfrac{1}{2}\{T(s, t) + T(s, u)\}\ . \tag{2.1}$$

Now it is well-known that $T(s, t)$ obeys a dispersion relation, the Khuri relation, for fixed t [2]; evidently $\overline{T}$ obeys no such simple relation for fixed t. We may ask what are the analytic properties of $\overline{T}$, and to find them we use the Mandelstam representation for T, which has recently been proved rigorously [3], *viz.*:

$$T(s, t) = \int\limits_{M^2}^{\infty} \mathrm{d}s' \int\limits_{\mu^2/4}^{\infty} \mathrm{d}t'\, \frac{A(s', t')}{(s' - s)(t' - t)}\ , \tag{2.2}$$

where the potential is supposed to be a superposition of Yukawa potentials with inverse ranges $\geqslant \mu$

$$V(t) = \int\limits_{\mu^2/4}^{\infty} \frac{\varrho(t')\,\mathrm{d}t'}{t' - t}\ . \tag{2.3}$$

Then

$$\overline{T} = \frac{1}{2}\int\limits_{M^2}^{\infty} \mathrm{d}s' \int\limits_{\mu^2/4}^{\infty} \mathrm{d}t'\, \frac{A(s', t')}{(s' - s)(t' - t)} + \frac{1}{2}\int\limits_{M^2}^{\infty} \mathrm{d}s' \int\limits_{\mu^2/4}^{\infty} \mathrm{d}u'\, \frac{A(s', u')}{(s' - s)(u' - u)}\ . \tag{2.4}$$

The one-dimensional dispersion relation obtained from this at fixed t is

$$\overline{T} = \int\limits_{0}^{\infty} \mathrm{d}\eta'^2\, \frac{B(\eta'^2, t)}{\eta'^2 - \eta^2 - i\varepsilon} - \int\limits_{\mu^2/4}^{\infty} \mathrm{d}\eta'^2\, \frac{C(\eta'^2, t)}{\eta'^2 - \eta^2 + t}\ , \tag{2.5}$$

(*) We recall that all particles are treated as bosons in the present paper.

(2) N. N. Khuri: *Phys. Rev.*, **107**, 1148 (1957).

(3) T. Regge: preprint; J. Bowcock and A. Martin: *Nuovo Cimento*, **14**, 516 (1959); R. Blankenbecker, M. L. Goldberger, N. N. Khuri and S. B. Treiman: preprint.

where

$$
(2.6)\qquad
\left\{
\begin{aligned}
B(\eta'^2, t) &= \frac{1}{2}\int\limits_{\mu^2/4}^{\infty} \mathrm{d}t'\, A(\eta'^2 + M^2, t') \left[\frac{1}{t'-t} + \frac{1}{t'+t+\eta'^2}\right],\\
C(\eta'^2, t) &= \frac{1}{2}\int\limits_{0}^{\infty} \mathrm{d}t'\, \frac{A(t', \eta'^2)}{\eta'^2 + t + t'}\,.
\end{aligned}
\right.
$$

This dispersion relation is formally identical with that of GOLDBERGER, NAMBU and OEHME [4], in that there is in addition to the cut for $\eta^2 > 0$, a cut on the left-hand side for $\eta^2 < -(\mu^2/4) - t$.

In this simple case we may summarize by observing that the scattering amplitude may be decomposed into two parts as in (2.1), the first satisfying a Khuri-type dispersion relation for fixed t, the second for fixed u. The more complicated form of the dispersion relation (2.5) for $\bar{T}$ itself originates in the fact that for fixed t the second term on the right hand side of (2.1) depends implicitly on s through $u = M^2 - s - t$.

B) Consider now the scattering of two particles, p and n, through a potential containing an exchange part. We wish to show that the analytic properties of the scattering amplitude T_{pn} are quite analogous to the ones discussed in subsection *A*): first, it is possible to separate

$$
(2.7)\qquad T_{pn} = T_D + T_E
$$

so that T_D satisfies a Khuri-type relation for fixed t and T_E for fixed u. Secondly, for fixed t, T_{pn} satisfies a GNO type of dispersion relation of the form (2.5).

To do this it is convenient to make use of the isotopic spin formalism. This enables us to consider p and n as two different charge states N_1 and N_2 of the same particle $\mathcal{N}$. Our problem is thus reduced to identical particle ($\mathcal{N}$-$\mathcal{N}$) scattering through an isotopic spin dependent potential. This is closely analogous to that treated in subsection *A*), the only additional complication being the charge degree of freedom possessed by each particle. We will show that the extra singularities coming from the exchange forces are just a consequence of symmetrisation.

We have seen that the simplest way of discussing the analytic properties of the scattering amplitude for identical particles is first to consider the scattering of non-identical particles, and then to symmetrize. This leads us to consider the scattering of two particles, $\mathcal{N}$ and Y, each with two charge states,

[4] M. L. GOLDBERGER, Y. NAMBU and R. OEHME: *Ann. Phys.*, **2**, 226 (1957).

through a potential which depends on isotopic spin

$$V(t) = V_D(t) + V_E(t)P\,, \tag{2.8}$$

where

$$P = \tfrac{1}{2}(1 + \boldsymbol{\tau}_1 \cdot \boldsymbol{\tau}_2)\,. \tag{2.9}$$

The Schrödinger equation for such a process is a pair of coupled differential equations, with only direct potentials. These equations can be trivially separated by considering states symmetric or antisymmetric in the exchange $Y \rightleftarrows \mathcal{N}$ (corresponding of course to isotopic singlet or triplet states). This is achieved by means of the projection operators:

$$\Lambda_{(\pm)} = \tfrac{1}{2}(1 \pm P) \tag{2.10}$$

and the separation yields two uncoupled Schrödinger equations with the effective potentials

$$V_{(\pm)} = V_D \pm V_E\,. \tag{2.11}$$

The resulting T-matrices, $T_{(\pm)}$ related by

$$T = T_{(+)}\Lambda_{(+)} + T_{(-)}\Lambda_{(-)} \tag{2.12}$$

will therefore have Mandelstam representations:

$$T_{(\pm)} = \int_{M^2}^{\infty} \mathrm{d}s' \int_{\mu^2/4}^{\infty} \mathrm{d}t' \, \frac{A_{(\pm)}(s', t')}{(s' - s)(t' - t)}\,. \tag{2.13}$$

It is also possible to separate T into a direct and an exchange part

$$T = T_D + T_E P\,, \tag{2.14}$$

$$\begin{cases} T_D = \tfrac{1}{2}(T_{(+)} + T_{(-)})\,, \\ T_E = \tfrac{1}{2}(T_{(+)} - T_{(-)})\,. \end{cases} \tag{2.15}$$

Evidently, T_D and T_E also have Mandelstam representations of the form (2.13) with weight functions $A_D(s', t')$, $A_E(s', t')$. In the iteration series for T_D and T_E are respectively the sums of terms in which the exchange potential acts an even or odd number of times.

Consider now the unitarity relation. Since the equations of motion are

separated by the projection operators $\Lambda_{(\pm)}$, the unitarity relations for $T_{(\pm)}$ take the same form as in a neutral theory, which we may symbolise as

$$\text{Im}\, T_{(\pm)} = \pi T^+_{(\pm)} * T_{(\pm)} \,. \tag{2.16}$$

Thus

$$\begin{cases} \text{Im}\, T_D = \pi(T^+_D * T_D + T^+_E * T_E)\,, \\ \text{Im}\, T_E = \pi(T^+_D * T_E + T^+_E * T_D)\,, \end{cases} \tag{2.17}$$

which confirms the even-odd character of T_D and T_E in the number of exchanges.

This completes the summary of the general properties of the amplitudes $T_{(\pm)}$ relevant to the $\mathcal{N}$-Y problem. It is now necessary to relate these quantities to the scattering amplitude for our original p-n problem. This is done by applying the appropriate symmetrization. The $\mathcal{N}$-$\mathcal{N}$ scattering amplitude $\overline{T}$ is

$$\overline{T} = \{T_{(+)}(s,t) + T_{(+)}(s,u)\}\Lambda_{(+)} + \{T_{(-)}(s,t) - T_{(-)}(s,u)\}\Lambda_{(-)}\,, \tag{2.18}$$

$$= \{T_D(s,t) + T_E(s,u)\} + \{T_E(s,t) + T_D(s,u)\}P\,. \tag{2.19}$$

The pp and pn scattering amplitudes are derived by taking matrix elements of P between the appropriate states

$$\begin{cases} (pn\,|P|\,pn) = 0\,, \\ (pp\,|P|\,pp) = 1\,, \end{cases} \tag{2.20}$$

so that

$$T_{\text{pn}} = T_D(s,t) + T_E(s,u)\,, \tag{2.21}$$

$$T_{\text{pp}} = T_{\text{nn}} = T_{\text{pn}}(s,t) + T_{\text{pn}}(s,u)\,. \tag{2.22}$$

Equations (2.21) shows clearly the striking analogy with the discussion of subsection A). The unsymmetrized amplitudes T_D and T_E have simple Mandelstam representations of the form (2.21), and satisfy a Khuri-type dispersion relation for fixed momentum transfer. The proton neutron scattering amplitude has the representation

$$T_{\text{pn}} = \iint \frac{A_D(s't')\,\mathrm{d}s'\,\mathrm{d}t'}{(s'-s)(t'-t)} + \iint \frac{A_E(s'u')\,\mathrm{d}s'\,\mathrm{d}u'}{(s'-s)(u'-u)}\,. \tag{2.23}$$

From eq. (2.23) it follows that for fixed t, T_{pn} satisfies a GNO type dispersion

relation:

$$(2.24)\qquad T_{\mathrm{pn}}(\eta^2, t) = \int_0^\infty \frac{\mathrm{d}\eta'^2}{\eta'^2 - \eta^2 - i\varepsilon}\,\alpha(\eta'^2, t) + \int_{\mu^2/4}^\infty \frac{\mathrm{d}\eta'^2}{\eta'^2 + \eta^2 + t}\,\beta(\eta'^2, t)\,,$$

where

$$(2.25)\qquad \alpha(\eta'^2, t) = \int_{\mu^2/4}^\infty \mathrm{d}t'\,\frac{A_D(M^2 + \eta'^2, t')}{t' - t} + \int_{\mu^2/4}^\infty \mathrm{d}u'\,\frac{A_E(M^2 + \eta'^2, u')}{u' + \eta'^2 + t}\,,$$

$$(2.26)\qquad \beta(\eta'^2, t) = \int_0^\infty \mathrm{d}y\,\frac{A_E(M^2 + y, \eta'^2)}{\eta'^2 + y + t}\,.$$

The separation of T_{pn} into parts corresponding to an even and odd number of exchanges has also been performed by Hamilton on the basis of perturbation theory (5). He also shows that each part satisfies a Khuri-type dispersion relation if the appropriate momentum transfer is kept fixed.

3. – Exchange effects in field theory.

In this section we relax some of the unphysical restrictions imposed on the model treated in Part I by allowing $\pi^\pm$ to be exchanged between the nucleons. In this case $\mathrm{p} + \bar{\mathrm{n}} \to \pi$'s is permitted, and the field-theoretic dispersion relations have the form derived in GNO with a pole at $\eta^2 = -(\mu^2/4) - t$ and a cut for $\eta^2 < -\mu^2 - t$. It is clear that this cannot be derived from a direct potential, which leads to a Khuri-type of dispersion relation with no singularities for negative energies. But we saw in the previous section that a potential with an exchange part gives rise to just such singularities, and so it is still possible that the T-matrix from a potential with exchange might be able to reproduce that of field theory at low energies.

In order to prove that this is indeed the case, one would have to identify the low-lying singularities of the two kinds of dispersion relations. This is not easy, because in the GNO form the exchange and direct forces are treated on entirely different bases. The simplest way is to demonstrate that the field-theoretic scattering amplitude can be split into two parts as in the previous section

$$(3.1)\qquad G_{\mathrm{pn}} = G_D(s, t) + G_E(s, u)\,,$$

(5) J. Hamilton: *Phys. Rev.*, **114**, 1170 (1959).

where G_D and G_E each satisfy dispersion relations similar to (I.3.1)

$$G_{D,E}(\eta^2, t) = G_{D,E}(0, t) + \frac{1}{\pi}\int_0^\infty \frac{\eta^2}{\eta'^2}\frac{\operatorname{Im} G_{D,E}(\eta'^2, t)\,d\eta'^2}{(\eta'^2 - \eta^2 - i\varepsilon)} - \frac{1}{\pi}\int_{M^2}^\infty \frac{\eta^2}{(u'+t)}\frac{\operatorname{Im} G^a_{D,E}(u', t)\,du'}{(u'+t+\eta^2)}\,. \tag{3.2}$$

This may be done in two ways. First, one may look at the perturbation expansion for G_{pn}; then G_D is the sum of all graphs of the type of Fig. 1*a* in which the net charge exchanged between the nucleons is zero, whilst G_E corresponds to graphs of the type of Fig. 1*b* in which there is an overall exchange of one unit of charge between the nucleons. Evidently this corresponds to an exchange of an even or an odd number of charged pions respectively, analogous to the occurrence of an even or an odd number of applications of the exchange potential in the corresponding treatment of the previous section.

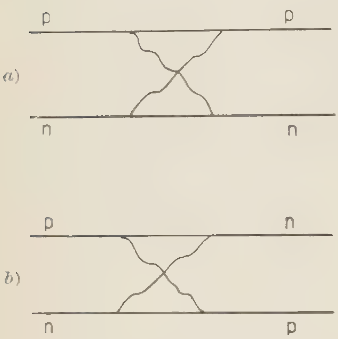

Fig. 1. – Graphs contributing to the direct and to the exchange parts of the scattering amplitude.

It is also clear that for graphs of the type of Fig. 1*a* $\mathrm{p}+\overline{\mathrm{n}}$ cannot give pions, whilst for graphs of the type of Fig. 1*b* $\mathrm{p}+\overline{\mathrm{p}}$ cannot give pions. This shows that there are no negative energy singularities coming from pion states for the dispersion relation at fixed t for the first type of graph, nor for fixed u for the second. This proves that G_D and G_E satisfy the relation (3.2) keeping the appropriate momentum transfer fixed.

A more compact and convenient way of looking at this same point is, as in Section 2, to attribute the separation (3.1) to the effect of a symmetrization. Here we again introduce to different nucleon types $\mathcal{N}$ and Υ, each having two different charge states, and interacting in the same way with an isotopic triplet pion field. Of course we do not allow transitions $\mathcal{N} \to \Upsilon + \pi$'s.

This model will allow us to consider both $\mathcal{N}$-Υ and $\mathcal{N}$-$\mathcal{N}$ scattering. Since the Hamiltonian for the model is symmetric under $\mathcal{N} \rightleftarrows \Upsilon$ exchange, $\mathcal{N}$-$\mathcal{N}$ scattering is obtained by properly symmetrizing the $\mathcal{N}$-Υ scattering amplitude (*).

(*) The $\mathcal{N}$-$\mathcal{N}$ scattering in this model is not exactly the same as that in the case in which the Υ-particle does not exist: this is because of the possibility of Υ-$\overline{\Upsilon}$ pairs in intermediate states. However, this can make no difference to the low-lying singularities which are all that are important for our problem. The pair effects can only

FONDAZIONE FRANCESCO SOMAINI
PRESSO IL TEMPIO VOLTIANO, A COMO

BANDI DI CONCORSI
AL PREMIO E ALLA BORSA PER IL 1961

Con lo scopo di premiare e incoraggiare nel nome di ALESSANDRO VOLTA gli studi di Fisica in Italia, la « Fondazione Francesco Somaini », presso il Tempio Voltiano a Como, indice i seguenti concorsi.

A) **Concorso al "Premio Triennale per la Fisica Francesco Somaini".**

1. – È aperto il Concorso al « Premio Triennale Francesco Somaini » per l'anno 1961, di L. 1 500 000 (un milione e cinquecentomila) nette, da assegnarsi al concorrente che, fra quelli che la Commissione Giudicatrice giudicherà in senso assoluto meritevoli del Premio per i risultati conseguiti nello studio della Fisica durante il Triennio 1º Luglio 1958-30 Giugno 1961, sia, a parere della Commissione stessa, il più meritevole.

2. – Al Concorso possono partecipare singolarmente i cittadini, d'ambo i sessi, italiani e svizzeri del Canton Ticino purchè di stirpe italiana, che siano di condotta morale incensurata e che non siano già risultati vincitori nel concorso immediatamente precedente. Sono esclusi dal Concorso i membri della Commissione Amministratrice e della Commissione Scientifica della « Fondazione Francesco Somaini ».

3. – Alla domanda, su carta libera, di partecipare al Concorso, diretta alla Commissione Amministratrice della Fondazione e contenente l'esatto recapito del concorrente, questi dovrà unire:

a) il certificato (di data non anteriore di tre mesi a quella di presentazione) di essere cittadino italiano o cittadino svizzero del Canton Ticino di stirpe italiana;

b) un breve *curriculum vitae* (in triplice copia);

c) i lavori, in triplice copia, che attestino le ricerche di Fisica svolte dal concorrente stesso nel triennio 1º Luglio 1958 - 30 Giugno 1961 e i risultati conseguiti;

d) gli altri eventuali documenti, titoli, lavori (in triplice copia) che il concorrente creda vantaggiosi a sé ai fini del concorso.

4. – La domanda, i documenti, i lavori ecc., presentati dai singoli concorrenti dovranno pervenire, tra il 1º Gennaio e le ore 12 del 1º Luglio 1961, alla Commissione Amministratrice della « Fondazione Francesco Somaini » a Como presso il Tempio Voltiano.

5. – I documenti di rito e una copia dei lavori presentati non verranno restituiti ai concorrenti.

6. – La Commissione Giudicatrice è formata dalla Commissione Scientifica della Fondazione, la quale è costituita da un Socio nazionale della Categoria III, Sezione A.

dell'Accademia Nazionale dei Lincei, nominato dall'Accademia stessa; da un Membro efttivo della Sezione IIª della Classe delle Scienze dell'Istituto Lombardo, nominato dall'Istituto stesso; dal Presidente della Società Italiana di Fisica o, in sua vece, da un Membro del Consiglio di Società nominato dal Consiglio stesso.

7. – Il premio è indivisibile.

8. – Il giudizio della Commissione Giudicatrice è inappellabile.

9. – Il Premio triennale per la Fisica potrà essere anche conferito a uno studioso che non abbia preso parte al concorso, ma sia stato segnalato da un Membro della Commissione Giudicatrice, con proposta motivata, come meritevole di particolare considerazione, oppure ritenuto degno di premio dalla Commissione Giudicatrice, indipendentemente da ogni segnalazione.

10. – Il conferimento del Premio al vincitore avrà luogo entro il Novembre 1961. Al vincitore sarà rilasciato inoltre il diploma e la medaglia in bronzo della Fondazione.

11. – La proclamazione del vincitore, e il conferimento del Premio, del diploma e della medaglia avranno luogo, se possibile, in occasione di Congressi di Fisica. La Commissione Amministratrice potrà chiamare il vincitore a illustrare pubblicamente, nella seduta di proclamazione e conferimento del Premio, i lavori presentati al Concorso.

B) Concorso alla "Borsa Francesco Somaini per lo studio della Fisica".

1. – È aperto il Concorso alla «Borsa Francesco Somaini» per l'anno 1961, di L. 750 000 (settecentocinquantamila) nette, per studi di Fisica, da assegnarsi al concorrente che, tra quelli che la Commissione Giudicatrice giudicherà in senso assoluto meritevoli della Borsa, verrà dalla Commissione stessa giudicato il più meritevole, sia per titoli, preparazione scientifica, lavori già svolti e risultati già conseguiti nella Fisica, anche per il vantaggio che gli studi, per i quali è richiesta la Borsa, possono portare allo sviuppo della Fisica, in Italia.

2. – Al Concorso possono prendere parte singolarmente i cittadini d'ambo i sessi, italiani e svizzeri del Canton Ticino purchè di stirpe italiana. Sono esclusi dal Concorso i membri della Commissione Amministratrice e della Commissione Scientifica della «Fondazione Francesco Somaini».

3. – Alla domanda, su carta libera, di partecipare al Concorso, diretta alla Commissione Amministratrice della Fondazione e contenente l'esatto recapito del concorrente, questi dovrà unire:

a) il certificato di essere cittadino italiano o cittadino svizzero del Canton Ticino di stirpe italiana;

b) un breve *curriculum vitae* (in triplice copia);

c) il certificato di laurea in Fisica o in Matematica e Fisica o in Ingegneria (in triplice copia);

d) l'indicazione scritta degli studi e delle ricerche in Fisica che, usufruendo della Borsa, intende svolgere e degli istituti, preferibilmente esteri, presso i quali intende a tal fine recarsi (in triplice copia);

e) i documenti e i lavori (in triplice copia) che attestino la sua preparazione e competenza nel campo degli studi e ricerche per il quale chiede la Borsa;

f) la dichiarazione olografa e firmata dal concorrente stesso di assumere l'impegno morale che, nel caso risulti vincitore, usufruirà della Borsa con le modalità stabilite da questo Bando e con lo scopo per cui la Borsa è stata posta a concorso dalla Fondazione e da lui richiesta;

g) gli altri documenti, titoli, lavori (in triplice copia) che il concorrente creda vantaggiosi a sè ai fini del concorso).

I certificati sopra indicati dovranno essere conformi alle vigenti disposizioni di legge, e debitamente legalizzati; quello di nazionalità dovrà essere in data non anteriore di tre mesi a quella di presentazione.

4. – La domanda, i documenti, i lavori presentati dai singoli concorrenti dovranno pervenire, tra il 1° Gennaio e le ore 12 del 1° Luglio 1961 alla Commissione Amministratrice della « Fondazione Francesco Somaini » a Como presso il Tempio Voltiano.

5. – I documenti di rito e una copia dei lavori presentati non verranno restituiti ai concorrenti.

6. – La Commissione Giudicatrice è la medesima nominata per il Concorso al « Premio triennale per la Fisica Francesco Somaini ».

7. – La Borsa è indivisibile.

8. – Il giudizio della Commissione Giudicatrice è inappellabile.

9. – La proclamazione del vincitore della Borsa avrà luogo, se possibile, in occasione di Congressi di Fisica.

10. – Il pagamento della Borsa al vincitore avverrà per metà entro il Novembre 1961, e per l'altra metà se gli studi per i quali la Borsa è stata richiesta si svolgeranno all'estero, avverrà un mese dopo l'inizio degli studi stessi, e se questi invece si svolgeranno in Italia, avverrà tre mesi dopo l'inizio.

11. – Il vincitore ha il dovere di iniziare gli studi per i quali ha richiesto la Borsa, entro due mesi dalla data di liquidazione della prima rata. La durata degli studi è di almeno tre mesi continuativi se essi sono svolti all'estero, e di almeno sei mesi continuativi se svolti in Italia.

All'inizio degli studi e delle ricerche presso l'Istituto scelto, il vincitore ha il dovere di far pervenire al Presidente della Commissione Amministratrice della Fondazione una dichiarazione in questo senso del Direttore dell'Istituto.

La Commissione Amministratrice ha il diritto, quando che voglia, di informarsi dal Direttore dell'Istituto presso il quale il vincitore si reca, del come proseguono gli studi e le ricerche del vincitore stesso.

Alla fine degli studi o delle ricerche, il vincitore ha il dovere di far pervenire alla Commissione Amministratrice della Fondazione una relazione (controfirmata dal Direttore dell'Istituto presso il quale ha compiuto i suoi studi o ricerche) che illustri l'attività svolta e i risultati conseguiti.

12. – Ricevuta la relazione di cui all'ultimo comma del precedente articolo, la Commissione Amministratrice della Fondazione rilascerà al vincitore il diploma di vincita del Concorso.

* * *

La procedura dei suddetti Concorsi è regolata secondo lo Statuto della Fondazione, il quale è ostensibile a Como presso il Tempio Voltiano ed è depositato negli atti del Notaio Dr. Raoul Luzzani di Como.

Como, dal Tempio Voltiano, il giorno 2 Agosto 1958.

Il Segretario
Conservatore del Tempio
GIUSEPPE BACCI

Il Presidente
Sindaco di Como
LINO GELPI

In this model the $\mathcal{N}$-Y scattering amplitude can be written (cf. (2.12))

$$G = G_{(+)} \Lambda_{(+)} + G_{(-)} \Lambda_{(-)} \,, \tag{3.3}$$

$G_{(+)}$ and $G_{(-)}$ satisfy dispersion relations of the form (3.2) for fixed t. The unitarity relation for elastic processes has the simple form

$$\mathrm{Im}^{\mathrm{el}}\, G_{(\pm)} = \pi \frac{M}{E} G^{+}_{(\pm)} * G_{\pm} \,. \tag{3.4}$$

The identical particle amplitude for $\mathcal{N}$-$\mathcal{N}$ scattering, $\bar{G}$, obtained by symmetrizing G is

$$\bar{G} = [G_{(+)}(s, t) + G_{(+)}(s, u)] \Lambda_{(+)} + [G_{(-)}(s, t) - G_{(-)}(s, u)] \Lambda_{(-)} = \tag{3.5}$$

$$= [G_D(s, t) + G_E(s, u)] + [G_E(s, t) + G_D(s, u)] P \,, \tag{3.6}$$

where

$$G_D = \tfrac{1}{2}(G_{(+)} + G_{(-)}) \,, \qquad G_E = \tfrac{1}{2}(G_{(+)} - G_{(-)}) \,, \tag{3.7}$$

G_D and G_E evidently also satisfy dispersion relations of the form (3.2), and it is clear that (3.1) is a special case of (3.6).

We need hardly remark on the close analogy between the equations derived in this section and those of the previous section.

4. – The definition of the potential.

In Section **4** of Part I we showed how the formal identity between the dispersion relation and the unitarity requirement for the field theory of proton-neutron scattering through neutral mesons and the scattering in a direct potential which obtains at sufficiently low kinetic energies, together with the requirement that the corresponding scattering amplitudes should be identical at zero kinetic energy, leads to a unique definition of the potential. An exactly parallel argument is used in this Section for the comparison between a field theory in which charged mesons also occur and a potential theory with exchange.

As was pointed out in the Introduction, the essential new feature introduced by the presence of charged pions is the pion continuum and pole for

contribute to the extremely short range part of the potential (as indeed hyperon-antihyperon pairs certainly do) and about this region the present theory can in any case say nothing.

proton-antineutron annihilation, which show up as additional singularities in the fixed t dispersion relation of GNO. The guiding principle of our method is to find a potential which leads to a scattering matrix with the same low-lying singularities as that of field theory. In Part I, when the negative energy cut in the field-theoretic fixed t dispersion relation began at $-M^2-t$, it was reasonable that the amplitude could be approximated by a local direct potential, which leads to a Khuri-type dispersion relation. Now that we have a pole at $-(\mu^2/4)-t$ and a cut starting at $-\mu^2-t$, a local direct potential, which cannot give rise to singularities on the negative axis, could only be useful in a very restricted energy range, so small in fact that an effective range theory would have a wider validity. To reproduce these negative energy singularities we must introduce some kind of non-locality into the potential. In general, of course, this would be very difficult, and indeed not very useful, as the general non-local potential is a function of two variables, just like the scattering amplitude itself. However, the separation of the field theoretic amplitude achieved in the previous Section into parts which, with the appropriate momentum transfer fixed, have one-dimensional dispersion relations exactly as in Part I *without* the pion continuum, together with the discussion of Section 2 on exchange potentials, make it clear that the very special kind of non-locality in a potential which is a superposition of a pure direct and a pure exchange part is adequate.

We saw in Section 2 how the T-matrix may be separated into $T_{(\pm)}$, each of which satisfies a Khuri-type dispersion relation

$$T_{(\pm)}(\eta^2, t) = V_{(\pm)}(t) + \frac{1}{\pi}\int_0^\infty \frac{\mathrm{Im}\, T_{(\pm)}(\eta'^2, t)\,\mathrm{d}\eta'^2}{\eta'^2 - \eta^2 - i\varepsilon}\,. \tag{4.1}$$

A similar separation of the field-theoretic amplitude into $G_{(\pm)}$ was shown in Section 3, and if we make the identification

$$T_{(\pm)}(0, t) = G_{(\pm)}(0, t) \tag{4.2}$$

we obtain

$$T_{(\pm)}(\eta^2, t) = G_{(\pm)}(0, t) + \frac{1}{\pi}\int_0^\infty \frac{\eta^2}{\eta'^2}\,\frac{\mathrm{Im}\, T_{(\pm)}(\eta'^2, t)\,\mathrm{d}\eta'^2}{\eta'^2 - \eta^2 - i\varepsilon}\,, \tag{4.3}$$

$$V_{(\pm)}(t) = G_{(\pm)}(0, t) - \frac{1}{\pi}\int_0^\infty \frac{\mathrm{Im}\, T_{(\pm)}(\eta'^2, t)\,\mathrm{d}\eta'^2}{\eta'^2}\,. \tag{4.4}$$

We also have the unitarity condition

$$\mathrm{Im}\, T_{(\pm)} = \pi\, T^+_{(\pm)} * T_{(\pm)}\,. \tag{4.5}$$

Exactly as in Part I, (4.3), (4.4) and (4.5) define the potential $V_{(\pm)}$ in terms of the zero-energy field-theoretic amplitude $G_{(\pm)}$: (4.3) and (4.5) are to be solved for $T_{(\pm)}$ which gives the potential through (4.4). Again we must show that this potential has a useful range of validity. A relation formally identical with (3.2) evidently exists for $G_{(+)}$, and this we may write as

$$G_{(\pm)}(\eta^2, t) = G_{(\pm)}(0, t) + \frac{1}{\pi}\int_0^\infty \frac{\eta^2}{\eta'^2}\, \frac{\mathrm{Im}^{\mathrm{el}}\, G_{(+)}(\eta'^2, t)\, \mathrm{d}\eta'^2}{\eta'^2 - \eta^2 - i\varepsilon} + 0\left(\frac{\eta^2}{\eta^2_{\mathrm{thresh}}}\right), \tag{4.6}$$

where

$$\eta^2_{\mathrm{thresh}} = M\mu + \frac{\mu^2}{4}. \tag{4.7}$$

For momenta sufficiently below the meson-production threshold η_{thresh}, (4.6) and the unitarity relation (3.4) are formally identical with (4.3) and (4.5), so we may conclude that

$$G_{(\pm)}(\eta^2, t) = T_{(\pm)}(\eta^2, t) + 0\left(\frac{\eta^2}{\eta^2_{\mathrm{thresh}}}\right), \tag{4.8}$$

i.e., that the potential is adequate to reproduce $G_{(\pm)}$ for energies sufficiently below meson-production threshold. Since the symmetrizations which lead to (2.18) on the one hand and to (3.5) on the other are equivalent, the potential

$$V = V_{(+)}\, \Lambda_{(+)} + V_{(-)}\, \Lambda_{(-)} \tag{4.9}$$

leads to a scattering matrix for identical particles which approximates well the field-theoretic nucleon-nucleon amplitude.

In Part I we gave a method of explicit construction of the potential as a superposition of Yukawa potentials

$$V(t) = \frac{1}{(2\pi)^3}\int \frac{\varrho(\sigma^2)\, \mathrm{d}\sigma^2}{\sigma^2 - 4t}, \tag{4.10}$$

in the physically interesting case when we may write

$$G(0, t) = \frac{1}{(2\pi)^3}\int \frac{F(\sigma^2)\, \mathrm{d}\sigma^2}{\sigma^2 - 4t}. \tag{4.11}$$

This method still applies, *mutatis mutandis*, to the present case, and we will not bore the reader with its repetition. We shall, however, illustrate an application to the one- and two-meson exchange potentials of perturbation theory.

The one-meson exchange amplitude is now

$$(4.12)\quad \begin{cases} G^{(1)}(\eta^2, t) = \boldsymbol{\tau}_1 \cdot \boldsymbol{\tau}_2\, G_0^{(1)}(\eta^2, t)\,, \\ \qquad\qquad\quad = (\Lambda_{(+)} - 3\Lambda_{(-)})\, G_0^{(1)}(\eta^2, t)\,, \end{cases}$$

where the suffix 0 indicates the corresponding quantity of the neutral theory. Similarly the amplitudes for the two-meson exchange uncrossed and crossed graphs are respectively

$$(4.13\text{A})\qquad G^{(A)}(\eta^2, t) = (\Lambda_{(+)} + 9\Lambda_{(-)})\, G_0^{(A)}(\eta^2, t)\,,$$

$$(4.13\text{B})\qquad G^{(B)}(\eta^2, t) = (5\Lambda_{(+)} - 3\Lambda_{(-)})\, G_0^{(B)}(\eta^2, t)\,.$$

In a direct application of perturbation theory, the potential is defined by a term-by-term identification of the T-matrix obtained by iterating a potential with the perturbation expansion of the field-theoretic scattering amplitude. This yields

$$(4{,}14)\qquad V^{(1)} = G^{(1)}\,,$$

$$(4.15)\qquad V^{(2)} = G^{(A)} + G^{(B)} + I\,,$$

where I is the iteration of $V^{(1)}$. In the neutral theory we saw that $G_0^{(1)}$, and hence $V_0^{(1)}$, is independent of η^2, and that in the adiabatic limit ($\eta^2 \ll M^2$) the same is true for $G_0^{(B)}$. Moreover, there is a cancellation between the energy-dependent parts of $G_0^{(A)}$ and I_0 which enables us to say that in the adiabatic limit $V_0^{(2)}$ is also energy-independent.

In the present case, it is clear from (4.12) and (4.14) that the one-meson exchange potential is energy-independent, being proportional to that of the neutral theory. Similarly in the adiabatic limit, $G^{(B)}$ is independent of η^2. It remains to show that the cancellation between the energy-dependent part of $G^{(A)}$ and I still occurs. But from (4.12)

$$(4.16)\quad \begin{cases} I = (\Lambda_{(+)} - 3\Lambda_{(-)})^2 I_0 \\ \quad = (\Lambda_{(+)} + 9\Lambda_{(-)}) I_0 \end{cases}$$

so that

$$(4.17)\quad \begin{cases} V^{(A)} = G^{(A)} + I \\ \qquad\; = (\Lambda_{(+)} + 9\Lambda_{(-)})\, V_0^{(A)} \end{cases}$$

is indeed energy-independent in the adiabatic limit.

It would, of course, have been possible to express the whole argument of this section in terms of a decomposition into direct and exchange parts instead

of using the projection operators $\Lambda_{(\pm)}$. The reason that the direct and exchange potentials can be separated in perturbation theory is that at each stage the field-theoretic amplitude is separated, and that since the lower-order potentials are already known and separated, so are their combinations in the iteration series.

We conclude this Section by stating the results of applying the method of Part I for obtaining the spectral-function for the potential, modified to deal with the separation by $\Lambda_{(\pm)}$. For $\sigma^2 < 4\mu^2$

$$\varrho(\sigma^2) = -\frac{g^2}{4M}\,\delta(\sigma^2-\mu^2)[\Lambda_{(+)}-3\Lambda_{(-)}]\,. \tag{4.18}$$

For $4\mu^2 < \sigma^2 < 9\mu^2$

$$\varrho(\sigma^2) = \frac{g^4}{64\pi^2}\,\frac{1}{M^3\mu^2}\,\frac{1}{\sigma}\left\{(\Lambda_{(+)}+9\Lambda_{(-)})\theta-(5\Lambda_{(+)}-3\Lambda_{(-)})\,\frac{\sin 2\theta}{2}\right\}+F_{\text{rescat.}}(\sigma^2)\,, \tag{4.19}$$

$$\theta(\sigma) = \operatorname{tg}^{-1}\left\{\frac{\mu}{M}\,\frac{\mu}{\sqrt{\sigma^2-4\mu^2}}\right\}. \tag{4.20}$$

The potential obtained from these equations by (4.10) yields a T-matrix which when symmetrized reproduces for $\eta^2 \ll \eta^2_{\text{thresh}}$ the one- and two-meson exchange parts of the field-theoretic problem.

5. – Conclusions.

In this second Part we have generalized the results of Part I to include the case of charged meson exchange, and have shown that apart from the appearance of exchange forces, the conclusions as to the existence of a potential are the same. Up to now all our considerations have been for spinless particles, and the discussion of the physically interesting case has been deferred to a further paper.

The reason for this is not entirely a consequence of the disinclination of the authors to tackle the considerable complexities introduced by the spin. The methods developed in Parts I and II cannot be extended immediately to the treatment of particles with spin because the mathematical tools required are not yet available. In particular the Khuri result has not yet been generalized to, for example, the spin orbit potential. Nor is it clear what choice of relativistic invariants gives the simple analytic properties required for the definition of the potential.

Only when these difficulties have been resolved will it be possible to extend

our formalism to cover the scattering of particles with spin. If no unexpected difficulties arise, we anticipate that a comparison of the ten field-theoretical dispersion relations with the corresponding ones for potential theory will lead to the definition of a potential

$$V = V_D + V_E P \,, \tag{5.1}$$

$$V_{D,E} = V^{(1)}_{D,E} + V^{(2)}_{D,E}(\boldsymbol{\sigma}_1 \boldsymbol{n})(\boldsymbol{\sigma}_2 \boldsymbol{n}) + V^{(3)}_{D,E}\, i(\boldsymbol{\sigma}_1 + \boldsymbol{\sigma}_2)\cdot \boldsymbol{n} + V^{(4)}_{D,E}(\boldsymbol{\sigma}_1 \boldsymbol{m})\boldsymbol{\sigma}_2 \boldsymbol{m}) + V^{(5)}_{D,E}(\boldsymbol{\sigma}_1 \boldsymbol{l})(\boldsymbol{\sigma}_2 \boldsymbol{l}) \,, \tag{5.2}$$

where the ten potentials $V^{i}_{D,E}$ are functions of the distance r alone (6). Since the μ/M corrections are not small, there is no reason to suppose that any of these ten potentials may be ignored.

* * *

During the preparation of Parts I and II, we have had many discussions with staff members at CERN and with visitors. We would particularly like to thank Professors G. F. CHEW, M. CINI, M. FIERZ and M. LÉVY.

One of us (J.M.C.) would like to express his gratitude to Professor FIERZ for his hospitality during his visits to the Theoretical Studies Division of CERN; he also acknowledges a D.S.I.R. Research Studentship, under which part of this work was conducted.

---

(6) Cfr. L. PUZIKOV, R. RYNDIN and YA. SMORODINSKIJ: *Journ. Exp. Theor. Phys.* **5**, 489 (1957).

RIASSUNTO

Si generalizzano i risultati della parte I al caso di forze di scambio prodotte da pioni carichi. L'ampiezza di scattering protone-neutrone dovuta ad un potenziale con una parte di scambio può ottenersi simmetrizzando l'ampiezza di scattering di due particelle non identiche dovuta ad un potenziale che dipende dallo spin isotopico. Questo ci permette di spezzare l'ampiezza in due parti ciascuna delle quali soddisfa una relazione di dispersione del tipo di Khuri nella variabile appropriata. Il metodo permette anche la generalizzazione della rappresentazione di Mandelstam al caso di forze di scambio. È possibile effettuare un'analoga separazione dell'ampiezza ottenuta in teoria dei campi in due parti che soddisfano a relazioni di dispersione unidimensionali senza singolarità pioniche per energie negative. Il confronto delle relazioni di dispersione e della condizione di unitarietà per le ampiezze di teoria dei campi con quelle di teoria del potenziale permette una definizione del potenziale (che è in parte diretto, in parte di scambio) che riproduce l'ampiezza della teoria dei campi al di-sotto della soglia per produzione di mesoni.

Solar Flare Effects on Cosmic Ray Intensity.

H. Ghielmetti, J. C. Anderson, J. M. Cardoso, J. R. Manzano, J. G. Roederer and O. R. Santochi

Comisión Nacional de Energía Atómica - Buenos Aires

(ricevuto il 24 Settembre 1959)

Summary. — In order to look for small cosmic ray increases associated with the development of solar flares, data from two neutron monitors located in the Southern Hemisphere were analysed. Solar flares of magnitude 2 or greater were selected, and the analysis was carried out for the detectors being located within the morning impact zones. The behaviour of nucleonic intensity, corrected for superposed daily variation, did not show any significative increase over the « zero hour ». This result contrasts with that of Firor, but agrees with the more recent paper by Towle and Lockwood. However, in the present work and for one station, there appears a significative peak if another type of correction is applied. Furthermore, another significative increase arises several hours after the onset of solar flares, closely peaked around the time of maximum in the mean daily variation. Data examined were extracted from records of the University of Tasmania at Mount Wellington (Hobart, Tasmania) and Mawson (Antarctica). The period investigated covers from July 1957 to August 1958.

1. – Introduction.

One of the most outstanding features of the large increases in cosmic ray intensity associated with important chromospheric outbursts on the sun, is that both events do not occur at comparable rates. Since the beginning of continuous recording of cosmic ray intensity there were only few instances of large cosmic ray increases, while the frequency of important solar flares is several times greater.

If one assumes that the intensity increases are due to a sudden production of high energy particles on the sun or near it, the fact that not every solar flare is accompanied by a rise in cosmic rays intensity might be explained by one or several of the following arguments:

a) The physical process occurring on the sun during the development of a solar flare has, in each case, a different effectiveness for particle acceleration. The resultant spectrum of the additional solar radiation changes in shape and total number of particles.

b) The accelerating mechanism being the same in each flare of similar magnitude, the electromagnetic conditions around the sun are different in each case. Only in few opportunities the accelerated particles would be able to reach the space beyond the solar atmosphere.

c) Electromagnetic conditions in interplanetary space are different in each case. Again, only in few instances the conditions would be favorable for particles to reach the earth.

d) Solar particles arrive at the earth in any case, but special conditions are required for the position of detectors, relative to the source, in order to show any increase in the recorded intensity.

The first calculated trajectories of particles initially travelling in the direction of the earth-sun line, already showed that argument *d*) is valid ([1,2]). In order to reveal a solar originated increase, the detector must be located within one of the impact zones ([3]). This however does not explain the rarity of reported increases, even less if one takes into account that the number of simultaneously operating observatories has increased substantially.

To find out whether *a*) or *b*) or both hold, it seems necessary to be sure of the true mechanism operating on the sun during a solar flare and of the correlated changes in magnetic fields around the sun. As to argument *a*), there are several plausible mechanisms proposed to explain how charged particles may be accelerated to cosmic ray energies during a solar flare ([4]); the point is to elucidate if physical conditions are reproduced for different flares, so that one accepted mechanism could operate with the same effectiveness in each case.

The « tunnel » theory of FORBUSH *et al.*, ([5]) that fits into *b*), is probably one of the few known arguments that might explain the scarcity of increases. Indeed, « tunnel » formation in a proper superposition of the sun's general field and the magnetic field of a sunspot would occur with a rare chance. However, new evidence about the permanent solar magnetic moment suggest that tunnels should arise more frequently than formerly supposed. Almost

([1]) A. EHMERT: *Zeits. f. Naturfor.*, **3***a*, 264 (1948).

([2]) A. SCHLÜTER: *Zeits. f. Naturfor.*, **6***a*, 613 (1951).

([3]) J. W. FIROR: *Phys. Rev.*, **94**, 1017 (1954) (and references therein).

([4]) S. F. SINGER: in *Progress in Cosmic Ray Physics*, edited by J. G. WILSON, vol. **4**, (Amsterdam, 1958), p. 313 (and references therein).

([5]) S. E. FORBUSH, P. S. GILL and M. S. VALLARTA: *Rev. Mod. Phys.*, **21**, 44 (1949).

every sunspot with a magnetic field of at least 1000 gauss is expected to give rise to a magnetic tunnel [6]. If this were the case, intensity increases should be expected after almost every solar flare, although the size of the increase cold be different from case to case, due to changes in energy spectra.

There is clear evidence that interplanetary magnetic fields influence the additional flux of charged particles arriving at the earth [7]. If this influence is the predominant one, it would be expected a difference in cosmic ray behaviour during solar flares in epochs of high or low solar activity. About the time of maximum solar activity, the increased number of magnetized beams and clouds ejected by the sun would prevent with a greater chance the arrival of solar particles at the earth.

Therefore it seems important to clarify whether a cosmic rays increase, no matter how small, is associated with every solar flare. The experimental difficulty lies in the fact that very small increases are masked by statistical fluctuations and by other superposed cosmic ray intensity variations.

DOLBEAR, ELLIOT and DAWTON [8] analysed data of a counter telescope, looking for increases associated with radio fade-outs accompanying solar flares. They found an increase of 0.3 percent, although impact zones were not taken into account. Near 1954 solar cycle minimum, analysing nucleonic component data at Climax, FIROR found an increase near 1 percent associated with solar flares of importance 1+ or greater, when the station was within a proper impact zone. In a similar analysis recently made by TOWLE and LOCKWOOD [9], no increase $\geqslant 0.25\%$ was found, even for flares of importance 2 or greater [*]. This result correspond to data obtained near 1957 solar maximum.

The task of the present work is to investigate the behaviour of nucleonic intensity recorded by two neutron monitors located in the Southern Hemisphere, during solar flares occuring at maximum solar activity.

2. – Sources of data.

In the present analysis, data reported by the University of Tasmania [**], since the beginning of the International Geophysical Year, were utilized. They correspond to two neutron monitors located at Mount Wellington (Hobart,

[6] L. I. DORMAN: *Cosmic Ray Variations* (Translation from Russian prepared by Technical Documents Liaison Office, Wright-Patterson Air Force Base, Ohio, 1957).

[7] P. MEYER, E. N. PARKER and J. A. SIMPSON: *Phys. Rev.*, **104**, 768 (1956).

[8] D. W. N. DOLBEAR, H. ELLIOT and D. I. DAWTON: *Journ. Atm. Terr. Phys*, **1**, 187 (1950).

[9] L. C. TOWLE and J. A. LOCKWOOD: *Phys. Rev.*, **113**, 641 (1959).

[*] This paper was known to the authors only when the present work was finished.

[**] We are very indebted to Prof. N. R. PARSONS for sending us the data.

Tasmania) and Mawson (Antarctica). Both stations supply pressure corrected hourly intensity values with standard deviations about 0.55 % or better.

Geomagnetic co-ordinates for the two stations are: 51.7° S, 225.2° E (Mt. Wellington), and 73.1° S, 103.0° E (Mawson); and geomagnetic time [10] is given by: $t+10.4$ h and $t+2.3$ h, where t is universal time (UT), in hours.

The epoch considered, around solar maximum, extends from July 1957 to August 1958.

3. – Selection criteria.

3·1. *Selection of solar flares.* – As it was shown by FIROR [3], the size of cosmic ray intensity increases during solar flares is correlated with flare magnitude. Due to this evidence, and to the fact that the maximum solar activity over the period considered *a priori* assures a reasonable number of events, we analysed only those solar flares of reported importance 2 or greater, confirmed by several observatories [11].

3·2. *Geomagnetic co-ordinate system.* – To locate the position of the detectors and to determine the variable position of the sun, the conventional geomagnetic system, in the centered dipole approximation, was utilized. Although the question of the effective co-ordinate system for cosmic rays is still open [12,13], PFOTZER showed that the conventional geomagnetic system was the better one to give account of the relative increases in cosmic ray intensity at several stations during the second phase of the cosmic ray disturbance following the solar flare of February 23, 1956 [14].

The geomagnetic latitude Φ_s of the source was determined using suitable curves deduced from McNish graphs [10].

3·3. *Impact zones.* – In order to locate the source position, the sun was considered as a point source, despite of the fact that evidence from large cosmic ray increases has shown that it acts as a finite source of considerable angular aperture (15° ÷ 30°) [3].

With the geomagnetic latitude Φ of the station and using Firor's graphs (curves 3 and 4 in ref. [3]) we determined both, the range in Φ_s for which the

[10] A. G. McNISH: *Terr. Magn. and Atm. Elec.*, **41**, 37 (1936).

[11] *Solar-Geophysical Data*, Part B (U. S. Dept. of Commerce, National Bureau of Standards, Central Radio Propagation Laboratory, Boulder Colorado, 1957, 1958).

[12] J. A. SIMPSON, F. JORY and M. PYKO: *Journ. Geophys. Res.*, **61**, 11 (1956).

[13] J. A. SIMPSON, K. B. FENTON, I. KATZMANN and D. C. ROSE: *Phys. Rev.* **102**, 1648 (1956).

[14] G. PFOTZER: *Suppl. Nuovo Cimento*, **8**, 220 (1958).

detector could be in an impact zone, and the range in geomagnetic time (*) corresponding to the center θ_c of this zone. Only the morning impact zones were considered, and as usual they were supposed to be four hours in width. If at the moment of the flare the detector was located within one of them, the event was classified as of type A. If the detector was at least one hour away from the edges of the zones (complementary region) the event was classified as of type B.

For Mawson (73° S) it was found that only the « 09 » impact zone is of importance. Effects are to be expected when Φ_s lies between 20° S and 35° S, roughly corresponding to particles of magnetic rigidities M between 1 and 3 GV. The center of the zone lies between 0930 and 1000 hours, in geomagnetic time.

For Mt. Wellington (52° S), effects are expected when the station is within the two morning impact zones: « 09 » and « 04 ». For the first one, we have roughly: $0° \leqslant \Phi_s \leqslant 20°$ N ($5 \leqslant M \leqslant 10$ GV) and $0630 \leqslant \theta_c \leqslant 0930$ hours. For the second one, $20°$ S $\leqslant \Phi_s \leqslant 20°$ N ($2.5 \leqslant M \leqslant 5$ GV) and θ_c ranges between 2330 and 0630 hours.

It must be noted that, in general, only « 09 » and « 04 » impact zones have been taken into account [3,9], in view of the greater relative increases to be expected in them. However, this is true only when the source is on the geomagnetic equator and the additional particles have a flat spectrum. The relative increases at the top of the atmosphere may be considerably different for certain Φ_s, as it has been shown by LÜST [15]. On the other hand, we must realize that the magnetic rigidity of the particles able to reach a particular point changes with Φ_s. As the effectiveness of a detector deeply immersed in the atmosphere depends on primary energy, the superposition of events occurring at distant epochs (different Φ_s), greatly affects the reliability of the method used to reveal such small increases.

3·4. *Procedure of analysis.* – Data were analysed according to the method of superposed epochs [16]. As « zero hour » we chose the interval containing the time of the first optical observation of the solar flare. The analysis was carried out for an interval extended from 6 hours before « zero hour » (preflare interval) to 12 hours after.

For each station, and each type of impact zone, hourly averages per column and percent deviations from the hourly mean over the preflare interval were

(*) The approximate relation $\theta = t + (\Lambda - 69)/15$ for geomagnetic time (t = UT; Λ geomagnetic longitude) was considered good enough for the present purposes [10].

(15) R. LÜST: *Phys. Rev.*, **105**, 1827 (1957) (and references therein).

(16) C. CHREE: *Phil. Trans.*, A **213**, 245 (1913); A **212**, 76 (1913).

calculated (*). Table I shows the number of events considered in each set of data. Standard errors of the percent deviations were in any case better than 0.15 %.

TABLE I.

Station	Type of impact zone	No. of events	Range of Φ_S	Range of M	Range of θ_c	Date of analysed events
Mawson	« 09 »	16	$20°$ S $\div$ $\div 35°$ S	$(1 \div 3)$ GV	$0930 \div$ $\div 1000$	1957: Oct., Nov., Dec. 1958: Jan., Feb.
	Compl. Region	20				
Mt. Wellington	« 09 »	16	$0° \div$ $\div 20°$ N	$(5 \div 10)$ GV	$0630 \div$ $\div 0930$	1957: Aug., Sep., Oct. 1958: Mar., Apr., Aug.
	Compl. Region	100				
	« 04 »	20	$20°$ S $\div$ $\div 20°$ N	$(2.5 \div 5)$ GV	$2330 \div$ $\div 0630$	1957: Aug., Sep., Oct., Nov., Dec. 1958: Jan., Mar., Apr., Jun., Aug.
	Compl. Region	69				

4. – Corrections.

It is obvious that the investigation of different time variations of cosmic ray primary intensity is made difficult due to their superposition; when attention is focused on one of them, it is not always easy to eliminate completely the influence of the others. In our case, we assumed that the most important additional variation to be considered is the daily variation, which masks the small effect looked for.

4·1. *Superposed daily variation.* – Data from Mawson were corrected with a daily variation averaged on five months around the main events; those from Mt. Wellington were corrected with a mean variation deduced from eleven months (see Table I).

As a check of this procedure, data from Mawson were tentatively grouped into months and corrected with a mean daily variation deduced from each month. No difference was found with respect to the use of an over all mean daily variation.

(*) A more reliable procedure, taking the percent deviations of hourly values from pre-flare mean in each single event, and then averaging these deviations over corresponding columns, showed no significative difference. This is due to the fact that hourly averages in each case do not differ in more than 5% from the over all hourly mean.

4·2. *Correction with « preceding day » daily variation.* – It is well known that daily variation suffers very irregular day to day changes, specially during times of increased solar activity. Furthermore, the appearence of an important solar flare generally means that a very disturbed area on the visible hemisphere on the sun has been acting since some days before. Days surrounding that of a flare are characterized by high geomagnetic activity and therefore by a daily variation different of the mean, showing significative increases in the amplitude of higher harmonics. For this reason, the weakest point in the usual correction arises in the use of a mean daily variation taken over a long period covering the intervals of the flares.

In order to take this into account, another way of correction was applied: data of each day preceding the occurrence of a flare (included in the former analysis) were superposed, taking in each case the same hours as in the nineteen hours interval around the flare. The percent deviations per column were subtracted from raw data. The resulting deviations were supposed to be free of daily variation effect, showing the true variation due to the additional radiation coming from the sun, if any.

As it will be shown below, there appears a significative difference in final results, if one applies correction *a*) or *b*).

5. – Results.

Table I gives details concerning analysed cases. In spite of the relatively large number of solar flares of importance 2 or greater during the considered period (*), the restrictions imposed decrease greatly the number of acceptable data.

Hourly deviations have a standard error of 0.15% or better; after correction *a*) the error is almost the same; correcting according to *b*) it increases to 0.20% or better. Notwithstanding, an increase of about 1% should be reliably detected.

Final results are presented in Figs. 1-8. Fig. 1 shows the mean daily

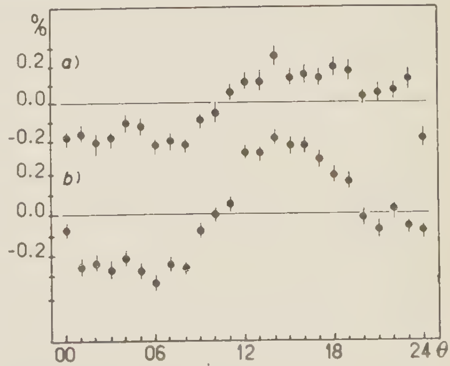

Fig. 1. – Mean daily variation of cosmic ray intensity at Mawson *a*) and Mt. Wellington *b*), calculated over several months around the selected solar flares (see Table I).

(*) During the last quarter of 1957 the relative sunspot number reached its highest value since many solar cycles.

variation during the period analysed (Mawson: curve a), Mt. Wellington: curve b)). Despite of the high flare activity in this epoch, no significative increase during morning hours is found, in contrast to Firor's results for daily variation of days of high flare activity index, obtained near the last solar minimum. However, flare activity index was not explicitly taken into account in the present case, so that these curves cannot be considered as evidence of no increase during morning hours.

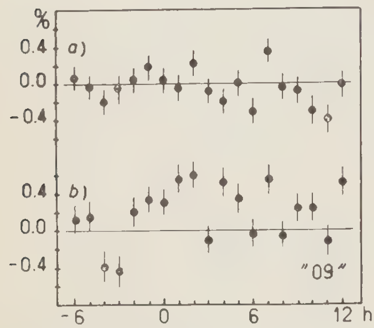

Fig. 2. – Cosmic ray intensity at Mawson (in the « 09 » impact zone) six hours before and twelve-hours after the onset of 16 solar flares. a) Corrected for mean solar cycle, b) corrected for « preceding day » effect.

Fig. 2 shows final results for Mawson in « 09 » impact zone, raw data being corrected with both above mentioned methods: mean daily variation a), and « preceding day » b). No statistically significative increase at « zero hour » is observed.

Figs. 3 and 4 show corrected deviations for Mt. Wellington in « 09 » and « 04 » impact zones, respectively. In both figures, a) corresponds to data corrected with mean daily cycle, and b) to those corrected with the « preceding day » method. Fig. 3 c) shows data after correction taking into account intensity variation from the day preceding and day following the occurrence of each flare. Here the correction applied results from hourly averages deduced by adding the total pairs of days embracing each flare, over the same intervals in UT corresponding to the flares. As it is apparent this procedure resembles the correction outlined under b), and it was applied simply to confirm the result obtained in Fig. 3 b).

Now, one considers only those results obtained after correction for mean daily cycle effect (Figs. 2 a), 3 a) and 4 a)), one comes to the conclusion that no significative effect is revealed in each of the three analysed cases. However, results are changed if one exclusively takes into account the mean

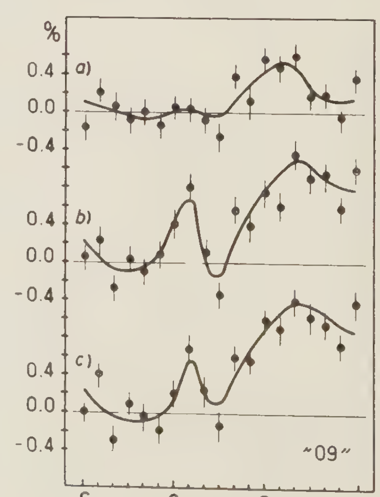

Fig. 3. – Cosmic ray intensity at Mt. Wellington (in the « 09 » impact zone) six hours before and twelve hours after the onset of 16 solar flares. a) Corrected for mean daily cycle; b) corrected for the « preceding » day effect; c) corrected with the pair of days around each solar flare (see text).

behaviour of the intensity for the day preceding that of the flare production. For Mt. Wellington in the « 09 » impact zone (Fig. 3 *b*)), there appears a significative peak around « zero hour » of 0.6%, similar to that found by Firor for Climax (48° N). For Mawson and Mt. Wellington in the « 04 » impact zone (Figs. 2 *b*) and 4 *b*)) it is more difficult to come to the same conclusions.

Fig. 5 shows the behaviour of the nucleonic intensity for events of type B, for Mawson (curve *a*)) and Mt. Wellington (curves *b*) and *c*)) within the complementary regions of both « 09 » and « 04 » impact zones. As it should be expected, no increase following the onset of solar flares is observed.

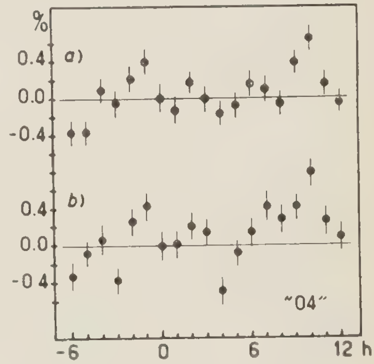

Fig. 4. – Cosmic ray intensity at Mt. Wellington (in the « 04 » impact zone) six hours before and twelve hours after the onset of 20 solar flares. *a*) Corrected for mean daily cycle; *b*) corrected for the « preceding day » effect.

Figs. 6, 7 and 8 show the distribution of « zero hours » for Mawson and Mt. Wellington. Hours in the dial are given in geomagnetic time. Weighted means of the position of « zero hours » are: 9.4 h for Mawson in the « 09 » impact zone, and 7.5 h and 1.4 h for Mt. Wellington in the « 09 » and « 04 » zones, respectively. This figures also show the distributions of « zero hours » for the stations in the complementary regions.

Further examination of Mt. Wellington curves (Figs. 3 and 4) indicates that, whatever the correction applied, the intensity increases nearly 1% several hours after the beginning of the flare. Considering the distribution in time of « zero hours » when the station is in the « 09 » impact zone (Fig. 7), one can deduce that this « second peak » appears near the time of the daily

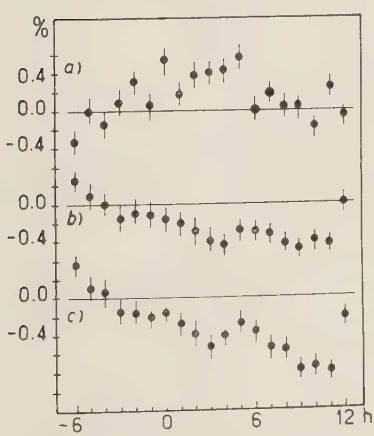

Fig. 5. – *a*): Cosmic ray intensity at Mawson, six hours before and twelve hours after the onset of 20 solar flares, occurring when the station was in the complementary region of the « 09 » impact zone (corrected for mean daily cycle). *b*) and *c*): Cosmic ray intensity at Mt. Wellington six hours before and twelve hours after the onset of 100 and 69 solar flares occurring when the station was in the complementary regions of the « 09 » and « 04 » impact zones, respectively. (Uncorrected for mean daily cycle).

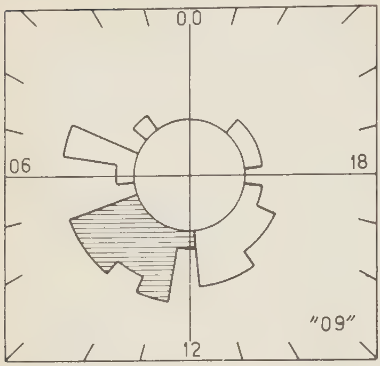

Fig. 6. – Distribution of « zero hours » at Mawson for solar flares occurring when the station was in the « 09 » impact zone (dashed area) and in the complementary region. It corresponds to Figs. 2 and 5*a*.

variation maximum. For the « 04 » impact zone, the distribution of « zero hours » is broader, nevertheless the peak falls again roughly after noon. This complementary result seems to be interesting enough for a further analysis. If this increase in amplitude of daily variation follows every solar flare, it would be revealed only when events are grouped in time over a more or less narrow distribution, as it is the case when impact zones are taken into account. This increase in amplitude after the production of a flare, if confirmed, could be explained by the same mechanism responsible for the normal daily variation, if one accepts that the additional radiation accelerated during the flare remains trapped for some time within the vicinity of the solar system.

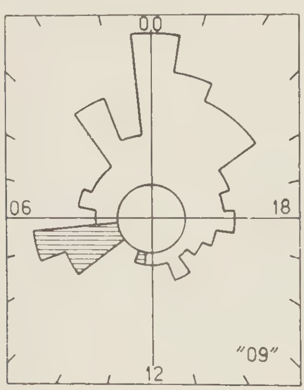

Fig. 7. – Distribution of « zero hours » at Mt. Wellington, for solar flares occurring when the station was in the « 09 » impact zone (dashed area) and in the complementary region. It corresponds to Figs. 3 and 5*b*.

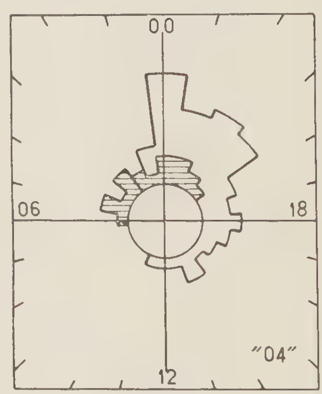

Fig. 8. – Distribution of « zero hours » at Mt. Wellington, for solar flares occurring when the station was in the « 04 » impact zone (dashed area) and in the complementary region. It corresponds to Figs. 4 and 5*c*.

6. – Conclusions.

From the results obtained above, it appears that if one considers the first point of view for data correction, namely, the use of an over all mean daily cycle properly weighted for « zero hours » distribution, our result agrees with

a similar analysis made by TOWLE and LOCKWOOD for Mt. Washington, and both differ from that given by FIROR. The first two were obtained near the 1957 solar maximum, while Firor's analysis was made near the 1954 solar minimum. If in both periods different mean electromagnetic conditions in interplanetary space existed, it would be easy to understand the observed difference in solar flare effects.

However, we believe that a better correction for daily variation is that of the « preceding day » method used in the present work. In this case, the fact that only Mt. Wellington in the « 09 » impact zone shows a significative increase at « zero hour » might be explained taking into account the difference in magnetic rigidities of the particles able to arrive at the detector for each of the three cases considered. It must be noted that during the 1954 solar minimum neither the correction for mean daily cycle applied by FIROR to his data, nor the correction with our « preceding day » method would reveal any significative difference, because of the low solar activity of the epoch and the lower magnitude of the flares analysed, which prevent large changes between the solar flare preceding days' behaviour and the mean behaviour of cosmic ray intensity.

In summary, one can arrive to the following conclusions from the results obtained in the present work:

1) In analysing small flare effects it is important to choose an appropriate method of correction to take into account the masking effect of daily variation. The results appear to be strongly dependent on the method employed, and we suggest to consider the behaviour of cosmic ray daily variation around each analysed interval as a more suitable index of the correction to be applied.

2) It seems reasonable to continue investigating small flare effects along the solar cycle in order to obtain further evidence. Besides, it would be interesting to confirm the existence of the post-flare increase, for detectors suitably located, after the onset of the solar flares.

3) The use of the method of superposed epochs in an analysis of small flare effects presents several disadvantages, mainly due to the mixing of events occuring under different conditions. Certainly, it would be most convenient to use devices of such high counting rates that conclusions might be driven from every individual solar flare. In this case, it would be unnecessary to correct for other superposed variations; hence no uncertainties related to their day to day changes would arise. Balloons and rockets carrying cosmic rays counters, recording very low energy particles, are suitable instruments to reveal these small increases, but the chance of a flare occuring during a

flight is low. Earth satellites equipped with cosmic rays detectors appear to be a better tool for the continuous recording of these small solar flare effects.

* * *

The authors wish to express their sincere appreciation to Prof. A. G. FENTON and Prof. N. R. PARSONS and to the staff of the Cosmic Ray Group of the University of Tasmania for sending them data of their cosmic ray stations on which this work is based. They also wish to thank Miss M. C. BAVA for her assistance in numerical calculations.

RIASSUNTO (*)

Per ricercare piccoli aumenti della radiazione cosmica associati allo sviluppo di brillamenti solari, abbiamo analizzato i dati registrati da due contatori di neutroni situati nell'emisfero meridionale. Si scelsero brillamenti di grandezza 2 o superiore, e l'analisi fu fatta solo quando i contatori si trovavano nelle zone d'impatto mattutine. Il comportamento dell'intensità dei nucleoni, al netto di correzione per la variazione giornaliera sovrapposta, non mostrò alcun aumento sensibile all'« ora zero ». Questo risultato è in contrasto con quello di FIROR, ma è in accordo con il più recente scritto di TOWLE e LOCKWOOD. Però nel presente lavoro e per una delle stazioni compare un sensibile picco se si applica un altro tipo di correzione. Per di più un altro sensibile aumento si verifica parecchie ore dopo l'insorgere dei brillamenti, con un picco molto stretto attorno al periodo di massimo della variazione giornaliera media. I dati esaminati vennero ricavati dalle registrazioni fatte a cura dell'Università di Tasmania a Mount Wellington (Hobart, Tasmania) e a Mawson (Antartide). Il periodo esaminato va dal luglio 1957 all'agosto 1958.

(*) *Traduzione a cura della Redazione.*

IL NUOVO CIMENTO Vol. XV, N. 1 1° Gennaio 1960

Analytic Properties of $l \neq 0$ Partial Wave Amplitudes for a Given Class of Potentials.

A. Martin
CERN - Geneva

(ricevuto l'8 Ottobre 1959)

Summary. — A preceding work on the analytic properties of the S wave amplitude for a family of potentials including the Yukawa case is extended to higher waves. Apart from a transformation in order to eliminate the centrifugal term, the method is essentially the same as in the S wave case. It makes use of the Laplace transforms of two quantities related to independent solutions of the Schrödinger equation. The singularities in the upper half complex k plane are bound states on the imaginary axis plus a cut $i(\mu/2) \to i\infty$. In any direction (except perhaps the cut) $\lim\limits_{|k|\to\infty} S(k)=1$, so it is possible to write dispersion relations.

1. – Introduction.

In a preceding paper designated hereunder by A (1), we have studied the analytic properties of the S wave scattering amplitude for the family of potentials:

$$V(r) = \exp[-\mu r]\int\limits_0^\infty C(\alpha)\exp[-\alpha r]\,\mathrm{d}\alpha\,, \tag{1}$$

with

$$|C(\alpha)| < M\,.$$

It was shown that the scattering amplitude is holomorphic in the upper half complex k plane, except for poles due to bound states on the imaginary

(1) A. Martin: *Nuovo Cimento*, **14**, 403 (1959).

axis and a cut from $i\mu/2$ to $i\infty$; the analytic properties in the lower half plane follow by use of symmetry properties. Furthermore, it was shown that in any direction, the scattering amplitude goes to zero as $|k|\to\infty$. We shall now prove that these properties hold for any partial wave. Due to the presence of the centrifugal term in the Schrödinger equation, the treatment presented in A must be seriously modified. Such a term cannot be merely included in the potential, since it is too singular at the origin and does not decrease fast enough at infinity.

2. – Summary of the method used in the S wave case.

In A it was shown that the scattering matrix can be written:

$$S(k)=\frac{f(0,k)}{g(0,k)}=\frac{f(0,k)}{f(0,-k)}\,, \tag{2}$$

where

$$f(r,k)\exp[-ikr]$$

is a solution of the Schrödinger equation, such that

$$\lim_{r\to\infty} f(r,k)=1\,, \tag{3}$$

$f(r,k)$ was expressed in terms of its Laplace transform:

$$f(r,k)-1=\int_0^\infty \exp[-\alpha r]\,\varrho_k^s(\alpha)\,\mathrm{d}\alpha\,, \tag{4}$$

where ϱ satisfies the equation:

$$\varrho_k^s(\alpha)\,\alpha(\alpha+2ik)=C(\alpha-\mu)+\int_0^{\alpha-\mu} C(\alpha-\mu-\beta)\,\varrho_k^s(\beta)\,\mathrm{d}\beta\,, \tag{5}$$

(notice a slight change in notations), which means, in particular, that $\varrho_k^s(\alpha)=0$ for $0<\alpha<\mu$. Equation (5) permits to compute by recursion $\varrho_k^s(\alpha)$ for any arbitrarily large value of α, and gives the information needed to establish the analytic properties of $f(r,k)$ and $f(r,-k)$. Moreover, it was shown that the zeros of $g(0,k)$ in the upper half plane, correspond to bound states with the

wave function:

$$u(r) = g(r, k) \exp[ikr]. \tag{6}$$

These poles cannot be outside the imaginary axis, because

$$|u' - iku|^2_{r_0} \geqslant 4 \operatorname{Im} k (\operatorname{Re} k)^2 \int_0^{r_0} |u|^2 \mathrm{d}r, \tag{7}$$

cannot be satisfied for $r_0 \to \infty$, $\operatorname{Im} k \neq 0$, $\operatorname{Re} k \neq 0$.

3. – Necessary changes in view of an extension to higher waves.

It is still possible to define two independent solutions of the Schrödinger equation

$$f(r, k) \exp[-ikr], \qquad f(r, -k) \exp[ikr],$$

satisfying the equation:

$$f'' - ikf' = \left[\frac{l(l+1)}{r^2} + V(r)\right] f. \tag{8}$$

One still writes:

$$f(r, k) = 1 + \int_0^\infty \varrho_k(\alpha) \exp[-\alpha r] \mathrm{d}\alpha, \tag{9}$$

but equation (5) is replaced by:

$$\varrho_k(\alpha)\alpha(\alpha + 2ik) = \tag{10}$$

$$= l(l+1)\alpha + C(\alpha - \mu) + \int_0^\alpha [l(l+1)(\alpha - \beta) + C(\alpha - \mu - \beta)] \varrho_k(\beta) \mathrm{d}\beta.$$

It is no longer true that $\varrho = 0$ for $\alpha < \mu$. One problem is to study the solution of equation (10), another one is to define, from this solution the scattering matrix. In the general case, $f(r, k)$ and $f(r, -k)$ are singular at the origin and behave like r^{-l}. Therefore one has to define $S(k)$ by a limiting process:

$$S(k) \times S_0(k) = \lim_{r \to 0} \frac{1 + \int_0^\infty \exp[-\alpha r] \varrho_k(\alpha) \mathrm{d}\alpha}{1 + \int_0^\infty \exp[-\alpha r] \varrho_{-k}(\alpha) \mathrm{d}\alpha}, \tag{11}$$

$S_0(k)$ is a factor, independent of the potential, such that $S(k)=1$ when no interaction is present. It will be shown in Section **5** that (11) can be replaced by a more convenient expression in terms of the asymptotic behaviour of $\varrho_k(\alpha)$ and $\varrho_{-k}(\alpha)$ for large α.

4. – Study of the equation defining $\varrho_k(\alpha)$.

In equation (10), the centrifugal term is treated on the same footing as the potential itself. This should be avoided, since for $V(r)=0$ the solution of the Schrödinger equation can be expressed in terms of half integer order Bessel functions. Then $f(r, k)$ and $f(r, -k)$ are polynomials of degree l of the quantity $1/ikr$. From this one can deduce by Laplace transformation:

$$\varrho_k^0(\alpha) = \frac{1}{(2ik)l!}\left(\frac{\mathrm{d}}{\mathrm{d}X}\right)^{l+1}[X(X+1)]^l, \tag{12}$$

where $X=\alpha/2ik$ (²); for $l=0$, $\varrho_k^0(\alpha)=0$.

Equation (10) can now be transformed in the following way: we introduce

$$y(\alpha) = 1 + \int_0^\alpha \varrho(\alpha)\,\mathrm{d}\alpha\,,$$

and we take the derivative of equation (10). This gives:

$$\alpha(\alpha+2ik)y'' + \{\alpha[\alpha+2ik]\}'y' - l(l+1)y = \\ = \frac{\mathrm{d}C(\alpha-\mu)}{\mathrm{d}\alpha} + \int_0^{\alpha-\mu}\frac{\mathrm{d}C(\alpha-\beta-\mu)}{\mathrm{d}\alpha}\,\varrho_k(\beta)\,\mathrm{d}\beta\,. \tag{13}$$

This equation can now be treated as a second order differential equation with « known » right hand side. The homogeneous equation has known solutions:

$$\begin{cases} y_1(\alpha) = \dfrac{1}{l!}\left(\dfrac{\mathrm{d}}{\mathrm{d}X}\right)^l[X(X+1)]^l\,, \\[2ex] y_2(\alpha) = y_1(\alpha)\displaystyle\int_\alpha^\infty \frac{\mathrm{d}\beta}{y_1^2(\beta)\beta(\beta+2ik)}\,. \end{cases} \tag{14}$$

Then one can get the general solution of equation (13).

By inspection of equation (10) one sees that the right boundary condition

(²) W. Magnus and F. Oberettinger: *Formulae and Theorems of the Functions of Mathematical Physics* (Chelsea, 1954), pp. 19, 22, 122, 124.

is that $\varrho(\alpha)$ and $\varrho_0(\alpha)$ coincide for $\alpha < \mu$. This gives the solution:

$$y = y_1(\alpha) + \int_0^\alpha [y_1(\alpha)\, y_2(\beta) - y_1(\beta)\, y_2(\alpha)] \frac{\mathrm{d}F(\beta)}{\mathrm{d}\beta}\, \mathrm{d}\beta\,,$$

where

$$F(\alpha) = C(\alpha - \mu) + \int_0^{\alpha-\mu} C(\alpha - \beta - \mu)\, \varrho_k(\beta)\, \mathrm{d}\beta\,.$$

This expression can be transformed by integration by parts, differentiation, and inversion of order of integration to get:

$$\varrho_k(\alpha) = \varrho_k^0(\alpha) + \frac{C(\alpha-\mu)}{\alpha(\alpha+2ik)} + \int_\mu^\alpha K(\alpha, \beta)\, C(\beta - \mu)\, \mathrm{d}\beta + \int_0^{\alpha-\mu} \mathrm{d}\gamma\, \varrho_k(\gamma) \left[\frac{C(\alpha-\gamma-\mu)}{\alpha(\alpha+2ik)} + \int_{\gamma+\mu}^\alpha K(\alpha, \beta)\, C(\beta-\gamma-\mu)\, \mathrm{d}\beta\right], \tag{15}$$

where

$$K(\alpha, \beta) = y_1'(\alpha)\, y_2'(\beta) - y_1'(\beta)\, y_2'(\alpha) \qquad (y_1' \equiv \varrho^0).$$

This new integral equation has the same structure as the S wave equation (5): when $\varrho(\alpha)$ is known for $\alpha < \alpha_0$ one can get $\varrho(\alpha)$ for $\alpha < \alpha_0 - \mu$ by inserting the known function in the right hand side. The derivation we give assumes that $C(\alpha)$ is continuous and derivable, but the final result is independent of this assumption; the derivative of C is not present in equation (15). As a check we see that $\varrho = \varrho^0$ when $C \equiv 0$, and the case $l = 0$ gives equation (5). Equation (15) has a well defined solution when $\alpha + 2ik$ can never vanish, α being in the range $\mu - +\infty$. This means that when k is outside the cut $(i\mu/2) - i\infty$, the solution exists.

Let us now study the behaviour of $\varrho_k(\alpha)$ for large α. It is perhaps more convenient to use equation (15) in the following form:

$$R_K(\alpha) = 1 + F_k(\alpha) + \int_0^{\alpha-\mu} \mathrm{d}\gamma\, R_k(\gamma)\, G_k(\gamma, \alpha)\,, \tag{15'}$$

with

$$R_k(\alpha) = \frac{\varrho_k(\alpha)}{\varrho_k^0(\alpha)}\,,$$

$$F_k(\alpha) = \frac{C(\alpha-\mu)}{y_1'(\alpha)\, \alpha(\alpha+2ik)} + \int_\mu^\alpha \left[y_2'(\beta) - \frac{y_2'(\alpha)}{y_1'(\alpha)}\, y_1'(\beta)\right] \cdot C(\beta - \mu)\, \mathrm{d}\beta\,,$$

$$G_k(\gamma, \alpha) = \frac{y_1'(\gamma)\, C(\alpha-\gamma-\mu)}{y_1'(\alpha)\, \alpha(\alpha+2ik)} + y_1'(\gamma) \int_{\gamma+\mu}^\alpha \left[y_2'(\beta) - y_1'(\beta)\, \frac{y_2'(\alpha)}{y_1'(\alpha)}\right] C(\beta-\gamma-\mu)\, \mathrm{d}\beta\,.$$

Here we just state the result which will be proven in Appendix I: in the union of the domains,

$$|\mathrm{Arg} - ik| \geqslant \varepsilon \,, \qquad |k| > \frac{\mu}{2} - \varepsilon \,,$$

(this excludes the cut $i(\mu/2) - i\infty$),

$$\lim_{\alpha\to\infty} R_k(\alpha)$$

is a finite holomorphic quantity, and

$$\lim_{|k|\to\infty} [\lim_{\alpha\to\infty} R_k(\alpha)] = 1 \,. \tag{16}$$

The proof of this result is based on upper and lower bounds of y_1, y_1', y_2, y_2' giving upper bounds of $F_k(\alpha)$ and $G_k(\gamma, \alpha)$.

5. - Connection between the solutions of equations (15′) and the scattering matrix.

We want to prove here that definition (11) of the scattering matrix is equivalent to the following:

$$S(k) = \frac{\lim\limits_{\alpha\to\infty} R_k(\alpha)}{\lim\limits_{\alpha\to\infty} R_{-k}(\alpha)} \,. \tag{17}$$

If we assume first that these two limits are different from zero, this means that

$$\varrho_k(\alpha) \simeq C_k \alpha^{l-1} \,,$$

$$\varrho_{-k}(\alpha) \simeq C_{-k} \alpha^{l-1} \,,$$

then it is not difficult to prove that

$$\lim_{r\to 0} r^l \frac{1 + \int\limits_0^\infty \exp[-\alpha r]\, \varrho_k(\alpha)\, \mathrm{d}\alpha}{(l-1)!\, C_k} = 1 \,,$$

hence, from (11):

$$S(k)\, S_0(k) = \frac{C_k}{C_{-k}} = \frac{\lim\limits_{\alpha\to\infty} R_k(\alpha)}{\lim\limits_{\alpha\to\infty} R_{-k}(\alpha)} \lim_{\alpha\to\infty} \frac{\varrho_k^0(\alpha)}{\varrho_{-k}^0(\alpha)} \,.$$

The last factor in this equation is easily seen to be $(-1)^l$, from equation (12),

so that:

$$S_0(k) = (-1)^l \,,$$

$$S(k) = \frac{\lim\limits_{\alpha\to\infty} R_k(\alpha)}{\lim\limits_{\alpha\to\infty} R_{-k}(\alpha)} \,.$$

It remains to prove that whenever $S(k)$, as defined by equation (11), has a pole, this pole appears also in the new definition (17): it is shown in Appendix II that whenever

$$\lim_{\alpha\to\infty} R_{-k}(\alpha) = 0 \,,$$

i.e. when

$$\lim_{\alpha\to\infty} \alpha^{-l+1} \varrho_{-k}(\alpha) = 0 \,,$$

$$\lim_{r\to 0}\left[1 + \int_0^\infty \exp\left[-\alpha r\right] \varrho_{-k}(\alpha)\, \mathrm{d}\alpha\right] \equiv \lim_{r\to 0} f(r, -k) = 0 \,.$$

6. – Final results.

From Section **4** and **5**, we obtain that $S(k)$ is an analytic function in the upper half plane with a cut going from $i\mu/2$ to $i\infty$, and poles corresponding to

$$\lim_{r\to 0} f(r, -k) = 0 \,.$$

The reasoning used in the S wave case to show that these poles correspond to bound states is still valid. At infinity, except perhaps in the direction $\mathrm{Re}\, k = 0$, $S(k)$ becomes equal to unity, so that it is possible to write a dispersion relation for the quantity $(S(k) - 1)/2i$ by following the contour indicated in Fig. 1 in the k^2 complex plane (the contribution from the large circle vanishes).

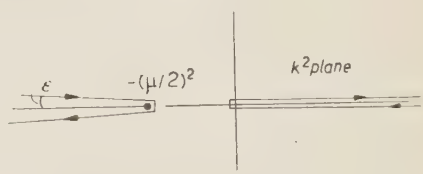

Fig. 1.

It is perhaps worth-while to add one remark: the quantity $\lim\limits_{\alpha\to\infty} R_{-k}(\alpha)$ has the phase of $\exp\left[-i\delta(k)\right]$ for real k, and is regular in the whole upper half plane; its zeros correspond to bound states. Application of the Cauchy formula to the function

$$\frac{\mathrm{d}}{\mathrm{d}k}\left[\lim R_{-k}(\alpha)\right] / \lim R_{-k}(\alpha) \,,$$

leads to the Levinson theorem

$$\delta(0) - \delta(\infty) = \pi \times \text{number of bound states} \,.$$

The properties derived here are essentially the same as those obtained in the S wave case. Of course these results could be derived from the Mandelstam representation of the total scattering amplitude [3] by taking the average of this amplitude over the angles, conveniently weighted by a Legendre polynomial.

* * *

The author would like to thank Professor GLASER and Dr. KANELLOPOULOS for encouraging him to extend the S wave method to higher angular momenta.

APPENDIX I

a) Upper and lower bounds for y_1, y_1', y_2, y_2'.

From equation (14)

$$y_1(\alpha) = \frac{1}{l\,!}\left(\frac{\mathrm{d}}{\mathrm{d}X}\right)^l [X(X+1)]^l\,,$$

where

$$X = \frac{\alpha}{2ik}\,,$$

one sees that the roots of $y_1(\alpha) = 0$ lie on a straight line between $\alpha = 0$ and $\alpha = -2ik$. This is sufficient to show

$$\text{(I.1)}\qquad \begin{cases} |y_1(\alpha)| < \text{const}\,[|X|+1]^l\,, \\ \text{and, in the same way} \\ |y_1'(\alpha)| < \text{const}\,\dfrac{[|X|+1]^{l-1}}{2k}\,. \end{cases}$$

Now, provided $\alpha > \mu$, it can be shown that if k lies inside the union of the domains $|\text{Arg} - ik| > \varepsilon$, $|k| < (\mu/2) - \varepsilon$, which excludes the cut,

$$C_1 < \left|\frac{\dfrac{\alpha}{2ik} + X_0}{\dfrac{\alpha}{2ik} + 1}\right| < C_2\,,$$

if $0 < \varepsilon < X_0 < 1 - \varepsilon$.

---

(3) T. REGGE: preprint; R. BLANKENBECKLER, M. L. GOLDBERGER, N. N. KHURI and S. B. TREIMAN: preprint; J. BOWCOCK and A. MARTIN *Nuovo Cimento*, **14**, 516 (1959).

So it is also possible to get lower bounds of $|y_1(\alpha)|$ and $|y_1'(\alpha)|$:

$$(\mathrm{I}.2)\qquad \begin{cases} \text{Const} < \dfrac{|y_1|}{[|X|+1]^l} < \text{Const}\,, \\[2ex] \text{Const} < \dfrac{2\,|y_1'|\,|k|}{[|X|+1]^{l-1}} < \text{Const}\,, \end{cases}$$

in the above defined domain. By substitution in

$$y_2(\alpha) = y_1(\alpha)\int\limits_{\alpha}^{\infty}\frac{\mathrm{d}\beta}{\beta[\beta+2ik]\,y_1^2(\beta)}$$

and in $y_2'(\alpha)$, of these upper and lower bounds, one can prove in the same way, *in the same domain:*

$$(\mathrm{I}.3)\qquad \begin{cases} |y_2(\alpha)| < \dfrac{\text{Const}}{\alpha[|X|+1]^l}\,, \\[2ex] |y_2'(\alpha)| < \dfrac{\text{Const}}{|2k|^2[|X|+1]^{l-1}|X|}\,. \end{cases}$$

b) *Upper bounds for the quantities entering in the integral equation* (15′).

Keeping in mind $|C(\alpha)| < M$ and using the bounds obtained in *a*), it is possible to get upper bounds for $F_k(\alpha)$ and $G_k(\gamma,\alpha)$. It must be noticed that $F_k(\alpha)$ is non-vanishing for $\alpha > \mu$ and that $G_k(\gamma,\alpha)$ is non-vanishing for $\alpha - \mu > \gamma > 0$. Then, by straightforward but tedious calculations, one gets

$$(\mathrm{I}.4)\qquad |F_k(\alpha)| < \frac{\text{Const}}{\left[\dfrac{\mu}{2|k|}+1\right]^l}\,.$$

This is not always sufficient: a more complicated bound can be obtained

$$(\mathrm{I}.5)\qquad F_k(\alpha) < \frac{\text{Const}}{|k|\left[\dfrac{\mu}{2|k|}+1\right]^{l+1}} + \frac{\text{Const}}{\left[\dfrac{\alpha}{2|k|}+1\right]^l}\,,$$

which means that

$$\lim_{|k|\to\infty}\,[\lim_{\alpha\to\infty} F_k(\alpha)] = 0$$

inside the domain excluding the cut.

It can also be shown:

$$(\mathrm{I}.6)\qquad |G_k(\gamma,\alpha)| < \frac{\text{Const}}{(\gamma+\mu)(\gamma+\mu+2|k|)}\,.$$

c) *Existence and analyticity of* $\lim_{\alpha\to\infty} [R_k(\alpha)]$ *outside the cut.*

The bounds obtained in *b*) will be used first to prove that $R_k(\alpha)$ is uniformly bounded, for any α, in the domain already defined for k. From *b*), one sees that

$$|R_k(\alpha)| < C_1 + \int_0^{\alpha-\mu} \frac{|R_k(\gamma)|\, C_2}{(\gamma+\mu)^2}\, d\gamma\,,$$

where C_1 is a constant larger than unity.

So $R_k(\alpha)$ is bounded by

$$B(\alpha) = C_1 + C_2 \int_0^{\alpha-\mu} \frac{B(\gamma)\, d\gamma}{(\gamma+\mu)^2}\,,$$

which is an increasing function of α. Then it can be shown as in A that

$$B(\infty) = C_1 + C_2 \int_0^{\infty} \frac{B(\alpha) d\alpha}{(\alpha+\mu)^2} < \frac{C_1 + C_2 \int_0^{\alpha_1} \frac{B(\alpha)\, d\alpha}{(\alpha+\mu)^2}}{1 - C_2 \int_{\alpha_1}^{\infty} \frac{d\alpha}{(\alpha+\mu)^2}}\,,$$

with $\alpha_1 + \mu > C_2$. This establishes that $R_k(\alpha)$ is uniformly bounded.

Now it is not difficult to establish that the right hand side of equation (15′) has a finite limit which is given by:

$$\text{(I.7)} \qquad \lim_{\alpha\to\infty} R_k(\alpha) = 1 + \int_{\mu}^{\infty} y_2'(\beta)\, C(\beta)\, d\beta + \int_0^{\infty} R_k(\gamma)\, y_1'(\gamma)\, d\gamma \int_{\gamma+\mu}^{\infty} y_2'(\beta)\, C(\beta-\gamma)\, d\beta\,.$$

The integrals appearing in (I.7) converge uniformly with respect to k in the domain excluding the cut; since $R_k(\alpha)$, for any finite α can be obtained by a finite number of integrations over holomorphic functions, $\lim_{\alpha\to\infty} R_k(\alpha)$ is holomorphic in this domain. Using again the bounds (I.2), (I.3), one can show by substitution in (I.7) that

$$\lim_{|k|\to\infty} [\lim_{\alpha\to\infty} R_k(\alpha)] = 1\,,$$

outside the cut. Further, one can see that this limit is reached faster than $\log|k|/|k|$.

Appendix II

We want to prove that whenever $\lim_{\alpha\to\infty} R_k(\alpha) = 0$

$$\lim_{r\to 0}\left[1 + \int_0^{\infty} \exp[-\alpha r]\, \varrho_k(\alpha)\, d\alpha\right] = \lim_{r\to 0} f(r,k) = 0\,.$$

One starts from the original equation (10), rather than from the transformed equation (15). Assume for ϱ the asymptotic behaviour

$$C_k \alpha^p .$$

Then, inserting in equation (10), one sees that if $p > -1$ the right hand side is equivalent to

$$C_k \frac{l(l+1)}{(p+1)(p+2)} \alpha^{p+2} ,$$

while the left hand side is equivalent to

$$C_k \alpha^{p+2} .$$

Hence, either $p = l - 1$ or $p \leqslant -1$. So if $\lim\limits_{\alpha\to\infty} R_k(\alpha) = 0$, $\varrho_k(\alpha)$ goes to zero as $\alpha \to \infty$ at least as fast as α^{-1}. The case $p = -1$ can be easily excluded by inserting the asymptotic $\varrho_k(\alpha)$ in equation (10). If $p < -1$, the left hand side behaves like $\alpha^{1-\varepsilon}$ while the right hand side is dominated by the term

$$\alpha l(l+1)\left[1 + \int\limits_0^\infty \varrho_k(\beta)\,\mathrm{d}\beta\right].$$

This means that

$$1 + \int\limits_0^\infty \varrho_k(\beta)\,\mathrm{d}\beta = 0 ,$$

and so

$$\lim_{r\to 0} f(r, k) = 0 .$$

RIASSUNTO (*)

Un precedente lavoro sulle proprietà analitiche dell'ampiezza dell'onda S per un gruppo di potenziali comprendente il caso di Yukawa viene esteso ad onde superiori. A prescindere da una trasformazione avente lo scopo di eliminare il termine centrifugo, il metodo è essenzialmente analogo a quello usato per il caso dell'onda S. Si fa uso della trasformazione di Laplace per due quantità collegate a soluzioni indipendenti dell'equazione di Schrödinger. Le singolarità nel semipiano complesso superiore k sono stati limitati sull'asse immaginario più un taglio $i(\mu/2) \to i\infty$. In ogni direzione (eccettuato forse il taglio) $\lim\limits_{|k|\to\infty} S(k) = 1$, cosicchè è possibile scrivere relazioni di dispersione.

(*) *Traduzione a cura della Redazione.*

Hyperfragment Production in K⁻-Meson Absorptions at Rest in Nuclear Emulsions. Mesic Decays (*).

J. Sacton (**)
Université Libre de Bruxelles

(ricevuto il 14 Ottobre 1959)

Summary. — The results of the analysis of 26 mesic hyperfragment decays found in a sample of 2236 K^--meson stars (excluding K^-_ρ) are given. 9 hyperfragment decays have been uniquely identified. Among these, a new decay mode of the $^8Li_\Lambda$ hyperfragment has been observed. We also mention the possible existence of a $^6He_\Lambda$ hyperfragment.

1. – Introduction.

The present experiment was undertaken to study the production of hyperfragments in K^--meson absorptions at rest. The absorption of K^--mesons by a nucleus takes place through one of the following processes:

$$K^- + \mathcal{N} \begin{cases} \Sigma + \pi & (1) \\ \Lambda^0 + \pi & (2) \end{cases}$$

$$K^- + 2\,\mathcal{N} \begin{cases} \Sigma + \mathcal{N} & (3) \\ \Lambda^0 + \mathcal{N} & (4) \end{cases}$$

The products of reactions (1) to (4) may suffer secondary interactions in the parent nucleus; in particular, the Σ-hyperons can be transformed into

(*) Preliminary results of this work have been reported by Dr. E. H. S. Burhop at the International Conference on High Energy Physics of Kiev (July 1959).

(**) Chercheur agréé à l'Institut Interuniversitaire des Sciences Nucléaires.

Λ^0-hyperons through the reaction $\Sigma + \mathcal{N} \to \Lambda^0 + \mathcal{N}$ (for the Σ^0-hyperon let us mention the electromagnetic decay modes $\Sigma^0 \to \Lambda^0 + \gamma$). Thus any K$^-$-meson absorption can lead to direct or indirect Λ^0 hyperon production and therefore eventually to hyperfragment formation. In fact, numerous hyperfragments emitted in K$^-$-meson absorption stars have already been observed in nuclear emulsions.

The purpose of the present paper is to report our results concerning the analysis of 26 mesic decays found in a sample of 2236 K$^-$-meson stars (excluding K$^-\varrho$), all stars lying within 20 μm from either surface of the unprocessed emulsion having been excluded.

2. – Experimental arrangement.

2·1. *Exposure and scanning.* – Two large emulsion stacks were exposed at the Berkeley Bevatron. The first one, stack K_1, consisted of 300 Ilford G-5 pellicles ($15 \times 25 \times 0.06$ cm^3) and was irradiated in 1956 by the first devised K$^-$-meson beam. 419 K$^-$-meson absorption stars at rest were observed in this stack (*). Stack K_2 built up with 300 Ilford K-5 emulsion sheets of 600 μm thickness and (18×20) cm^2 area was exposed during December 1957 for the European Collaboration (**) to the separated K$^-$-meson beam. 40 plates of this stack were scanned in Brussels and 1817 K$^-$-meson absorption stars were found.

Once detected, each K$^-$-meson star was carefully scrutinized by at least two observers under a microscope magnification of 50×25 or 100×25. A particular attention was reserved to stars of more than three prongs in order to detect any double centered star with very short connecting track. A part of the events (~ 200) was re-examined using a vertically moving ocular (1) but this last check did not reveal any additional pecularity. The black prongs (***) of all the stars were followed to the end of their range in order to avoid any loss of hyperfragments of long range. The track ends were also carefully examined.

(*) General characteristics of some 300 of those stars were already published. See: G. L. BACCHELLA, A. BERTHELOT, A. BONETTI, O. GOUSSU, F. LÉVY, M. RENÉ, D. REVEL, J. SACTON, L. SCARSI, G. TAGLIAFERRI and G. VANDERHAEGHE: *Nuovo Cimento*, **8**, 215 (1958). 100 events were found by the emulsion group of Göttingen. We are indebted to Prof. CECCARELLI for the gift of these events.

(**) European Collaboration: *Nuovo Cimento*, **12**, 91 (1959).

(***) A black prong is characterized by a specific ionization equal to, or greater than, 4 or 5 times the minimum; this corresponds to a residual range of 5 mm.

(1) J. HEUGHEBAERT: *Thesis*, Brussels (1957).

Experimental biases may affect the observation of some specific kind of mesic hyperfragments. Great care has been taken in this analysis to minimize the effect of these biases. As a result we are able to postulate that the detection of mesic hyperfragments is rather free from any experimental loss except perhaps for cryptofragments.

2·2. *Measurements.* – All the constants and standards adopted in computing the binding energies were taken from the World Survey of R. LEVI-SETTI and coll. (²).

The stopping power of our emulsion was found to be equal within the experimental errors to that of the Barkas standard emulsion (range measurements on the μ-mesons from the $\pi \to \mu + \nu$ decays at rest). The initial thickness of the individual pellicles being unknown, a rather large error of 10% was taken on the nominal 600 μm value.

The kinetic energy of all singly charged particles was determined from the range energy curves of W. H. BARKAS (³); these curves were also used for doubly charged particles of range greater than 20 μm. For short range helium isotopes we adopted the Wilkins curves normalized by R. LEVI-SETTI and coll. (²) and for heavier fragments use was made of the Papineau curves (⁴).

The kinematic analysis of the decay stars has been performed with the help of the electronic computer Gamma 3B. The program was the one developped by F. W. INMAN (⁵) slightly modified to reduce machine time.

3. – Results.

The characteristics of the 26 mesic hyperfragment decay stars are given in Table I. 22 of these events were completely analyzed and the binding energy of the Λ^0-hyperon was computed whenever possible. In the 4 other cases the π-meson interacted in flight (Bx 3122, Bx 5002, Go 52) or left the stack (Bx 5026) after a range too short to allow accurate energy determination by ionization or scattering measurements.

The results of the analysis are given separately in Tables II and III for the uniquely and non-uniquely identified events.

The following points appear in Table II:

(²) R. LEVI-SETTI, W. E. SLATER and V. L. TELEGDI: *Suppl. Nuovo Cimento*, **10**, 68 (1958).

(³) W. H. BARKAS: *Nuovo Cimento*, 8, 201 (1958).

(⁴) A. PAPINEAU: *Range-energy curves for ions of* $3 < Z < 10$ (C.E.N. Saclay).

(⁵) F. W. INMAN: *U.C.R.L.* 3815, June 1957 (Thesis).

TABLE I. – *Characteristics of 26 hyperfragment decay stars.*

No. event	Track	Range (μm)	Energy (MeV)	Dip angle (deg.)	Azimuth (deg.)
Go 83	π^-	14924	29.34	-2.3	0
	p	80	3.07	-61.1	139
	^{3}He	5.7	1.59	$+14$	202
Go 85	$\pi^\pm$	>13300	—	-35.7	0
	$Z=1$ or 2	11.8	—	-24	222.5
	recoil	2.3	—	$+35.2$	156.5
Go 52	π^-	11370	24.99	-2.5	0
	p	197	5.34	$+54.8$	156
	H or He	2.9	—	-53.5	250
Go 97	π^-	13662	27.80	-4	0
	p	258	6.22	$+6$	164.5
Bx 16	π^-	17224	31.93	-16.1	0
	p	6.1	0.53	$+21.1$	168
	^{4}He	6	1.70	0	312
Bx 92	π^-	13113	27.10	-3	0
Bx 178	π^-	17713	32.48	-46.3	0
	p	8.3	0.67	-4	102
	$^{3\text{-}4}$He	5.7	—	$+37.3$	196
Bx 1460	π^-	15171	29.63	-7.1	0
	p	35.4	1.82	$+20$	0.5
	^{4}He	11	3.01	0	179
Bx 2125	π^-	10410	23.73	-7.1	0
	d	7.1	0.69	$+53$	62
	p	3	0.25	0	146
Bx 2154	$\pi^\pm$	>22000	—	$+49.7$	0
	$^{3\text{-}4}$He	9.3	—	-49.7	177
Bx 2213	π^-	38720	52.30	$+20.5$	0
	^{4}He	8.5	2.37	-22.4	180.5
Bx 3122	$\pi^\pm$	>13600	—	-61.7	0
	$Z=1$ or 2	60	—	$+2.7$	189.5
Bx 4034	$\pi^\pm$	>24800	—	$+38.2$	0
	$^{3\text{-}4}$He	8.2	—	-34.4	184 ± 5

TABLE I (*continued*).

No. event	Track	Range (μm)	Energy (MeV)	Dip angle (deg.)	Azimuth (deg.)
Bx 4222	π^-	29 204	43.93	+ 14.7	0
	^{4}He	12.3	3.30	— 25.2	183
	^{4}He	1	0.40	—	—
Bx 5001	π^-	12 365	26.25	— 28.2	0
	p	65.9	2.72	— 17.9	126.5
	d	15.7	1.25	+ 33.2	300
	^{4}He	2.5	0.62	+ 13.4	189
Bx 5002	$\pi^\pm$	> 3 755	—	+ 5.8	0
	recoil	6.3	—	— 5.2	180
Bx 5010	π^-	11 588	25.27	— 54.5	0
	p	280	6.60	— 45.6	212
	^{4}He	10	2.75	+ 68.6	83.5
Bx 5012	π^-	16 396	31.01	— 31.9	0
	p	105.1	3.64	+ 16.6	204.5
	$^{3\text{-}4}$He	1.2	—	0 ± 10	109 ± 5
Bx 5016	π^-	15 152	29.61	+ 66.1	0
	$^{1\text{-}2\text{-}3}$H	56	—	+ 53.1	11.5
	$^{3\text{-}4}$He	20.5	—	— 56.2	190.5
Bx 5017	π^-	17 932	32.72	— 40.9	0
	p	21.6	1.32	+ 18.5	120
	$^{3\text{-}4}$He	2.9	—	+ 20.8	215
Bx 5018	π^-	25 771	40.80	+ 8.4	0
	recoil	1.2	0.40	0 ± 10	180 ± 5
Bx 5026	$\pi^\pm$	> 11 943	—	— 67.1	0
	recoil	1.2	—	—	—
	recoil	0.6	—	—	—
Bx 5029	π^-	5 656	16.60	— 41	0
	t	152.2	6.09	+ 32.1	268.5
	p	34.2	1.80	0	115
	^{4}He	10.7	2.95	— 17.5	61
Bx 5036	π^-	10 518	—	— 40.8	0
	$^{1\text{-}2\text{-}3}$H	36.5	—	+ 25.6	173.5
	recoil	1	—	—	—
Bx 6000	π^-	14 351	28.67	+ 72.5	0
	p	134.5	4.22	— 14.2	208.5
	p or $^{3\text{-}4}$He	2.4	—	— 25.2	56
Bx 10	π^-	5 792	16.90	0	0
	$^{1\text{-}2\text{-}3}$H	343	—	+ 5.5	173

TABLE II. – *Uniquely identified hyperfragments.*

No. event	Decay scheme	Q (MeV)	B_Λ (MeV)	δB_Λ (MeV)	P_r (MeV/c)	R_i (μm)	R_o (μm)
Bx 2213	${}^4H_\Lambda \to \pi^- + {}^4He$	54.65	2.38	0.70	—	—	—
Bx 2125	${}^4H_\Lambda \to \pi^- + p + d + n$	29.37	1.59	0.50	—	—	—
Go 83	${}^4He_\Lambda \to \pi^- + p + {}^3He$	34.00	3.22	1.00	99	6.4	5.7
Bx 16	${}^5He_\Lambda \to \pi^- + p + {}^4He$	34.16	3.06	0.70	120	6.8	6.1
Bx 1460	${}^5He_\Lambda \to \pi^- + p + {}^4He$	34.45	2.76	0.80	152	11.4	11.0
Bx 5010	${}^5He_\Lambda \to \pi^- + p + {}^4He$	34.63	2.59	0.60	157	12.5	10.0
Bx 5001	${}^7Li_\Lambda \to \pi^- + p + d + {}^4He$	31.07	4.67	0.90	73 *	2.8	2,6
Bx 4222	${}^8Li_\Lambda \to \pi^- + {}^4He + {}^4He$	47.62	6.94	1.40	—	—	—
Bx 5029	${}^8Li_\Lambda \to \pi^- + p + t + {}^4He$	28.30	6.45	0.90	150 *	11.1	10.7

Explanation of symbols:

Q = Sum of the kinetic energies of the decay products.
B_Λ = Binding energy of the Λ^0-hyperon into the fragment.
δB_Λ = Error on B_Λ (see R. LEVI SETTI *et al.* (²)).
P_r = Resultant momentum of the π^--proton system, for three body decays:

$$ {}^A_Z X_\Lambda \to \pi^- + p + {}^{A-1}_{\ Z} X_\Lambda . $$

R_i = Recoil range, inferred from P_r.
R_o = Observed recoil range.
(*) In these cases « P_r » means resultant momentum of the π^--p-d or π^--p-t systems.

a) Two different decay modes are observed for the ${}^4H_\Lambda$ hyperfragment

$$ {}^4H_\Lambda \to \pi^- + {}^4He $$

and

$$ {}^4H_\Lambda \to \pi^- + p + d + n $$

leading respectively to (2.38 ± 0.70) MeV and (1.59 ± 0.50) MeV binding energies for the Λ^0-hyperon.

b) All the uniquely identified helium hyperfragments decay through the channel

$$ {}^AHe_\Lambda \to \pi^- + p + {}^{A-1}He . $$

TABLE III. – *Non uniquely identified hyperfragments.*

No. event	Decay scheme	Q (MeV)	B_Λ (MeV)	δB_Λ (MeV)	P_r (MeV/c)	R_i (μm)	R_σ (μm)
Bx 2154	${}^{3\text{-}4}H_\Lambda \to \pi^- + {}^{3\text{-}4}He$	The π-meson track leaves the stack					
Bx 4034	${}^{3\text{-}4}H_\Lambda \to \pi^- + {}^{3\text{-}4}He$	The π meson track leaves the stack					
Bx 5017	${}^4He_\Lambda \to \pi^- + p + {}^3He$	34.79	2.43	—	68	3.1	2.9
	${}^5He_\Lambda \to \pi^- + p + {}^4He$	34.79	2.43	—	68	2.6	2.9
Bx 178	${}^4He_\Lambda \to \pi^- + p + {}^3He$	34.75	2.48	—	102	6.8	5.8
	${}^5He_\Lambda \to \pi^- + p + {}^4He$	34.77	2.45	—	102	5.0	5.8
Bx 5012	${}^4He_\Lambda \to \pi^- + p + {}^3He$	35.05	2.17	—	45	1.4	1.2
	${}^5He_\Lambda \to \pi^- + p + {}^4He$	35.05	2.17	—	45	1.2	1.2
Go 97	${}^4He_\Lambda \to \pi^- + p + {}^3He$	34.02	3.20	—	30	< 1.0	blob?
	${}^5He_\Lambda \to \pi^- + p + {}^4He$	34.02	3.20	—	30	< 1.0	blob?
Go 52	${}^3H_\Lambda \to \pi^- + p + p + n$	32.98	2.02	—	—	—	—
	${}^4He_\Lambda \to \pi^- + p + {}^3He$	31.08	6.14	—	56	2.0	2.9
	${}^5He_\Lambda \to \pi^- + p + {}^4He$	31.08	6.14	—	56	2.0	2.9
Bx 6000	${}^3H_\Lambda \to \pi^- + p + p + n$	36.07	−1.07	—	—	—	—
	${}^4He_\Lambda \to \pi^- + p + {}^3He$	33.59	3.63	—	92	5.5	2.8
	${}^5He_\Lambda \to \pi^- + p + {}^4He$	33.59	3.63	—	92	4.1	2.8
Bx 5016	${}^4He_\Lambda \to \pi^- + p + {}^3He$	33.67	0.60	0.70	161	21.4	20.5
	${}^6He_\Lambda \to \pi^- + d + {}^4He$	38.22	2.18	0.70	203	23.1	20.5

Bx 10 see table IV. Bx 5036 see table IV.
Bx 92 see text. Bx 5018 see text.

For explanation of symbols see footnotes to Table II.

c) The mean binding energy deduced from the three cases of ${}^5He_\Lambda$ hyperfragments is $\bar{B}_\Lambda = (2.80 \pm 0.50)$ MeV.

d) A new three-body decay mode of the ${}^8Li_\Lambda$ hyperfragment is observed

$$ {}^8Li_\Lambda \to \pi^- + p + t + {}^4He $$

involving the break up of the lithium nuclear core into an α-particle and a hydrogen isotope; the energy required for such a break-up is 2.47 MeV. The binding energy of the Λ^0-hyperon is found to be (6.45 ± 0.90) MeV.

e) The events Bx 4222 and Bx 5001 confirm the existence of the corresponding decay schemes previously reported by W. E. SLATER [6] and by O. SKJEGGESTAD and S. O. SØRENSEN [7].

Among the non-uniquely identified hyperfragments, some cases are rather ambiguous and only a lower limit can be put on the charge of the hyperfragment. These events are now briefly discussed.

The hyperfragment Bx 92 decays after a range of 6 μm into a single π^--meson of 27.1 MeV kinetic energy; no blob is visible at the decay point. The simplest decay scheme involving the emission of an invisible recoil taking away the unbalanced momentum due to the π-meson (91 MeV/c) leads us to consider hyperfragments as heavy as ${}^{12}C_\Lambda$ or ${}^{13}C_\Lambda$. By introducing neutrons among the decay products, the charge of the hyperfragment can be lowered to 2 or 3. The assumption of this event being due to the disintegration in flight of a Σ-hyperon of short range can easily be excluded on kinematical grounds.

The decay star of event Bx 5018 contains a π^--meson of 40.8 MeV kinetic energy and a very short recoil of (1.2 ± 1.0) μm range. The collinearity of the two tracks cannot be tested. Assuming a two-body decay, the following identities are possible for this hyperfragment:

$$
\begin{aligned}
{}^{7}He_\Lambda &\to \pi^- + {}^{7}Li \qquad & B_\Lambda &= 5.42\ \text{MeV}\,,\\
{}^{12}B_\Lambda &\to \pi^- + {}^{12}C \qquad & B_\Lambda &= 11.79\ \text{MeV}\,,\\
{}^{13}B_\Lambda &\to \pi^- + {}^{13}C \qquad & B_\Lambda &= 13.41\ \text{MeV}\,.
\end{aligned}
$$

If the recoiling nucleus is emitted in an excited state, some other solutions may be considered. They are not detailed here. Postulating the emission of one or more neutrons, the only possible scheme is

$$
{}^{13}B_\Lambda \to \pi^- + {}^{12}C + n
$$

leading to a binding energy lower than 8.5 MeV.

The hyperfragment Bx 10 decays into a π^--meson and a stable particle of unit charge; any admissible decay channel involves at least the emission of a very short fragment. A list of some possible identities for this event and for event Bx 5036 which is of the same type (but with a visible recoil of ~ 1 μm) is given in Table IV.

(6) W. E. SLATER: *Suppl. Nuovo Cimento*, **10**, 1 (1958).
(7) O. SKJEGGESTAD and S. O. SØRENSEN: *Phys. Rev.*, **104**, 511 (1956).

TABLE IV. – *Events* Bx 10 *and* Bx 5036.

Decay scheme	Q (MeV)		B_Λ (MeV)	
	Bx 10	Bx 5036	Bx 10	Bx 5036
${}^{7}\mathrm{Li}_\Lambda \to \pi^- + \mathrm{p} + {}^{6}\mathrm{Li}$	24.67	25.74	12.55	11.48
${}^{8}\mathrm{Li}_\Lambda \to \pi^- + \mathrm{p} + {}^{7}\mathrm{Li}$	24.63	25.74	12.58	11.48
${}^{8}\mathrm{Be}_\Lambda \to \pi^- + \mathrm{p} + {}^{7}\mathrm{Be}$	24.63	25.74	12.58	11.48
${}^{10}\mathrm{Be}_\Lambda \to \pi^- + \mathrm{p} + {}^{9}\mathrm{Be}$	24.59	25.74	12.62	11.48
${}^{11}\mathrm{Be}_\Lambda \to \pi^- + \mathrm{p} + {}^{10}\mathrm{Be}$	24.61	25.74	12.64	11.48
${}^{10}\mathrm{B}_\Lambda \to \pi^- + \mathrm{p} + {}^{9}\mathrm{B}$	24.59	25.74	12.62	11.48
${}^{11}\mathrm{B}_\Lambda \to \pi^- + \mathrm{p} + {}^{10}\mathrm{B}$	24.61	25.74	12.64	11.48
${}^{12}\mathrm{B}_\Lambda \to \pi^- + \mathrm{p} + {}^{11}\mathrm{B}$	24.62	25.74	12.65	11.48
${}^{13}\mathrm{B}_\Lambda \to \pi^- + \mathrm{p} + {}^{12}\mathrm{B}$	24.63	25.74	12.66	11.48
${}^{12}\mathrm{C}_\Lambda \to \pi^- + \mathrm{p} + {}^{11}\mathrm{C}$	24.62	25.74	12.65	11.48
${}^{13}\mathrm{C}_\Lambda \to \pi^- + \mathrm{p} + {}^{12}\mathrm{C}$	24.63	25.74	12.66	11.48
${}^{14}\mathrm{C}_\Lambda \to \pi^- + \mathrm{p} + {}^{13}\mathrm{C}$	24.64	25.74	12.67	11.48
${}^{15}\mathrm{C}_\Lambda \to \pi^- + \mathrm{p} + {}^{14}\mathrm{C}$	24.64	25.74	12.67	11.48
${}^{8}\mathrm{Li}_\Lambda \to \pi^- + \mathrm{d} + {}^{6}\mathrm{Li}$	—	26.22	—	5.97
${}^{9}\mathrm{Li}_\Lambda \to \pi^- + \mathrm{d} + {}^{7}\mathrm{Li}$	—	26.22	—	11.18
${}^{11}\mathrm{Be}_\Lambda \to \pi^- + \mathrm{d} + {}^{9}\mathrm{Be}$	27.72	26.22	4.90	6.40
${}^{11}\mathrm{B}_\Lambda \to \pi^- + \mathrm{d} + {}^{9}\mathrm{B}$	27.72	26.22	2.18	4.78
${}^{12}\mathrm{B}_\Lambda \to \pi^- + \mathrm{d} + {}^{10}\mathrm{B}$	27.82	26.22	0.16	—
${}^{13}\mathrm{B}_\Lambda \to \pi^- + \mathrm{d} + {}^{11}\mathrm{B}$	27.92	26.22	8.15	9.85
${}^{14}\mathrm{C}_\Lambda \to \pi^- + \mathrm{d} + {}^{12}\mathrm{C}$	27.92	26.22	6.57	8.27
${}^{15}\mathrm{C}_\Lambda \to \pi^- + \mathrm{d} + {}^{13}\mathrm{C}$	28.02	26.22	3.25	5.05
${}^{9}\mathrm{Li}_\Lambda \to \pi^- + \mathrm{t} + {}^{6}\mathrm{Li}$	—	26.52	—	9.89
${}^{13}\mathrm{B}_\Lambda \to \pi^- + \mathrm{t} + {}^{10}\mathrm{B}$	—	26.52	—	4.35
${}^{15}\mathrm{C}_\Lambda \to \pi^- + \mathrm{t} + {}^{12}\mathrm{C}$	—	26.52	—	6.06
${}^{16}\mathrm{C}_\Lambda \to \pi^- + \mathrm{t} + {}^{13}\mathrm{C}$	—	26.52	—	8.67

Let us finally mention the possible existence of a ${}^{6}\mathrm{He}_\Lambda$ hyperfragment (event Bx 5016). As can be seen from Table III, the kinetics of the decay is very well fitted by this assumption.

The binding energy we find for the Λ^0-hyperon is (2.18 ± 0.70) MeV which is rather low compared with the expected value inferred from the work of R. LEVI-SETTI and coll. (1) ($\bar{B}_\Lambda$ $({}^{5}\mathrm{He}_\Lambda) = (2.82 \pm 0.20)$ MeV and $\bar{B}_\Lambda$ $({}^{7}\mathrm{Li}_\Lambda) = (4.80 \pm 0.50)$ MeV). A similar event has been reported recently by F. BREIVIK and coll. (8) with $B_\Lambda = (3.80 \pm 0.70)$ MeV.

(8) F. BREIVIK, O. SKJEGGESTAD, S. O. SORENSEN and A. SOLEHIM: *Nuovo Cimento*, **12**, 531 (1959).

4. – Conclusion.

The production rate of mesic hyperfragments in K^--meson absorptions at rest (K_σ^--stars only) is 26/2236, *i.e.* $(1.2 \pm 0.2)\%$. This value is not corrected for any contribution of mesic cryptofragments. About this point let us mention that out of a total of 27 double centered stars with vanishingly short connecting track no example of mesic hyperfragment has been found. Thus we do not expect a very large contribution of mesic cryptofragments.

The charge distribution of the hyperfragments for which the charge is uniquely determined is given in Fig. 1 (solid line). We did not identify unambiguously any mesic hyperfragment of charge greater than 3. In fact such events may exist among the 4 hyperfragments for which only a lower limit of the charge could be found. Adding to our results those of S. MORA and I. ORTALLI (9) one obtains the distribution given in Fig. 1 (dotted line). The maximum of the distribution arises for $Z = 2$.

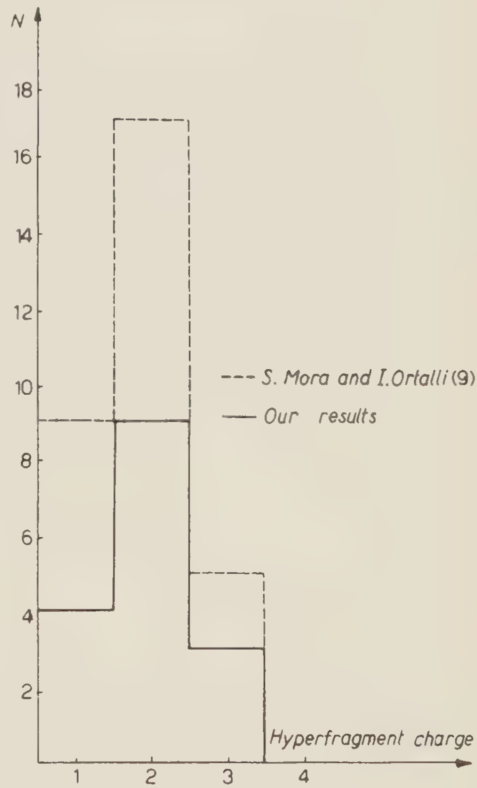

Fig. 1. – Charge distribution of the hyperfragments for which the charge is uniquely determined.

* * *

I wish to thank the organizators of the European Collaboration and especially Professors E. H. S. BURHOP and G. P. S. OCCHIALINI for having given me the opportunity to perform this work.

I am glad to express my thanks to Professors A. BERTHELOT, M. CECCARELLI and G. P. S. OCCHIALINI who where kind enough to lend me the plates and the experimental material available in their laboratories.

(9) S. MORA and I. ORTALLI: *Nuovo Cimento*, **12**, 635 (1959).

I am also indebted to the «Société Belge de Machines Bull S.A.» for studying the programmation of the kinetic analysis of the decay stars.

My further thanks are due to the scanners Mrs. F. JOHNSON and I. SACTON and Miss F. CAMBIER for their efficient work.

RIASSUNTO (*)

Si espongono i risultati dell'analisi del decadimento di 26 iperframmenti mesici trovati in un gruppo di 2236 stelle da mesoni K^- (esclusi i K_ρ^-). Si sono identificati soltanto 9 decadimenti di iperframmenti. Fra di essi si è osservato un nuovo modo di decadimento dell'iperframmento ${}^8Li_\Lambda$. Menzioniamo anche la possibilità dell'esistenza dell'iperframmento ${}^6He_\Lambda$.

(*) *Traduzione a cura della Redazione.*

IL NUOVO CIMENTO Vol. XV, N. 1 1° Gennaio 1960

On the Relative Abundances of Cosmic Ray Nuclei of Charge $Z \geqslant 3$.

C. M. GARELLI, B. QUASSIATI and M. VIGONE

Istituto di Fisica dell'Università - Torino
Istituto Nazionale di Fisica Nucleare - Sezione di Torino

(ricevuto il 30 Ottobre 1959)

Summary. — The charge spectrum of heavy primaries ($Z \geqslant 3$) of cosmic radiation has been measured in nuclear emulsion exposed in a high altitude ballon flight at a residual atmospheric thickness of about 6 g/cm². The fluxes of light, medium and heavy nuclei at the top of the atmosphere, and also the relative abundances of charges between $Z=3$ and $Z=14$, are given.

1. – Introduction.

In a previous work (paper I) (1) we studied the charge and energy spectrum of the heavy primaries of the cosmic radiation, using a stack of emulsions exposed at an atmospheric depth of 15 g/cm². In a second time, the very heavy component of the cosmic radiation has been studied more accurately; in this experiment (paper II) (2) a stack exposed under 13.5 g/cm² of air has been used.

From the experimental results of our first experiment, and using the diffusion equation reported by KAPLON *et al.* (3) we found for the fluxes at the

(1) Paper I: R. CESTER, A. DEBENEDETTI, C. M. GARELLI, B. QUASSIATI, L. TALLONE and M. VIGONE: *Nuovo Cimento*, **7**, 371 (1958).

(2) Paper II: V. BISI, R. CESTER, C. M. GARELLI and L. TALLONE: *Nuovo Cimento*, **10**, 881 (1958).

(3) M. F. KAPLON, G. H. NOON and G. W. RACETTE: *Phys. Rev.*, **96**, 1408 (1954).

top of the atmosphere the values:

$$\Phi_L^0 = (1.67 \pm 0.39) \text{ particles/m}^2 \text{ sr s}$$
$$\Phi_M^0 = (5.52 \pm 0.40) \quad » \quad »$$
$$\Phi_H^0 = (2.82 \pm 0.40) \quad » \quad »$$

where: L = light elements $(3 \leqslant Z \leqslant 5)$,

M = medium elements $(6 \leqslant Z \leqslant 9)$,

H = heavy elements $(Z \geqslant 10)$.

The knowledge of these fluxes, and in particular of the percentage of light nuclei, is important in the investigation of the origin of the cosmic rays; but the values at the top of the atmosphere depend in a very critical way from the parameters used in the diffusion equation. The purpose of the present work is to check the flux values using a stack exposed at an atmospheric depth of about 6 g/cm², so that the uncertainties in the extrapolation to the top of the atmosphere do not influence the final results in a sensible way.

2. – Exposure details.

The emulsion stack used in this research has been exposed over Texas at a geomagnetic latitude of 41° N in September 1958. The flight curve is shown in Fig. 1.

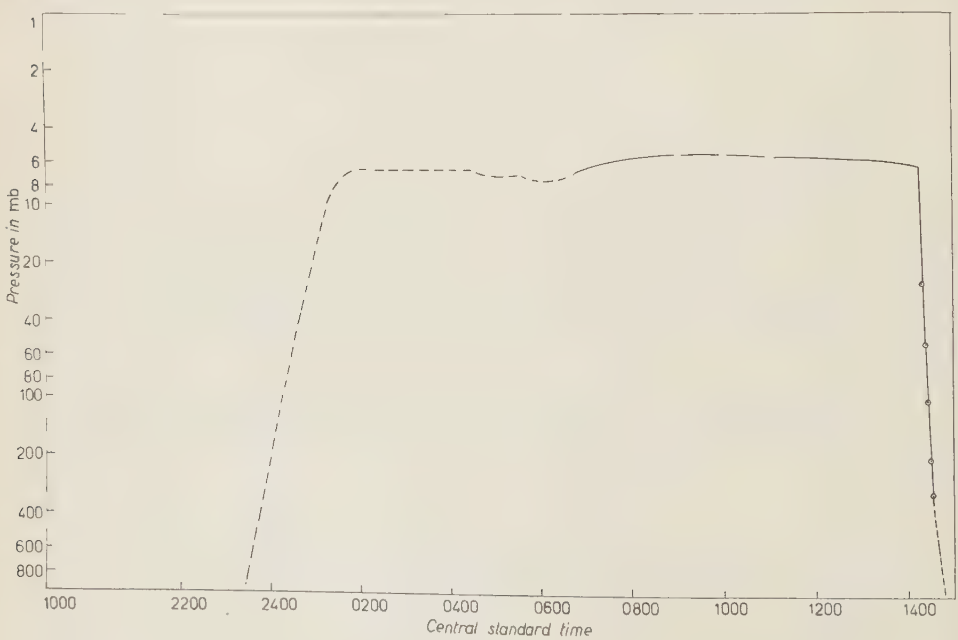

Fig. 1.

An other stack of emulsions was flown together with ours, and settled on the same vertical line, 20 feet higher. Owing to this unfortunate fact, the tracks that arrive vertically on our plates can be secondaries produced by interactions of the heavy primaries in the overlaying stack. For this reason we accepted in this experiment only those tracks whose zenith angle was higher than 10°.

3. – Scannings method and charge measurements.

The stack used in the present experiment is made of 80 sheets, of dimensions 12.5 cm $\times$12.5 cm $\times$600 μm; the emulsions are of two different types, G-5 and L-4, settled in the succession: 2 G-5, 1 L-4, and so on. The scanning has been done in the G-5 emulsions, 3 mm below the top edge, with the same criteria given in paper I [1]; the scanned area is 15.2 cm². In order to know the scanning losses, 8.0 cm² have been re-scanned and in this way we could evaluate the correction factors to be applied to the numbers of primaries with $Z \geqslant 5$ found in the first scanning. For the very light nuclei, Li and Be, we made a special scanning on 12.3 cm²; the criteria of this special scanning have also been given in paper I [1]. Moreover, an additional area of 13.0 cm² has been scanned, looking only for heavy nuclei in order to increase their statistics.

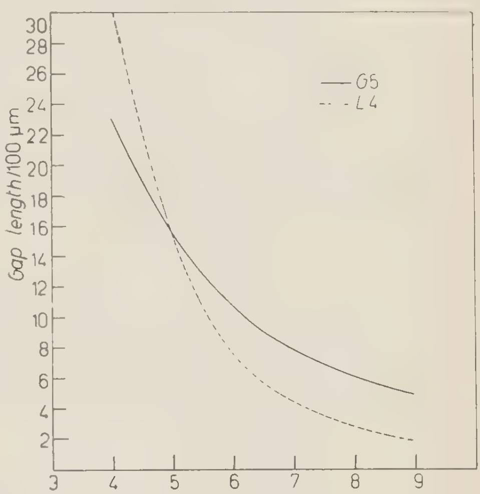

Fig. 2.

Each track has been followed through the whole stack. The data obtained from the interactions of the heavy primaries in this stack, have not been used to check the fragmentation probabilities that we gave in the previous works; in fact, the minimum ionization in these emulsions is so low (10 grains/100 μm) that we probably missed a large number of splittings of a primary into a secondary plus a proton.

The charge measurements have been done using the methods described in paper I [1], *i.e.*: gap length, photometric absorption and δ-rays counting. Each time the geometrical conditions were suitable, gap length measurements were done on a total track length of 5 mm, in four different sheets (2 G-5 and 2 L-4); photometric measurements on a total track length of 2 mm in five different sheets (3 G-5 and 2 L-4); δ-rays counting has been used as a

check in the doubtful cases. The curves « gap length – Z » and « photometric absorption – Z » are different for the two different types of emulsions, and this fact gave us a very useful check for the charge measurements. As an example, we show in Fig. 2 the curves « gap length *vs.* Z » for G-5 and L-4 emulsions.

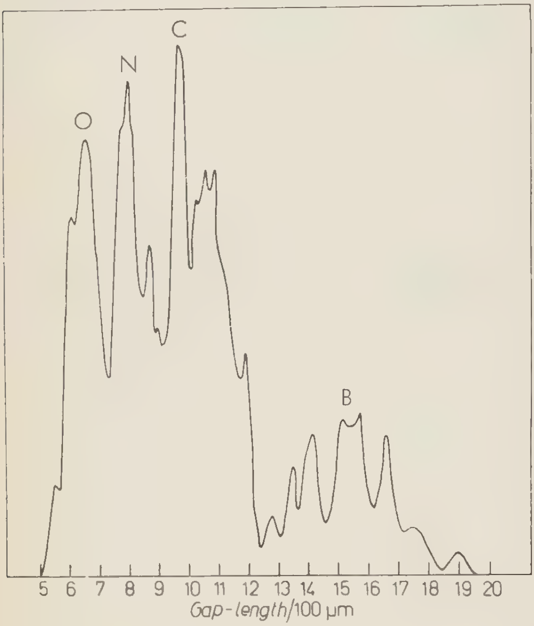

Fig. 3.

The hystograms of Figs. 3 and 4 show the results of gap length measurements (for B, C, N, O) and of photometric measurements (for nuclei of charge $Z \geqslant 8$) in G-5 emulsions. As it can be easily seen, the resolution is very good, and for a very large part of the tracks, the identification of the charge could be done with an uncertainty $\Delta Z \ll 1$.

The uncertainty was bigger for a 5% of the tracks be-

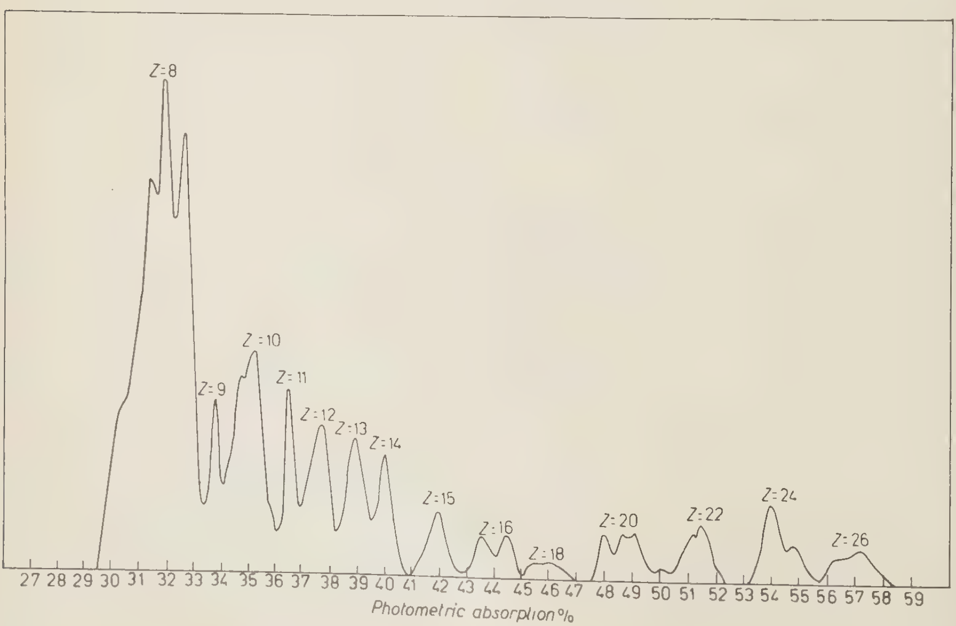

Fig. 4.

cause of their bad geometrical conditions; in these cases it has only been possible to attribute the tracks to one of the three charge groups, L, M, H.

4. – Experimental results and discussion.

A total of 299 tracks (30 Li and Be tracks, found in an area of 12.3 cm²; 176 tracks of the group B, C, N, O and F, found in an area of 15.2 cm²; 93 tracks of the group with $Z \geqslant 10$, found in an area of 28.2 cm²) have been included in the calculations. All these accepted tracks have a zenith angle $> 10°$ and $< 70°$. The numbers of available tracks, divided in three charge groups, referred to the same scanned area (15.2 cm²) and corrected for scanning losses, are the following:

number of light tracks	$(3 \leqslant Z \leqslant 5)$	$n_L = 72$,
» » medium »	$(6 \leqslant Z \leqslant 9)$	$n_M = 156$,
» » heavy »	$(Z \geqslant 10)$	$n_H = 52$.

From these figures we obtain the relative abundances at flight altitude:

$$n_L/n_M = 0.46 \, , \qquad n_H/n_M = 0.33 \, .$$

In order to evaluate the fluxes at the top of the atmosphere, we divided the tracks in three groups with different mean zenith angle ($10° \div 30°$; $30 \div 50°$; $50° \div 70°$); we made a separate calculation for each group, using the diffusion equation given by KAPLON *et al.* [3] and the following parameters:

$$\lambda_L = 33.6 \text{ g/cm}^2 \qquad P_{LL} = 0.13$$

$$\lambda_M = 26.9 \text{ g/cm}^2 \qquad P_{MM} = 0.18 \qquad P_{ML} = 0.23$$

$$\lambda_H = 19.0 \text{ g/cm}^2 \qquad P_{HH} = 0.31 \qquad P_{HM} = 0.39 \qquad P_{HL} = 0.18 \, .$$

The values of the mean free path in air (λ_L, λ_M, λ_H) are the ones calculated using an empirical expression given by BRADT and PETERS [4] (see also Table IV, paper I [1]); the values of the fragmentation probabilities in air are the ones obtained averaging over the results of the Turin group (see Table VI, paper I [1]) and the ones of the Bristol group [5]. The thickness of matter laying upon the scanned area has been estimated in 7 g/cm², taking into

(4) H. L. BRADT and B. PETERS: *Phys. Rev.*, **77**, 54 (1950).
(5) V. Y. RAJOPADHYE and C. J. WADDINGTON: *Phil. Mag.*, **3**, 9 (1958).

account the atmospheric depth, the packing material and the 3 mm of emulsion thickness between the scanning line and the top edge of the stack.

The flux values obtained in the three angular intervals are equal within the statistical and experimental uncertainties. This fact is in agreement with the recent observations of DANIELSON *et al.* (6).

The mean flux values at the top of the atmosphere results to be:

$$\Phi_L^0 = (1.87 \pm 0.25) \text{ particles/m}^2 \text{ sr s}$$

$$\Phi_M^0 = (4.39 \pm 0.37) \quad » \quad »$$

$$\Phi_H^0 = (1.64 \pm 0.17) \quad » \quad »$$

and the relative abundances:

$$\Phi_L^0/\Phi_M^0 = 0.43 \pm 0.09\,, \qquad \Phi_H^0/\Phi_M^0 = 0.37 \pm 0.07\,.$$

The quoted errors are the statistical ones.

The most important result is that the percentage of light nuclei incident on the top of the atmosphere is certainly not negligible.

This conclusion is in agreement with the results obtained by the Minnesota (7), Chicago (8) and Rochester (9) groups, that made the experiments at an atmospheric depth nearly equal to the one of the present work, and also with the results obtained previously by our group (1) and by the Bristol group (10) at greater atmospheric depth.

On the contrary, the Bombay group (11), extrapolating their results to the top of the atmosphere, found that the abundance of light nuclei at that point is nearly negligible. We think that this conclusion is ruled out by the results of the flights at very high altitude, owing to the fact that in this case the uncertainties in the parameters used in the extrapolation do not affect considerably the values of the fluxes.

Since our measurements give a quite good resolution of the charges of the heavy primaries, we give in the following table the percentages of the various nuclei with respect to the total flux; in the same table we show the percentages obtained by the Chicago (8) and the Rochester (9) groups, that have been obtained with exposures at an altitude comparable with the one of our

(6) R. E. DANIELSON and P. S. FREIER: *Phys. Rev.*, **109**, 151 (1958).

(7) P. S. FREIER, E. P. NEY and C. J. WADDINGTON: *Phys. Rev.*, **113**, 921 (1959).

(8) H. KOSHIBA, G. SCHULTZ and M. SCHEIN: *Nuovo Cimento*, **9**, 1 (1958).

(9) A. ENGLER, M. F. KAPLON and J. KLARMANN: *Phys. Rev.*, **112**, 597 (1958).

(10) P. H. FOWLER, R. R. HILLIER and C. J. WADDINGTON: *Phil. Mag.*, **2**, 293 (1957), C. J. WADDINGTON: *Phil. Mag.*, **2**, 1059 (1957).

(11) M. V. K. APPA RAO, S. BISWAS, R. R. DANIEL, K. A. NEELAKANTAN and B. PETERS: *Phys. Rev.*, **110**, 751 (1958).

exposure; in the last line of the table we show, for comparison, the cosmic abundances given by SUESS and UREY ([12]). The quoted errors are the statistical ones.

	Turin (*)	Chicago (**)	Rochester (**)	Suess and Urey
Li	5.7 ± 1.7	—	—	negligible
Be	7.5 ± 2.1	8.7 ± 1.7	7.0 ± 1.8	»
B	12.5 ± 2.7	10.9 ± 2.0	14.8 ± 2.7	»
C	21.0 ± 4.0	25.0 ± 3.2	27.0 ± 3.9	4.9
N	13.5 ± 3.0	16.7 ± 2.5	16.5 ± 2.9	9.3
O	18.1 ± 4.0	15.4 ± 2.4	13.5 ± 2.6	30.4
F	1.9 ± 1.0	2.2 ± 0.8	7.0 ± 1.8	negligible
$Z \geqslant 10$	18.6 ± 4.0	21.2 ± 2.9	14.4 ± 2.7	16.8
$Z = 10$	5.0 ± 1.2	—	—	12.1
$Z = 11$	2.1 ± 0.7	—	—	0.06
$Z = 12$	2.1 ± 0.7	—	—	1.3
$Z = 13$	1.7 ± 0.6	—	—	0.13
$Z = 14$	1.9 ± 0.7	—	—	1.4
$Z > 14$	5.0 ± 1.2	—	—	1.8

(*) The numbers are quoted in percentages of the total number of particles with $Z \geqslant 3$.
(**) The numbers are quoted in percentages of the total number of particles with $Z > 3$.

The knowledge of the flux values at the top of the atmosphere allows us to evaluate, at least as an order of magnitude, the mean path traversed by the cosmic radiation from the origin to the earth.

We made the calculation with the method of the one dimensional diffusion equation ([3]), under the hypothesis that at the origin the flux of light nuclei is zero. For fragmentation probabilities in interstellar matter we took the same values used in paper II ([2]), that are a weighted average of the Chicago ([8]) and Bristol ([5]) data:

$$P_{LL} = 0.07$$

$$P_{MM} = 0.09 \qquad P_{ML} = 0.34$$

$$P_{HH} = 0.29 \qquad P_{HM} = 0.36 \qquad P_{HL} = 0.27 \, .$$

We assumed for the interstellar matter a density of 0.1 atoms/cm³ and a composition of 90% H and 10% He; the mean free paths used are the fol-

([12]) H. E. SUESS and M. C. UREY: *Rev. Mod. Phys.*, **28**, 53 (1956).

lowing [9]:

$$\lambda_L = 5.78 \cdot 10^{25}\ \text{cm}\ , \quad \lambda_M = 3.88 \cdot 10^{25}\ \text{cm}\ , \quad \lambda_H = 2.08 \cdot 10^{25}\ \text{cm}\ .$$

For flux values at the top of the atmosphere we used the mean of the data of the present work and of the Minnesota group [5] that is:

$$\Phi_L^0 = 1.9\ \text{particles/m}^2\ \text{sr s}$$

$$\Phi_M^0 = 4.7\ \text{»} \quad \text{»}$$

$$\Phi_H^0 = 1.7\ \text{»} \quad \text{»}$$

The value found for the mean path traversed by the cosmic radiation is:

$$2.7 \cdot 10^{25}\ \text{cm}$$

and the ratio of the heavy nuclei to the medium ones, at the origin, turns out to be:

$$Q_H/Q_M = 0.58$$

to be compared with the cosmic abundance given by SUESS and UREY [12]

$$H/M = 0.375\ .$$

An other point that we wish to outline is the following: if the composition of the source of the cosmic radiation is equal to the mean composition of the universe [12], and the value $2.7 \cdot 10^{25}$ cm obtained in the present calculation for the mean path traversed is correct, it is very difficult to understand the big difference in the relative abundances of the nuclei C, N, O:

top of the atmosphere (present work): $C:N:O = 1.16:0.75:1$,

cosmic abundance (SUESS and UREY [12]): $C:N:O = 0.16:0.31:1$.

This fact seems to indicate that the composition of the source of the cosmic radiation is different from the mean composition of the universe and can support the hypothesis that the source has to be situated in the supernovae.

* * *

We express our thanks to the Office of Naval Research for the exposure of our stack and especially to Dr. ZAFFARANO for valuable assistence.

Our thanks are also due to the Bristol group for the processing of the plates. We are grateful to Professors R. DEAGLIO and G. WATAGHIN for their constant interest in our work, to Drs. A. DEBENEDETTI and R. CESTER for useful discussions and advices, to Drs. MORENO and ORSINI, Mr. BORREANI and Miss MARZARI for help in the course of the measurements.

RIASSUNTO

Si é studiato lo spettro di carica dei primari pesanti ($Z \geqslant 3$) della radiazione cosmica utilizzando emulsioni nucleari esposte ad una profondità atmosferica di 6 g/cm^2. Si sono determinati i valori dei flussi dei nuclei leggeri, medi e pesanti incidenti sull'atmosfera terrestre, ed anche le relative abbondanze dei nuclei di carica compresa fra $Z=3$ e $Z=14$.

IL NUOVO CIMENTO Vol. XV, N. 1 1° Gennaio 1960

Incompatibilité entre l'hypothèse de la symétrie restreinte et certains résultats expérimentaux.

B. d'Espagnat et J. Prentki

CERN - Genève

(ricevuto il 5 Novembre 1959)

Summary. — Methods for testing global symmetry ($g_{NN\pi}=g_{\Lambda\Sigma\pi}=g_{\Sigma\Sigma\pi}=g_{\Xi\Xi\pi}$) and restricted symmetry ($g_{\Lambda\Sigma\pi}=g_{\Sigma\Sigma\pi}$) with the help of K^-p scattering and absorption data are discussed and an application to restricted symmetry is made. The principle of all the approximation methods that have been used for that purpose is to infer some knowledge about the matrix elements pertaining to $\Sigma\pi$ scattering with K interactions present from the assumed knowledge of what these same matrix elements would be if the K interactions were switched off. It is shown in Section **1**: *a*) that there are at least two such methods: either one assumes that a rough equality holds between the $T_{\Sigma\pi,\Sigma\pi}$ (or $K_{\Sigma\pi,\Sigma\pi}$) matrix elements with and without K interactions, or one assumes that a similar equality holds between the $(T^{-1})_{\Sigma\pi,\Sigma\pi}$ matrix elements under the same conditions; *b*) that when the K interactions are large enough to allow for appreciable absorption (which is experimentally the case) these two methods lead to essentially different results. This general remark already throws serious doubts on the usefulness of the global or restricted symmetry concepts as regards K-nucleon processes. It is, however, interesting to investigate whether one of these approximations, or both, would lead to results compatible with the experimental data. It is shown in Sections **3**, **4**, **5**: *a*) that assuming the validity of the 1-st method, a straightforward extension of Amati and Vitale's argument leads to incompatibility between restricted symmetry and the observed data; *b*) that, if one assumes the validity of the second method, the arguments used by Salam to reject global symmetry can be extended to restricted symmetry and that, for quite different reasons than in *a*), incompatibility with the experimental data also results (*). It is concluded that restricted symmetry is definitely not a useful concept as far as low energy K-p phenomena are considered; either it does not hold, or it is completely veiled by the K interactions.

(*) See however the *Note added in proof.*

1. – Considérations générales et présentation de la méthode.

Lorsqu'il s'agit de tests expérimentaux pour les hypothèses de la symétrie globale ou de la symétrie restreinte, il est nécessaire d'introduire dans la description des processus réels les données caractéristiques des systèmes composés de Λ, Σ et de π (comme, par exemple, les déphasages des diffusion $\Sigma\pi$, $\Lambda\pi$). Celles-ci sont supposées connues (symétrie globale) ou reliées entre elles par des relations simples (symétrie restreinte) lorsque les intéractions K sont coupées et que les symétries s'appliquent pleinement. Il est donc nécessaire de faire une certaine approximation.

Lorsque les interactions peuvent être traitées comme des perturbations par rapport aux intéractions π la procédure à suivre est simple et univoque. Le problème de l'absorption des K^- sur des protons par exemple a été traité en détail (intéractions K faibles par rapport aux interactions π) par AMATI et VITALE [1]. Par contre, quand les interactions K ne sont pas beaucoup plus faibles que les interactions π (ce qui semble être le cas) le problème (pour autant qu'il ait un sens) est beaucoup plus complexe. La manière d'introduire les approximations n'est pas *a priori* claire. Différentes méthodes peuvent être imaginées et nous montrerons que les résultats peuvent être très différents les uns des autres en fonction de la méthode choisie.

A cet effet considérons un exemple abstrait afin de ne pas introduire dès le début les complications liées au spin isotopique, etc., qui ne peuvent qu'obscurcir le raisonnement.

Considérons donc les réactions à deux voies

$$(1.1)\qquad \left\{\begin{array}{l} a+\alpha \longrightarrow a+\alpha \\ \qquad\quad \times \\ b+\beta \longrightarrow b+\beta \end{array}\right.$$

avec $m_a+m_\alpha > m_b+m_\beta$, et les réactions

$$(1.2)\qquad \left\{\begin{array}{l} a+\alpha \rightarrow a+\alpha \\ b+\beta \rightarrow b+\beta \end{array}\right.$$

que l'on obtient de (1.1) en supprimant les interactions qui conduisent de $a+\alpha$ à $b+\beta$. La matrice T^{-1} pour (1.1) (l'inverse de la matrice de diffusion)

---

[1] D. AMATI et B. VITALE: *Nuovo Cimento*, 9, 895 (1958).

peut être écrite (²) (invariance par rapport au renversement du sens du temps):

$$\text{(1.3)} \qquad \left\{ T^{-1} = \begin{pmatrix} a - ik_a\,, & h \\ h\,, & b - ik_b \end{pmatrix} \right.$$

où a, h et b sont des nombres réels (*), k_a et k_b les moments relatifs dans le c.m.

Pour la réaction (1.2) on a

$$\text{(1.4)} \qquad T'^{-1} = \begin{pmatrix} a' - ik_a\,, & 0 \\ 0 & ,\; b' - ik_b \end{pmatrix} = \begin{pmatrix} a' - ik_a\,, & 0 \\ 0 & ,\; \dfrac{k_b}{\sin\alpha}\exp[-i\alpha] \end{pmatrix}$$

où α est le déphasage de la réaction $b \to b$. De (1.3) on calcule T et l'on a facilement

$$\text{(1.5)} \qquad T_{11} = \frac{1}{z - ik_a} = \frac{A}{1 - iAk_a} = |T_{11}|\exp[i\Theta]\,,$$

$$\text{(1.6)} \qquad T_{12} = T_{11}\sqrt{\frac{y}{k_b}}\exp[i\varphi]\,,$$

$$\text{(1.7)} \qquad T_{22} = T_{11}\sqrt{\frac{a^2 + k_a^2}{b^2 + k_b^2}}\exp[i\varphi]\cdot\exp[i\psi]\,,$$

avec

$$\text{(1.8)} \qquad \operatorname{tg}\psi = -\frac{k_a}{a}\,; \qquad \operatorname{tg}\varphi = \frac{k_b}{b}\,,$$

$$\text{(1.9)} \qquad z = x + iy\,, \qquad A = \frac{1}{z}\,,$$

$$\text{(1.10)} \qquad x = a - \frac{h^2 b}{b^2 + k_b^2}\,, \qquad y = \frac{h^2 k_b}{b^2 + k_b^2}\,.$$

(²) P. T. MATTHEWS et A. SALAM: *Nuovo Cimento*, **13**, 381 (1959).

(*) T est défini ici par

$$\text{(1.3')} \qquad S_{fi} = \delta_{fi} + 2i\sqrt{k_f}\,T_{fi}\sqrt{k_i}\,.$$

(1.3) découle de

$$\text{(1.3'')} \qquad T^{-1} = K^{-1} - iC\,,$$

où K est la matrice de réaction hermitique et symétrique (invariance par rapport au renversement du sens du temps) et $C_{ij} = k_i\delta_{ij}$. La forme T^{-1} est particulièrement simple. Le T qui s'en déduit satisfait nécessairement à la relation découlant de l'unitarité de la matrice S.

De même

$$T' = \begin{pmatrix} \dfrac{1}{a' - ik_a} & 0 \\ 0 & \dfrac{1}{k_b} \sin\alpha \ \exp[i\alpha] \end{pmatrix}. \tag{1.11}$$

Supposons maintenant (et ceci correspond à la situation pour les réactions $K^- + p \begin{smallmatrix} \nearrow K^- + p \\ \searrow \Sigma \ + \pi \end{smallmatrix}$ que nous allons discuter en détail) que T_{11} soit connu et que T_{12} soit connu à la phase φ près. Nous voulons alors déterminer l'élément de matrice T'_{22} (et par là même la phase φ) à l'aide de l'élément de matrice (supposé connu) T'_{22}. Plusieurs méthodes distinctes s'offrent alors:

Méthode I. – Elle consiste à remplacer pour $k_a = 0$, l'élément T_{22} par T'_{22} donc

$$T_{22} \approx T'_{22}. \tag{1.12}$$

Nous appellerons cette méthode « *comparaison des T* ».

Pour $k_a = 0$ (1.5)–(1.10) donnent $(\vartheta = \Theta(k_a = 0))$

$$T_{11} = A = |A| \exp[i\vartheta], \tag{1.13}$$

$$T_{12} = |T_{12}| \exp[i(\vartheta + \varphi)], \tag{1.14}$$

$$T_{22} = |T_{22}| \exp[i(\vartheta + \varphi)], \tag{1.15}$$

avec

$$\operatorname{tg}\vartheta = -\frac{y}{x}, \qquad \operatorname{tg}\varphi = \frac{k_b}{b}, \qquad \psi = 0. \tag{1.16}$$

Il est facile alors de prouver que

$$T_{22} = \frac{1}{k_b} \sin(\vartheta + \varphi) \exp[i(\vartheta + \varphi)] \quad \text{avec} \quad \operatorname{tg}(\vartheta + \varphi) = \frac{k_b}{b - (h^2/a)}.$$

Par (1.12) et (1.11)

$$\vartheta + \varphi = \alpha,$$

donc

$$\frac{k_b}{b - (h^2/a)} \approx \operatorname{tg}\alpha, \tag{1.17}$$

(1.14) et (1.15) montrent que la phase de T_{12} est α

$$T_{12} = |T_{12}| \exp[i\alpha]. \tag{1.18}$$

De la matrice T pour $k_a = 0$ on passe à la matrice T pour k_a quelconque en utilisant (1.3) ce qui, évidemment, préserve l'unitarité de la matrice S (*).

Méthode II. – Elle consiste à remplacer l'élément $(T^{-1})_{22}$ par $(T'^{-1})_{22}$

$$(T^{-1})_{22} \approx (T'^{-1})_{22} .$$

Nous appellerons cette méthode « *comparaison des* T^{-1} ».

De (1.4) et (1.3)

$$\frac{b - ik_b}{k_b} \approx \frac{1}{\sin\alpha} \exp[-i\alpha] ,$$

d'où

(1.19) $$\frac{k_b}{b} \approx \operatorname{tg}\alpha .$$

D'après (1.8) et (1.19), $\varphi \approx \alpha$ et d'après (1.6) et (1.5), la phase de T_{12} est alors $\Theta + \alpha$

(1.20) $$T_{12} = |T_{12}| \exp[i(\Theta + \alpha)] .$$

Pour $k_a = 0$ on a

(1.21) $$T_{12} = T_{12} \exp[i(\vartheta + \alpha)] ,$$

avec ϑ donné par (1.16) (**).

Discussion. – La comparaison de (1.20) et (1.18) ou de (1.19) et (1.17) montre que les méthodes I et II conduisent à des résultats qui sont différents. Que ces résultats puissent différer notablement lorsque h est grand est tout à fait évident. Ceci tient au fait que pour la matrice T (qui n'est pas diagonale) l'inverse de l'élément de matrice est différent de l'élément de matrice correspondant de la matrice inverse, $T_{22}^{-1} \neq (T^{-1})_{22}$, tandis que pour la matrice T' (qui est diagonale) on a $T'^{-1}_{22} = (T'^{-1})_{22}$.

h grand correspond à y grand donc à ϑ grand ((1.10, (1.16)). Quand l'aborption $a \to b$ devient importante il devient impossible donc d'introduire d'une manière univoque dans l'ensemble des réactions (1.1) les résultats que l'on désirerait prendre des réactions (1.2). Or, dans le cas réel des réactions $K^- + p$ que nous voulons discuter, l'analyse de DALITZ et TUAN [3] montre que ϑ est grand.

(*) Un autre procédé pour préserver l'unitarité de la matrice S consiste à identifier K_{22} avec $K'_{22} = k_b^{-1} \operatorname{tg}\alpha$, K étant la matrice de réaction réelle et symétrique. On vérifie aisément en faisant le calcul au seuil ($k_a = 0$) que — dans le problème ici étudié — ceci conduit en fait aux mêmes résultats.

(**) Il est évident, en vertu de (1.3″), que l'identification de $(K^{-1})_{22}$ avec $(K'^{-1})_2$ conduirait aux mêmes résultats.

(3) R. H. DALITZ et S. F. TUAN: *Annals of Physics*, 8, 100 (1959).

On pourrait donc dès maintenant conclure que les symétries globale ou restreinte ne sont pas des idées utiles car leur introduction dans les processus réels conduit à des résultats contradictoires en fonction de l'approximation utilisée. Ceci est un point de vue parfaitement légitime.

Néanmoins on peut aussi adopter un point de vue plus prudent. Il se pourrait en effet que l'une de ces méthodes d'approximation fut plus proche de la réalité que l'autre. Nous n'avons pas été capables de trouver un argument général qui pourrait donner une préférence à la méthode I par rapport à la méthode II ou vice versa. Nous doutons même de son existence. Car si les perturbations s'appliquent au problème, c'est la méthode I qui doit être utilisée tandis que pour un couplage très fort l'approximation utilisés dans la méthode II semblerait préférable. Dans le cas d'intérêt physique où les couplages K sont du domaine intermédiaire il semble impossible de se prononcer *a priori*.

Pour cette raison nous allons montrer dans ce qui suit que les deux méthodes donnent des résultats en contradiction avec les résultats expérimentaux même si l'on ne considère que la symétrie restreinte. Nous montrerons donc que la symétrie restreinte n'est pas un concept utile. Ceci, bien entendu, s'applique *a fortiori* à la symétrie globale (cas discuté déjà par SALAM [4]) qui apporte des restrictions supplémentaires.

2. – Quelque remarques sur la symétrie restreinte.

Cette Section est consacrée à un très bref rappel des propriétés de la symétrie restreinte. Nous suivons ici de très près la présentation due à AMATI et VITALE [1].

L'hamiltonien des interactions des Σ et Λ avec les π s'écrit

$$H = ig_2(\bar{\Lambda}\gamma_5\boldsymbol{\Sigma}\boldsymbol{\pi} + \bar{\boldsymbol{\Sigma}}\gamma_5\Lambda\boldsymbol{\pi}) + g_3\boldsymbol{\Sigma}\times\gamma_5\boldsymbol{\Sigma}\cdot\boldsymbol{\pi}\,. \tag{2.1}$$

L'hypothèse de la symétrie restreinte consiste à supposer que, en l'absence des interactions K, $g_2 = g_3$ et $m_\Lambda = m_\Sigma$. (2.1) peut alors s'écrire

$$H = ig(\bar{\boldsymbol{Y}}\gamma_5\boldsymbol{\tau}Y + \bar{\boldsymbol{Z}}\gamma_5\boldsymbol{\tau}Z)\boldsymbol{\pi} \tag{2.2}$$

avec les doublets de spin isotopique définis par

$$Y = \begin{pmatrix}\Sigma^+\\ Y_0\end{pmatrix}; \qquad Z = \begin{pmatrix}Z^0\\ \Sigma^-\end{pmatrix},$$

avec $Y_0 = (\Lambda - \Sigma_0)/\sqrt{2}$ et $Z_0 = (\Lambda + \Sigma_0)/\sqrt{2}$.

---

[4] A. SALAM: *Conférence de Kiev* (Juillet 1959).

Si en plus la constante g est égale à la constante d'interaction $g_{\mathcal{N}\pi}$ et $g_{\Xi\pi}$ et si l'on néglige les différences des masses entre tous les baryons on a affaire à la symétrie globale.

(2.1) et (2.2) montrent que, pour les systèmes Σ, Λ, π, deux attributions distinctes de spin isotopique existent:

a) le spin isotopique ordinaire I avec $I = 0$ pour Λ et $I = 1$ pour Σ et π;

b) le spin isotopique i de la symétrie restreinte avec $i = \frac{1}{2}$ pour Y et Z.

Il en découle que (en particulier) les amplitudes de diffusion dans les états de spin isotopique 0 et 1 des systèmes $\Sigma\pi$ ed $\Lambda\pi$ peuvent être exprimées à l'aide des amplitudes de diffusion $T'_{\frac{1}{2}}$ et $T'_{\frac{3}{2}}$ des systèmes $Y\pi$ et $Z\pi$ ($i = \frac{1}{2}$ et $\frac{3}{2}$) définies par

$$\langle \tfrac{1}{2} | T' | \tfrac{1}{2} \rangle = T'_{\frac{1}{2}}\,; \qquad \langle \tfrac{3}{2} | T' | \tfrac{3}{2} \rangle = T'_{\frac{3}{2}} \tag{2.3}$$

avec la relation d'orthogonalité

$$\langle \tfrac{1}{2} | T' | \tfrac{3}{2} \rangle = 0\,. \tag{2.4}$$

On a alors ($|\Sigma\pi\rangle_1$ signifiant état de $\Sigma\pi$ de spin isotopique $I = 1$, etc.)

$$\langle \Sigma\pi | T' | \Sigma\pi \rangle_0 = T'_{\frac{1}{2}}\,, \tag{2.5}$$

$$\langle \Sigma\pi | T' | \Sigma\pi \rangle_1 = \tfrac{2}{3} T'_{\frac{1}{2}} + \tfrac{1}{3} T'_{\frac{3}{2}}\,, \quad \text{etc.} \tag{2.6}$$

Les états $|\frac{1}{2}\rangle$ et $|\frac{3}{2}\rangle$ son reliés aux états $|\Sigma\pi\rangle_1$ et $|\Lambda\pi\rangle_1$ par

$$\begin{pmatrix} |\frac{1}{2}\rangle \\ |\frac{3}{2}\rangle \end{pmatrix} = U \begin{pmatrix} |\Sigma\pi\rangle_1 \\ |\Lambda\pi\rangle_1 \end{pmatrix} \quad \text{avec} \quad U = \begin{pmatrix} \sqrt{\frac{2}{3}}\,, & \sqrt{\frac{1}{3}} \\ \sqrt{\frac{1}{3}}\,, & -\sqrt{\frac{2}{3}} \end{pmatrix}. \tag{2.7}$$

Il est très important de réaliser que la diffusion $\Sigma\pi$ dans l'état $I = 0$ est complètement déterminée par l'amplitude $T'_{\frac{1}{2}}$ correspondant aux états $|\frac{1}{2}\rangle$ de la description à l'aide de i (*).

Les considérations ci-dessus concernant les éléments de matrice de la matrice T' sont évidemment valables pour les éléments de matrice des matrices K', K'^{-1} et T'^{-1}, la matrice U possédant une inverse.

(*) En fait l'état $|\frac{1}{2}\rangle$ qui apparaît dans $|\Sigma\pi\rangle_1$ et $|\Lambda\pi\rangle_1$ est de la forme $\psi_Y^{\frac{1}{2}} - \psi_Z^{\frac{1}{2}}$ tandis que celui qui apparaît dans $|\Sigma\pi\rangle_0$ est $\psi_Z^{\frac{1}{2}} + \psi_Y^{\frac{1}{2}}$. Mais vu l'orthogonalité des états $\psi_Y^{\frac{1}{2}}$ et $\psi_Z^{\frac{1}{2}}$ c'est le même $T'_{\frac{1}{2}}$ qui intervient dans (2.5) et (2.6).

3. – Diffusion et absorption des K⁻ sur les protons.

Considérons l'ensemble des réactions

$$
\left\{
\begin{array}{c}
\mathrm{K}^- + \mathrm{p} \longrightarrow \mathrm{K}^- + \mathrm{p} \\
\times \\
\Sigma(\Lambda) + \pi \longrightarrow \Sigma(\Lambda) + \pi
\end{array}
\right.
\tag{3.1}
$$

Deux états de spin isotopique I sont possibles: l'état $I=0$ et l'état $I=1$. La réaction totale est décrite par la matrice ($I=0$)

$$
T_0^{-1} = \begin{pmatrix} a_0 - iK_k\,, & h_0 \\ h_0 & ,\quad b_0 - iK_\Sigma \end{pmatrix}
\tag{3.2}
$$

et par la matrice (*) ($I=1$)

$$
T_1^{-1} = \begin{pmatrix} a_1 - iK_k\,, & h_1\,, & g_1 \\ h_1\,, & b_1 - iK_\Sigma\,, & f_1 \\ g_1\,, & f_1\,, & c - iK_\Sigma \end{pmatrix}.
\tag{3.3}
$$

La matrice T_0 est une matrice 2×2 car l'état $\Lambda\pi$ est un état $I=1$ pur. Les résultants de la Section précédente montrent que pour la matrice T_1 on peut utiliser directement la description en termes du spin isotopique i, ceci en vertu de (2.7) qui donne $|\Sigma\pi\rangle_1$, et $|\Lambda\pi\rangle_1$ en fonction de $|\frac{1}{2}\rangle$ et $|\frac{3}{2}\rangle$. T^{-1}, de la forme (3.3), s'écrit

$$
T_1^{-1} = \begin{array}{c|ccc}
 & I=1\,, & i=\frac{1}{2}\,, & i=\frac{3}{2} \\
\hline
I=1 & & & \\
i=\frac{1}{2} & & & \\
i=\frac{3}{2} & & &
\end{array}
\tag{3.3'}
$$

c'est à dire que dans T_{ij} $(i, j = 1, 2, 3)$ l'indice 1 correspond au système $\overline{\mathrm{K}}\mathfrak{N}$ avec $I=1$, l'indice 2 au système $\mathrm{Y}\pi$ $\mathrm{Z}\pi$ avec $i=\frac{1}{2}$ et l'indice 3 au système $\mathrm{Y}\pi$, $\mathrm{Z}\pi$ avec $i=\frac{3}{2}$.

La matrice T_0 et les relations entre les phases de ses éléments de matrice T_{0ij} sont données par les formules (1.5)–(1.8). Pour la matrice T_1 les formules sont plus compliquées. On a

$$
T_{1,ij} = \frac{D_{ij}}{\mathscr{D}} = \frac{D_{11}}{\mathscr{D}}\cdot\frac{D_{ij}}{D_{11}} = T_{1,11}\frac{D_{ij}}{D_{11}}\,,
\tag{3.4}
$$

(*) On néglige la différence des masses entre Λ et Σ.

où $\mathscr{D} = \text{Det}\, T_1^{-1}$ et $D_{ij} = (-)^{i+j} m_{ij}$ où m_{ij} est le mineur du déterminant correspondant à l'élément a_{ij} de la matrice T^{-1}. $T_{1,11}$ peut être écrit sous la forme

$$T_{1.11} = \frac{1}{\mathscr{D}/A_{11}} = \frac{1}{Z_1 - iK_k} = \frac{A_1}{1 - iK_k A_1}\,, \tag{3.5}$$

où

$$z_1 = x_1 - iy_1\,, \tag{3.6}$$

x_1 et y_1 s'expriment aisément en fonction des $a \dots f$. Nous n'expliciterons pas les D_{ij}. Nous remarqueron seulement que D_{11}, D_{12} et D_{13} ne dépendent pas de K_k.

Soit ψ_{ij} la phase de D_{ij}: $D_{ij} = |D_{ij}| \exp[i\psi_{ij}]$ et Θ_1 la phase de $T_{1,11}$: $T_{1,11} = |T_{1,11}| \exp[i\Theta_1]$.

(3.4) montre que

$$T_{1ij} = |T_{1ij}| \exp[i(\Theta_1 + \psi_{ij} - \psi_{11})]\,. \tag{3.7}$$

Si l'on se place au seuil $(K_k = 0)$ on trouve:

$$T_{1,11} = \frac{1}{Z_1} = A_1\,; \qquad \operatorname{tg} \vartheta_1 = \frac{y_1}{x_1} \qquad (\vartheta_1 = \Theta_{1\text{seuil}}) \tag{3.8}$$

et

$$\left\{\begin{array}{ll} \operatorname{tg} \psi_{11} = \dfrac{-(b+c)K_\Sigma}{bc - f^2 - K_\Sigma^2}\,; & \operatorname{tg} \psi_{23} = 0\,, \\[2ex] \operatorname{tg} \psi_{12} = \dfrac{hK_\Sigma}{-hc + fg}\,; & \operatorname{tg} \psi_{22} = \dfrac{-aK_\Sigma}{ac - g^2}\,, \\[2ex] \operatorname{tg} \psi_{13} = \dfrac{gK_\Sigma}{hf - bg}\,; & \operatorname{tg} \psi_{33} = -\dfrac{-aK_\Sigma}{ab - h^2}\,. \end{array}\right. \tag{3.9}$$

Noter que les expressions pour ψ_{11}, ψ_{12}, ψ_{13} sont également valables pour $K_k \neq 0$ en vertu de la remarque qui suit (3.6).

4. – Introduction de la symétrie restreinte.

Les réactions (3.1) sont complètement décrites à l'aide des 9 paramètres réels $a_0 \dots h_1$ intervenant dans T_0^{-1} et T_1^{-1}. Ceci est dû au fait que l'absorption des K^- que nous étudions s'effectue à partir d'une onde S (5). L'introduction

(5) T. B. Day, G. A. Snow et J. Sucher: *Phys. Rev. Letters*, 3, 61 (1959).

de la symétrie restreinte réduit ce nombre à 7, celle de la symétrie globale le réduit à 5. Il y a de bonnes raisons de penser [3,4,6] que, dans le domaine d'énergies actuellement exploré, ces paramètres ne varient guère. Le problème consiste à rechercher s'il est possible de déterminer ces paramètres de manière a satisfaire aux données expérimentales. Celles-ci portent sur les rapports de branchement au seuil de l'absorption K^-p:

$$\Sigma^-:\Sigma^+:\Sigma^0:\Lambda \approx 2:1:1:\tfrac{1}{4}\,, \tag{4.1}$$

sur la diffusion et l'absorption K^-p à 175 MeV/c (analyse de DALITZ et TUAN [3]) et sur la variation avec l'énergie du rapport de branchement Σ^-/Σ^+ [1]. Comme il a été largement discuté dans la Section **1** la symétrie restreinte (ou globale) peut être introduite de plusieurs manières essentiellement différentes.

Méthode I. « Comparaison des T ». – Cette méthode consiste à prendre pour la sous-matrice de T concernant la diffusion $\Lambda\pi$, $\Sigma\pi$ la sous-matrice correspondante de T'. Les éléments de matrice $T_{0,22}$ et $T_{1,ij}$ $(i, j = 2,3)$ doivent être remplacés par $T'_{0,22}$ et $T'_{1,ij}$ $(i, j = 2,3)$.

D'après (2.5) et (2.3) on a

$$T'_{0,22} = T'_{\frac{1}{2}} = \frac{1}{K_\Sigma}\sin\alpha_{\frac{1}{2}}\exp[i\alpha_{\frac{1}{2}}]\,, \tag{4.2}$$

où $\alpha_{\frac{1}{2}}$ $(\alpha_{\frac{3}{2}})$ est le déphasage de la diffusion $Y\pi$, $Z\pi$ dans l'état s de spin isotopique $i = \frac{1}{2}$ $(\frac{3}{2})$.

De même d'après (3.3′), (2.3) et (2.4)

$$T'_{1,22} = T'_{\frac{1}{2}} = \frac{1}{K_\Sigma}\sin\alpha_{\frac{1}{2}}\exp[i\alpha_{\frac{1}{2}}]\,, \tag{4.3}$$

$$T'_{1,33} = T'_{\frac{3}{2}} = \frac{1}{K_\Sigma}\sin\alpha_{\frac{3}{2}}\exp[i\alpha_{\frac{3}{2}}]\,, \tag{4.4}$$

$$T'_{1,23} = \langle\tfrac{1}{2}|T'|\tfrac{3}{2}\rangle = 0\,, \tag{4.5}$$

$T_{1,23} \approx T'_{1,23} = 0$ entraîne d'après (3.4) $D_{23} \approx 0$. Si l'on se place au seuil $(K_k = 0)$ où

$$D_{23} = -af + hg$$

la condition (4.5) donne

$$af = hg\,, \tag{4.6}$$

[6] R. H. DALITZ: *Proceedings of the CERN Conference* (1958), p. 187.

(4.6) et (3.9) entraînent les relations suivantes ($K_k = 0$):

(4.7) $$\operatorname{tg} \psi_{22} = \operatorname{tg} \psi_{12} = \frac{k_\Sigma}{-c + (g^2/a)}; \qquad \psi_{22} = \psi_{12},$$

(4.8) $$\operatorname{tg} \psi_{33} = \operatorname{tg} \psi_{13} = \frac{k_\Sigma}{-b + (h^2/a)}; \qquad \psi_{33} = \psi_{13},$$

(3.7), (4.7), (4.8), (4.3), (4.4) et $T_{22} \approx T'_{22}$ et $T_{33} \approx T'_{33}$ (par hypothèse) montrent que (*)

(4.9) $$\begin{cases} \text{Phase } (T_{13}) = \vartheta_1 + \psi_{13} - \psi_{11} = \text{phase } T_{33} \approx \alpha_{\frac{3}{2}}, \\ \text{Phase } (T_{12}) = \vartheta_1 + \psi_{12} - \psi_{11} = \text{phase } T_{22} \approx \alpha_{\frac{1}{2}}. \end{cases}$$

De (4.9) on déduit

(4.11) $$T_{1,12} = |T_{1,12}| \exp [i\alpha_{\frac{1}{2}}],$$

(4.12) $$T_{1,13} = |T_{1,13}| \exp [i\alpha_{\frac{3}{2}}].$$

En ce qui concerne $T_{0,12}$ il résulte des formules (1.14)-(1.18) et de (4.2) que

(4.13) $$T_{0,12} = |T_{0,12}| \exp [i\alpha_{\frac{1}{2}}],$$

avec

(4.14) $$\operatorname{tg} (\vartheta + \varphi) = \frac{k_\Sigma}{b_0 - (h_0^2/a_0)} \simeq \operatorname{tg} \alpha_{\frac{1}{2}}.$$

Méthode II. « Comparaison des T^{-1} ». – On suppose ici $(T^{-1})_{ij} = (T_1'^{-1})_{ij}$

(*) Pour que les relations $T_{22} \approx T'_{22}$ et $T_{33} \approx T'_{33}$ soient possibles il faut évidemment que T_{22} et T_{33} aient la forme générale $1/K_\Sigma \sin \gamma e^{i\gamma}$, ce qui au seuil est garanti par (1.3′) et par l'unitarité de la matrice S, elle-même garantie par la forme (3.3) de T^{-1} Le calcul donne ces phases en fonction des a, b, c, g, h:

(4.10) $$\begin{cases} \operatorname{tg} \gamma_2 = \dfrac{k_\Sigma}{b - (h^2/a)} \approx \operatorname{tg} \alpha_{\frac{1}{2}}, \\ \operatorname{tg} \gamma_3 = \dfrac{k}{c - (g^2/a)} \approx \operatorname{tg} \alpha_{\frac{3}{2}}. \end{cases}$$

Noter que les identifications faites au seuil permettent de fixer certains des paramètres parmi les $a \dots f$ et que la forme (3.3) continue alors à garantir l'unitarité de la matrice S à toutes les énergies K_k.

$(i, j = 2, 3)$; (3.3) donne:

$$(4.15)\qquad b - iK_\Sigma \approx \left[\frac{1}{K_\Sigma}\sin\alpha_{\frac{1}{2}}\exp\left[i\alpha_{\frac{1}{2}}\right]\right]^{-1} \qquad \text{donc} \qquad \operatorname{tg}\alpha_{\frac{1}{2}} = \frac{K_\Sigma}{b},$$

$$(4.16)\qquad (c - iK_\Sigma) \approx \left[\frac{1}{K_\Sigma}\sin\alpha_{\frac{3}{2}}\exp\left[i\alpha_{\frac{3}{2}}\right]\right]^{-1} \qquad \text{donc} \qquad \operatorname{tg}\alpha_{\frac{3}{2}} = \frac{K_\Sigma}{c},$$

$$(T^{-1})_{23} = f \approx (T'^{-1})_{23} = 0 \qquad\qquad f = 0.$$

A l'aide de (3.9) avec la condition $f = 0$ on prouve $\operatorname{tg}\psi_{12} = -(K_\Sigma/c) = -\operatorname{tg}\alpha_{\frac{3}{2}}$; $\psi_{12} = -\alpha_{\frac{3}{2}}$ ainsi que $\psi_{13} = -\alpha_{\frac{1}{2}}$ et $\psi_{11} = -(\alpha_{\frac{1}{2}} + \alpha_{\frac{3}{2}})$. (3.7) donne alors

$$(4.17)\qquad T_{1,12} = |T_{1,12}|\exp\left[i(\Theta_1 + \alpha_{\frac{1}{2}})\right] = M,$$

$$(4.18)\qquad T_{1,13} = |T_{1,13}|\exp\left[i(\Theta_1 + \alpha_{\frac{3}{2}})\right] = N,$$

Procédant de même avec T_0^{-1} on obtient (cf. (1.19), (1.21) et (4.2))

$$(4.19)\qquad T_{0,12} = |T_{0,12}|\exp\left[i(\Theta_0 + \alpha_{\frac{1}{2}})\right] = \mathrm{L},$$

et

$$(4.20)\qquad \operatorname{tg}\alpha_{\frac{1}{2}} = \frac{K_\Sigma}{b_0}.$$

Soulignons encore une fois que les résultats fournis par les méthodes I et II sont très différents pour la situation physique discutée ici. En effet les phases ϑ_1 et ϑ_0 données par les solutions de DALITZ [3] sont grandes. Pour les solutions a^+, par exemple, on a $\vartheta^\circ = 75°\,20'$ et $\vartheta_1 = 13°\,20'$.

5. – Comparaison avec l'expérience.

Méthode I. – Les phases obtenues par cette méthode ((4.11), (4.12), (4.13)) pour les éléments de matrice sont exactement celles données par AMATI et VITALE [1]. Les résultats obtenus par ces auteurs par une voie essentiellement perturbative sont donc d'une validité beaucoup plus générale que celle déterminée par le cadre des perturbations, à condition cependant que l'on postule la validité des approximation de la méthode I. Par conséquent, dans le cadre de la méthode I, l'inégalité obtenue par AMATI et VITALE, à savoir

$$(5.1)\qquad (W_{\Sigma^+\pi^-} + W_{\Sigma^-\pi^+} - 4W_{\Sigma^0\pi^0})^2 + 4W_{\Sigma^0\pi^0}\cdot W_{\Lambda\pi^0} \geqslant 4W_{\Sigma^+\pi^-}\cdot W_{\Sigma^-\pi^+}$$

reste valable, car la validité de cette inégalité est liée au fait que $T_{0,12}$ et $T_{1,12}$ ont les mêmes phases. (5.1) cependant est en violent désaccord avec le résultat expérimental (4.1). Il en résulte donc que la symétrie restreinte ne peut être introduite de cette manière. Il en va *a fortiori* de même pour la symétrie globale qui donne simplement aux phases $\alpha_{\frac{1}{2}}$ et $\alpha_{\frac{3}{2}}$ les valeurs $\delta_{\frac{1}{2}}$ et $\delta_{\frac{3}{2}}$ respectivement des déphasages de la diffusion $\pi\mathcal{N}$ sur une onde s.

Méthode II. – Du fait que $T_{0,12}$ et $T_{1,12}$ ont maintenant des phases différentes l'inégalité (5.1) n'est plus valable. Il faut donc reprendre l'analyse. Calculons alors en fonction des M, N et L définis par (4.17)-(4.19) les éléments de matrice $T_1(\Sigma)$, $T_1(\Lambda)$ et T_0 des transitions K^-p vers les systèmes $\Sigma\pi$, $\Lambda\pi$ et $\Sigma\pi$ dans les états de spin isotopique $I=1,\ 1,\ 0$ respectimevent. Tenant compte de (2.7) on a

$$\left\{\begin{aligned} T_1(\Sigma) &= \sqrt{\tfrac{2}{3}}\,M + \sqrt{\tfrac{1}{3}}\,N\,, \\ T_1(\Lambda) &= \sqrt{\tfrac{1}{3}}\,M - \sqrt{\tfrac{2}{3}}\,N\,. \\ T_0(\Sigma) &= \mathrm{L} \end{aligned}\right. \tag{5.2}$$

Les données expérimentales (4.1) au seuil conduisent essentiellement (cf. [6]) aux résultats suivants

$$\left|\frac{T_1(\Sigma)}{T_0(\Sigma)}\right|^2 \simeq \frac{1}{3}\,, \qquad \left|\frac{T_1(\Lambda)}{T_0(\Sigma)}\right|^2 \simeq \frac{1}{12}\,. \tag{5.3}$$

Phase $T_1(\Sigma)/T_0(\Sigma) \simeq \pm 70°$.

(5.2) et (5.3) donnent, compte tenu de (4.17), (4.18), (4.19),

$$\exp\,[i\alpha] = \sqrt{2}\,m + n\exp\,[i\beta]\,, \tag{5.4}$$

$$|m - \sqrt{2}\,n\exp\,[i\beta]\,|^2 = \tfrac{1}{4}\,, \tag{5.5}$$

avec $\beta = \alpha_{\frac{3}{2}} - \alpha_{\frac{1}{2}}$, $m = |M/L|$, $n = |N/L|$ et

$$\alpha = \pm 70° - \Theta_1 + \Theta_0 \tag{5.6}$$

pour que (5.5) soit possible il faut que $|\sqrt{2}n\sin\beta| \leqslant \frac{1}{2}$. (5.4) donne d'autre part $\sin\alpha = n\sin\beta$, d'où la condition de compatibilité

$$\sin^2\alpha \leqslant \tfrac{1}{8}\,. \tag{5.7}$$

Cas de solutions $b^{\pm}$ de Dalitz [3]. – (5.7) exclut immédiatement la validité de la méthode II lorsque l'on prend les solutions $b^{\pm}$ de Dalitz [3] qui sont

$A_0 = \pm 1.88 + 0.82i$; $A_1 = \pm 0.40 + 0.41i$ (A_0 et A_1 sont définis par (1.13) et (3.8) respectivement). Elles donnent $\vartheta_0 \simeq \pm 23°$; $\vartheta_1 \simeq \pm 45°$ donc $\vartheta_1 - \vartheta_0 = \pm 22°$. (5.6) donne alors $\alpha \approx \pm 92°$ ou $\alpha \approx \pm 48°$ ce qui est incompatible avec (5.7).

Cas de solutions $a^{\pm}$ de Dalitz (3). – Reste encore à prendre en considération les solutions $a^{\mp}$ de Dalitz (3) qui sont $A_0 = \pm 0.20 + i0.76$; $A_1 = \pm 1.62 \pm i0.38$; $\vartheta_0 = \pm 13°20'$, $\vartheta_1 = \pm 75°20'$. $\vartheta_1 - \vartheta_0 = -62°$. De (5.6) on a alors soit $\alpha \approx \pm 8°$ soit $\alpha \simeq \pm 130°$. Les valeurs $\alpha = \pm 130°$ sont incompatibles avec (5.7). $\alpha \simeq 8°$ permet par contre de satisfaire (5.4) et (5.5) conduisant donc au seuil au rapport (4.1). Il n'y a donc pas incompatibilité, au seuil, entre les résultats obtenus par la méthode II à partir de la symétrie restreinte (et même globale! car (5.4) montre que $\beta = \alpha_{\frac{3}{2}} - \alpha_{\frac{1}{2}} = \delta_{\frac{3}{2}} - \delta_{\frac{1}{2}}$ petit dans ce cas entraine α petit) et les données expérimentales.

Il y a cependant un fait expérimental très significatif. Le rapport au seuil ($K_k = 0$) de $\Sigma^-/\Sigma^+ = 2$ décroît très rapidement avec l'énergie pour atteindre la valeur 1 vers les énergies où $K_k \simeq 30$, 40 MeV/c et pour rester ensuite autour de cette valeur pour des énergies plus élevées. Ceci, comme il a été souligné par SALAM (4) est une propriété très importante et constitue un critère très strict pour l'étude de la validité de la symétrie globale, conduisant même à son rejet. Le fait que α soit petit montre tout de suite qu'il peut en être ainsi pour la symétrie restreinte.

Le rapport Σ^-/Σ^+ est donné par

$$\frac{\left|1 + \sqrt{\frac{3}{2}}\,\frac{T_1}{T_0}\right|^2}{\left|1 - \sqrt{\frac{3}{2}}\,\frac{T_1}{T_0}\right|^2}.$$

D'après (5.2) et (4.7)-(4.19)

$$\frac{T_1}{T_0} = \sqrt{\frac{2}{3}}\,\frac{M}{L} + \sqrt{\frac{1}{3}}\,\frac{N}{L} = \sqrt{\frac{2}{3}}\,\frac{|M|}{|L|}\exp\left[i(\Theta_1 - \Theta_0)\right] +$$

$$+ \sqrt{\frac{1}{3}}\,\frac{|N|}{|L|}\exp\left[i(\Theta_1 - \Theta_0 - \beta)\right] = \exp\left[i(\Theta_1 - \Theta_0)\right]\left(\sqrt{\frac{2}{3}}\,m + \sqrt{\frac{1}{3}}\,n\exp\left[i\beta\right]\right).$$

Mais avec (3.4) et (1.6)

$$m = \frac{|T_{1,11}|}{|T_{0,11}|}\,\frac{|D_{12}|}{|D_{11}|}\sqrt{\frac{k_\Sigma}{y}}\,; \qquad n = \frac{|T_{1,11}|}{|T_{0,11}|}\,\frac{|D_{13}|}{|D_{11}|}\sqrt{\frac{k_\Sigma}{y}}\,,$$

donc

$$\frac{T_1}{T_0} = \exp\left[i(\Theta_1 - \Theta_0)\right]\cdot\frac{|T_{1,11}|}{|T_{0,11}|}\left\{\sqrt{\frac{2}{3}}\,D_{12} + \frac{1}{\sqrt{3}}\,D_{13}\exp\left[i\beta\right]\right\}\frac{1}{|D_{11}|}\sqrt{\frac{k_\Sigma}{y}}\,.$$

Pour les valeurs de K_k comprises entre 0 et 150 MeV/c K_Σ varie peu et peut être considéré comme constant. β est un angle fixe, et, comme il a été remarqué D_{12}, D_{13}, D_{11} et Y, ne dépendant pas de K_k, restent pratiquement constants. Il en résulte donc que l'on peut écrire

$$\frac{T_1}{T_0} = \exp\left[i(\Theta_1 - \Theta_0)\right] \frac{|T_{1,11}|}{|T_{0,11}|} \cdot \text{const} = \frac{T_{1,11}}{T_{0,11}} \cdot \text{const}\,.$$

La variation avec l'énergie de T_1/T_0 est donc essentiellement déterminée par la variation correspondante de $T_{1,11}/T_{0,11}$.

D'après (1.5) et (3.5)

$$\frac{T_{1,11}}{T_{0,11}} = \frac{A_0 - ik_K A_0 A_1}{A_1 - ik_K A_0 A_1}$$

Prenant la solution a^+ de Dalitz pour A_0 et A_1 on a

$$\frac{T_{1,11}}{T_{0,11}} = \frac{A_0 + 1.24\,k_K + i\,0.03\,k_K}{A_1 + 1.24\,k_K + i\,0.03\,k_K}$$

Ceci peut se représenter à l'aide de la Fig. 1. La Fig. 1 montre que $\Theta_0 - \Theta_1$ varie rapidement avec l'énergie et diminue tandis que $|T_1|/|T_0|$ reste pratiquement constant. Ceci va dans le mauvais sens. En effet, pour avoir

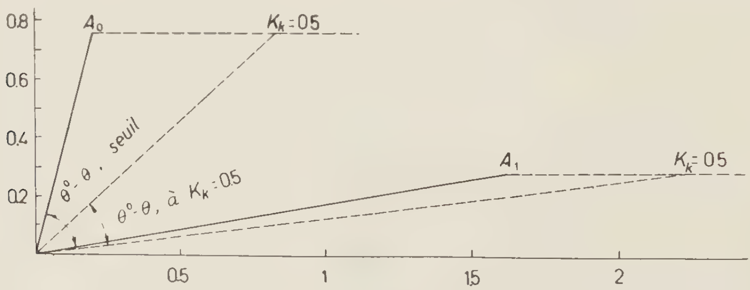

Fig. 1.

$\Sigma^-/\Sigma^+ \approx 1$ avec $|T_1|/|T_0|$ constant il faudrait que la phase de T_1/T_0 se rapproche rapidement de 90° ce qui n'est pas le cas.

La solution a^- de Dalitz conduit au même résultat: sur le graphique elle correspond à une symétrie par rapport à l'axe des ordonnées.

Il est donc ainsi prouvé que bien que la méthode II donne un résultat satisfaisant pour $k_K = 0$ elle conduit, au dessus du seuil, à des résultats qui sont en violent désaccord avec les données expérimentales. Il faut donc en conclure encore une fois que la symétrie restreinte (ou globale) n'est pas de grande utilité pour l'interprétation des résultats expérimentaux.

6. – Conclusions.

Il est évident qu'une condition suffisante pour l'utilité de la symétrie restreinte (supposée valable pour les intéractions des π) serait d'avoir affaire à des interactions K faibles. Cette condition cependant, qui n'est pas réalisée dans la nature, peut *a priori* n'être pas nécessaire et pour cette raison nous avons étudié le problème de la réaction $K+\mathcal{N}\to\Sigma(\Lambda)+\pi$ sans introduire une telle propriété. Il a été alors constaté que l'introduction de la symétrie restreinte (ou globale) conduit à des résultats qui différent essentiellement entre eux, ceci en fonction de l'approximation choisie, lorsque les interactions K ne peuvent pas être traitées en perturbations. Ceci déjà jette un doute sur l'utilité du concept de la symétrie restreinte.

Il s'est trouvé en plus que toutes les méthodes d'approximation envisagées dans ce travail (et ce sont les approximations simples) conduisent à un désaccord entre les prévisions théoriques et les données expérimentales. En toute rigueur ceci, bien entendu, ne signifie pas que l'idée même de la symétrie restreinte (ou globale) soit dénuée de sens. Simplement, même si elle existe, on ne peut en tirer aucun profit car elle est complétement masquée par les interactions K. Ce dernier effet toutefois peut, en principe, dépendre du phénomène envisagé. Il nous semble donc peut-être indiqué de poursuivre l'étude expérimentale dans ce domaine car on pourrait concevoir que pour des processus qui peuvent avoir lieu sans aucune intervention des interactions K un souvenir plus précis de la symétrie restreinte (ou globale) se manifesterait dans le processus physique. C'est, par exemple, le cas de la création des paires d'antihypérons [7] $\Sigma\overline{\Sigma}$, $\Lambda\overline{\Lambda}$, $\Lambda\overline{\Sigma}$.

Pour terminer, ajoutons une remarque. Il serait tentant de raisonner à l'envers, c'est-à-dire, partant de la connaissance de la diffusion K^-p et de l'absorption $K^-+p\to\Sigma(\Lambda)+\pi$, de déduire les phases réelles du scattering $\Sigma\pi$ et $\Lambda\pi$ en supposant ces phases connues lorsque les interactions K sont supprimées. Vu cependant la discussion de la Section **1** ceci ne peut pas être fait d'une manière univoque.

* * *

Nous tenons à remercier le professeur A. SALAM pour la communication de ses résultats avant leur publication et pour des discussions très intéressantes lors de son séjour au CERN. De même des échanges de vue avec MM. D. AMATI et Y. YAMAGUCHI nous en été très profitables.

[7] B. D'ESPAGNAT et J. PRENTKI: *Nuclear Physics*, **9**, 326 (1958-59).

Note sur épreuve

Il est possible que le résultat négatif obtenu par comparaison des résultats fournis par la méthode II avec l'expérience doive être révisé à la lumière de récentes données expérimentales. En effet, une modification, même relativement minime, des rapports de branchement au seuil peut conduire à un accroissement du second membre de (5.7) assez substantiel pour que la valeur de α correspondant aux solutions $a^{\pm}$ de Dalitz et comprise entre $\pi/2$ et π ne soit plus éliminée. Or cette valeur de α conduit précisément à un rapport Σ^-/Σ^+ décroissant avec l'énergie, ce qui est conforme aux observations. De fait, utilisant pour l'étude du même problème des données expérimentales qui seraient plus récentes, M. L. GUPTA est parvenu, par le jeu du mécanisme qui vient d'être décrit, à une compatibilité entre les résultats de la méthode II et l'expérience. Nous le remercions vivement de nous avoir communiqué cet intéressant résultat.

RIASSUNTO (*)

Si discutono i metodi per mettere alla prova la simmetria globale ($g_{NN\pi}=g_{\Lambda\Sigma\pi}=g_{\Sigma\Sigma\pi}=g_{\Xi\Xi\pi}$) e la simmetria ristretta ($g_{\Lambda\Sigma\pi}=g_{\Sigma\Sigma\pi}$) con l'aiuto dello scattering K⁻-p e dei dati d'assorbimento e se ne fa un'applicazione alla simmetria ristretta. La base di tutti i metodi di approssimazione usati a questo scopo sta nel dedurre alcune informazioni sugli elementi di matrice relativi allo scattering $\Sigma\pi$ in presenza di interazioni K premessa la conoscenza di ciò che sarebbero questi stessi elementi di matrice se fossero eliminate le interazioni K. Si mostra nella Sez. **1**: *a*) che vi sono almeno due di tali metodi: o si presume che una approssimata eguaglianza valga fra gli elementi di matrice $T_{\Sigma\pi,\Sigma\pi}$ (o $K_{\Sigma\pi,\Sigma\pi}$) con e senza interazioni K, o si presume che un'analoga eguaglianza valga fra gli elementi di matrice $(T^{-1})_{\Sigma\pi,\Sigma\pi}$ nelle stesse condizioni; *b*) che quando le interazioni K sono abbastanza grandi da dar luogo ad apprezzabili assorbimenti (come è il caso sperimentale) questi due metodi portano a risultati essenzialmente diversi. Questa osservazione generale pone seri dubbi sulla utilità dei concetti di simmetria globale o ristretta nei riguardi dei processi con nucleoni K. Comunque è interessante investigare se una di queste approssimazioni, od entrambe, portino a risultati compatibili con i dati sperimentali. Si mostra nelle Sez. **3**, **4**, **6**: *a*) che presunta la validità del 1° metodo, una diretta estensione della teoria di Amati e Vitale porta ad incopatibilità fra la simmetria ristretta ed i dati osservati; *b*) che, se si assume la validità del secondo metodo, i motivi usati da SALAM per rifiutare la simmetria globale si possono estendere alla simmetria ristretta e che, per motivi un po' diversi che in *a*), si ha ancora incompatibilità con i dati sperimentali (**). Si conclude che la simmetria ristretta non è assolutamente un concetto utile sinchè si considerano fenomeni K-p a bassa energia; o non è valida o è completamente offuscata dalle interazioni K.

(*) *Traduzione a cura della Redazione.*

(**) Vedi, tuttavia la *Nota aggiunta in bozze.*

LETTERE ALLA REDAZIONE

(La responsabilità scientifica degli scritti inseriti in questa rubrica è completamente lasciata dalla Direzione del periodico ai singoli autori)

Dispersion Relation Predictions for π, p Scattering.

T. D. SPEARMAN

St. John's College - Cambridge

(ricevuto il 17 Ottobre 1959)

The dispersion relations for forward elastic π, p scattering were used by PUPPI and STANGHELLINI [1] to calculate the real parts $D_B^{(\pm)}(\omega)$ of the forward scattering amplitudes. For π^+ scattering, the values thus obtained were in agreement with the experimental results, using as coupling constant

$$f^2 = 0.095 \pm 0.005 ,$$

and the s-wave scattering lenths of OREAR [2]

$$a_1 = \quad 0.165 ,$$

$$a_3 = -0.105 .$$

A discrepancy was observed in the case of π^- scattering. SALZMAN and SCHNITZER [3], using later values for the total cross-section, reduced this discrepancy. A calculation by the author [4], using more recent cross-sectional data, gave reasonable agreement in the case of both π^+ and π^- for a value of the renormalized coupling constant

$$f^2 = 0.08 \pm 0.01 ,$$

using again the scattering lengths of OREAR [2]. The values of the total π^-, p cross-section $\sigma^-(\omega)$, in the range 0 to 275 MeV were those of ANDERSON and METROPOLIS [5]; the points at 307 and 330 MeV were due to KORENCHENKO and ZINOV [6]; in the range 450 to 1200 MeV the values of BURROWES *et al.* [7] were used; and for energies above 1200 MeV $\sigma^-(\omega)$ was assumed to have the constant value 30 mb. For the total π^+, p cross-section $\sigma^+(\omega)$, the results of ANDERSON, DAVIDON and KRUSE [8];

(1) G. PUPPI and A. STANGHELLINI: *Nuovo Cimento*, **5**, 1305 (1957)

(2) J. OREAR: *Phys. Rev.* **96**, 176 (1954).

(3) H. J. SCHNITZER and G. SALZMAN: *Phys. Rev.*, **112**, 1802 (1958).

(4) See article by J. HAMILTON: *Progr. Nucl. Phys.*, **8**, to be published.

(5) H. L. ANDERSON and N. METROPOLIS: *Proc. of the Sixth Annual Rochester Conference on High Energy Nuclear Physics* (New York, 1956), Sect. I, p. 20.

(6) S. M. KORENCHENKO and V. G. ZINOV: *Sowiet Physics J.E.T.P.*, **6**, 1006 (1958).

(7) H. C. BURROWES, D. O. CALDWELL, D. H. FRISCH, D. A. HILL, D. M. RITSON, R. A. SCHLUTER and M. A. WAHLIG: *Phys. Rev. Lett.*, **2**, 119 (1959).

(8) F. ANDERSON, W. C. DAVIDON and U. E. KRUSE: *Phys. Rev.*, **104**, 339 (1956).

Cool, Piccioni and Clark [9]; and Burrowes *et al.* [7] were used and it was assumed that for energies above 1900 MeV $\sigma^+(\omega)$ had the constant value 30 mb.

From an investigation of low energy pion phenomena Hamilton and Woolcock [10] have recently obtained the values

$$a_1 = \quad 0.178\,,$$

$$a_3 = -0.087\,,$$

for the *s*-wave scattering lengths. These values differ appreciably from those of

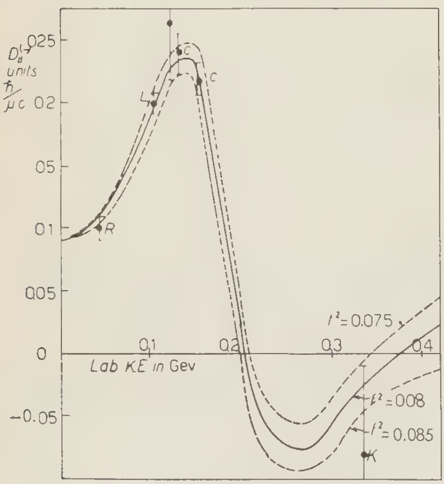

Fig. 1.

Orear and it seemed of interest to study their effect on the dispersion relation result. Fig. 1 and 2 show the calculated values for $D_B^{(-)}$ and $D_B^{(+)}$ respectively, using these new values, and their agreement with the experimental results [11]. The consequence of the new values for the scattering lengths is to improve the fit in the case of π^-, for $f^2 = 0.08$, while retaining good agreement for π^+.

An interesting consequence of the new data is that the values of the renormalized coupling constant which will give a good fit with the experimental results for both π^+ and π^- are now closely restricted. The π^- results using $f^2=0.075$ and $f^2=0.085$ are shown by the two dotted curves in Fig. 1. It is seen that for both of these values the agreement with the experimental data breaks down. The dotted curve in Fig. 2 shows the calculated π^+ value

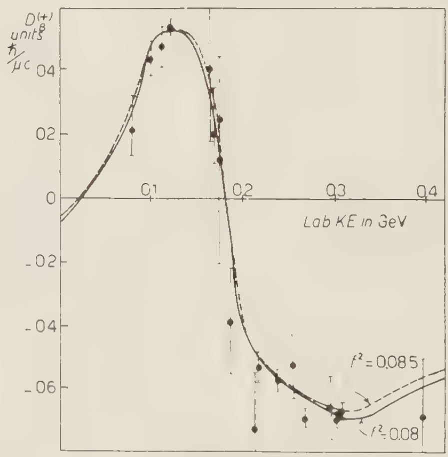

Fig. 2.

for $f^2 = 0.085$. Here again the fit is not as good as for $f^2 = 0.08$.

(9) R. Cool, O. Piccioni and D. Clark: *Phys. Rev.*, **103**, 1082 (1956).

(10) J. Hamilton and W. S. Woolcock: to be published. I am indebted to Dr. Hamilton and Mr. Woolcock for permission to use their results.

(11) The experimental values for $D_B^{(-)}$ are due to: S. W Barnes *et al.*: Rochester University preprint NYO-2170 (1958); (denoted in Fig. 1 by R). D. N. Edwards, S. G. F. Frank and J. R. Holt: *Proc. Phys. Soc.*, **73**, 856 (1959); (denoted in Fig. 1 by L). U. E. Kruse and R. G. Arnold: University of Chicago, preprint (1959); (denoted by C). S. M. Korenchenko and V. G. Zinov: *Sowiet Physics J.E.T.P.*, **6**, 1006 (1958); (denoted by K). The results K are as recalculated by Hamilton and Chiu: *Phys. Rev. Lett.*, **1**, 146 (1958).

We conclude that the discrepancy, observed by PUPPI and STANGHELLINI [1], in the dispersion relation prediction for π^-, p scattering, has been satisfactorily resolved using more accurate experimental data [12]. It would appear moreover that to obtain a satisfactory agreement a value of the renormalized coupling constant f^2 such that

$$0.075 < f^2 < 0.085 .$$

must be used.

[12] A similar conclusion has been obtained by H. P. NOYES and D. N. EDWARDS (private communication), who also point out that the dispersion relations favour the values obtained by HAMILTON and WOOLCOCK [10] for the scattering lengths.

Proton-Proton Scattering Phase Shifts at 150 MeV (*).

R. C. Stabler and E. L. Lomon (**)

Laboratory of Nuclear Studies, Cornell University - Ithaca, N. Y.

(ricevuto il 20 Ottobre 1959)

We would like to report the results of a phase shift analysis of proton-proton scattering data at 150 MeV (1). Using a set of experimental quantities f_j a limited search with an I.B.M. 650 computer has been performed by expanding

$$M = \sum_j [f_j(\delta_i) - f_{j(\text{exp})}]^2/[\Delta f_{j(\text{exp})}]^2\,,$$

in a Taylor series to second order about several trial solutions. Then

$$M = M_0 + 2\sum_i T_i\,\Delta\delta_i + \sum_{ij} S_{ij}\,\Delta\delta_i\,\Delta\delta_j\,,$$

is mimized by setting $\delta_i = \delta_{i(\text{trial})} + \Delta\delta_i$ where $\Delta\delta_i = -S_{ij}^{-1}T_j$ (2). We have used the Harvard cross section, polarization, and depolarization data (3) fitting with phase shifts up to F waves. As noted by Chamberlain *et al.* (4) these three experiments are sufficient to over-determine the phase shifts providing that l is cut off at some $l_{\max}$. Thus well localized minima are to be expected.

We have searched for solutions in two regions roughly corresponding to Stapp's solutions 1 and 6 (5). Preliminary results of the search in the 6 region have been previously reported. A good fit was obtained by iterating the search procedure from Phillip's solution (3*b*) (6). However, with the addition of small angle polarization data this solution (B) could not be brought into the acceptable range for M. This may be due to the importance of linear combinations of scattering matrix elements in the Coulomb interference region. This yields independent information through the known Coulomb interaction. Moreover the R values for this solution are in substantial disagreement with the recent Harwell results, not being sufficiently negative (7). A fit

(*) Supported by the joint program of the Office of Naval Research and the U. S. Atomic Energy Commission.

(**) Permanent address: Dept. of Mathematics, McGill University, Montreal, Canada.

(1) Preliminary results reported at London Few Nucleon Conf. and Kiev High Energy Conf. (1959).

(2) For a more detailed discussion of this method see H. Y. Chiu and E. L. Lomon: *Ann. of Phys.*, **6**, 50 (1959).

(3) J. N. Palmieri, A. M. Cormack, N. F. Ramsey and R. Wilson: *Ann. of Phys.*, **5**, 299 (1958). Harwell data is also available. The main discrepancy with the Harvard data is in the depolarization measurement and the normalization. This data was not included due to the length of the program.

(4) O. Chamberlain, E. Segrè, R. D. Tripp, C. Wiegand and T. Ypsilantis: *Phys. Rev.*, **105**, 288 (1957).

(5) H. P. Stapp, T. Ypsilantis and N. Metropolis: *Phys. Rev.*, **105**, 302 (1957).

(6) R. C. Stabler: *Bull. Am. Phys. Soc.*, **4**, 267 (1959).

(7) Bird, Edwards, Rose, Taylor and Wood: *London Few Nucleon Conf.* (1959).

also was obtained to the Harwell depolarization data which had to be discarded due to its behavior in the Coulomb interference region.

In the region of Stapp's solution no. 1 iterations were performed starting from both the Gammel and Thaler (GT) and Signell and Marshak (SM1) solutions [8].

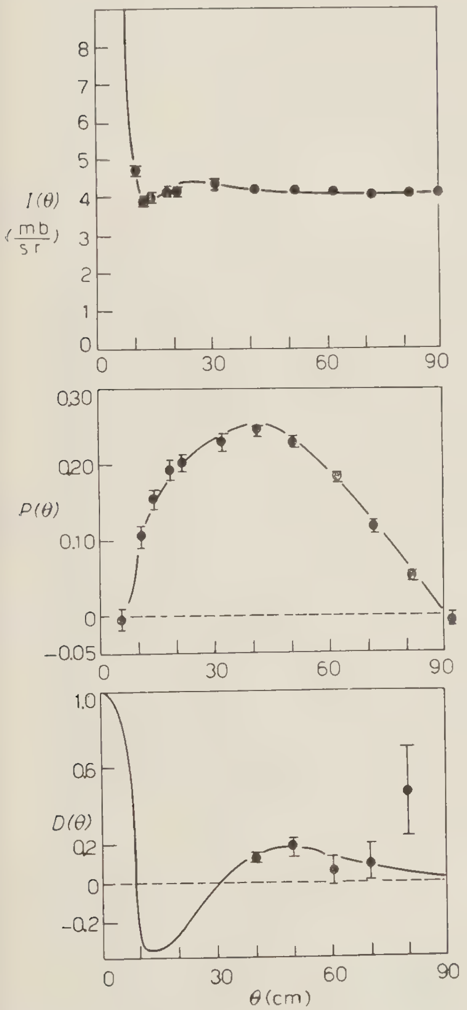

Fig. 1. – The Harvard cross section, polarization and depolarization data at 147 MeV and the curves for solution A.

Both of these converged to solution A. See Table I. Twenty-nine representative data were used: twelve $I(\theta)$, twelve $P(\theta)$, and five $D(\theta)$. Thus the most probable value of M for the true solution with the eight phase shifts and one coupling parameter would be 20. The predicted values for the other triple scattering parameters from solution A are shown in Fig. 2. The agreement with the now available data on R is adequate. Data available from earlier iterations indicates that a better fit of R can be made without substantially affecting the fit to the other parameters. The ranges of the phase shifts given for solution A are the changes necessary to increase the value of M to 37.6, corresponding to a 1% correlation with the experiments.

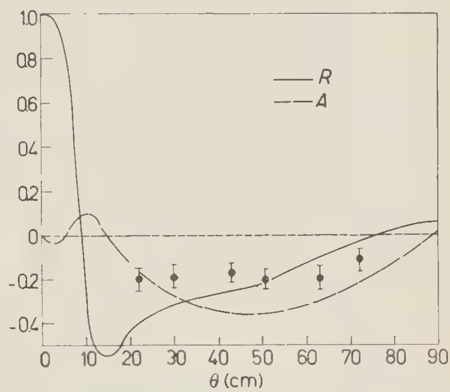

Fig. 2. – The triple scattering parameters $R(\theta)$ and $A(\theta)$ at 147 MeV for solution A. The experimental points are those obtained at Harwell for $R(\theta)$ at 140 MeV. No attempt has been made to fit this data.

Thus $\Delta\delta_i = \sqrt{(37.6 - M)/S_{ii}}$ (*). This neglects the correlations between the errors in the various phase shifts. The correlated sensitivities can be obtained from the inverted S_{ij} matrix. The

[8] G. L. GAMMEL and R. M. THALER: *Phys. Rev.*, **107**, 291 (1957), and R. MARSHAK: private communication.

(*) The standard deviations, upon neglecting correlations, are given by $\sqrt{1/S_{ii}}$.

TABLE I. – *Total bar phase shifts in degrees.*

Phase	GT	SM1	A	P (3b)	B
$^1S_0$	11.7	19.2	13.9 ± 1.5	18.0	12.7
$^1D_0$	9.9	6.9	7.0 ± 0.5	− 2.0	5.3
$^3P_0$	4.1	10.6	7.4 ± 2.5	− 36.0	− 51.6
$^3P_1$	− 17.0	− 18.7	-18.2 ± 0.4	14.0	1.7
$^3P_2$	14.2	12.6	14.9 ± 0.3	6.0	6.9
ε_2	− 2.7	− 4.3	-2.5 ± 0.3	—	0.0
$^3F_2$	3.1	0.83	2.7 ± 0.5	—	1.9
$^3F_3$	− 1.4	0.02	-1.3 ± 0.4	—	1.9
$^3F_4$	3.9	3.3	2.9 ± 0.3	0.8	2.5
M	748	365	18.6	1970	123

TABLE II. – S_{ij} *in (degrees)*$^{-2}$ *for solution* A.

	$^1S_0$	$^1D_0$	$^3P_0$	$^3P_1$	$^3P_2$	ε_2	$^3F_2$	$^3F_3$	$^3F_4$
$^1S_0$	8.9	24.5	3.4	− 25.8	21.4	16.7	− 10.8	− 27.7	19.0
$^1D_0$		94.9	11.2	− 58.9	24.6	95.1	− 27.9	− 92.4	47.1
$^3P_0$			3.1	− 9.5	4.3	10.5	− 1.9	− 10.0	7.6
$^3P_1$				147.7	− 139.5	18.9	26.3	72.6	− 0.3
$^3P_2$					187.3	− 65.5	− 36.7	− 27.5	42.0
ε_2						246.7	− 79.7	− 131.0	130 2
$^3F_2$							75.6	69·9	− 106 5
$^3F_3$								145·2	− 76.7
$^3F_4$									234.7

expectation that the $I(\theta)$, $P(\theta)$ and $D(\theta)$ measurements would be sufficient to yield localized minima has so far been borne out. The minima are deep and narrow, the background M being of the order of several hundred or more. The Coulomb interference eliminated one minimum which would otherwise appear. We expect any more minima found to be of this type. It is not likely that any more exist in regions extrapolating to the 310 MeV solutions.

The program is being modified to include data from R and A experiments and is being transferred to a Burroughs 220 computer. A more extensive search will be made.

* * *

We are indebted to Miss A. WALBRAN of the Cornell Computing Center for doing the programming and to Dr. A. CROMER for discussions and the computation of the triple scattering parameters.

TCP as a Space Reflection (*).

E. Lubkin

Lawrence Radiation Laboratory, University of California - Berkeley, Cal.

(ricevuto il 9 Novembre 1959)

1. – The remark that parity conservation implies the impossibility of the experimental definition of a right-handed coordinate system was somewhat disturbing in the days before the discovery of parity non-conservation, because one would have liked to argue in the reverse direction, but one was blocked by the fallaciousness of the converse (1). This very difficulty has been turned to advantage to show that the present experimental situation does not involve an experimental definition of a right-handed coordinate system, because the present situation is consistent with *CP* invariance (2). In order to accept this conclusion, one must abandon *a priori* choice of sign of charge; this choice, if it is at all involved in the discussion of an experimental definition of right and left, must itself be part of the experiment.

If one oversimplifies the situation by accepting the conclusion—namely, that *CP* invariance be a reasonable substitute for *P* invariance in providing for left-right symmetry—merely on the ground that the factor *P* occurs once in *CP*, one is thereby led to the conjecture that *TCP* invariance alone may provide for left-right symmetry, in the sense that a theory which possesses *TCP* invariance must also satisfy the condition that an observer be incapable of experimentally defining a right-handed coordinate system, for indeed the factor *P* occurs once in *TCP*, as well as in *P* and in *CP*.

This conclusion is valid only if one takes even greater care not to make any choice prior to the attempted experimental determination of a screw sense. In fact, one must not allow an *a priori* determination of a sense of time.

This may be seen most rapidly as follows. Consider a system which contains an observer, and its image under *TCP*. The notebooks of the *TCP*'ed observer will have the same text as those of the original observer; *e.g.*, there will be no extra minus signs. But the coordinates employed by the *TCP*'ed observer differ objectively from those of the initial observer with regard to spatial orientation, sense of time, and

(*) This work was performed under the auspices of the U. S. Atomic Energy Commission

(1) The possibility of *CP* as a space reflection appears in the famous footnote of G. C. Wick, A. S. Wightman and E. P. Wigner: *Phys. Rev.*, **88**, 104 (1952).

(2) T. D. Lee and C. N. Yang: *Phys. Rev.*, **105**, 1671 (1957); L. Landau: *Nucl. Phys.*, **3**, 127 (1957); E. P. Wigner: *Rev. Mod. Phys.*, **29**, 258 (1957).

sign of charge (*). Consequently, for each asymmetry observed by the original observer, the objectively reversed asymmetry is seen by the TCP'ed observer, providing over-all symmetry with respect to choice of a screw sense, of a time sense, and of a sign of charge.

It is not necessary, of course, to explicitly consider time-reversed observers, and in the following the situation will be examined from the standpoint of the various asymmetries that may be seen by a single observer.

It is convenient to use proper Lorentz invariance to reduce all observables to proper Lorentz scalars. One then asks how these observables transform under pure space reflection or « parity », P; pure charge conjugation, C; and pure time reversal, T. Since these three operations commute and square to 1 in their action on the scalar observables, the operations they induce on the scalar observables may be simultaneously diagonalized (**), so that we may speak of eight types of proper Lorentz scalars, according to their behavior in regard to change of sign under the transformations of scalar observables induced by P, C, T. Convenient notation for these eight types of scalars is as follows: a $1+$ scalar changes its sign under none of the three operations, a $1-$ scalar changes its sign under all of them, a $P-$, $C-$, or $T-$ changes its sign only under the transformation induced by P, C, or T, respectively, and a $P+$, $C+$, or $T+$ does not change its sign under the transformation induced by P, C, or T, respectively, but does change its sign under the two other transformations.

(*) This comparison of the objective situations may be facilitated by considering the two relatively TCP' ed states as descriptions of only parts of a system observed by a super-observer to whom the operation does not apply.

(**) Note that scalars so incomparable that they may not be added also cannot be expected to mix under an inversion operation, so that their existence does not really damage the classification argument.

Instead of considering the general conditions for an experimental definition of just an absolute screw sense to be impossible—a matter that is easily discussed in the present framework of the eight classes of proper Lorentz scalars—we will consider the general conditions for the impossibility of an experimental definition of either an absolute screw sense, or an absolute sign of charge, or an absolute sense of time. Bias introduced by the observer is easily eliminated by the free use of coordinate systems: thus, instead of considering a time-reversed observer, one may consider the use of a reversed time coordinate for a fixed observer.

The three impossibility conditions are then easily seen to be incompatible with the existence of a nonzero $P-$, $C-$, or $T-$. Since the conjoint existence of a nonzero $1-$ and a nonzero $P+$, $C+$, or $T+$ would give rise to the existence of a nonzero $P-$, $C-$, or $T-$, respectively, the three impossibility conditions allow either the conjoint existence of the nonzero types $1+$, $1-$, or the conjoint existence of the nonzero types $1+, P+, C+, T+$. The parity asymmetries already discovered are of form $T+$. Therefore, the impossibility conditions and the present experimental situation limit the types to $1+$, $P+$, $C+$, $T+$. This set coincides with that determined by the requirement of invariance under the transformation induced by TCP. Either from the previous argument using the TCP image of an observer, or from the observation that neither a $P+$ nor a $T+$ can determine a convention without a prior choice of another convention, one concludes that the impossibility conditions provide no further restriction on the possible types of nonzero proper Lorentz scalar observables than is imposed by TCP invariance.

That the left-right symmetry inherent in TCP invariance alone necessitates the contemplation of a time-reversed observer, or equivalently, the acceptance

of coordinate systems with t running opposite to the usual sense, is easily shown in an example. Suppose a spinless particle A decays into particles B and C, and that B has spin, and is in fact totally longitudinally polarized. Further, suppose that the charge-conjugate decay involves the same longitudinal polarization of B, so that CP invariance is violated. Then TCP invariance may still be maintained by allowing only the B and $\overline{\mathrm{B}}$ particles of reverse helicity to be captured in the inverse processes $\mathrm{B}+\mathrm{C}\to\mathrm{A}$, $\overline{\mathrm{B}}+\overline{\mathrm{C}}\to\overline{\mathrm{A}}$. The only way to argue that a screw sense is not absolutely determined in this example is to admit the time-reversed description on a footing equal with the usual description, so that the capture reactions may be regarded as decays involving the opposite helicity.

2. – The three general indistinguishability conditions regarding screw sense, time sense, and sign of charge have been shown to impose no restriction beyond what is imposed by TCP invariance. If one seeks a general indistinguishability principle that rules out the possibility of nonzero $P+$ and $C+$ scalars, in conformity with the apparent validity of CP invariance, one must go beyond a requirement of left-right symmetry.

It is easy to find such a principle. The known existence of a nonzero $T+$ has already correlated choice of sign of charge with choice of a screw sense, so that the existence of a nonzero $P+$ or $C+$ would imply a correlation of all three choices. One may then postulate a principle of *independence* of choice of screw sense from choice of time sense to rule out the unobserved asymmetries.

Such a postulate may seem of questionable form, because the apparently similar postulate forbidding dependence of choice of sign of charge on choice of screw sense is wrong.

However, these two kinds of dependence are of quite different character. The charge-screw sense dependence may be viewed as an actual spatial structure of charge, in analogy to stereoisomerism in chemistry, and it may therefore be considered a welcome step in the unification of charge with space-time. But a time-screw sense dependence has no similar concretization, and would constitute, in more symmetric language, an orientation of 4-space. A rule forbidding dependence between screw sense and time sense is therefore an analogue of the rule forbidding an experimental definition of a screw sense, stepped up to four dimensions.

The Sigma-Neutron Interaction (*).

G. Eder

Institute for Theoretical Physics, University of Vienna - Vienna

(ricevuto il 14 Novembre 1959)

At the Kiev Conference on High Energy Physics 1959 Gandolfi *et al.* submitted an event which probably represents a Σ^-n bound state. As this state is not observed in experiments where K^--mesons are absorbed from S-states in deuterium, one has to assume that Σ^- and n are bound in a singlet S-state. It therefore seems that the Σ^--n interaction in even parity states is more attractive in the singlet than in the triplet spin state. In this note we shall show that a meson-theoretical calculation allows us to understand this behavior.

The adiabatic potential in the second and fourth order is calculated following the methods of Brueckner and Watson (1). The static approximation used here and the restriction to second and fourth order potential means that the results have a qualitative meaning only.

The interaction Hamiltonian shall be the following:

$$H' = H'_{\mathcal{N}\mathcal{N}} + H'_{\Sigma\Sigma} + H'_{\Sigma\Lambda}\,,$$

where

$$H'_{\mathcal{N}\mathcal{N}} = \frac{\sqrt{4\pi}}{\mu} f_1(\boldsymbol{\sigma}\boldsymbol{\nabla})(\boldsymbol{\tau}\boldsymbol{\varphi})\,,\quad H'_{\Sigma\Sigma} = \frac{\sqrt{4\pi}}{\mu} f_2(\boldsymbol{\sigma}\boldsymbol{\nabla})\,2(\boldsymbol{I}_\Sigma\boldsymbol{\varphi})\,,\quad H'_{\Lambda\Sigma} = \frac{\sqrt{4\pi}}{\mu} f_3(\boldsymbol{\sigma}\boldsymbol{\nabla})(\boldsymbol{w}_\Sigma\boldsymbol{\varphi})\,.$$

The baryons are treated as heavy particles (recoil effects are neglected), $\boldsymbol{\sigma}$ is the Pauli spin vector of the baryons, which are all supposed to have spin $\frac{1}{2}$. τ_k are the nucleon isobaric spin matrices. $\boldsymbol{I}_\Sigma$ and $\boldsymbol{w}_\Sigma$ are the isobaric spin vector and isobaric spin function of the Σ-particle. μ is the pion mass. $\boldsymbol{\varphi}$ represents the pion field operator. We introduce $x = \mu|\boldsymbol{r}|$, where $\boldsymbol{r}$ means the separation be-

(*) Sponsored in part by the U. S. Government.

(1) K. A. Brueckner and K. M. Watson: *Phys. Rev.*, **92**, 1023 (1953).

tween nucleon and Σ-particle. We then get for the adiabatic Σ-nucleon potential:

$$V(x) = \frac{2}{3} f_1 f_2 \mu (\boldsymbol{\tau I}_\Sigma) \left(\boldsymbol{\sigma}_1 \boldsymbol{\sigma}_2 + \frac{3+3x+x^2}{x^2} S_{12} \right) \frac{e^{-x}}{x} -$$

$$- \frac{2 f_1^2 f_2^2}{\pi x^3} \mu \left\{ (3 - 4\, \boldsymbol{\tau I}_\Sigma) \left[(2 + 2x + x^2) k_0(x) + \frac{4+4+x^2}{x} k_1(x) \right] e^{-x} + \right.$$

$$+ 2(\boldsymbol{\tau I}_\Sigma) \left[(23 + 4x^2) k_0(2x) + \frac{23+12x^2}{x} k_1(2x) \right] - 4(\boldsymbol{\sigma}_1 \boldsymbol{\sigma}_2) \left[3k_0(2x) + \frac{3+2x^2}{x} k_1(2x) \right] +$$

$$+ \frac{2}{3} (\boldsymbol{\sigma}_1 \boldsymbol{\sigma}_2)(3 - 4 \boldsymbol{\tau I}_\Sigma) \left[(1+x) k_0(x) + \frac{2+2x+x^2}{x} k_1(x) \right] e^{-x} +$$

$$\left. + \frac{1}{3} S_{12} \left[36 k_0(2x) + \frac{45+12x^2}{x} k_1(2x) - (3 - 4\boldsymbol{\tau I}_\Sigma) \left((1+x) k_0(x) + \frac{5+5x+x^2}{x} k_1(x) \right) e^{-x} \right] \right\},$$

where

$$S_{12} = (3/r^2)(\boldsymbol{\sigma}_1 \boldsymbol{r})(\boldsymbol{\sigma}_2 \boldsymbol{r}) - (\boldsymbol{\sigma}_1 \boldsymbol{\sigma}_2) \, .$$

On account of $H'_{\Sigma\Lambda}$ we also get a contribution to the potential in fourth order arising from intermediate Λ-states of the hyperon. The rest energy difference between the σ and the Λ-particle,

$$\delta = m_\Sigma - m_\Lambda = (77.8 \pm 3.6) \text{ MeV},$$

has been neglected in comparison with the energy of the exchanged pions. We thus get the further contribution

$$V_\Lambda(x) = - \frac{f_1^2 f_3^2}{3\pi x^3} \mu \left\{ 6 \left[(2 + 2x + x^2) k_0(x) + \frac{4+4x+x^2}{x} k_1(x) \right] e^{-x} + \right.$$

$$+ 3(\boldsymbol{\tau I}_\Sigma) \left[(23 + 4x^2) k_0(2x) + \frac{23+12x^2}{x} k_1(2x) - \right.$$

$$\left. - 2 \left((2 + 2x + x^2) k_0(x) + \frac{4+4x+x^2}{x} k_1(x) \right) e^{-x} \right] +$$

$$+ 4(\boldsymbol{\sigma}_1 \boldsymbol{\sigma}_2) \left[\left((1+x) k_0(x) + \frac{2+2x+x^2}{x} k_1(x) \right) e^{-x} - 6k_0(2x) - \frac{6+4x^2}{x} k_1(2x) \right] +$$

$$+ 2S_{12} \left[12k_0(2x) + \frac{15+4x^2}{x} k_1(2x) - \left((1+x) k_0(x) + \frac{5+5x+x^2}{x} k_1(x) \right) e^{-x} \right] +$$

$$+ 4(\boldsymbol{\tau I}_\Sigma) \left[S_{12} \left((1+x) k_0(x) + \frac{5+5+x^2}{x} k_1(x) \right) - \right.$$

$$\left. \left. - 2 (\boldsymbol{\sigma}_1 \boldsymbol{\sigma}_2) \left((1+x) k_0(x) + \frac{2+2x+x^2}{x} k_1(x) \right) \right] e^{-x} \right\}.$$

For $\delta \neq 0$ we have to take into account that δ has to be subtracted from the meson energies in the intermediate states. This means that δ will have the effect of a longer range for the Σ-nucleon potential (about 0.9 fermi instead of 0.7 fermi). For the singlet and triplet spin states we have $(\boldsymbol{\sigma}_1 \boldsymbol{\sigma}_2) = -3$ and 1. $(\boldsymbol{\tau I}_\Sigma) = 1$ and

-2 for the total isobaric spin quantum number $I=\frac{3}{2}$ and $\frac{1}{2}$, respectively. As Σ^-n has $I_3=-1-\frac{1}{2}=-\frac{3}{2}$ only $I=\frac{3}{2}$ is possible. The potential of the Σ^--n system is thus given by $V+V_\Lambda$ with $(\boldsymbol{\tau I}_\Sigma)=1$. With $f_1^2=f_2^2=f_3^2=f^2$ we get for the singlet spin state

$$V_s=-f^2\mu\left\{\frac{2e^{-x}}{x}+\frac{f^2}{\pi x^3}\left[2\left((2+2x-x^2)k_0(x)+\frac{4+4x+3x^2}{x}\,k_1(x)\right)e^{-x}+\right.\right.$$
$$\left.\left.+(211+20x^2)k_0(2x)+\frac{211+124x^2}{x}\,k_1(2x)\right]\right\}.$$

For the triplet spin potential we have

$$V_{tr}=V_c+V_T S_{12}\,,$$

where the central and tensor part are given by

$$V_c=\frac{2f^2\mu}{3}\left\{\frac{e^{-x}}{x}+\frac{f^2}{\pi x^3}\left[\left(3\,(2+2x+x^2)k_0(x)+\frac{20+20x+7x^2}{x}\,k_1(x)\right)e^{-x}-\right.\right.$$
$$\left.\left.-\left((124.5+30x^2)k_0(2x)+\frac{124.5+58x^2}{x}\,k_1(2x)\right)\right]\right\},$$

$$V_T=\frac{2f^2\mu}{3x^3}\left\{(3+3x+x^2)e^{-x}-\frac{2f^2}{\pi}\left[24k_0(2x)+\frac{30+8x^2}{x}\,k_1(2x)+\right.\right.$$
$$\left.\left.+\left((1+x)k_0(x)+\frac{5+5x+x^2}{x}\,k_1(x)\right)e^{-x}\right]\right\}.$$

The potential is shown in Fig. 1 for $f^2=0.08$. Here S stands for the singlet potential; C and T stand for the central and tensor part of the triplet spin state potential. We immediately see that the singlet potential is much stronger than the triplet potential. In a wide range the tensor part is even repulsive. A repulsive core with a radius in the usual order of magnitude can therefore easily give binding in the singlet state, but not in the triplet state.

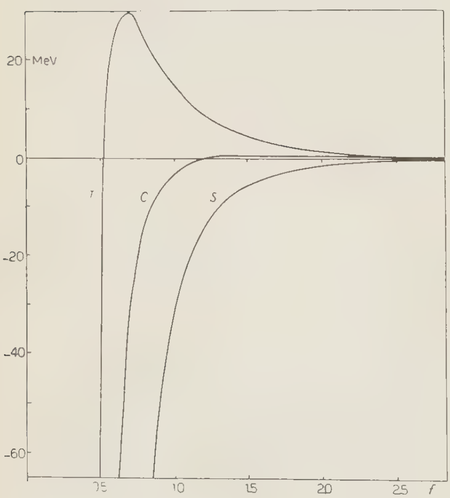

Fig. 1. – Σ^--n potential in the singlet (S) and triplet (C, T) spin states for $f_1^2=f_2^2=f_3^2=0.08$.

* * *

I wish to thank Professor Dr. W. Thirring for the inspiration of this work.

IL NUOVO CIMENTO Vol. XV, N. 1 1° Gennaio 1960

The Non-Renormalization Hypothesis for the vector β-Decay and Rare Decay Models of Hyperons.

N. Cabibbo and R. Gatto

Istituto di Fisica e Scuola di Perfezionamento in Fisica Nucleare dell'Università - Roma
Istituto Nazionale di Fisica Nucleare - Sezione di Roma

(ricevuto il 26 Novembre 1959)

It is known that the non-renormalization hypothesis for the vector strangeness-conserving current allows one to relate some weak decay amplitudes to corresponding electromagnetic amplitudes ([1]). We have used this relation to express the vector amplitude for $\Sigma^{\pm}\to\Lambda^0+e^{\pm}+\nu$ in terms of the Σ^0-Λ^0 transition magnetic moment. Such a magnetic moment determines the Σ^0 lifetime and it also appears in the residuum of a pole in the amplitude for $\gamma+N\to Y+K$. Global symmetry would give a value for such a moment equal, except for the sign, to that of the neutron magnetic moment ([2]). The vector amplitude for $\Sigma\to\Lambda+e+\nu$ derived in this way turns out to be very small, corresponding to a branching ratio $\simeq 10^{-7}$. Thus if a rate for such a process would ever be detected it should entirely come from the axial current. One would then conclude, using a theorem due to Weinberg ([3]), that, after averaging over the lepton momenta and spins, all parity non-conserving effects (up-down asymmetry for the Λ-momentum with respect to the plane of production of the decaying Σ, and forward-backward asymmetry in the subsequent Λ decay) must be absent. If such tests were not satisfied the non-renormalization hypothesis could not be maintained.

It must be noted that under the non-renormalization hypothesis allowed vector transition must satisfy, together with the condition $\Delta J=0$ (no), also the condition $\Delta I=0$ in the isotopic spin change. Examples of such allowed transitions are $n\to p+e+\nu$, $\pi^{\pm}\to\pi^0+e^{\pm}+\nu$, $\Sigma^-\to\Sigma^0+e^-+\nu$, $K^0\to K^++e^-+\nu$, possibly $\Xi^-\to\Xi^0+e^-+\nu$, and transitions between nuclear energy levels of the same supermultiplet (however even without the non-renormalization hypothesis the vector matrix element for a nuclear transition not satisfying $\Delta I=0$ would anyway be very small as long as one can regard the nucleus as built up from independent dressed nucleons, see ref. ([1])).

([1]) M. Gell-Mann and R. P. Feynman: *Phys. Rev.*, **109**, 193 (1958); M. Gell-Mann: *Phys. Rev.*, **111**, 362 (1958).

([2]) M. Gell-Mann: *Proc. of the 1958 Annual International Conference on High Energy Physics at CERN* (Geneva) edited by B. Ferretti, p. 162.

([3]) S. Weinberg: *Phys. Rev.*, **115**, 481 (1959 .

The reaction $\Sigma \to \Lambda + e + \nu$ could thus be classified as a forbidden transition for the vector under the non-renormalization hypothesis, but it could have an allowed vector matrix element without such a hypothesis.

One should also remark that the non-renormalization hypothesis for the vector current, together with the assumption that the baryons appear in the Lagrangian with a definite spirality, implies also the absence of a bare axial coupling. Therefore detection of a rate for $\Sigma \to \Lambda + e + \nu$ would indicate a big renormalization of the A coupling (the first induced terms come from the 3π states and are negligible).

The matrix element for $\Sigma^+ \to \Lambda^0 + e^+ + \nu$ is given by

$$\langle \Lambda^0 e^+ \nu; \text{out} \,|\, \Sigma^+; \text{in} \rangle = 2\pi i G(\bar{\nu}\gamma_\mu\, ae) \langle \Lambda^0 \,|\, J_\mu^{(A)}(0) + J_\mu^{(V)}(0) \,|\, \Sigma^+ \rangle \delta(p_\Sigma - p_\Lambda - p_\nu - p_e) ,$$

where G is the weak coupling constant, ν and e are the neutrino and electron spinor respectively, $a = \frac{1}{2}(1 + \gamma' s)$, $J_\mu^{(A)}(x)$ and $J_\mu^{(V)}(x)$ are the axial and vector strangeness-conserving currents. With the hypothesis of non-renormalization for the vector strangeness-conserving current, $J_\mu^{(V)}(x)$ can be identified with the minus component $J_\mu^{(-)}(x)$ of the total isotopic spin current. Next one notes that in the matrix element of the electromagnetic current $J_\mu(x)$ between a Σ^0 and a Λ^0, $\langle \Lambda^0 \,|\, J_\mu(x) \,|\, \Sigma^0 \rangle$, only that part of $J_\mu(x)$ contributes which behaves as the zero-component of a vector in isotopic spin space. This part is $J_\mu^{(0)}(x)$ and it is related to $J_\mu^{(-)}(x)$ by an isotopic-spin rotation. It follows that $\langle \Lambda^0 \,|\, J_\mu^{(V)}(0) \,|\, \Sigma^+ \rangle$ in (1) is equal to the electromagnetic matrix element $\langle \Lambda^0 \,|\, J_\mu(0) \,|\, \Sigma^0 \rangle$, which for real photons determines the amplitude for $\Sigma^0 \to \Lambda^0 + \gamma$. The general form of such a matrix element, assuming even relative parity between Σ and Λ, is on invariance arguments,

$$(1) \qquad \langle \Lambda^0 \,|\, J_\mu(0) \,|\, \Sigma^0 \rangle = \frac{1}{(2\pi)^3}\, \bar{u}(q_\mu^{(\Lambda)})[a(q^2)\gamma_\mu + b(q^2)\sigma_{\mu\nu} q_\nu + c(q^2) q_\mu] u(q_\mu^{(\Sigma)}) ,$$

where $\bar{u}(q_\Lambda)$ and $u(q_\Sigma)$ are Λ and Σ spinors, and a, b, c, are form factors depending on the invariant momentum transfer $q_\mu q_\mu$ with $q_\mu = q_\mu^{(\Sigma)} - q_\mu^{(\Lambda)}$.

The form factors a, b, c are not all independent because of the relation

$$(2) \qquad q_\mu \langle \Lambda^0 \,|\, J_\mu(0) \,|\, \Sigma^0 \rangle = 0 ,$$

expressing the absence of divergence for the charge current $J_\mu(x)$. In the problem of $\Sigma^+ \to \Lambda^0 + e^+ + \nu$ the corresponding equation $q_\mu \langle \Lambda^0 \,|\, J_\mu^{(V)}(0) \,|\, \Sigma^+ \rangle = 0$ expresses the absence of divergence for the vector strangeness-conserving current.

From (2) one obtains

$$(3) \qquad c(q^2) = -i\, \frac{a(q^2)}{q^2}\, (m_\Sigma - m_\Lambda) .$$

For physical reasons we expect $c(q^2)$ to have a finite limit for $q^2 \to 0$. We are thus led to conjecture that $a(q^2)$ vanishes for $q^2 \to 0$. Such a conjecture is verified in perturbation theory at lowest order. In $\Sigma^0 \to \Lambda^0 + \gamma$, $q^2 = 0$ and $q_\mu \varepsilon_\mu = 0$, where ε_μ is the polarization four-vector of the emitted γ, and therefore only the $\sigma_{\mu\nu}$ term in (1) contributes. In the non-relativistic limit the transition matrix is proportional

to $\boldsymbol{\sigma}\cdot\boldsymbol{e}\wedge\boldsymbol{q}$, giving a $M1$ transition (⁴). In terms of a transition magnetic moment $\mu_\times$ one can write $b(0)$ in the form

$$b(0)=\frac{\mu_\times}{m_\Sigma+m_\Lambda}\,. \tag{4}$$

The inverse lifetime for $\Sigma^0\to\Lambda^0+\gamma$ is then given by

$$\frac{1}{\tau}=\frac{e^2|\mu_\times|^2}{8}\,\frac{(m_\Sigma-m_\Lambda)^3(m_\Sigma+m_\Lambda)}{\pi m_\Sigma^3}\,. \tag{5}$$

Differently from the case of real photons, in the decay $\Sigma^+\to\Lambda^0+e^++\nu$ the invariant momentum transfer is no longer rigorously zero; however it is still very small if compared to the relevant mass values, presumably of the order of the nucleon mass, since one has $|q^2|<(m_\Sigma-m_\Lambda)^2$. Therefore neglecting terms of the order $(m_\Sigma-m_\Lambda)$, both a, because of the conjecture we have made, and c, because of the form of (3), can be ignored in (1). Actually it turns out in the complete calculation that this is also true, in this case of even relative parity between Σ and Λ, up to terms proportional to $(m_\Sigma-m_\Lambda)^2$, certainly very small compared to the main terms [the ratio $(m_\Sigma-m_\Lambda)^2/(\text{nucleon mass})^2$ is $\simeq 0.006$], WEINBERG has recently shown that in leptonic decays, summing over lepton spins and momenta, there are no V-A interferences contributing to scalar correlations, whereas only V-A interference terms can contribute to pseudoscalar correlations (³). In particular the total transition rate for $\Sigma^+\to\Lambda^0+e^++\nu$ will be the sum of a vector rate R_V and of an axial rate R_A. The evaluation of R_V, under the above conjecture for the vertex function, gives.

$$R_V=G^2\,\frac{2}{105(2\pi)^4}|\mu_\times|^2\,\frac{(m_\Sigma-m_\Lambda)^7}{(m_\Sigma+m_\Lambda)^2}\left(\frac{m_\Lambda}{m_\Sigma}\right)^{\frac{3}{2}}, \tag{6}$$

where, consistently with the approximation made in neglecting higher order terms in $m_\Sigma-m_\Lambda$, we have assumed $b(q^2)\simeq b(0)$. The value (6) is thus expected to be accurate up to terms proportional to $(m_\Sigma-m_\Lambda)^2$. It is known that $\mu_\times$, the transition magnetic moment between Σ^0 and Λ^0, also appears in the theory of strange particle photoproduction (⁵) (it is related to the residuum of a pole for the crossed reaction $K+N\to Y+K$). An order of magnitude for $\mu_\times$ can be obtained from the use of global symmetry which gives $\mu_\times\simeq-\mu_n=1.9$ (²). Using this value we find for R_V a value of $0.9\cdot10^3\ \text{s}^{-1}$ giving a branching rate of about 10^{-7}. With the same value of $\mu_\times$ the Σ^0 lifetime would be, from (5), $\tau=8\cdot10^{-20}$ s. The smallness of the vector rate for $\Sigma^+\to\Lambda^0+e^++\nu$ implies that the detection of such a process would mean a big contribution from the uncalculable axial part R_A. If all baryons appear in the bare interaction with the factor $\frac{1}{2}(1+\gamma_5)$ in front, no bare axial coupling exists for the process under the non-renormalization hypothesis. Therefore detection of the process, even with a branching ratio $\simeq10^{-4}$, would indicate a remarkably large

(⁴) See R. GATTO: *Phys. Rev.*, **109**, 610 (1958).
(⁵) A. FUJII and R. E. MARSHAK: *Phys. Rev.*, **107**, 570 (1951); M. MORAVCSIK: *Phys. Rev.*, **107**, 600 (1957); and ref. (²).

renormalization of the axial constant. Experiments to detect such decay may become possible in the future when higher intensities will be available. A check of the scheme would then be the following. Because of the nearly total absence of a vector amplitude in the decay, there will be no V-A interferences. Averaging over the lepton spins and momenta the final distribution must in general have the form

$$w = A(\boldsymbol{q}^2) + (\boldsymbol{P}_\Sigma \cdot \boldsymbol{P}_\Lambda) B(\boldsymbol{q}^2) + (\boldsymbol{P}_\Sigma \cdot \boldsymbol{q}) C(\boldsymbol{q}^2) + (\boldsymbol{P}_\Lambda \cdot \boldsymbol{q}) D(\boldsymbol{q}^2) \, ,$$

where $\boldsymbol{q}$ is the Λ momentum in Σ rest frame and $\boldsymbol{P}_\Sigma$ and $\boldsymbol{P}_\Lambda$ are the Σ and Λ polarization vectors. As a consequence of our result $C(\boldsymbol{q}^2)$ and $D(\boldsymbol{q}^2)$ must be identically zero. This means that there should be no up-down asymmetry in the distribution of $\boldsymbol{q}$ with respect to the plane of production of the Σ (whenever this plane is defined) and no forward-backward asymmetry in the subsequent Λ-decay. The relation between (6) and (5) can also be used, rather peculiarly, to put a lower limit for the $\Sigma^0 \to \Lambda^0 + \gamma$ lifetime from a measurement of the $\Sigma^+ \to \Lambda^0 + e^+ + \nu$ rate. However even from a measured branching ratio of 10^{-4} for such a mode the lower limit for the lifetime would be only $8 \cdot 10^{-23}$ s. In conclusion we note that all the qualitative results we have derived also apply in the case of odd relative parity between Σ and Λ. In this case first order terms in $m_\Sigma - m_\Lambda$ also appear in the Σ^+ rate but this should not change our main conclusions. All of our conclusions can be applied to Σ^- decays. Experiments of the sort considered here are difficult at present but they may become feasible when machines with larger intensities and energies will be available.

Decay Electron Spectrum from Bound μ^--Mesons.

H. Überall

Carnegie Institute of Technology - Pittsburgh, Penn.

(ricevuto il 1° Dicembre 1959)

Some recent experiments [1,2] indicate that the binding of μ^--mesons in the K shell of mesic atoms has a strong influence on the muon decay rate. The effect of the binding on the spectrum of decay electrons has been pointed out earlier in some theoretical papers [3,4], which take into account non-relativistic and relativistic aspects, respectively, of the muon bound to a point nucleus. However, the Coulomb interaction between the nucleus and the decay electron cannot be neglected, and some calculations taking this into account have been performed by Tenaglia [5].

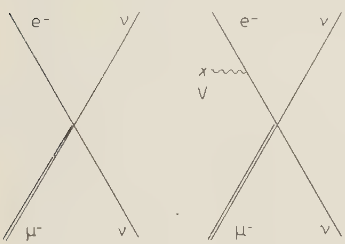

Fig. 1. – Feynman diagrams for the decay of bound μ^--mesons. The double line indicates a bound state, V the final electron interaction.

We have made a systematic evaluation of the μ^- decay electron spectrum for light point nuclei, accurate up to the first power in $\gamma = Z/137$. A hydrogen-type wave function, including small components, was used for the muon in the K shell; for the electron, we took a Dirac plane wave plus a wave scattered by a Coulomb potential in first Born approximation. The two diagrams corresponding to this process are shown in Fig. 1. The muon decay Hamiltonian was assumed to be of V, A type only,

$$H_{\mu e} = \sum_{i=V,A} f_i (\psi_e^\dagger O_i \psi_\mu)(\psi_\nu^\dagger O_i \psi_\nu) \,, \tag{1}$$

$O_V = \gamma_4 \gamma_\mu$, $O_A = i\gamma_4\gamma_5\gamma_\mu$, with left-handed two-component neutrinos.

(1) J. C. Sens, R. A. Lundy, R. A. Swanson, V. L. Telegdi and D. D. Yovanovich: *Bull. Am. Phys. Soc.*, **3**, 198 (1958).
(2) W. A. Barrett, F. E. Holmstrom and J. W. Keuffel: *Phys. Rev.*, **113**, 661 (1959).
(3) C. E. Porter and H. Primakoff: *Phys. Rev.*, **83**, 849 (1951).
(4) T. Muto, M. Tanifuji K. Inoue and T. Inoue: *Progr. Theor. Phys.*, **8**, 13 (1952).
(5) L. Tenaglia: *Nuovo Cimento*, **13**, 284 (1959).

The expected effects of the muon binding, as compared to the decay of a free μ^+-meson, are as follows:

1) The reduction in phase space. This provides an over-all factor ε^5 to the rate and spectrum, with $\varepsilon = 1 - \gamma^2/2$, which is 1 in our approximation.

2) The orbital motion of the muon causes a Doppler smearing [3] of the upper end of the electron spectrum over a fractional range of the order γ.

3) Relativistic time dilatation connected with the small component of the muon wave function. In the spectrum, it adds to the effect of 2), and is expected to decrease the decay rate.

4) Coulomb attraction between nucleus and decay electron. It causes the decay electrons to appear with diminished momentum.

Our results for the spectrum, keeping terms of order 1 and γ^1, are:

$$
(2)\quad \left\{
\begin{aligned}
w_{\mathrm{NR}} &= w_+ \frac{\varepsilon^5}{\pi}\left\{\mathrm{tg}^{-1}\frac{1}{\gamma} + \mathrm{tg}^{-1}\frac{1-x}{\gamma} + \gamma\frac{2-x}{X}\left[(1-x)\left(1+\frac{2}{3}\frac{\gamma^2}{X}\right) + \frac{\gamma^2}{3}\left(1-\frac{2\gamma^2}{X}\right)\right]\right\},\\
w_{\mathrm{R}} &= w_{\mathrm{NR}} + w_+ \frac{\varepsilon^5}{\pi}\frac{2\gamma^5}{3}\frac{2-x}{X^2},\\
w_{\mathrm{Re}} &= w_{\mathrm{R}} + w_+\gamma\frac{\varepsilon^5}{\pi}\left\{2\gamma\frac{1-x}{X}\left(1+\frac{2}{3}\frac{\gamma^2}{X}\right)\mathrm{tg}^{-1}\frac{1-x}{\gamma} + \left(\mathrm{tg}^{-1}\frac{1-x}{\gamma}\right)^2 - \right.\\
&\qquad\qquad\left. - \frac{\pi^2}{4} + \frac{\gamma^2}{X}\left(1-\frac{2}{3}\frac{\gamma^2}{X}\right)\right\},
\end{aligned}
\right.
$$

the indices referring to non-relativistic and relativistic muon, and inclusion of electron-nucleus interaction, respectively; w_{Re} is then the complete electron spectrum. The free muon decay spectrum is given by

$$
(3)\qquad w_+ = \frac{\mu^5}{3 \cdot 2^7 \pi^3}\left(|f_V|^2 + |f_A|^2\right)(3-2x)x^2\,\mathrm{d}x\,;
$$

furthermore, $x = 2p/\varepsilon\mu$, $X = (1-x)^2 + \gamma^2$, and p is the electron momentum, μ the rest mass of the muon. The curves (2) are plotted in Fig. 2 for $Z = 25$, and show agreement with predictions 2)-4). For higher Z, the spectrum w_{Re} would become slightly negative for $x \gtrsim 1.2$, indicating that higher terms in γ are not completely negligible.

When integrated over $\mathrm{d}x$, w_{Re} gives the free muon decay rate λ_+ and no correction term linear in γ. The point nucleus model is thus not sufficient to explain the experimental results [1,2]: $\lambda_- > \lambda_+$ for $Z \lesssim 30$, $< \lambda_+$ for $Z \gtrsim 30$. The terms in λ_- of order γ^2 obtained from the integration of w_{Re} are not the only ones of this order. Correctly up to order γ^2, we have found [6]:

$$
(4)\qquad (\lambda_-)_{\mathrm{NR}} = (1 - 9\gamma^2/2)\lambda_+\,, \qquad (\lambda_-)_{\mathrm{R}} = (1 - 11\gamma^2/2)\lambda_+\,,
$$

---

[6] These results were also obtained by J. DREITLEIN and by R. HUFF; I wish to thank Prof. H. PRIMAKOFF for a private communication about this work.

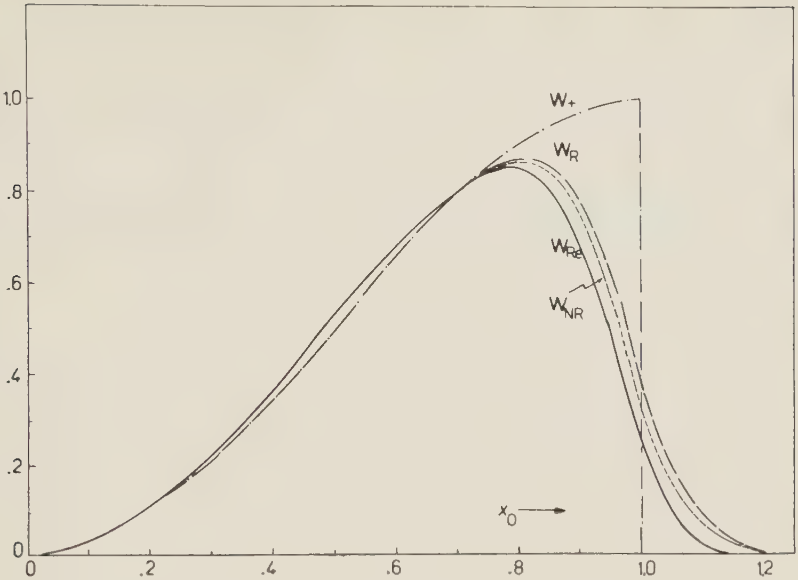

Fig. 2. – Decay electron spectra of bound μ^--mesons for $Z=25$: w_{NR} and w_R for non-relativistic and relativistic muons and no final electron-nucleus interaction; w_{Re} (the actual spectrum) for a relativistic muon and with final electron interaction; w_+ is the decay electron spectrum of free muons. All is plotted *vs.* $x_0 = \varepsilon x$.

but for a calculation of $(\lambda_-)_{Re}$, second Born approximation on the electron wave function would have to be used.

* * *

I am indebted to Professor L. Wolfenstein for discussions.

IL NUOVO CIMENTO VOL. XV, N. 1 1° Gennaio 1960

On the Possible Existence of Doubly Strange Heavy Mesons (*).

J. C. POLKINGHORNE

Trinity College - Cambridge

A. SALAM

Imperial College of Science and Technology - London

(ricevuto il 12 Dicembre 1959)

Recently there have been revived indications (1) of the possible existence of doubly strange heavy mesons of approximately 1500 electron masses. In this note we wish to discuss some of the theoretical implications of this.

The positive meson ω^+ ($S=2$) could first be produced by 1.8 GeV/c pions in the reaction

$$(1) \qquad \pi^- + \mathrm{p} \to \Xi^- + \omega^+ \, .$$

This process also gives a markedly lower threshold for Ξ production than the conventional one arising from association with two K-mesons. However since all Ξ interactions seem to be anomalously weak (2) perhaps the threshold of greater importance might prove to be that for the reaction

$$(2) \qquad \pi^- + \mathrm{p} \to \Lambda^0 + \mathrm{K}^- + \omega^+ \, ,$$

which occurs at 2.5 GeV/c pion momentum. Just above this at 2.7 GeV/c is the first threshold for ω^- ($S=-2$) production, by the process

$$(3) \qquad \pi^- + \mathrm{p} \to \mathrm{N} + \omega^+ + \omega^- \, .$$

The mesons find a natural place in a four dimensional classification scheme (3) as the charged members of the (0, 1) triplet. The neutral member (*) ω^0 would be expected to be highly unstable since it has $S=0$ and would only manifest itself as an $I=\frac{1}{2}$ resonance in pion-nucleon scattering. If the mass were

(*) Research supported in part by the United States Air Force, Research and Development Command, Europe.

(1) W. KAN-CHANG: *Proc. of the Kiev Conference on High Energy Nuclear Physics* (1959); T. YAMANOUCHI and M. F. KAPLON: *Phys. Rev. Lett.*, **3**, 283 (1959).

(2) L. W. ALVAREZ: *Proc. of the Kiev Conference on High Energy Nuclear Physics* (1959).

(*) It is in requiring the existence of ω^0 (and X^0) as well as in the insistence that if ω-particles exist, X-particles do so too, that the application of our scheme differs from just filling gaps in the Gell-Mann-Nishijima strangeness assignments.

(3) A. SALAM and J. C. POLKINGHORNE: *Nuovo Cimento*, **4**, 848 (1955); J. C. POLKINGHORNE: *Nuovo Cimento*, **6**, 864 (1957).

the same as that of the charged mesons this would occur around 1 GeV/c.

The requirement that strangeness changes only by one unit in weak decays enforces the cascade decays of $\omega^{\pm}$ by which it is hoped they have been identified. The $\Delta I = \frac{1}{2}$ rule requires that the branching ratio

$$\frac{\omega^{+} \to K^{+} + \pi^{0}}{\omega^{+} \to K^{0} + \pi^{+}}, \tag{4}$$

be $\frac{1}{2}$. Presumably this would be easy to determine experimentally.

Apart from the (0, 0) meson (which could easily be unstable) the existence of $\omega^{\pm}$ would fill all the gaps in the four dimensional scheme for the mesons. It would be tempting to suppose therefore that the (0, 1) baryon triplet existed also. The resulting new baryons would be X^{-} ($S = -3$), X^{0} ($S = -1$), X^{+} ($S = 1$). Nothing can be said *a priori* about their masses which, on the analogy of N-Ξ splitting, might be all different. X^{-} would be hard to produce, the reaction with the lowest threshold being

$$\pi^{-} + p \to X^{-} + \omega^{+} + K^{0}. \tag{5}$$

Since X^{0} must be heavier than the Λ^{0} (for the sake of the latter's quasi-stability) it must be highly unstable. X^{+} must be heavier than ~ 1430 MeV to avoid lowering the well established threshold for K^{-} production and so must also be highly unstable. The practical effects of X^{0} and X^{+} would be to produce $I = 0$ resonances in K-nucleon scattering.

It is possible that the widths of the resonances associated with ω^{0}, X^{0} and X^{+} would be less than might be anticipated. If μ-isospin (3) were a good quantum number their decay into the currently known particles would be forbidden so that their instability would be the result of electromagnetic interactions alone. The splitting of nucleons and cascades shows that μ-isospin is not conserved but it is in the spirit of our scheme to suppose that the interactions that break it are of lesser importance than those that do not, so that some residual effect might remain.

* * *

We wish to thank Dr. J. HAMILTON for an interesting discussion.

Multiple Scattering of Polarized Particles.

L. WALDMANN

Max-Planck-Institut für Chemie (Otto Hahn Institut) - Mainz

(*Nuovo Cimento*, **14**, 898 (1959))

In eq. (3) read $\frac{8}{7}$ instead of $\frac{7}{8}$.

Note on the Electric Quadrupole Absorption in the Nuclear Photoreaction.

S. FUJII

Department of Physics, College of Science and Engineering, Nihon University - Tokyo

O. SUGIMOTO

Department of Physics, Hiroshima University - Hiroshima

(*Nuovo Cimento*, **12**, 513 (1959))

Add to Figures following captions:

Fig. 1. – The computed result for the EQ cross-section in $^{40}A(\gamma, p)^{39}Cl$.

Fig. 2. – The computed result for the EQ cross section in $^{59}Co(\gamma, p)^{58}Fe$.

Fig. 3. – The angular distribution in $^{40}A(\gamma, p)^{39}Cl$: the theoretical curve at $E_\gamma = 18$ MeV; the experimental result of proton of energy greater than 4 MeV from ^{40}A irradiated with 22.5 MeV bremsstrahlung.

Fig. 4. – The angular distribution in $^{59}Co(\gamma, p)^{58}Fe$: the theoretical curve at $E_\gamma = 21.5$ MeV; the theoretical curve at $E_\gamma = 19.5$ MeV; the experimental result of proton of energy greater than 10 MeV from ^{59}Co irradiated with 24 MeV bremsstrahlung.

LIBRI RICEVUTI E RECENSIONI

J. Rzewuski – *Field Theory* - Part I: *Classical Theory*. Polish Academy of Sciences, Physical Monographs, Warsavia, 1958, pp. 297.

È questo il primo volume di una monografia sulla teoria dei campi che l'autore si ripromette di completare con un secondo volume dedicato ai campi quantizzati. L'usuale metodo di esposizione della teoria dei campi formulato sul modello dello sviluppo dell'elettrodinamica, si presta, entro certi limiti, a questa suddivisione in due parti, una classica ed una quantistica. Personalmente riteniamo superato, da un punto di vista logico, questo tipo di esposizione. I recenti sviluppi hanno infatti mostrato come la teoria assiomatica offra un quadro più conveniente per la presentazione delle basi della teoria: principi di invarianza e principi dinamici. Mentre per quanto riguarda i principi di invarianza le due presentazioni sono probabilmente ugualmente adatte, è presumibile che la teoria assiomatica riesca più direttamente ad individuare le possibili teorie relativistiche ed a legarle a semplici e forse essenziali postulati. Didatticamente, peraltro, può riuscire ancora utile una esposizione secondo il vecchio stile, il cui principale inconveniente è di non offrire apparentemente nuove possibilità di sviluppo. Diamo ora un'idea del contenuto di questo primo volume, scritto con molta cura e molta originalità in alcune parti.

Il primo capitolo tratta degli spazi e dei tensori. Dopo la presentazione del gruppo di Lorentz, l'autore discute il gruppo unimodulare a due dimensioni, le cui rappresentazioni sono connesse al gruppo di Lorentz. Viene quindi svolta in dettaglio l'analisi spinoriale e tensoriale. Il secondo capitolo sui principi variazionali contiene la discussione del principio di azione stazionaria, e dei principi di conservazione integrale e differenziali. Segue anche una discussione del principio di azione nella dinamica di particelle. Il capitolo III è dedicato agli esempi fisici. Per i vari campi non interagenti vengono esaminati il principio variazionale, le equazioni di campi, le leggi di conservazione e risolte le equazioni del moto per valori iniziali assegnati. Lo stesso viene quindi fatto per campi interagenti con sorgenti esterne e per campi accoppiati, come il campo elettromagnetico interagente col campo degli elettroni. Le molteplici difficoltà di una teoria classica conducono l'autore a discutere problemi di smorzamento per radiazione ed esempi di teorie classiche non locali. L'ultimo capitolo molto ben fatto e che riuscirà senz'altro utile al lettore, discute le soluzioni fondamentali delle equazioni di campo mediante le varie funzioni di Green per campi bosonici e per campi fermianici, di cui vengono esibite le varie rappresentazioni integrali e le relazioni tra di esse.

In conclusione, a parte le critiche che

abbiamo mosse all'inizio, e che certamente non si applicano in pieno ad una opera che vuole avere carattere introduttivo e didattico, riteniamo che la lettura di questo volume di RZEWUSKI riuscirà interessante tanto agli studiosi dell'argomento, che potranno con poca fatica controllarvi le loro nozioni, quanto ai principianti che, data l'estrema chiarezza e semplicità di tono dell'esposizione, troveranno facile apprendervi concetti e metodi di uso corrente.

R. GATTO

A. VAN DER ZIEL – *Fluctuation Phenomena in Semi-Conductors.* London, Butterworths scientific publications, 1959.

Il libro ha lo scopo di presentare un panorama delle conoscenze attuali sui fenomeni statistici che contribuiscono al rumore di fondo nei materiali semiconduttori.

L'argomento, oltre a rivestire interesse per l'enorme diffusione avutasi nelle applicazioni tecniche dei semiconduttori, è importante anche per altri motivi. Le fluttuazioni di corrente e di tensione nei semiconduttori riflettono il carattere atomistico del meccanismo di conduzione e quindi il loro studio aiuta a comprendere meglio le leggi fisiche che definiscono il comportamento di questi materiali. Inoltre, la comprensione dei predetti fenomeni permette sia di stabilire i limiti d'applicatilità degli attuali elementi di circuito a semiconduttori sia di migliorarne successivamente le caratteristiche.

Il nome dell'autore, universalmente noto per i suoi studi sui rumori nei circuiti elettronici, è già una garanzia per la serietà e la competenza con cui l'argomento viene trattato.

Ci sembra che uno dei meriti del libro risieda nella trattazione unitaria data a tutta la materia; per cui i diversi argomenti non sono semplicemente un rifacimento di articoli già noti e magari sparsi in diverse riviste, ma costituiscono gli sviluppi consequenti alla teoria elaborata nei primi capitoli.

Nel classificare i tipi di rumore, giustamente l'Autore osserva che i nomi finora usati sono stati introdotti su una base più o meno euristica spesso tenendo presente analogie con i tubi elettronici non sempre valide.

Perciò, invece delle denominazioni « thermal noise », « flicker noise » e « shot noise » ben precise nel loro significato riferito ai tubi a vuoto, suggerisce per i semiconduttori di classificarne i rumori tenendo presente i veri fenomeni fisici che li determinano e propone le denominazioni:

a) generation-recontinuation noise;

b) diffusion noise;

c) modulation noise.

Ad esempio il rumore del tipo $\text{cost}/f\alpha$ con α costante e prossimo ad 1, è presentato come una consequenza della teoria del generation-recontinuation noise.

Leggendo il libro ci si accorge come l'Autore non si sia solo preoccupato di illustrare e discutere i risultati finora conseguiti in questo campo di ricerche, ma di sottolineare anche dove risiedono e quali sono i problemi ancora non risolti. Senza dubbio ciò avrà il merito di stimolare nuove ricerche.

U. PELLEGRINI

M. J. LIGHTHILL – *Introduction to Fourier Analysis and generalised functions.* Ed. Cambridge University Press, 1958, pag. 79.

È noto che l'ordinario concetto di funzione è stato ampiamente generalizzato da L. SCHWARTZ con la nozione di *distribuzione*, nella quale rientrano, come casi particolari, la classica funzione δ

di Dirac e le sue derivate successive. Un altro punto di vista per introdurre *funzioni generalizzate* è quello dovuto a G. TEMPLE e questo volumetto è appunto destinato ad illustrarlo (nel caso di funzioni di una variabile) ed a presentarne le più semplici applicazioni.

In sostanza si tratta di questo: 1) diciamo G la classe delle funzioni $f(x)$ (in senso ordinario) definite in $(-\infty, +\infty)$, che sono dotate di tutte le derivate e che, assieme a queste derivate, si annullano all'infinito di ordine comunque elevato; 2) chiamiamo *regolare* una successione $\{f_n(x)\}$ di funzioni della classe G quando, per ogni funzione $F(x)$ della stessa classe, esiste determinato e finito il limite

$$(1) \qquad \lim_{n\to\infty} \int_{-\infty}^{+\infty} f_n(x) F(x)\, dx\,;$$

3) riguardiamo come *equivalenti* due successioni regolari $\{f_n(x)\}$, $\{g_n(x)\}$ quando, per ogni funzione $F(x)$ della classe G, risulta

$$\lim_{n\to\infty} \int_{-\infty}^{+\infty} f_n(x) F(x)\, dx = \lim_{n\to\infty} \int_{-\infty}^{+\infty} g_n(x) F(x)\, dx\,;$$

4) definiamo come *funzione generalizzata* $f(x)$ la totalità di tutte le successioni regolari ed equivalenti. Ovviamente ciò porta subito a definire, per ogni funzione generalizzata $f(x)$, integrali del tipo

$$\int_{-\infty}^{+\infty} f(x) F(x)\, dx$$

ponendoli uguali al limite (1) ove $\{f_n(x)\}$ è una qualunque delle predette successioni regolari ed equivalenti. Si possono poi introdurre per le funzioni generalizzate vari concetti, fra cui quello di trasformata di Fourier, ecc. Abbiamo così descritto, in modo rapidissimo, il contenuto dei primi due capitoli; il libro prosegue poi con altri tre capitoli dedicati alle trasformate di Fourier di particolari funzioni generalizzate, alle valutazioni asintotiche di tali trasformate ed alle serie di Fourier di funzioni generalizzate.

Il contenuto del volume, mantenuto su un tono molto elementare, è indubbiamente interessante; tuttavia riteniamo preferibile l'impostazione data da SCHWARTZ.

A. GHIZZETTI

L. V. KANTOROVICH and V. I. KRYLOV – *Approximate Methods of Higher Analysis*, tradotto dal russo da C. D. Benster. Ed. P. Noordhoff Ltd., Groningen, The Netherlands, 1958.

È la traduzione in inglese di opera russa. Si tratta di un grosso volume ove sono esposti numerosi metodi per il calcolo numerico approssimato delle soluzioni dei problemi ai limiti per le equazioni differenziali ordinarie lineari, dei problemi al contorno per le equazioni lineari a derivate parziali, delle equazioni integrali di Fredholm, ecc. Le equazioni a derivate parziali sono considerate esclusivamente in due variabili indipendenti, le equazioni integrali in una; vi è da aggiungere, per quanto riguarda le prime, che si parla quasi sempre delle classiche equazioni $\Delta u = f$, $\Delta\Delta u = f$, con pochi cenni ad equazioni di tipo ellittico più generali o di tipo diverso. I fondamenti teorici relativi ai vari argomenti trattati si suppongono di regola noti al lettore, ma vengono sempre brevemente richiamati. Ogni metodo è illustrato da esempi numerici; fra questi se ne trovano alcuni veramente notevoli ed interessanti. È da notare poi che nella descrizione di ogni metodo sono anche segnalati molti piccoli accorgimenti pratici di indubbia utilità.

Si può dire complessivamente che il

volume in discorso costituisce una eccellente guida per chi debba occuparsi di analisi numerica ed anche una buona fonte di notizie per studiosi nel campo dell'analisi pura.

Diamo un'idea del vasto contenuto del libro che è suddiviso in sette capitoli. Nel Cap. I sono esposti i metodi risolutivi dei problemi al contorno, basati sulla rappresentazione della soluzione per mezzo di sviluppi in serie. Nel Cap. II si prendono in considerazione le equazioni integrali di Fredholm e si espongono metodi per il calcolo numerico approssimato delle soluzioni. Nel Cap. III viene studiato il metodo delle differenze finite. Il Cap. IV tratta dei metodi variazionali per lo studio dei problemi al contorno. Il Cap. V, assai vasto, è dedicato alla rappresentazione conforme. Nel Cap. VI sono mostrate le applicazioni della rappresentazione conforme alla risoluzione di classici problemi al contorno per le funzioni armoniche o biarmoniche in alcuni domini tipici. Il Cap. VII infine è dedicato al metodo alternato di Schwarz per la risoluzione del problema di Dirichlet posto nella somma di due dominii ed all'analogo metodo di Neumann nel caso del prodotto di due dominii.

Per terminare, diremo ancora che figurano nel libro numerose citazioni bibliografiche, in grandissima parte dedicate ad Autori russi.

A. GHIZZETTI

Direttore responsabile: G, POLVANI

Tipografia Compositori - Bologna

Questo Fascicolo è stato licenziato dai torchi il 28-I-1960